Cover Page

Universiteit Leiden

The handle http://hdl.handle.net/1887/26502 holds various files of this Leiden University dissertation.

Author: Willems, Lianne Irene
Title: Direct and two-step activity-based profiling of proteases and glycosidases
Issue Date: 2014-06-24

Direct and two-step activity-based profiling of proteases and glycosidases

PROEFSCHRIFT

ter verkrijging van
de graad van Doctor aan de Universiteit Leiden,
op gezag van Rector Magnificus prof. mr. dr. C. J. J. M. Stolker,
volgens het besluit van het College voor Promoties
te verdedigen op dinsdag 24 juni 2014
klokke 13:45 uur

door

Lianne Irene Willems

geboren te Leiden in 1986

Promotiecommissie

Promotoren	Prof. dr. H. S. Overkleeft
	Prof. dr. G. A. van der Marel
Overige leden	Prof. dr. J. M. F. G. Aerts
	Prof. dr. J. Brouwer
	Prof. dr. D. J. Vocadlo
	Dr. M. Verdoes
	Prof. dr. J. Lugtenburg

Drukker Ridderprint B.V., Ridderkerk, Nederland

Table of contents

List of abbreviations 6

Chapter 1 9
General introduction

Chapter 2 25
Bioorthogonal chemistry

Chapter 3 39
Two-step labeling of endogenous enzymatic activities by Diels-Alder ligation

Chapter 4 57
Triple bioorthogonal ligation strategy for simultaneous labeling of multiple enzymatic activities

Chapter 5 83
Synthesis of epoxide- and aziridine-based probes to target retaining galactosidases

Chapter 6 103
A potent and selective activity-based probe for human retaining α-galactosidases

Chapter 7 117
Activity-based profiling of human retaining β-galactosidases

Chapter 8 129
Summary and future prospects

Samenvatting 157

List of publications 163

Curriculum vitae 166

List of abbreviations

4-mu	4-methylumbelliferyl
ABP	activity-based probe
ABPP	activity-based protein profiling
Ac	acetyl
ACN	acetonitrile
α-gal	α-D-galactopyranoside
αGal A	α-galactosidase A
αGal B	α-galactosidase B
Ahx	6-aminohexanoic acid
APT	attached proton test
ATP	adenosine triphosphate
β-gal	β-D-galactopyranoside
Bn	benzyl
Boc	*tert*-butoxycarbonyl
Bodipy	boron-dipyrromethene
BOP	benzotriazol-1-yloxy-tris-(dimethylamino)phosphonium hexafluorophosphate
bs	broad singlet
BSA	bovine serum albumin
Bz	benzoyl
c/m	chloroform/methanol
calcd.	calculated
cDNA	complementary DNA
Cos-7	African green monkey kidney fibroblast cell line
COSY	correlation spectroscopy
d	doublet
δ	chemical shift
D	Aspartic acid
DBU	1,8-diazabicycloundec-7-ene
DCE	dichloroethane
DCM	dichloromethane
dd	double doublet
ddd	double double doublet
ddt	double double triplet
DFT	density functional theory
DiPEA	*N*,*N*-diisopropylethylamine
DMAP	4-(*N*,*N*-dimethylamino)pyridine
DMEM	Dulbecco's modified Eagle's medium
DMF	*N*,*N*-dimethylformamide
DMSO	dimethylsulfoxide
DNA	deoxyribonucleic acid
dt	double triplet
dtd	double triple doublet
DTNB	5,5'-dithiobis-(2-nitrobenzoic acid)
DTT	dithiothreitol
E	Glutamic acid
EDC	1-ethyl-3-(3-dimethylamino-propyl)-carbodiimide
EEDQ	2-ethoxy-1-ethoxycarbonyl-1,2-dihydroquinoline
El-4	murine lymphoid cell line
eq.	molar equivalents
Et	ethyl
FBS	fetal bovine serum
FCS	fetal calf serum
Fmoc	(9*H*-fluoren-9-yl)methoxy-carbonyl
G	Glycine
GBA1	glucocerebrosidase

GLA	gene encoding αGal A
GM1	monosialotetrahexosyl-ganglioside
HCTU	*O*-(6-chlorobenzotriazol-1-yl)-*N*,*N*,*N*',*N*'-tetramethyluronium hexafluorophosphate
HEK-293T	human embryonic kidney cell line
HPLC	high-performance liquid chromatography
hr(s)	hour(s)
HRMS	high resolution mass spectrometry
HRP	horseradish peroxidase
HSQC	heteronuclear single quantum coherence
Hz	Hertz
IC_{50}	half maximal inhibitory concentration
J	coupling constant
LC/MS	liquid chromatography/mass spectrometry
Leu	Leucine
Lys	Lysine
M	multiplet
m/z	mass to charge ratio
*m*CPBA	*meta*-chloroperoxybenzoic acid
Me	methyl
MES	2-(*N*-morpholino)ethanesulfonic acid
min	minutes
mRNA	messenger ribonucleic acid
MS	mass spectrometry
NAGA	*N*-acetylgalactosamine
NCBI	National Center for Biotechnology Information
NMP	*N*-methyl-2-pyrrolidone
NMR	nuclear magnetic resonance
2-OG	2-oxoglutarate
PAGE	polyacrylamide gel electrophoresis
PBS	phosphate-buffered saline
pcDNA	partial complementary single strand DNA
PetEt	petroleum ether
ppm	parts per million
PVDF	polyvinylidene difluoride
q	quartet
RAW	mouse leukaemic monocyte macrophage cell line
R_f	retention factor
R_t	retention time
rt	room temperature
s	singlet
SD	standard deviation
SDS	sodium dodecyl sulfate
Su	succinimidyl
t	triplet
TBAF	tetrabutyl ammonium fluoride
TBDMS	*tert*-butyldimethylsilyl
TBS	Tris-buffered saline
TBS-t(+)	TBS with 0.1% Tween-20
TBTA	*N*,*N*,*N*-tris((1-benzyl-1*H*-1,2,3-triazol-4-yl)methyl)amine
*t*Bu	*tert*-butyl
TCEP	tris(2-carboxyethyl)phosphine
td	triple doublet
tdd	triple double doublet
TEV	Tobacco Etch virus
TFA	trifluoroacetic acid
THF	tetrahydrofuran
TIS	triisopropylsilane
TLC	thin layer chromatography
TMS	trimethylsilane
Tr	trityl
Tris	2-amino-2-(hydroxymethyl)-1,3-propanediol
Ts	*para*-toluenesulfonyl
Tyr	Tyrosine
UV	ultraviolet
WT	wild-type

1

General introduction

Chemical biology is defined as the field of research in which chemical tools and approaches are applied to understand and control biological processes. The chemical techniques that are developed for this objective involve contributions from many areas of chemistry, in particular from organic chemistry. Principles and knowledge inherent to organic chemistry, such as reactivity and selectivity, are applied to manipulate specific biomolecules in biological samples (cell extracts, living cells, and sometimes even animal models) in order to gain insight into the mechanisms underlying the biological processes in which these molecules participate or to identify potential new therapeutic strategies. Chemical biology research spans a wide range of applications including the use of small molecule chemical probes to inhibit, modify or enrich a particular protein of interest, the targeting of cell surface receptors with synthetic molecules, and the use of synthetic oligonucleotides or other small molecules to control gene expression. Further applications involve the synthesis of modified glycosides and lipids and their incorporation into glycoconjugates and post-translationally modified proteins by the cell's metabolic machinery, the introduction of unnatural amino acids into recombinant proteins, and the design of synthetic and enzymatic methods to manipulate and study post-translational modifications. The work described in this thesis involves the development of chemical tools and methods for activity-based protein profiling (ABPP), an area of chemical biology research that aims to obtain information on the activity of a protein or protein family within the larger context of a biological system.

1.1 Activity-based protein profiling

ABPP has emerged as a powerful strategy to study the activity of enzymes in complex proteomes.[1-6] Enzyme expression levels do frequently not correlate directly to their activity, as the activity of many enzymes is regulated by post-translational modifications, protein-protein interactions and/or the action of endogenous small molecule inhibitors. The importance of monitoring enzymatic activity can be illustrated by the class of cysteine proteases. These enzymes are synthesized as inactive precursors that need to be proteolytically cleaved in order to become catalytically active.[7,8] Therefore, methods to quantify mRNA or protein levels would provide only limited information on the amount of active cysteine proteases, a parameter of great physiological relevance for these enzymes. To enable the profiling of enzymatic activity, ABPP approaches make use of chemical probes termed activity-based probes (ABPs) that are directed to the active site of an enzyme or enzyme family. These probes are designed to be recognized by a specific target protein and react in a mechanism-based manner with an active site residue, thereby labeling only the catalytically active form of the enzyme. The binding of the probe to the enzyme should be covalent and irreversible in order to facilitate the analysis of labeled proteins by for instance SDS-PAGE or mass spectrometry. A large number of ABPs that target many different enzyme classes has been developed over the past decades, enabling the selective labeling of enzymatic activity in complex biological samples such as cell lysates, cell cultures and sometimes even living organisms.[1-3] Besides the monitoring of a specific enzymatic activity, ABPP strategies are also used to identify and characterize (unknown) protein functions, to study up- and down-regulation of enzymatic activity in various disease states, to discover and evaluate putative new enzyme inhibitors and to identify the protein targets of covalently binding natural products.[1-6]

In general, ABPs contain three essential structural elements as depicted schematically in Figure 1.1A. These elements are a reactive group, also named the 'warhead', a recognition element and a detectable agent. The warhead mediates irreversible binding of the probe to the enzyme of interest by reacting in a mechanism-based manner with the catalytically active amino acid residue of the enzyme. It is often an electrophilic moiety that is susceptible to attack by the active site nucleophile. The warhead needs to be sufficiently reactive to allow reaction with the intended active site residues while it should not react with off-target amino acid residues or any other functionalities present in the sample. Most ABPs also contain a recognition element that confers selectivity towards a specific protein of interest and that, by binding in the active site, brings the warhead of the probe and the active site nucleophile in close proximity, thereby stimulating their reaction. Together, the

structure of the recognition element and the reactivity of the warhead can be tuned to provide selective targeting of a specific enzyme or multiple members of an enzyme class. The third common feature of all ABPs is a means to visualize, isolate, identify and/or quantify the labeled proteins by for example SDS-PAGE, microscopy or mass spectrometry analysis. This functionality can either be a reporter group that enables the direct visualization and/or isolation of target enzymes (Figure 1.1B) or a reactive moiety that can be used to introduce the tag in a later stage (Figure 1.1C). Based on the nature of this third element ABPs are classified as either direct or two-step ABPs, respectively. Commonly used reporter entities for ABPP studies include fluorescent tags that enable visualization of the labeled proteins on gel and by fluorescence microscopy, affinity tags such as biotin for enrichment of labeled proteins and subsequent mass spectrometry analysis or detection by Western blotting, or a combination of these. Quenched fluorophores that only become fluorescent after binding of the ABP to a target enzyme can strongly reduce background labeling and thereby provide significant advantages for (*in vivo*) imaging applications.[9] The three main elements of ABPs may be separated by additional linkers that can be used to minimize steric hindrance or modulate solubility and membrane-permeability of the probe.

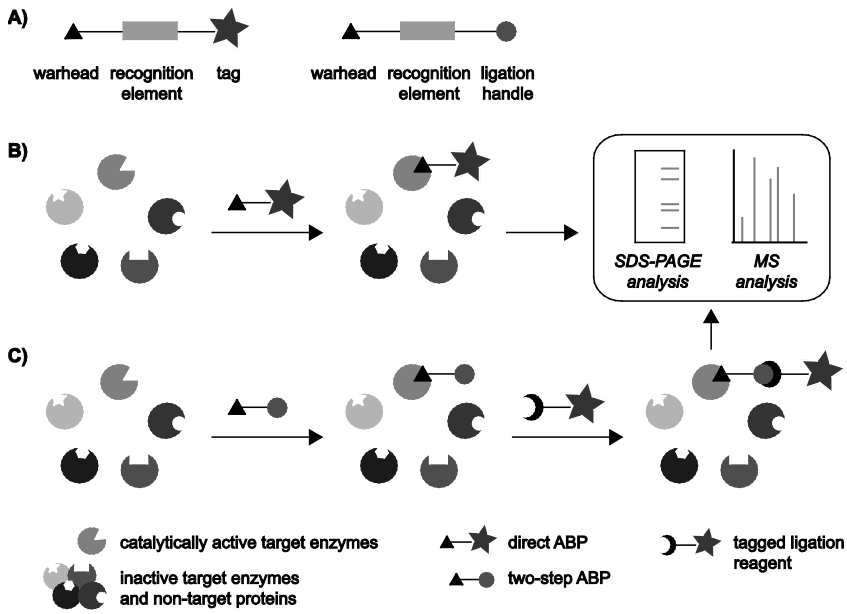

Figure 1.1. Schematic representations of one- and two-step ABPP strategies. A) General composition of a direct ABP (left) and a two-step ABP (right). B,C) Labeling of enzymatic activity by a direct ABP (B) or a two-step ABP (C). SDS-PAGE: sodium dodecyl sulfate polyacrylamide gel electrophoresis. MS: mass spectrometry.

Moreover, chemically-cleavable linkers may be included to facilitate the selective release of target proteins after affinity purification[10-15] and targeting elements can be added for targeted delivery of the probe to a specific cell type or cellular compartment.[16,17]

The enzymes that are most readily targeted by ABPs are those that form a covalent intermediate with their substrate at some point in the catalytic mechanism. The formation of such an intermediate can be exploited for the design of a probe that reacts in a manner similar to the substrate and thereby forms a covalent and irreversible bond with the active site of the enzyme. An example is the labeling of cysteine proteases using the biotinylated peptide epoxysuccinate DCG-04 (**1**) (Figure 1.2), which was shown to react specifically with a number of cysteine proteases of the cathepsin family in cell extracts.[18] The epoxide moiety of the ABP, which functions as the warhead, is attacked by the catalytically active cysteine residue in the active site, resulting in opening of the epoxide ring and the formation of a stable covalent bond between the enzyme and the probe (Figure 1.3A).[19] In cases where no covalent enzyme-substrate intermediate is formed, activity-based profiling can be achieved by applying suicide substrates that act via an indirect binding mechanism. For example, fluorogenic ABP **2** (Figure 1.2) was developed to report on the activity of β-galactosidases by reacting as shown in Figure 1.3B.[20] This probe contains a latent quinone methide precursor which is released upon hydrolysis by a target enzyme. The highly reactive species that is formed can subsequently react with a nearby nucleophilic amino acid residue, yielding an immobilized fluorescent label. Although suicide substrates bind in a mechanism-based manner, the reactive species that is released may react with a nucleophile distant from the active site or even another component in the sample, so that this type of ABP does not specifically label the protein of interest. In this thesis the focus is on the first class of ABPs which directly modify a catalytically active amino acid residue. It should be kept in mind that the use of these probes results in the subsequent inhibition of catalytic activity and may thereby potentially disturb the system at hand, especially when applied to living organisms.

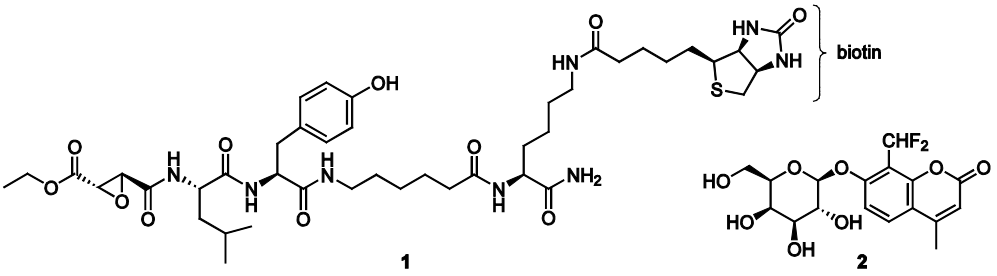

Figure 1.2. Structures of biotin-tagged cysteine protease ABP **1** and fluorogenic β-galactosidase ABP **2**.

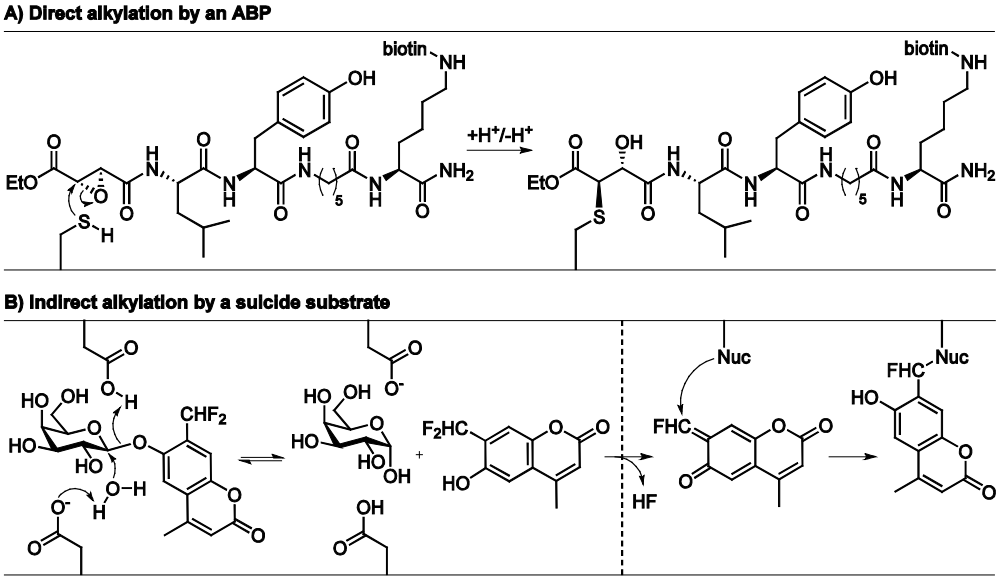

Figure 1.3. Examples of two mechanisms by which ABPs can bind to their target enzymes. A) Direct alkylation of the catalytically active amino acid residue: labeling of cysteine proteases by ABP **1**. B) Targeting with suicide substrates: labeling of inverting β-galactosidases by fluorogenic ABP **2**. 'Nuc': nucleophile.

1.2 Two-step activity-based probes

In contrast to direct ABPs such as DCG-04 (**1**, Figure 1.2), two-step ABPs do not contain a reporter group but are instead functionalized with a small reactive moiety, or 'ligation handle', that can be used to introduce a tag via a selective ligation reaction after binding of the probe to a target enzyme (Figure 1.1C). Two-step labeling experiments are particularly useful when the covalent attachment of a fluorescent group or an affinity tag to an ABP interferes with binding to the intended enzyme(s), selectivity and/or cell-permeability of the probe. An inherent consequence of the introduction of a tag is that it reduces the resemblance a probe may possess to an enzyme substrate. Furthermore, the presence of a relatively bulky reporter group is not always tolerated in the active site of an enzyme and the tag might also render the ABP less cell-permeable or reduce its bioavailability. Two-step ABPP strategies may solve these issues by allowing the temporal separation of an ABP and a reporter group. A further advantage as compared to direct ABPP is the option to use different reporter groups depending on the experimental settings and the desired method of analysis while using a single ABP. In order to achieve selective labeling of the enzymes

that are targeted by a two-step ABP, the ligation handle of the probe needs to react selectively and efficiently with a reactive group to which the tag is attached. At the same time interference with any other (biological) functionalities should be avoided. Therefore reactions are used which are commonly referred to as bioorthogonal ligation reactions.[21] A frequently used example of a bioorthogonal ligation reaction is the copper(I)-catalyzed [2+3] cycloaddition of an azide with an alkyne, a reaction generally referred to as 'click' reaction (Figure 1.4A).[22,23] Both of the reactive moieties are small and can be incorporated into an ABP without significantly affecting the properties of the probe. The power of this strategy was first illustrated by the labeling of enzymatic activity in cell extracts with azide-functionalized sulfonate **3** followed by reaction with rhodamine-alkyne **4** and copper(I) as the catalyst (Figure 1.4C).[24] A second example of a bioorthogonal ligation reaction is the Staudinger-Bertozzi ligation, in which an azide is again used as a ligation handle. In this case two-step labeling is achieved via selective reaction with a phosphine reagent (Figure 1.4B).[25] This strategy has been applied to profile the activity of the proteasome β-subunits by treating cultured cells with azide-modified proteasome inhibitor **5** (Figure 1.4C) and labeling the target proteins after cell lysis with biotin-phosphine **6**.[26] A further description of the various bioorthogonal ligation techniques and their application in two-step ABPP is given in Chapter 2.

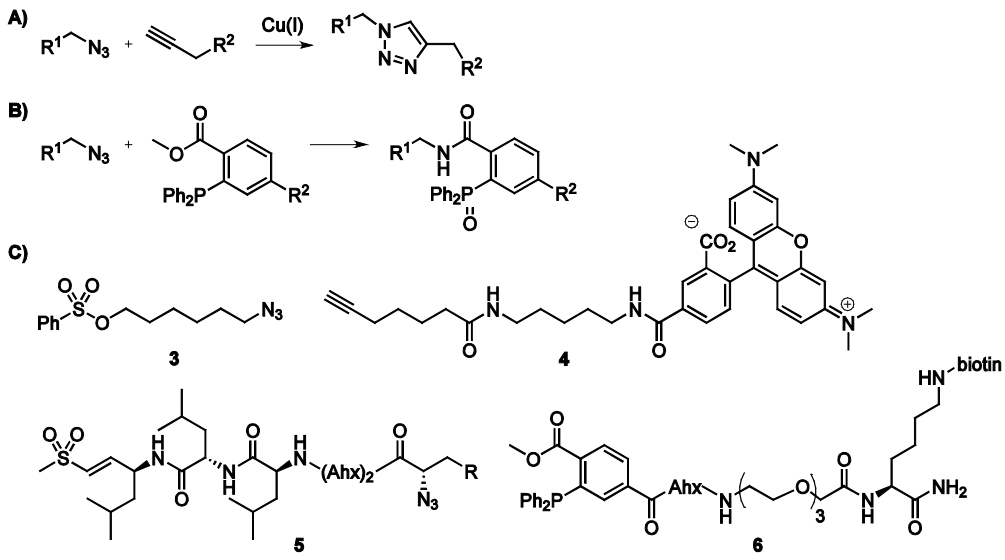

Figure 1.4. A) Copper(I)-catalyzed azide-alkyne [2+3] cycloaddition. B) Staudinger-Bertozzi ligation. C) Structures of azide-functionalized ABPs **3** and **5**, fluorescently labeled click reagent **4** and biotinylated phosphine **6**.

1.3 Probe design and selected examples

As a starting point for the design of novel ABPs, the structure of a natural substrate of the enzyme of interest can be used, which is then equipped with a tag and modified in such a way that reaction with the enzyme results in covalent and irreversible binding. Knowledge of the catalytic mechanism and/or reactivity towards particular electrophiles is essential. In many cases known mechanism-based inhibitors, in turn frequently based on natural substrates, are used as a scaffold to which a reporter entity is attached for analysis of the target proteins. In this respect, nature often provides a source of inspiration. For example, the structure of the potent biotin-tagged proteasome ABP **7** was derived from the naturally occurring irreversible proteasome inhibitor epoxomicin by extension of the *N*-terminus of the peptide epoxyketone with a biotinylated linker (Figure 1.5).[27,28] The proteasome contains three catalytically active β-subunits that have different substrate preferences but each employ an *N*-terminal threonine residue as the active site nucleophile, a distinctive feature that is only found in a few other proteases. This particular aspect of the proteasome's catalytic mechanism is exploited by the inhibitor to achieve selective targeting of this enzyme. The binding mechanism involves reaction of both the hydroxyl group and the primary amine of a catalytic threonine residue with the ketone and the epoxide of the inhibitor warhead, respectively, to form a stable morpholine ring (Figure 1.6A).[29]

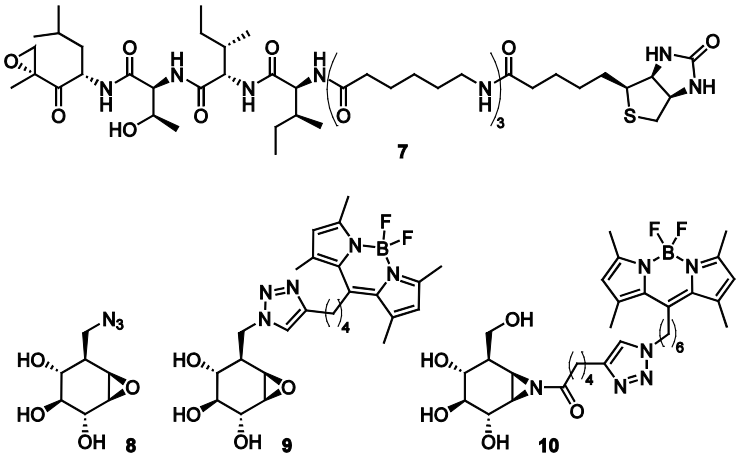

Figure 1.5. Structures of biotinylated epoxomicin-derived proteasome probe **7**, azide-tagged (**8**) and fluorescently labeled (**9**) cyclophellitol derivatives that target retaining β-glucosidases and fluorescently labeled aziridine-based retaining β-glucosidase probe **10**.

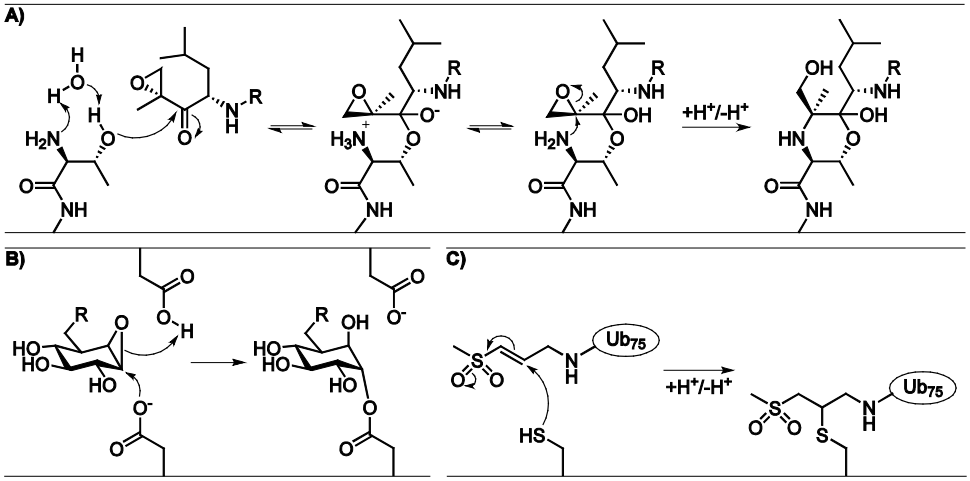

Figure 1.6. Binding mechanisms of various classes of ABPs. Inhibition of the proteasome by epoxomicin derivatives (A), retaining β-glucosidases by cyclophellitol analogues (B) and deubiquitinating enzymes by ubiquitin-vinyl sulfone (C). Ub_{75}: Ubiquitin lacking its *C*-terminal glycine residue.

Another example of ABP development guided by a mechanism-based inhibitor is based on the retaining β-glucosidase inhibitor cyclophellitol, which is itself a remarkable example of rational design coinciding with the isolation of the natural product.[30-32] This mechanism-based inhibitor has served as a basis for the synthesis of direct and two-step ABPs (**8** and **9**, Figure 1.5) that selectively label the human enzyme glucocerebrosidase in cell extracts and cultured cells.[33] Interestingly, the introduction of the hydrophobic fluorescent tag in probe **9** proved to strongly enhance its affinity as compared to the parent compound cyclophellitol. Irreversible binding of these probes is thought to occur by attack of the nucleophilic glutamic acid residue in the active site of retaining β-glucosidases on the epoxide moiety of the ABPs (Figure 1.6B).[34] A second glutamic acid residue, which is essential for substrate hydrolysis by acting as a general acid/base, was shown to be also requisite for binding of the epoxide probes.[33] In a later study, an aziridine-based ABP (**10**) was revealed to inhibit retaining β-glucosidases with enhanced potency and enabled *in vivo* profiling of enzymatic activity.[35] However, labeling also occurred in the absence of the general acid/base residue in the active site, presumably due to the high reactivity of the aziridine moiety. As a result the probe is capable of labeling enzymes that lack catalytic activity on their natural substrate and therefore it may be considered not to be a 'true' ABP.

The biotinylated peptide epoxysuccinate DCG-04 (**1**, Figure 1.2) represents a further example of an ABP that is derived from a natural product, the irreversible cysteine protease inhibitor E-64.[36] The structure of this inhibitor, which contains the thiol-reactive

epoxysuccinate warhead, was modified by elaboration of the peptide portion to allow incorporation of an affinity tag.[18]

Besides inhibitor-inspired probe design, the structure of a substrate and its binding mechanism to the protein of interest can also serve directly as a basis for novel ABPs. This strategy was illustrated by the synthesis of ABPs based on the small (76 amino acids) protein ubiquitin to target deubiquitinating enzymes, a class of cysteine proteases that recognize a range of substrates modified with one or more ubiquitin units which are linked via their *C*-terminus to a lysine residue of another ubiquitin or to the protein substrate. The substitution of the *C*-terminal glycine residue of recombinant ubiquitin with a vinyl sulfone warhead and subsequent radioiodination led to an ABP that labels a number of deubiquitinating enzymes in cell extracts (Figure 1.6C).[37] In later studies, other thiol-reactive electrophiles were attached to epitope-tagged ubiquitin to modify the reactivity of the probes towards specific deubiquitinating and ubiquitin-conjugating enzymes.[38,39] These probes also exemplify the uncommon use of protein-derived ABPs rather than small molecule chemical probes, with a major drawback being that their large size excludes *in situ* and *in vivo* applications.

The fine balance between reactivity and selectivity of an ABP is essential to achieve specific labeling of a desired protein or set of proteins. The rational design of a warhead, in particular its reactivity, can be an important factor to modify the range of enzymes that is targeted by an ABP. This aspect of ABP design is clearly illustrated by the development of probes **11**-**13** (Figure 1.7), which all contain an α-halogenated methylketone as the warhead.[40-42] Iodide is a good leaving group and the iodomethylketone is an excellent electrophile for S_N2 reactions with soft nucleophiles such as thiolates, while being stable towards nucleophilic attack by hard nucleophiles such as water. As a result, iodoacetamide has a high intrinsic reactivity towards cysteine residues, so that tagged derivatives such as biotinylated probe **11**[40] and two-step probe **12**[41] are capable of labeling virtually all cysteine residues within a biological sample. Consequently these reagents are not applicable as ABPs but they are generally used for the global profiling of protein expression by mass spectrometry analysis. The incorporation of a 'light' (hydrogen) or 'heavy' (deuterium) isotope-labeled linker into the ABP (**11**) or, in case of probe **12**, into the ligation reagent enables the relative quantification and parallel identification of individual proteins from two complex biological samples. In addition to these global labeling experiments, probe **12** was used to demonstrate how selectivity can be realized without lowering the reactivity of the probe.[41] Highly reactive cysteine residues, which likely include catalytic residues and for example sites of post-translational modification, were discriminated from cysteine residues

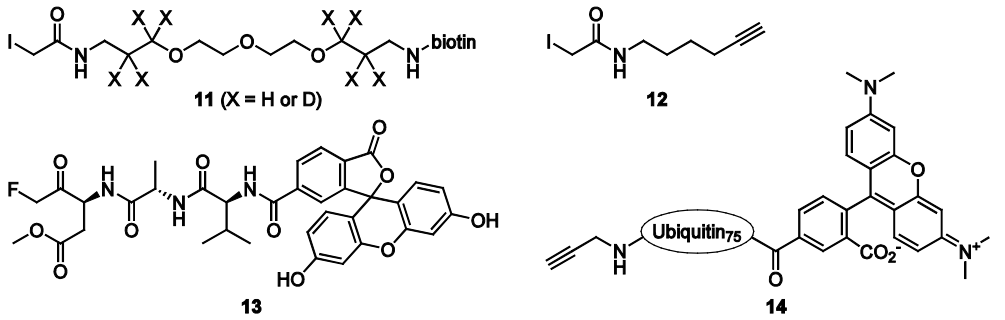

Figure 1.7. Structures of biotinylated (**11**) and alkyne-functionalized (**12**) iodoacetamide reagents and fluorescently labeled ABPs that target caspases (**13**) and deubiquitinating enzymes (**14**).

with low reactivity by using varying concentrations of the iodoacetamide reagent. While the cysteine residues with low reactivity are labeled in a concentration-dependent manner, labeling of the most reactive cysteine residues is equally efficient when a substoichiometric amount or an excess of the reagent is used. This strategy enables the annotation of highly reactive cysteines regardless of their natural abundance and can be used to identify new residues with putative catalytic activity.

In contrast to the iodoacetamide reagents, fluoromethylketone inhibitors and their derivatives, such as the fluorescein-functionalized ABP **13** (Figure 1.7),[42] have a very low intrinsic reactivity towards cysteine residues because the fluoride is a very poor leaving group and the carbon-fluorine bond is much more stable than the carbon-iodine bond. In this case, selective activity-based labeling of a specific class of cysteine proteases, the caspases, was achieved by incorporation of a peptide into the ABP that specifically binds these enzymes and thereby brings the warhead in close proximity to the active site cysteine residue so that a reaction takes place.

Another example of the use of a warhead which is essentially a very poor electrophile is the terminal alkyne in ABP **14**, which was shown to label deubiquitinating enzymes in an activity-based manner.[43] While the alkyne moiety is generally considered to be unreactive towards nucleophiles and therefore frequently used for bioorthogonal ligation reactions, attachment to a specific and tightly binding substrate of deubiquitinating enzymes was demonstrated to induce attack of the catalytically active cysteine residue on the alkyne warhead. The same strategy was also applied to label caspase activity.[43] Small molecule cysteine protease inhibitors that were derivatized with an alkyne warhead showed no considerable inhibitory potential, presumably due to their low affinity for these enzymes. In

contrast, the functionalization of larger peptide fragments of a natural caspase-1 substrate with an alkyne warhead yielded selective caspase-1 ABPs.

1.4 Aim and outline of this thesis

Most of the ABPs that have been developed to date target hydrolytic enzymes, in particular proteases and esterases, that employ an amino acid residue (serine, threonine, cysteine) as the active site nucleophile. Novel ABPP strategies are increasingly more directed towards the development of ABPs that target other enzyme families, often with different catalytic mechanisms or low expression levels. At the same time the targeting of enzyme activities with tight substrate specificity and the interest in *in vivo* applications of ABPP necessitates the use of ABPs that are modified with a small ligation handle instead of a reporter group. Relatively few bioorthogonal ligation methods, however, have been applied to the two-step profiling of enzymatic activity. The first part of this thesis therefore aims to develop new bioorthogonal ligation methods for use in ABPP. In addition, the complexity of biological processes and the involvement of many proteins and other biomolecules in cellular processes and disease development often requires the study of multiple targets simultaneously, and therefore attention is also focused on tandem labeling strategies in which multiple ligation reactions are performed concurrently in a single experiment.

Chapter 2 gives an overview of the various bioorthogonal ligation methods that have been described in literature, with an emphasis on the application of bioorthogonal chemistry in ABPP. Frequently used ligation reactions include copper(I)-catalyzed as well as strain-promoted [2+3] cycloadditions of an azide with an alkyne, Staudinger-Bertozzi ligation of an azide with a phosphine, Diels-Alder reactions between electron-rich dienes and an electron-deficient dienophiles and inverse-electron-demand Diels-Alder reactions of tetrazine with strained alkenes (Figure 1.8).[21]

While many examples exist of the use of azides and alkynes as ligation handles in two-step ABPs (Figures 1.8A and 1.8B, respectively),[1,44] Diels-Alder [4+2] cycloadditions have not yet been applied to ABPP. The selectivity of these reactions together with the generally small size of the reagents renders Diels-Alder ligations promising new strategies for two-step ABPP. **Chapter 3** describes the development of a Diels-Alder based approach (Figure 1.8C) for the labeling of endogenous enzymatic activity. Four different diene-conjugated proteasome ABPs are applied to the labeling of proteasome activity in cell extracts by reaction with a fluorescently labeled maleimide as a dienophile. The application of the Diels-Alder ligation to the labeling of another class of enzymes, cysteine proteases of the cathepsin family, is also demonstrated. Furthermore, a combined ligation strategy is

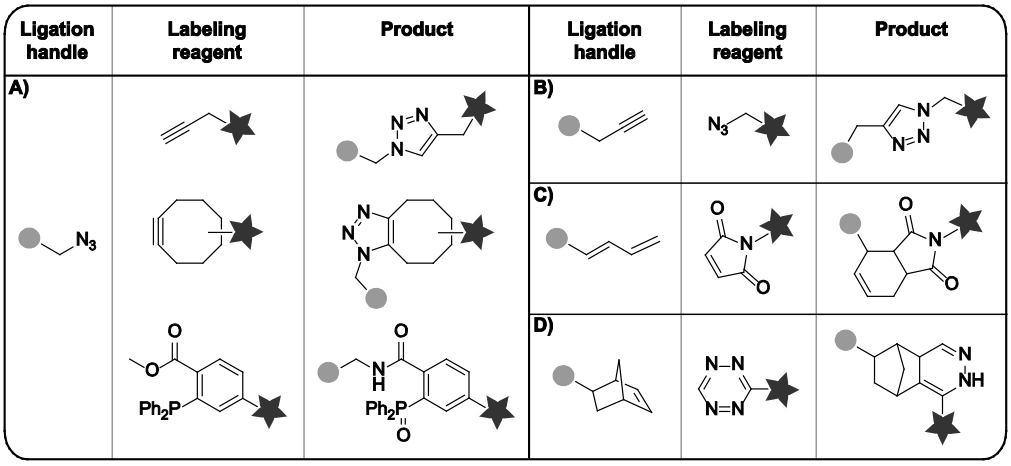

Figure 1.8. Reagents for commonly used bioorthogonal ligation reactions.

presented in which the Diels-Alder ligation is used together with the Staudinger-Bertozzi ligation for the labeling of multiple enzymatic activities in the same sample.

The inherent reactivity of maleimide towards cysteine residues poses severe limitations on its use in bioorthogonal labeling experiments. In order to improve the selectivity of the ligation reaction, an alternative two-step ABPP strategy that is based on the inverse-electron-demand Diels-Alder reaction of tetrazine with norbornene (Figure 1.8D) is investigated in **Chapter 4**. Labeling of proteasome activity is accomplished by using a norbornene-functionalized proteasome ABP and a fluorescently labeled or biotin-tagged tetrazine reagent. This approach enables the selective labeling of active proteasome β-subunits *in vitro* and *in situ*. Moreover, a triple ligation strategy involving tetrazine ligation, Staudinger-Bertozzi ligation and copper(I)-catalyzed click reaction is developed for the simultaneous labeling of three different proteolytic activities in a single experiment.

An enzyme class that has remained somewhat resistant to ABPP is that of the glycosidases, though at least a number of glycosidases employ a mechanism involving a covalent enzyme-substrate intermediate and are thus possible candidates for ABP development. The first ABPs for this class of enzymes were based on 2-deoxy-2-fluoroglycosides, substrate mimics in which the hydroxyl group next to the anomeric center has been substituted with a fluorine.[45] A drawback of these inhibitors, though well suited for structural studies on transition states, is that they bind in a reversible manner. Nonetheless it was shown that the covalent intermediate formed between a number of these ABPs and their respective target enzymes is sufficiently stable to enable visualization of the labeled

proteins on gel.[45,46] In a later study another type of glycosidase ABPs was developed based on the irreversible retaining β-glucosidase inhibitor cyclophellitol (see Figure 1.5).[33,35] In a comparative study the cyclophellitol derivatives proved to be superior to 2-deoxy-2-fluoroglucosides in terms of potency and labeling efficiency on two retaining β-glucosidases.[46] The second part of this thesis describes the development of differently configured isomers of the cyclophellitol-based ABPs for the labeling of two mechanistically related glycosidases, retaining α- and β-galactosidases, for which at present no covalent and irreversible probes have been reported in literature.

Chapter 5 details the synthesis of galactopyranose-configured probes that contain an electrophilic aziridine or epoxide moiety in either an α- or a β-configuration[47] with the aim to achieve activity-based profiling of retaining α- and β-galactosidases, respectively (Figure 1.9). Both direct ABPs functionalized with a fluorescent Bodipy tag or a biotin tag are synthesized as well as probes that are derivatized with an azide for two-step labeling experiments. The biological evaluation of these probes is presented in the following two chapters. In **Chapter 6** the inhibitory potency of the α-configured epoxide- and aziridine-based probes (**15** and **16**, Figure 1.9) is evaluated on the recombinant human enzyme α-galactosidase A. The most potent compounds, the aziridines ABPs, are then used to visualize the active enzyme on gel. In addition, it is demonstrated that the fluorescently labeled aziridine ABP enables the labeling of endogenous retaining α-galactosidase activity in cell extracts. **Chapter 7** describes the evaluation of the β-configured epoxide-based probes (**17**, Figure 1.9) for their ability to inhibit and label the recombinant enzyme galactocerebrosidase, a human retaining β-galactosidase. Furthermore, it is revealed that the small structural difference between the β-galactopyranose probe scaffold developed in this thesis and the previously reported β-glucopyranose-configured isomers (e.g. ABPs **8** and **9**, Figure 1.5), namely only the stereochemistry of a single hydroxy substituent, has resulted in a dramatic change in selectivity. Consequently, the two differently configured ABPs allow the selective labeling of retaining β-galactosidases and retaining β-glucosidases, respectively, without any observed cross-reactivity.

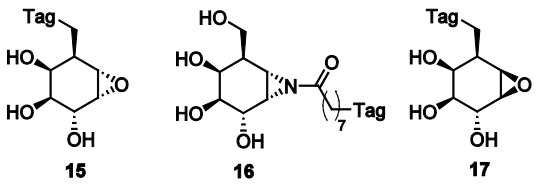

Figure 1.9. Structures of galactopyranose-configured ABPs for retaining α- and β-galactosidases.

References

1. Cravatt, B. F.; Wright, A. T.; Kozarich, J. W. *Annu. Rev. Biochem.* **2008**, *77*, 383.
2. Fonovic, M.; Bogyo, M. *Expert Rev. Proteomics* **2008**, *5*, 721.
3. Schmidinger, H.; Hermetter, A.; Birner-Gruenberger, R. *Amino Acids* **2006**, *30*, 333.
4. Nomura, D. K.; Dix, M. M.; Cravatt, B. F. *Nat. Rev. Cancer* **2010**, *10*, 630.
5. Krysiak, J.; Breinbauer, R. *Top. Curr. Chem.* **2012**, *324*, 43.
6. Heal, W. P.; Dang, T. H. T.; Tate, E. W. *Chem. Soc. Rev.* **2011**, *40*, 246.
7. Cygler, M.; Sivaraman, J.; Grochulski, P.; Coulombe, R.; Storer, A. C.; Mort, J. S. *Structure* **1996**, *4*, 405.
8. Coulombe, R.; Grochulski, P.; Sivaraman, J.; Ménard, R.; Mort, J. S.; Cygler, M. *EMBO J.* **1996**, *15*, 5492.
9. Blum, G.; Von Degenfeld, G.; Merchant, M. J.; Blau, H. M.; Bogyo, M. *Nat. Chem. Biol.* **2007**, *3*, 668.
10. Geurink, P. P.; Florea, B. I.; Li, N.; Witte, M. D.; Verasdonck, J.; Kuo, C.-L.; van der Marel, G. A.; Overkleeft, H. S. *Angew. Chem. Int. Ed.* **2010**, *49*, 6802.
11. Speers A. E.; Cravatt, B. F. *J. Am. Chem. Soc*. **2005**, *127*, 10018.
12. Verhelst, S. H. L.; Fonovic, M.; Bogyo, M. *Angew. Chem. Int. Ed.* **2007**, *46*, 1284.
13. Dirksen, A.; Yegneswaran, S.; Dawson, P. E. *Angew. Chem. Int. Ed.* **2010**, *49*, 2023.
14. Yang, Y.; Hahne, H.; Kuster, B.; Verhelst, S. H. L. *Mol. Cell. Proteomics* **2013**, *12*, 237.
15. Gartner, C. A.; Elias, J. E.; Bakalarski, C. E.; Gygi, S. P. *J. Proteome Res.* **2007**, *6*, 1482.
16. Hillaert, U.; Verdoes, M.; Florea, B. I.; Saragliadis, A.; Habets, K. L.; Kuiper, J.; van Calenbergh, S.; Ossendorp, F.; van der Marel, G. A.; Driessen, C.; Overkleeft, H. S. *Angew. Chem. Int. Ed.* **2009**, *48*, 1629.
17. Edgington, L. E.; Berger, A. B.; Blum, G.; Albrow, V. E.; Paulick, M. G.; Lineberry N.; Bogyo, M. *Nat. Med.* **2009**, *15*, 967.
18. Greenbaum, D.; Medzihradszky, K. F.; Burlingame, A.; Bogyo, M. *Chem. Biol.* **2000**, *7*, 569.
19. Matsumoto, K.; Mizoue, K.; Kitamura, K.; Tse, W.-C.; Huber, C. P.; Ishida, T. *Biopolymers* **1999**, *51*, 99.
20. Kwan, D. H.; Chen, H.-M.; Ratananikom, K.; Hancock, S. M.; Watanabe, Y.; Kongsaeree, P. T.; Samuels, A. L.; Withers, S. G. *Angew. Chem. Int. Ed.* **2011**, *50*, 300.
21. For reviews see: a) Sletten, E. M.; Bertozzi, C. R. *Acc. Chem. Res.* **2011**, *44*, 666; b) Devaraj, N. K.; Weissleder, R. *Acc. Chem. Res.* **2011**, *44*, 816; c) Ngo, J. T.; Tirell, D. A. *Acc. Chem. Res.* **2011**, *44*, 677; d) Hao, Z.; Hong, S.; Chen, X.; Chen, P. R. *Acc. Chem. Res.* **2011**, *44*, 742; e) Heal, W. P.; Tate, E. W. *Org. Biomol. Chem.* **2010**, *8*, 731; f) Willems, L. I.; van der Linden, W. A.; Li, N.; Li, K.-Y.; Liu, N.; Hoogendoorn, S.; van der Marel, G. A.; Florea, B. I.; Overkleeft, H. S. *Acc. Chem. Res.* **2011**, *44*, 718; g) Ramil, C. P.; Lin, Q. *Chem. Commun.* **2013**, *49*, 11007; h) Lang, K.; Chin, J. W. *ACS Chem. Biol.* **2014**, *9*, 16.
22. Rostovtsev, V. V. ; Green, L. G.; Fokin, V. V.; Sharpless, K. B. *Angew. Chem. Int. Ed.* **2002**, *41*, 2596.
23. Wang, Q.; Chan, T. R.; Hilgraf, R.; Fokin, V. V.; Sharpless, K. B.; Finn, M. G. *J. Am. Chem. Soc.* **2003**, *125*, 3192.
24. Speers, A. E.; Adam, G. C.; Cravatt, B. F. *J. Am. Chem. Soc.* **2003**, *125*, 4686.
25. Saxon, E.; Bertozzi, C. R. *Science* **2000**, *287*, 2007.
26. Ovaa, H.; van Swieten, P. F.; Kessler, B. M.; Leeuwenburgh, M. A.; Fiebiger, E.; van den Nieuwendijk, A. M. C. H.; Galardy, P. J.; van der Marel, G. A.; Ploegh, H. L.; Overkleeft, H. S. *Angew. Chem. Int. Ed.* **2003**, *42*, 3626.
27. Hanada, M.; Sugawara, K.; Kaneta, K.; Toda, S.; Nishiyama, Y.; Tomita, K.; Yamamoto, H.; Konishi, M.; Oki, T. *J. Antibiot*. **1992**, *45*, 1746.
28. Sin, N.; Kim, K. B.; Elofsson, M.; Meng, L.; Auth, H.; Kwok, B. H. B.; Crews, C. M. *Bioorg. Med. Chem. Lett*. **1999**, *9*, 2283.
29. Groll, M.; Kim, K. B.; Kairies, N.; Huber, R.; Crews, C. M. *J. Am. Chem. Soc.* **2000**, *122*, 1237.
30. Caron, G.; Withers, S. G. *Biochem. Biophys. Res. Commun.* **1989**, *163*, 495.
31. Tatsuta, K.; Niwata, Y.; Umezawa, K.; Toshima, K.; Nakata, M. *Tetrahedron Lett.* **1990**, *31*, 1171.

32. Atsumi, S.; Umezawa, K.; Iinuma, H.; Naganawa, H.; Nakamura, H.; Iitaka, Y.; Takeuchi, T. *J. Antibiot.* **1990**, *43*, 49.
33. Witte, M. D.; Kallemeijn, W. W.; Aten, J.; Li, K.-Y.; Strijland, A.; Donker-Koopman, W. E.; van den Nieuwendijk, A. M. C. H.; Bleijlevens, B.; Kramer, G.; Florea, B. I.; Hooibrink, B.; Hollak, C. E. M.; Ottenhoff, R.; Boot, R. G.; van der Marel, G. A.; Overkleeft, H. S.; Aerts, J. M. F. G. *Nat. Chem. Biol.* **2010**, *6*, 907.
34. Gloster, T. M.; Madsen, R.; Davies, G. J. *Org. Biomol. Chem.* **2007**, *5*, 444.
35. Kallemeijn, W. W.; Li, K.-Y.; Witte, M. D.; Marques, A. R. A.; Aten, J.; Scheij, S.; Jiang, J.; Willems, L. I.; Voorn-Brouwer, T. M.; van Roomen, C. P. A. A.; Ottenhoff, R.; Boot, R. G.; van den Elst, H.; Walvoort, M. T. C.; Florea, B. I.; Codée, J. D. C.; van der Marel, G. A.; Aerts, J. M. F. G.; Overkleeft, H. S. *Angew. Chem. Int. Ed.* **2012**, *51*, 12529.
36. Barrett, A. J.; Kembhavi, A. A.; Brown, M. A.; Kirschke, H.; Knight, C. G.; Tamai. M.; Hanada, K. *Biochem. J.* **1982**, *201*, 189.
37. Borodovsky, A.; Kessler, B. M.; Casagrande, R.; Overkleeft, H. S.; Wilkinson, K. D.; Ploegh, H. L. *EMBO J.* **2001**, *20*, 5187.
38. Borodovsky, A.; Ovaa, H.; Kolli, N.; Gan-Erdene, T.; Wilkinson, K. D.; Ploegh, H. L.; Kessler, B. M. *Chem. Biol.* **2002**, *9*, 1149.
39. Love, K.; Pandya, R.; Spooner, E.; Ploegh, H. *ACS Chem. Biol.* **2009**, *4*, 275.
40. Gygi, S. P.; Rist, B.; Gerber, S. A.; Turecek, F.; Gelb, M. H.; Aebersold, R. *Nat. Biotechnol.* **1999**, *17*, 994.
41. Weerapana, E.; Wang, C.; Simon, G. M.; Richter, F.; Khare, S.; Dillon, M. B.; Bachovchin, D. A.; Mowen, K.; Baker, D.; Cravatt, B. F. *Nature* **2010**, *468*, 790.
42. Bedner, E.; Smolewski, P.; Amstad, P.; Darzynkiewicz, Z. *Exp. Cell Res.* **2000**, *259*, 308.
43. Ekkebus, R.; van Kasteren, S. I.; Kulathu, Y.; Scholten, A.; Berlin, I.; Geurink, P. P.; De Jong, A.; Goerdayal, S.; Neefjes, J.; Heck, A. J.; Komander, D.; Ovaa, H. *J. Am. Chem. Soc.* **2013**, *135*, 2867.
44. Martell, J.; Weerapana, E. *Molecules* **2014**, *19*, 1378.
45. Vocadlo, D. J.; Bertozzi, C. R. *Angew. Chem. Int. Ed.* **2004**, *43*, 5338.
46. Witte, M. D.; Walvoort, M. T. C.; Li, K.-Y; Kallemeijn, W. W.; Donker-Koopman, W. E.; Boot, R. G.; Aerts, J. M. F. G.; Codée, J. D. C.; van der Marel, G. A.; Overkleeft, H. S. *ChemBioChem* **2011,** *12*, 1263.
47. Throughout this thesis, the designation of the α-/β-stereochemistry of all galactopyranose-configured epoxides and aziridines is based on α-/β-galactopyranose nomenclature.

2

Bioorthogonal chemistry

2.1 Introduction

A bioorthogonal ligation is defined as a process in which two reactants that are added to a biological sample react with each other in a chemoselective manner. This implies that the reagents are non-toxic and inert to any other functionality present and that the chemistry does not interfere with the biological system at hand. Ideally, the reactants that participate in a bioorthogonal ligation reaction should react fast in aqueous environments, in a 1:1 ratio and in a quantitative yield with respect to each other. Furthermore, easy access to the required reagents and stability under physiological conditions are requisite for the successful use of bioorthogonal chemistry in a wide range of applications and in different fields of research. The biological samples in which bioorthogonal reactions are intended to take place increase in complexity ranging from a cell extract (tissue lysate), to a cell or tissue culture to an animal model, with each of these posing additional demands that may complicate the accomplishment of a selective chemical transformation. The actual complexity of a biological sample is also dependent on the type of experiment. Whereas labeling of a biomolecule in cell extracts has to occur in the presence of (nearly) all possible biomolecules, in a cell-surface labeling experiment only those molecules present at the outer cell membrane may interfere with the reaction. In contrast to many biological processes, in which the problem of selectivity is solved by catalysts that recognize intrinsically relatively inert functionalities and cause these to react in a highly controlled and

selective manner, bioorthogonal chemistry aims to develop reagent pairs that react without the assistance of a (biological) catalyst. The chemical reactants thus need to have a high intrinsic reactivity towards each other whereas at the same time they need to be inert towards any other biological functionality. Considering the required level of selectivity combined with the fact that a quantitative process of two isolated reactants in a stoichiometric ratio is not easily achieved, it is not surprising that to date a truly bioorthogonal reagent pair has not yet been developed. Nonetheless, significant progress is being made and gradually more ligation reactions have emerged that fulfill most of the criteria of bioorthogonality.

2.2 Bioorthogonal chemistry: scope and limitations

The concept of bioorthogonal chemistry was first introduced by the labeling of cell surface *N*-glycoproteins using a ketone-functionalized analogue of *N*-acetylmannosamine.[2] It was demonstrated that *N*-levulinoyl-mannosamine is a valid substrate of the sialic acid biosynthesis machinery of mammalian cells. When added to a cell culture it is converted into levulinoyl sialic acid and subsequently incorporated into *N*-glycoprotein chains to eventually end up on the cell surface. The ketone moiety of the levulinoyl groups can then be reacted with a tagged hydrazide in a bioorthogonal fashion (Figure 2.1A), as neither of the two reactants is present in naturally occurring cell surface biomolecules. In a subsequent study the same objective was achieved with much higher efficiency by making use of another ligation reaction, referred to as the Staudinger ligation or Staudinger-Bertozzi ligation (Figure 2.1B, top panel).[3] Metabolic incorporation of an azide-functionalized mannosamine derivative followed by reaction with a biotinylated phosphine enabled the selective labeling of cell surface *N*-glycoproteins that contained the azide-modified sialic acids. Azides and phosphines are both unreactive towards biological functionalities but react readily with each other in an aqueous environment. The phosphine reagents used for this ligation strategy are designed such that the aza-ylide intermediate is captured by intramolecular reaction with a methyl ester to form a stable amide bond between the two reagents. Whereas ketones are present in a number of endogenous molecules, azides have not yet been detected in eukaryotes, which together with their small size and general inertness towards biological functionalities renders them ideal reagents for bioorthogonal chemistry. Another bioorthogonal ligation dating from the same period as the Staudinger-Bertozzi ligation is the copper(I)-catalyzed Huisgen [2+3] cycloaddition of an azide with a terminal alkyne, a reactive group that is also non-perturbing to biological systems. This cycloaddition, termed ‘click’ reaction, has found many applications in synthetic organic chemistry, bioorganic chemistry

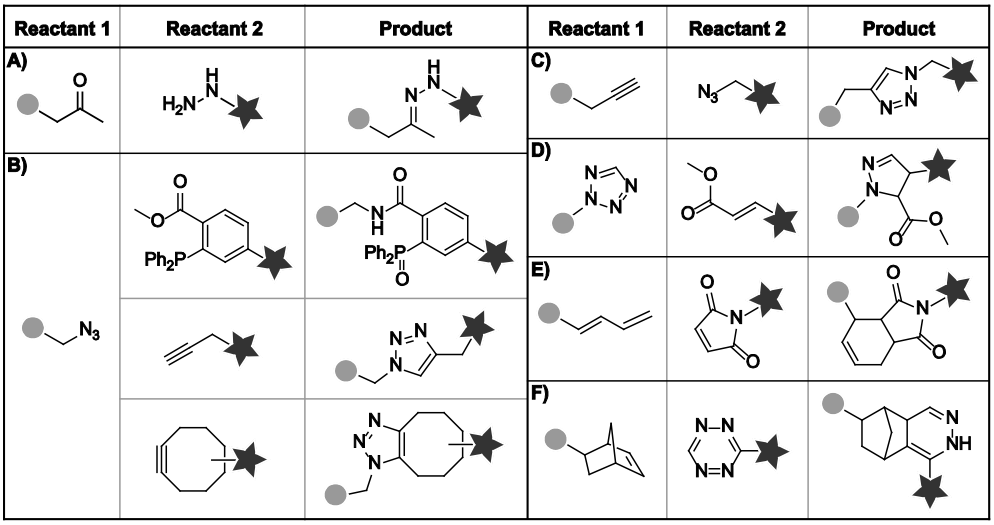

Figure 2.1. Schematic representations of commonly used bioorthogonal ligation reactions. A) Ketone-hydrazide condensation. B,C) Reactions using an azide as one of the reagents: copper(I)-catalyzed Huisgen [3+2] azide-alkyne cycloaddition, strain-promoted azide-alkyne cycloaddition and Staudinger-Bertozzi ligation of an azide with a phosphine. D) Light-induced reaction of tetrazole with an alkene. E) Diels-Alder [4+2] cycloaddition of a conjugated diene with a dienophile. F) Inverse-electron-demand Diels-Alder reaction of tetrazine with a strained alkene.

and, in particular, chemical biology.[4-8] As a bioorthogonal ligation strategy the click reaction requires the installation of either an azide or an alkyne in a biomolecule and subsequent reaction with the complementary reactant to which a reporter entity is attached (Figures 2.1B, middle panel and 2.1C). Click chemistry was first used as a bioorthogonal ligation method for the labeling of enzymatic activity in cell extracts using an azide-functionalized ABP and a fluorescently labeled alkyne.[8] The fact that this reaction is catalyzed by copper(I), which is toxic to cells and living organisms, precludes its use for *in situ* and *in vivo* labeling. Although this aspect makes the click reaction not strictly bioorthogonal, it is still one of the most widely used ligation reactions in chemical biology research due to the small size of the reagents and the selectivity and speed of the reaction, which proceeds considerably faster than the Staudinger-Bertozzi ligation.[9] In order to solve the issue of toxicity, a 'strain-promoted' click reaction has been developed that makes use of ring strain to drive the reaction and thereby eliminates the need for a copper catalyst.[10] A wide and rapidly growing number of substituted cyclooctynes has been reported to enable the labeling of biomolecules on the cell-surface and in living animals via strain-promoted cycloaddition with azides (Figure 2.1B, bottom panel).[10-21] In addition to the azide-alkyne cycloaddition several alternative 1,3-dipolar cycloadditions have also been used as bioorthogonal ligation

reactions, for example the reaction of cyclooctynes with other dipoles such as nitrones[22] and the light-induced cycloaddition of tetrazole and an alkene (Figure 2.1D), termed 'photoclick' chemistry, which occurs via the *in situ* formation of a nitrile imine.[23,24]

Of the various bioorthogonal reactions alternative to click chemistry and Staudinger-Bertozzi ligation, those based on Diels-Alder [4+2] cycloadditions are probably the most promising since they are generally very selective and efficient under mild, aqueous conditions. 'Standard' Diels-Alder chemistry involves the reaction of a conjugated electron-donating diene with an electron-deficient dienophile such as maleimide (Figure 2.1E). An inherent disadvantage of these Diels-Alder reactions is the propensity of the dienophile to undergo 1,4-conjugate addition, which necessitates the masking of free thiols in the biological sample at hand in order to prevent cross-reactivity and thereby essentially precludes *in situ* and *in vivo* applications.[25] This problem can be overcome by the use of inverse-electron-demand Diels-Alder cycloadditions in which tetrazine, an electron-deficient diene, is reacted with a strained alkene such as norbornene (Figure 2.1F). These reagents generally show no reactivity towards cysteine residues. The potential of the tetrazine ligation strategy was first demonstrated by the live cell imaging of cancer cells that were treated with norbornene-modified antibodies and subsequently labeled through reaction with a fluorescently labeled tetrazine.[26] In the following years, the selectivity and exceptionally fast kinetics of the tetrazine ligation have led to a rapidly growing number of *in situ* and *in vivo* applications.[27-33] The set of available reagents has been expanded with different dienophiles, most notably cyclopropene[27,28] and *trans*-cyclooctene,[29-35] as well as various substituted tetrazines that exhibit altered reactivity and/or stability.[36] A related ligation strategy that is based on the reaction of tetrazines with isonitriles has recently been applied to the imaging of cell surface glycans.[37] In another study it was demonstrated that the tetrazine moiety possesses an intrinsic property that may provide an additional advantage for imaging applications, namely its ability to quench specifically conjugated Bodipy fluorophores.[33] Cultured cells were treated with a *trans*-cyclooctene-modified taxol derivative and subsequently with Bodipy-functionalized tetrazine **1** (Figure 2.2) to visualize microtubule structures, the intracellular target of taxol. The Bodipy tag was revealed to be intrinsically only weakly fluorescent but turned brightly fluorescent upon reaction with the dienophile (**2**), which strongly reduces background fluorescence and eliminates the need to wash out the excess of reagents prior to fluorescence imaging. More recently, other tetrazine-fluorophore conjugates were described for which the 'turn-on' ratio of fluorescence intensity before and after reaction with a dienophile is much higher.[38]

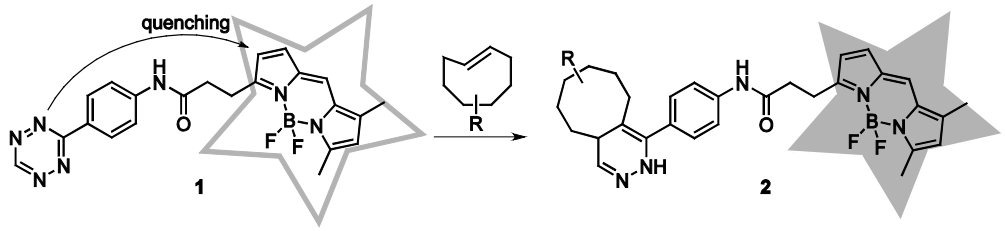

Figure 2.2. Quenched Bodipy-tetrazine (**1**) that becomes strongly fluorescent after reaction with a dienophile (**2**).

In synthetic organic chemistry the utility of chemical transformations is judged by their efficiency, so that at least the most elaborate or expensive reaction partner is transformed in (near) quantitative fashion, as well as their selectivity, so that unwanted side reactions are limited. Yield, the nature of (side) products and reaction kinetics are also parameters that should be considered when evaluating the merits of a bioorthogonal ligation. Whereas the kinetics of newly developed ligation reactions are frequently analyzed using isolated reagents, the efficiency of a particular ligation reaction is likely to be influenced by the nature of the biological sample, for example a cell extract or an intracellular environment, and the experimental conditions. A detailed study in which the copper(I)-catalyzed click reaction, strain-promoted click reaction and Staudinger-Bertozzi ligation were directly compared for the labeling of proteins in cell extracts and glycoproteins on live cell surfaces revealed that, as expected, the former reaction is superior in terms of efficiency but its use is restricted to *in vitro* experiments.[9] The strain-promoted azide-alkyne cycloaddition and Staudinger ligation performed similarly well, with the efficiency of the latter reaction depending on the specific structure of the azide.

The efficiency of bioorthogonal chemistry in the context of two-step profiling of enzymatic activity has been evaluated by making use of a trifunctional ABP (**3**, Figure 2.3A), which contains an electrophilic vinyl sulfone warhead to target the catalytically active subunits of the proteasome (β1, β2 and β5), a fluorescent Bodipy tag and also an azide as a ligation handle.[39] Using this probe, endogenous proteasome activity was fluorescently labeled in cell extracts and subsequently reacted with biotin-phosphine **4**. Visualization of the labeled proteins by SDS-PAGE revealed not only the fluorescent labeling of the three active proteasome subunits by ABP **3** but also a gel-shift of the fluorescent bands in those samples that were exposed to biotin-phosphine **4** (Figure 2.3B). This phenomenon is due to the increase in molecular weight of the labeled proteins (roughly 1 kDa) resulting from the reaction of the enzyme-bound ABP with the phosphine reagent. Hence, the efficiency of the ligation reaction can be determined from the ratio of fluorescence intensity between protein bands that are shifted, and thus represent proteins that are labeled via Staudinger-

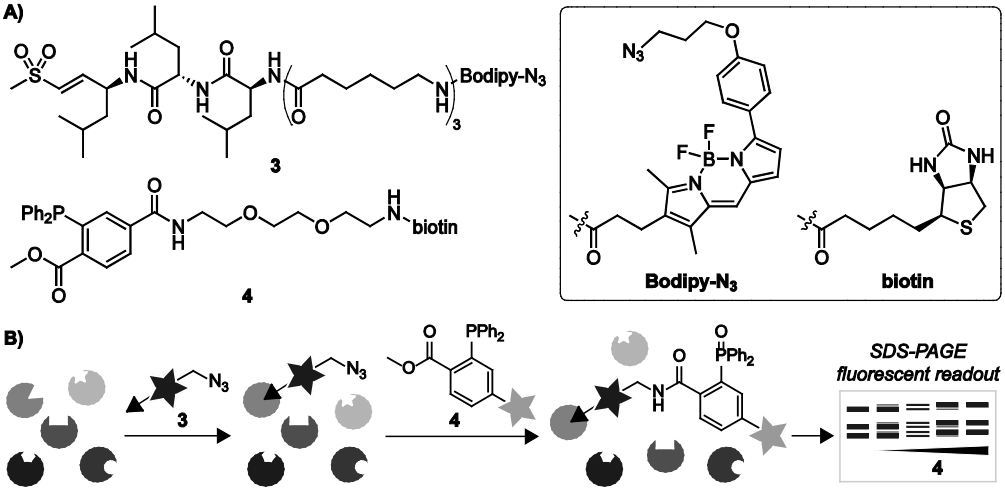

Figure 2.3. Staudinger-Bertozzi ligation in two-step labeling of proteasome activity. A) Structures of azide-functionalized fluorescent proteasome ABP **3** and biotin-phosphine **4**. B) Strategy to evaluate the efficiency of the Staudinger-Bertozzi ligation using ABP **3** and phosphine **4**. Ligation with the phosphine reagent results in a concentration-dependent gel-shift of the fluorescently labeled proteasome subunits. SDS-PAGE: sodium dodecyl sulfate polyacrylamide gel electrophoresis.

Bertozzi ligation, as compared to the corresponding lower-running bands. The ligation reaction was shown to reach completion, provided that a large excess of biotin-phosphine **4** was added relative to ABP **3**. The poor yield in terms of conversion of reagent **4** is most likely due to the inherent instability of the trivalent phosphine, which has been shown to be susceptible to aerobic and metabolic oxidation.[40]

A similar approach was used to directly compare the efficiency of the strain-promoted azide-cyclooctyne cycloaddition with the Staudinger-Bertozzi ligation in addressing azide-modified biomolecules in cell extracts. For this purpose, biotinylated cyclooctynes **6**,[18] **7**[21] and **8**[12] were applied to a two-step proteasome profiling assay using azide-functionalized and fluorescently labeled ABP **5** (Figure 2.4).[41] The results were compared to those obtained after Staudinger ligation with **4**, revealing that in these settings a quantitative transformation with respect to the azide is achieved with much lower concentrations of the cyclooctyne reagents than the phosphine. However, a shortcoming of all three strain-promoted click reagents is that they suffered from considerable cross-reactivity, resulting in the appearance of numerous background protein bands. This is in agreement with previously reported observations of non- specific labeling with dibenzocyclooctyne reagents in cell lysates.[42] The nature of the side products has been analyzed in detail, demonstrating

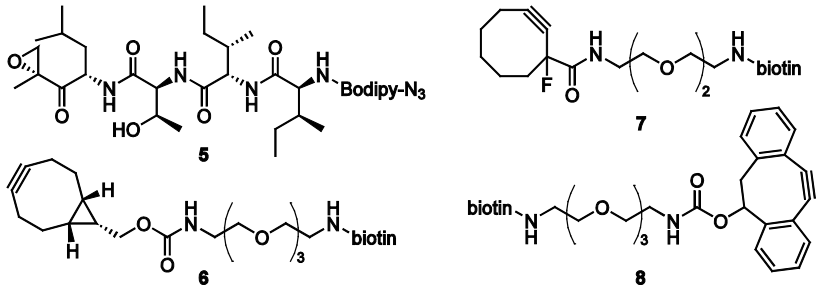

Figure 2.4. Reagents for two-step labeling of proteasome activity via strain-promoted click reaction. Structures of azide-functionalized fluorescent proteasome ABP **5** and biotin-functionalized cyclooctynes **6**-**8**.

that most of the azide-independent labeling by cyclooctynes occurs via thiol-yne addition with cysteine residues.[43] Consequently, while the use of functionalized cyclooctynes is an effective strategy for addressing cell surface azides, alkylation of free thiols appears to be requisite to limit background labeling when strain-promoted click chemistry is applied to complex biological samples such as cell extracts.

After the first reports describing the use of the tetrazine ligation as a bioorthogonal ligation strategy had appeared, its efficiency and selectivity have quickly led to an increasing use of this reaction for *in situ* and *in vivo* applications instead of azide-cyclooctyne cycloadditions and the Staudinger-Bertozzi ligation. At the same time the development of ligation handles other than azides and alkynes has opened up a means to explore another aspect of bioorthogonal chemistry, namely the simultaneous use of multiple bioorthogonal ligations to study several biomolecules at the same time. Whereas it has been shown that samples tagged with both azide and alkyne groups can be efficiently labeled by step-wise click ligation,[44,45] the cross-reactivity between the reagents precludes the simultaneous performance of both ligation reactions and also necessitates the use and efficient removal of large excesses of the reagents. The availability of reagents for bioorthogonal ligations that are orthogonal to azides enables the use of two or more individual ligation reactions at the same time. A first demonstration of a dual labeling strategy involved the simultaneous labeling of two different cell surface glycans by ketone-hydrazide ligation and Staudinger-Bertozzi ligation.[46] The use of ketones, however, restricts the application of this strategy to the labeling of molecules on the cell surface. In a later study it was shown that the Diels-Alder [4+2] cycloaddition and the Staudinger-Bertozzi ligation can be used in tandem to label different proteolytic activities in cell lysates (see Chapter 3), although the reactivity of the dienophile towards cysteine residues forms severe limitations to the application and practical use of this labeling method.[25]

The selectivity of the inverse-electron-demand Diels-Alder reaction has stimulated the development of improved tandem labeling strategies. In a first report it was revealed that the reaction between tetrazine and *trans*-cyclooctene can be used concurrently with the strain-promoted azide-cyclooctyne cycloaddition for the simultaneous labeling of two different cell surface receptors (Figure 2.5).[47] A co-culture of two cell lines was first treated with two different *trans*-cyclooctene- or dibenzocyclooctyne-modified antibodies and then labeled by reaction with azide- and tetrazine-functionalized fluorescent tags. A limitation of this strategy is that *trans*-cyclooctene reacts (albeit slowly) with azides and that some tetrazines display reactivity towards specific cyclooctynes,[47,48] so that the proper reagents need to be carefully selected in order to minimize cross-reactivity. Related dual labeling strategies were used for cell surface glycan imaging in which ligation with tetrazine was accomplished by making use of cyclopropene or terminal alkene ligation handles instead of *trans*-cyclooctene.[49-51] In addition, it has been demonstrated that properly substituted cyclopropenes enable orthogonal reactions with either tetrazines or nitrile imines[52] and that the reaction of tetrazine with isonitriles is orthogonal to the azide-dibenzocyclooctyne cycloaddition,[53] although in both cases no tandem bioorthogonal labeling experiments were performed. A triple ligation strategy that involves the copper(I)-catalyzed click reaction, the Staudinger-Bertozzi ligation and the inverse-electron-demand Diels-Alder reaction of tetrazine with norbornene was shown to enable the simultaneous labeling of three different enzymatic activities in cell extracts (Figure 2.6). Despite the fact that tetrazines revealed to be poorly compatible with click chemistry, the successive performance of these ligation reactions in the same sample proved to result in efficient and selective labeling of the intended target enzymes (see Chapter 4).[54]

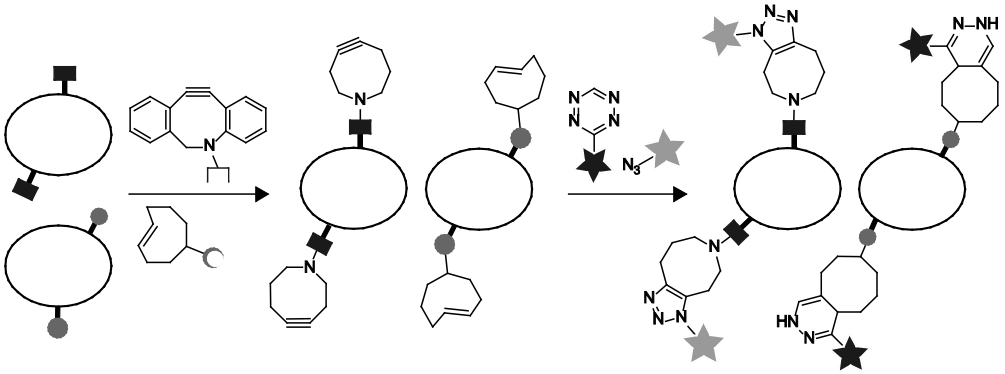
N
N
N

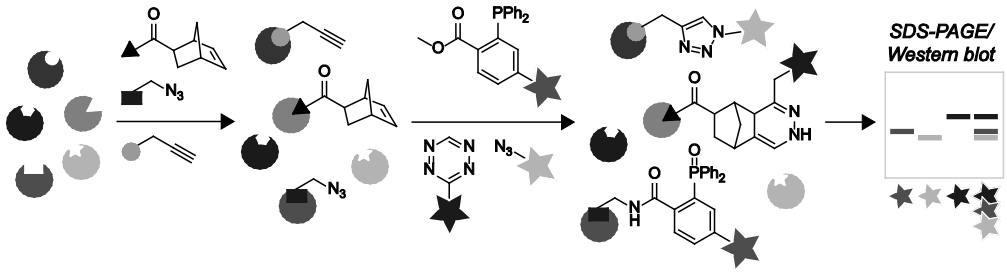

Figure 2.6. Schematic representation of a triple ligation strategy involving copper(I)-catalyzed click reaction, Staudinger-Bertozzi ligation and tetrazine ligation for simultaneous labeling of three enzymatic activities.

2.3 Bioorthogonal chemistry in ABPP

An area of research that has benefited greatly from the development of bioorthogonal chemistry is activity-based protein profiling (ABPP), which aims to obtain information on the activity of an enzyme (family) within the larger context of the full biological system. Bioorthogonal ligation reactions are essential for a specific type of ABPP studies that make use of two-step ABPs, which in contrast to directly labeled ABPs are modified with a small ligation handle instead of a reporter group. In this way the structural modifications to the ABP core, which is frequently derived from a small molecule inhibitor, are kept as small as possible in order to limit the disadvantageous consequences that can be associated with the direct attachment of a reporter group. Furthermore, the temporal separation of an ABP and a tag also provides the opportunity to select different tags depending on the desired method of analysis while using a single ABP. Most two-step ABPP strategies make use of either azide- or alkyne-functionalized ABPs that can be labeled via azide-alkyne cycloaddition or Staudinger-Bertozzi ligation. The first report describing the use of bioorthogonal chemistry for ABPP involved the two-step profiling of enzymatic activity via copper(I)-catalyzed click reaction between an azide-functionalized ABP and an alkyne-rhodamine tag.[55] At the same time another study was reported in which the Staudinger-Bertozzi-ligation was used to label enzymatic activity in cell extracts.[56] In this strategy, again an azide-modified ABP was used but two-step labeling was achieved by reaction with a biotinylated phosphine. The efficacy of the tetrazine-norbornene cycloaddition for the labeling of enzymatic activities in cell extracts and in cultured cells has also been demonstrated.[54] The relatively large size of the norbornene ligation handle may hinder its general application in activity-based profiling and in this respect the use of the much smaller cyclopropene tag forms an attractive alternative. Up till now, however, the tetrazine ligation has not yet found broad application in ABPP.

The value of two-step protein profiling can be illustrated by the development of a subunit-specific ABP for one of the proteasome active sites, β1. The two-step ABP **9** (Figure 2.7) was derived from a β1-subunit selective mechanism-based proteasome inhibitor by the installment of an azide and displayed selectivity similar to the parent compound.[57] In contrast, a direct ABP that was synthesized from the azide-functionalized probe by reaction with an alkyne-modified fluorescent tag (**10**) showed cross-reactivity towards other proteolytically active proteasome subunits, demonstrating that the installment of the fluorescent tag had resulted in a loss of selectivity.[58] An example of an enzyme class for which two-step labeling strategies appear to be indispensable is that of the exo-glycosidases, which typically have a sterically confined active site so that modification of a substrate (analogue) with a large tag is usually not tolerated. This limitation is likely responsible for the fact that few ABPs have been developed for this class of enzymes. The first ABPs that were reported to target exo-glycosidases are based on 2-deoxy-2-fluoroglycosides, mechanism-based retaining exo-glycosidase inhibitors,[59] in which the primary hydroxyl is substituted with an azide to enable two-step labeling of target enzymes. For instance, retaining β-galactosidase inhibitor **11** served as a basis for the development of the two-step ABP **12** (Figure 2.8).[60] Even though this small modification resulted in some loss of affinity, the probe retained sufficient affinity to enable labeling of target enzymes via Staudinger-Bertozzi ligation with a tagged phosphine reagent. In an alternative approach, ABPs for retaining β-glucosidases were designed by making use of the potent irreversible retaining β-glucosidase inhibitor cyclophellitol (**13**)[61,62] which contains an epoxide moiety with which it covalently binds its target enzymes. Substitution of the primary hydroxyl with an azide led to an equally potent two-step ABP (**14**).[63] This probe can be used to label recombinant retaining β-glucosidases via copper(I)-catalyzed azide-alkyne cycloaddition.[64] Suprisingly, however, a direct ABP that was derived from **14** by installment of a Bodipy fluorophore (**15**) proved to label the human enzyme glucocerebrosidase with much higher potency than the azide-functionalized ABP.[63] It was suggested that a hydrophobic pocket near the active site of the enzyme is responsible for tight binding of the hydrophobic fluorescent tag, thereby enhancing the affinity of the probe.

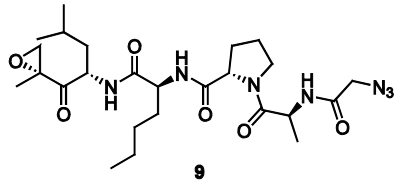

9

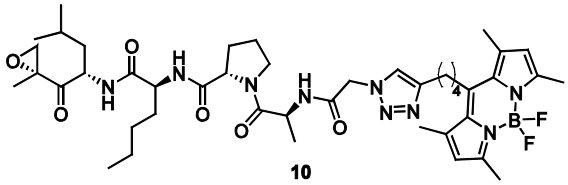

10

Figure 2.7. Structures of azide-functionalized β1-subunit selective proteasome ABP **9** and fluorescent derivative **10**.

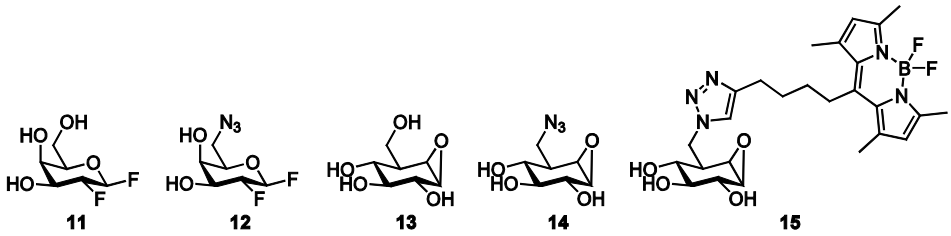

Figure 2.8. Structures of retaining β-galactosidase inhibitor **11** and azide-functionalized analogue **12**, retaining β-glucosidase inhibitor cyclophellitol (**13**) and derivatives functionalized with an azide (**14**) or Bodipy fluorophore (**15**).

2.4 Cleavable linkers in ABPP

A conceptually different application of selective organic chemistry in chemical biology research involves the use of cleavable linker systems that allow mild cleavage under conditions orthogonal to functionalities present in the biological system at hand. A major application of these linkers in ABPP is their use in the purification of enzymes that are tagged by either direct or two-step labeling with a biotin tag. Affinity tags are regularly used for the enrichment of target proteins, for instance by pull-down with streptavidin-coated beads, to facilitate subsequent analysis. This approach often requires the release of captured proteins from the beads, which generally involves harsh conditions due to the strong affinity of streptavidin for biotin. Another drawback is that the purified samples may be contaminated with endogenously biotinylated proteins, non-specifically bound proteins and (denatured) streptavidin. To solve these issues, several cleavable linker systems have been designed that can be incorporated in an ABP or in a reagent for bioorthogonal ligation and that can be cleaved in a chemoselective manner after affinity pull-down in order to selectively release the target proteins. Examples include redox-cleavable linkers based on a disulfide (**16**)[65,66] or a diazobenzene (**17**)[67] moiety, bisaryl hydrazones (**18**)[68] which are cleaved by transimination, and photocleavable linkers such as **19** (Figure 2.9A).[69] Protecting groups used in organic synthesis have also served as a basis for the design of cleavable linkers, for instance acid-cleavable linker **20**[70] and levulinoyl derivative **21**.[71] The latter moiety can be cleaved by the addition of hydrazine, which results in imine formation and intramolecular cyclization with concomitant cleavage of the ester bond (Figure 2.9B). Alternatively, enzymatic hydrolysis can be used to achieve the selective release of target proteins, as exemplified by linker **22** (Figure 2.9A) which contains a peptide sequence that is specifically cleaved by TEV proteases.[72] Recently, a linker containing a vicinal diol was developed for the enrichment of proteins and subsequent release via oxidative cleavage (**23**).[73]

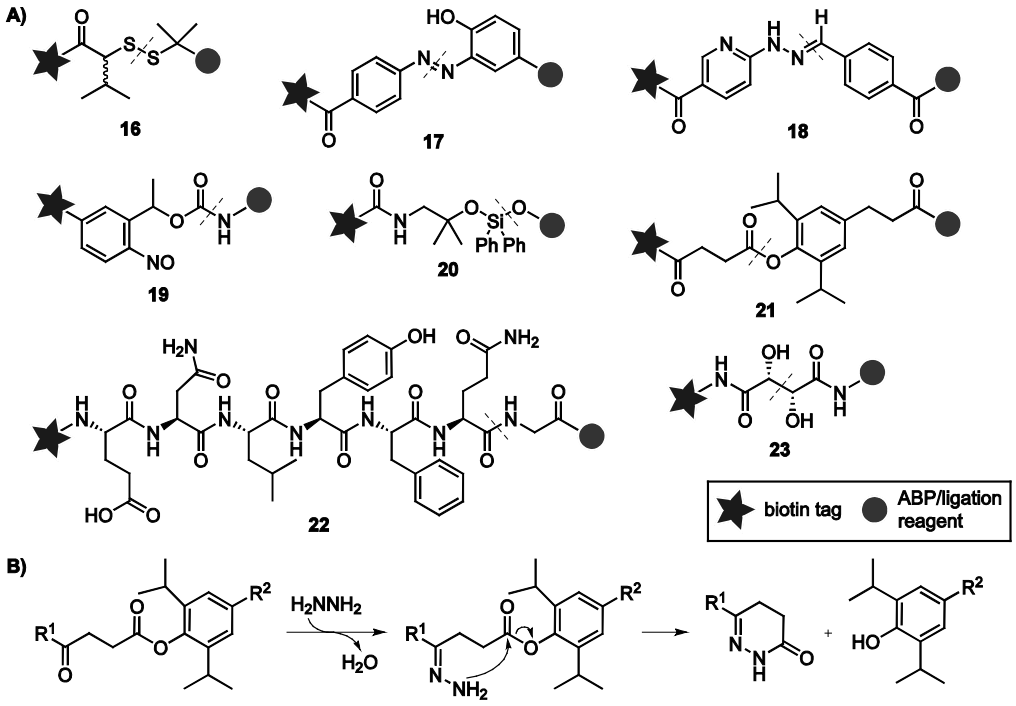

Figure 2.9. A) Structures of commonly used cleavable linker systems for the enrichment of proteins from biological samples. Cleavage sites are indicated by dashed lines. B) Mechanism of hydrazine-mediated cleavage of levulinoyl-based linker **21**.

References

1. Part of this chapter has been published in: Willems, L. I.; Van der Linden, W. A.; Li, N.; Li, K.-Y.; Liu, N.; Hoogendoorn, S.; van der Marel, G. A.; Florea, B. I.; Overkleeft, H. S. *Acc. Chem. Res.* **2011**, *44*, 718.
2. Mahal, L. K.; Yarema, K. J.; Bertozzi, C. R. *Science* **1997**, *276*, 1125.
3. Saxon, E.; Bertozzi, C. R. *Science* **2000**, *287*, 2007.
4. Huisgen, R. *1,3-Dipolar Cycloaddition Chemistry*; Padwa, A., Ed.; Wiley-Interscience: New York **1984**; Chapter 1, pp 1–176.
5. Tornøe, C. W.; Christensen, C.; Meldal, M. *J. Org. Chem.* **2002**, *67*, 3057.
6. Rostovtsev, V. V. ; Green, L. G.; Fokin, V. V.; Sharpless, K. B. *Angew. Chem. Int. Ed.* **2002**, *41*, 2596.
7. Wang, Q.; Chan, T. R.; Hilgraf, R.; Fokin, V. V.; Sharpless, K. B.; Finn, M. G. *J. Am. Chem. Soc.* **2003**, *125*, 3192.
8. Speers, A. E.; Adam, G. C.; Cravatt, B. F. *J. Am. Chem. Soc.* **2003**, *125*, 4686.
9. Agard, N. J.; Baskin, J. M.; Prescher, J. A.; Lo, A.; Bertozzi, C. R. *ACS Chem. Biol.* **2006**, *1*, 644.
10. Agard, N. J.; Prescher, J. A.; Bertozzi, C. R. *J. Am. Chem. Soc.* **2004**, *126*, 15046.
11. Baskin, J. M.; Prescher, J. A.; Laughlin, S. T.; Agard, N. J.; Chang, P. V.; Miller, I. A.; Lo, A.; Codelli, J. A.; Bertozzi, C. R. *Proc. Natl. Acad. Sci. USA* **2007**, *104*, 16793.
12. Ning, X.; Guo, J.; Wolfert, M. A.; Boons, G. J. *Angew. Chem. Int. Ed.* **2008**, *47*, 2253.
13. Sletten, E. M.; Bertozzi, C. R. *Org. Lett.* **2008**, *10*, 3097.

14. Jewett, J. C.; Sletten, E. M.; Bertozzi, C. R. *J. Am. Chem. Soc.* **2010**, *132*, 3688.
15. Chang, P. V.; Prescher, J. A.; Sletten, E. M.; Baskin, J. M.; Miller, I. A.; Agard, N. J.; Lo, A.; Bertozzi, C. R. *Proc. Natl. Acad. Sci. USA* **2010**, *107*, 1821.
16. Debets, M. F.; van Berkel, S. S.; Schoffelen, S.; Rutjes, F. P. J. T.; van Hest, J. C. M.; van Delft, F. L. *Chem. Commun.* **2010**, *46*, 97.
17. Kuzmin, A.; Poloukhtine, A.; Wolfert, M. A.; Popik, V. V. *Bioconjugate Chem.* **2010**, *21*, 2076.
18. Dommerholt, J.; Schmidt, S.; Temming, R.; Hendriks, L. J. A.; Rutjes, F. P. J. T.; van Hest, J. C. M.; Lefeber, D. J.; Friedl, P.; van Delft, F. L. *Angew. Chem, Int. Ed.* **2010**, *49*, 9422.
19. van den Bosch, S. M.; Rossin, R.; Renart Verkerk, P.; Ten Hoeve, W.; Janssen, H. M.; Lub, J.; Robillard, M. S. *Nucl. Med. Biol.* **2013**, *40*, 415.
20. Debets, M. F.; van der Doelen, C. W. J.; Rutjes, F. P. J. T.; van Delft, F. L. *ChemBioChem* **2010**, *11,* 1168.
21. Schultz, M. K.; Parameswarappa, S. G.; Pigge, F. C. *Org. Lett.* **2010**, *12*, 2398.
22. McKay, C. S.; Blake, J. A.; Cheng, J.; Danielson, D. C.; Pezacki, J. P. *Chem. Commun.* **2011**, *47*, 10040.
23. Song, W.; Wang, Y.; Qu, J.; Madden, M. M.; Lin, Q. *Angew. Chem. Int. Ed.* **2008**, *47*, 2832.
24. Song, W.; Wang, Y.; Qu, J.; Lin, Q. *J. Am. Chem. Soc.* **2008**, *130*, 9654.
25. Willems, L. I.; Verdoes, M.; Florea, B. I.; van der Marel, G. A.; Overkleeft, H. S. *ChemBioChem* **2010**, *11*, 1769.
26. Devaray, N. K.; Weissleder, R.; Hilderbrand, S. A. *Bioconjug. Chem.* **2008**, *19*, 2297.
27. Yang, J.; Seckute, J.; Cole, C. M.; Devaraj, N. K. *Angew. Chem. Int. Ed.* **2012**, *51*, 7476.
28. Patterson, D. M.; Nazarova, L. A.; Xie, B.; Kamber, D. N.; Prescher, J. A. *J. Am. Chem. Soc.* **2012**, *134*, 18638.
29. Devaray, N. K.; Upadhyay, R.; Haun, J. B.; Hilderbrand, S. A.; Weissleder, R. *Angew. Chem. Int. Ed.* **2009**, *48*, 7013.
30. Rossin, R.; Renart Verkerk, P.; van den Bosch, S. M.; Vulders, R. C. M.; Verel, I.; Lub, J.; Robillard, M. S. *Angew. Chem. Int. Ed.* **2010**, *49*, 3375.
31. Rossin, R.; van den Bosch, S. M.; Ten Hoeve, W.; Carvelli, M.; Versteegen, R. M.; Lub, J.; Robillard, M. S. *Bioconjugate Chem.* **2013**, *24*, 1210.
32. Neves, A. A.; Stöckmann, H.; Wainman, Y. A.; Kuo, J. C.-H.; Fawcett, S.; Leeper, F. J.; Brindle, K. M. *Bioconjugate Chem.* **2013**, *24*, 934.
33. Devaray, N. K.; Hilderbrand, S.; Upadhyay, R.; Mazitschek, R.; Weissleder, R. *Angew. Chem. Int. Ed.* **2010**, *49*, 2869.
34. Blackman, M. L.; Royzen, M.; Fox, J. M. *J. A. Chem. Soc.* **2008**, *130*, 13518.
35. Taylor, M. T.; Blackman, M. L.; Dmitrenko, O.; Fox, J. M. *J. Am. Chem. Soc.* **2011**, *133*, 9646.
36. Karver, M. R.; Weissleder, R.; Hilderbrand, S. A. *Bioconjugate Chem.* **2011**, *22*, 2263.
37. Stairs, S.; Neves, A. A.; Stöckmann, H.; Wainman, Y. A.; Ireland-Zecchini, H.; Brindle, K. M.; Leeper, F. J. *ChemBioChem* **2013**, *14*, 1063.
38. Carlson, J. C. T.; Meimetis, L. G.; Hilderbrand, S. C.; Weissleder, R. *Angew. Chem. Int. Ed.* **2013**, *52*, 6917.
39. Verdoes, M.; Florea, B. I.; Hillaert, U.; Willems, L. I.; van der Linden, W. A.; Sae-Heng, M.; Filippov, D. V.; Kisselev, A. F.; van der Marel, G. A.; Overkleeft, H. S. *ChemBioChem* **2008**, *9*, 1735.
40. Lin, F. L.; Hoyt, H. M.; van Halbeek, H.; Bergman, R. G.; Bertozzi, C. R. *J. Am. Chem. Soc.* **2005**, *127*, 2686.
41. van der Linden, W. A.; Li, N.; Hoogendoorn, S.; Ruben, M.; Verdoes, M.; Guo, J.; Boons, G-J.; van der Marel, G. A.; Florea, B. I.; Overkleeft, H. S. *Bioorg. Med. Chem.* **2012**, *20*, 662.
42. Berry, A. F.; Heal, W. P.; Tarafder, A. K.; Tolmachova, T.; Baron, R. A.; Seabra, M. C.; Tate, E. W. *Chembiochem* **2010**, *11*, 771.
43. van Geel, R.; Pruijn, G. J. M.; van Delft, F. L.; Boelens, W. C. *Bioconjugate Chem.* **2012**, *23*, 392.
44. Zhang, M. M.; Tsou, L. K.; Charron, G.; Raghavan, A. S.; Hang, H. C. *Proc. Natl. Acad. Sci. USA* **2010**, *107*, 8627.
45. Heal, W. P.; Jovanovic, B.; Bessin, S.; Wright, M. H.; Magee, A. I.; Tate, E. W. *Chem. Commun.* **2011**, *47*, 4081.

46. Chang, P. V.; Prescher, J. A.; Hangauer, M. J.; Bertozzi, C. R. *J. Am. Chem. Soc.* **2007**, *129*, 8400.
47. Karver, M. R.; Weissleder, R.; Hilderbrand, S. A. *Angew. Chem. Int. Ed.* **2012**, *51*, 920.
48. Chen, W.; Wang, D.; Dai, C.; Hamelberg, D.; Wang, B. *Chem. Commun.* **2012**, *48*, 1736.
49. Cole, C. M.; Yang, J.; Seckute, J.; Devaraj, N. K. *ChemBioChem* **2013**, *14*, 205.
50. Niederwieser, A.; Späte, A.-K.; Nguyen, L. D.; Jüngst, C.; Reutter, W.; Wittmann, V. *Angew. Chem. Int. Ed.* **2013**, *52*, 4265.
51. Späte, A.-K.; Busskamp, H.; Niederwieser, A.; Schart, V. F.; Marx, A.; Wittmann, V. *Bioconjugate Chem.* **2014**, *25*, 147.
52. Kamber, D. N.; Nazarova, L. A.; Liang, Y.; Lopez, S. A.; Patterson, D. M.; Shih, H.-W.; Houk, K. N.; Prescher, J. A. *J. Am. Chem. Soc.* **2013**, *135*, 13680.
53. Stairs, S.; Neves, A. A.; Stöckmann, H.; Wainman, Y. A.; Ireland-Zecchini, H.; Brindle, K. M.; Leeper, F. J. *ChemBioChem* **2013**, *14*, 1063.
54. Willems, L. I.; Li, N.; Florea, B. I.; Ruben, M.; van der Marel, G. A.; Overkleeft, H. S. *Angew. Chem. Int. Ed.* **2012**, *51*, 4431.
55. Speers, A. E.; Adam, G. C.; Cravatt, B. F. *J. Am. Chem. Soc.* **2003**, *125*, 4686.
56. Ovaa, H.; van Swieten, P. F.; Kessler, B. M.; Leeuwenburgh, M. A.; Fiebiger, E.; van den Nieuwendijk, A. M. C. H.; Galardy, P. J.; van der Marel, G. A.; Ploegh, H. L.; Overkleeft, H. S. *Angew. Chem. Int. Ed.* **2003**, *42*, 3626.
57. Britton, M.; Lucas, M. M.; Downey, S. L.; Screen, M.; Pletnev, A. A.; Verdoes, M.; Tokhunts, R. A.; Amir, O.; Goddard, A. L.; Pelphrey, P. M.; Wright, D. L.; Overkleeft, H. S.; Kisselev, A. F. *Chem. Biol.* **2009**, *16*, 1278.
58. Verdoes, M.; Willems, L. I.; van der Linden, W. A.; Duivenvoorden, B. A.; van der Marel, G. A.; Florea, B. I.; Kisselev, A. F.; Overkleeft, H. S. *Org. Biomol. Chem.* **2010**, *8*, 2719.
59. Withers, S. G.; Rupitz, K.; Street, I. P. *J. Biol. Chem.* **1988**, *263*, 7929.
60. Vocadlo, D. J.; Bertozzi, C. R. *Angew. Chem. Int. Ed.* **2004**, *43*, 5338.
61. Tatsuta, K.; Niwata, Y.; Umezawa, K.; Toshima, K.; Nakata, M. *Tetrahedron Lett.* **1990**, *31*, 1171.
62. Atsumi, S.; Umezawa, K.; Iinuma, H.; Naganawa, H.; Nakamura, H.; Iitaka, Y.; Takeuchi, T. *J. Antibiot.* **1990**, *43*, 49.
63. Witte, M. D.; Kallemeijn, W. W.; Aten, J.; Li, K.-Y.; Strijland, A.; Donker-Koopman, W. E.; van den Nieuwendijk, A. M. C. H.; Bleijlevens, B.; Kramer, G.; Florea, B. I.; Hooibrink, B.; Hollak, C. E. M.; Ottenhoff, R.; Boot, R. G.; van der Marel, G. A.; Overkleeft, H. S.; Aerts, J. M. F. G. *Nat. Chem. Biol.* **2010**, *6*, 907.
64. Witte, M. D.; Walvoort, M. T. C.; Li, K.-Y; Kallemeijn, W. W.; Donker-Koopman, W. E.; Boot, R. G.; Aerts, J. M. F. G.; Codée, J. D. C.; van der Marel, G. A.; Overkleeft, H. S. *ChemBioChem* **2011,** *12*, 1263.
65. Shimkus, M.; Levy, J.; Herman, T. *Proc. Natl. Acad. Sci. USA* **1985**, *82*, 2593.
66. Gartner, C. A.; Elias, J. E.; Bakalarski, C. E.; Gygi, S. P. *J. Proteome Res.* **2007**, *6*, 1482.
67. Verhelst, S. H. L.; Fonovic, M.; Bogyo, M. *Angew. Chem. Int. Ed.* **2007**, *46*, 1284.
68. Dirksen, A.; Yegneswaran, S.; Dawson, P. E. *Angew. Chem. Int. Ed.* **2010**, *49*, 2023.
69. Olejnik, J.; Sonar, S.; Krzymañska-Olejnik, E.; Rothschild, K. J. *Proc. Natl. Acad. Sci. USA* **1995**, *92*, 7590.
70. Szychowski, J.; Mahdavi, A; Hodas, J. J.; Bagert, J. D.;, Ngo, J. T.; Landgraf, P.; Dieterich, D. C.; Schuman, E. M.; Tirrell, D. A. *J. Am. Chem. Soc.* **2010**, *132*, 18351.
71. Geurink, P. P.; Florea, B. I.; Li, N.; Witte, M. D.; Verasdonck, J.; Kuo, C.-L.; van der Marel, G. A.; Overkleeft, H. S. *Angew. Chem. Int. Ed.* **2010**, *49*, 6802.
72. Speers A. E.; Cravatt, B. F. *J. Am. Chem. Soc*. **2005**, *127*, 10018.
73. Yang, Y.; Hahne, H.; Kuster, B.; Verhelst, S. H. L. *Mol. Cell. Proteomics* **2013**, *12*, 237.

3

Two-step labeling of endogenous enzymatic activities by Diels-Alder ligation

*Lianne I. Willems, Martijn Verdoes, Bogdan I. Florea, Gijsbert A. van der Marel, Herman S. Overkleeft, ChemBioChem **2010**, 11, 1769-1781.*

3.1 Introduction

A bioorthogonal reaction can be defined as a chemical transformation between two functional groups that takes place selectively within complex biological samples such as cell extracts, tissues or even living organisms. By allowing the temporal separation of a molecular probe and a reporter group, bioorthogonal chemistry creates the potential to selectively modify a specific biomolecule in the desired experimental setting. The power of this strategy was initially demonstrated by the cell surface labeling of *N*-glycoproteins by means of the Staudinger-Bertozzi ligation.[1-3] The success of this strategy led to the development of many other bioorthogonal ligation reactions, of which the copper(I)-catalyzed Huisgen [2+3] cycloaddition between an azide and an alkyne, referred to as 'click' reaction, is at present one of the most widely used bioconjugation methods.[4,5] Bioorthogonal ligation reactions have been applied to study a variety of biological processes, in particular those involving post-translational modifications.[6-10] Another area of research that has benefited from bioorthogonal chemistry is two-step activity-based protein profiling (ABPP), in which it enables the temporal separation of an active site-directed chemical probe (or activity-based probe, ABP) and a tag. Introduction of the tag after binding of the ABP to a

target enzyme may overcome problems associated with the direct introduction of a reporter group into an ABP such as interference with cell permeability, bioavailability, affinity for a target enzyme and/or selectivity over other enzymes. The value of bioorthogonal chemistry in ABPP was first demonstrated by the two-step activity-based profiling of serine hydrolases by making use of the copper(I)-catalyzed click reaction between an azide-functionalized ABP and an alkyne-modified fluorescent tag.[11] At the same time, a two-step ABPP method based on the Staudinger-Bertozzi ligation was reported for the labeling of the 20S proteasome, a highly conserved protease complex responsible for degrading the majority of cellular proteins. The use of an azide-functionalized ABP and subsequent reaction with a biotin-phosphine reagent enabled labeling of active proteasome subunits and also facilitated the direct identification of a novel subunit-specific inhibitor.[12,13]

While the examples described above make use of either azides or alkynes as ligation handles, other small reactive groups also warrant consideration to complement the repertoire of two-step ABPP strategies. In view of its selectivity and efficiency under mild, aqueous conditions, the Diels-Alder [4+2] cycloaddition presents an attractive alternative. Several reports have described the use of the Diels-Alder ligation for bioconjugation, including the modification of oligonucleotides and DNA,[14-21] surface immobilization of oligonucleotides,[22,23] conjugation of carbohydrates and proteins,[24,25] and the surface immobilization and site-specific ligation of peptides and proteins.[26,27] Recently, a number of related strategies based on the inverse-electron-demand Diels-Alder reaction has been reported for the bioorthogonal labeling of proteins.[28-30] None of these methods, however, has been applied to ABPP. The first part of this chapter describes the development of a Diels-Alder based ligation procedure for the profiling of endogenous enzymatic activities in complex biological samples. As outlined in Figure 3.1A, this approach involves the labeling of active enzymes with a diene-functionalized ABP followed by reaction with a dienophile containing a fluorescent tag to enable visualization of the labeled proteins. In the second part of this chapter, the potential use of a combined Diels-Alder and Staudinger-Bertozzi ligation strategy is examined in order to realize simultaneous two-step labeling of different enzymatic activities in a single experiment (Figure 3.1B). The application of the inverse-electron-demand Diels-Alder reaction as a two-step ABPP strategy for the monitoring of endogenously expressed enzymes is described in Chapter 4.

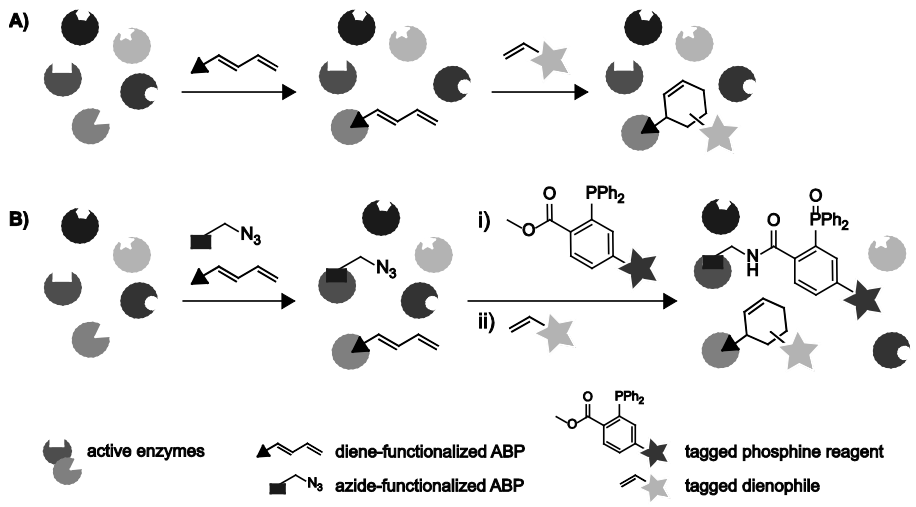

Figure 3.1. The Diels-Alder cycloaddition in activity-based protein profiling. Schematic representations of a two-step labeling strategy based on the Diels-Alder ligation (A) and the simultaneous labeling of two different catalytic activities in the same sample by successive Staudinger-Bertozzi ligation and Diels-Alder ligation (B). ABP: activity-based probe.

The validity of the Diels-Alder based ABPP strategy is evaluated by using the 20S proteasome as a model protein. This multi-subunit protein complex contains three catalytically active subunits (β1, β2 and β5) that each have a different substrate preference and can be targeted by either broad-spectrum or subunit-specific ABPs.[13,31-34] In order to enable two-step labeling of the catalytically active proteasome β-subunits by Diels-Alder ligation, a panel of four diene-modified ABPs (**1a**-**d**) was designed as well as a maleimide-functionalized fluorescent Bodipy tag (**3**) (Figure 3.2). The ABPs are based on the potent broad-spectrum proteasome inhibitor epoxomicin,[35,36] extended at the *N*-terminus with either a linear (**1b**, **1c**) or a cyclic (**1a**, **1d**) conjugated diene. The maleimide moiety is a very reactive dienophile which has been used successfully for Diels-Alder based ligation procedures on recombinant proteins.[26,27] Besides the labeling of proteasome activity, the Diels-Alder approach is also applied to the labeling of another class of enzymes, lysosomal cysteine proteases of the cathepsin family. For this purpose a diene-functionalized derivative of the cathepsin ABP DCG-04[37] (**2b**) was designed.

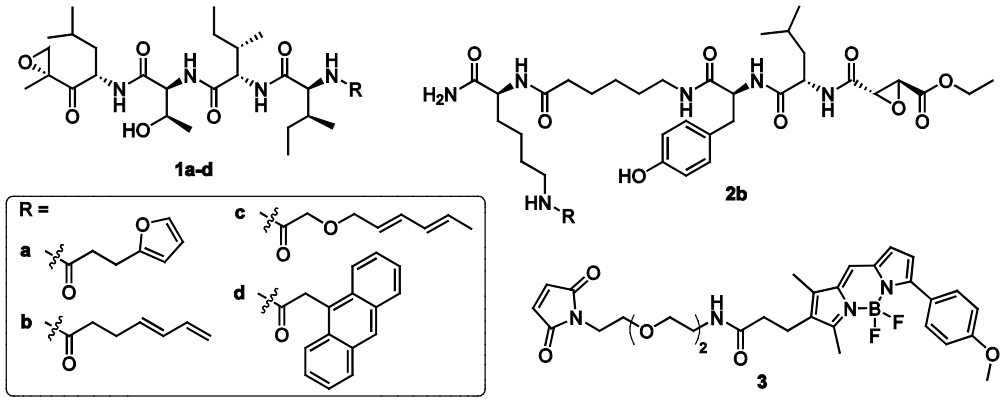

Figure 3.2. Structures of target compounds: diene-functionalized proteasome ABPs **1a**-**d**, cathepsin probe **2b** and Bodipy-tagged maleimide **3**.

3.2 Results and discussion

The synthesis of diene-derivatized proteasome ABPs **1a**-**d** and Bodipy-tagged maleimide reagent **3** has been described elsewhere.[38] The ability of the four epoxomicin derivatives **1a**-**d** to inhibit the activity of the 20S proteasome was established by performing a competition experiment against the fluorescent activity-based proteasome probe MV151[32] in El-4 cell extracts (Figure 3.3). El-4 cells contain next to the constitutive proteasome also the immunoproteasome, in which the β1, β2 and β5 subunits are replaced by β1i, β2i and β5i subunits having slightly different substrate preferences.[39-41] All six catalytically active subunits are targeted by MV151. Exposure of El-4 cell extracts to increasing concentrations of **1a**-**d** followed by labeling of residual proteasome activity with MV151 revealed that all probes are able to block the fluorescent labeling of the six proteasome β-subunits with

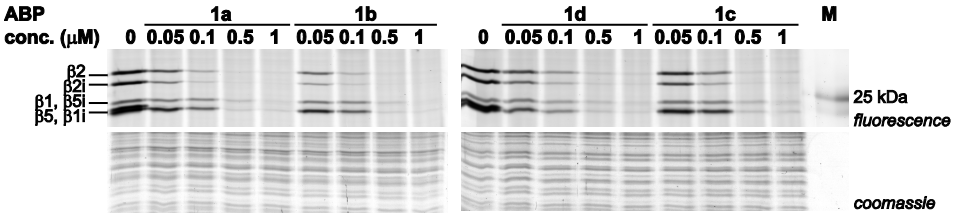

Figure 3.3. Inhibition of proteasome activity *in vitro* by probes **1a**-**d**. El-4 cell lysates were treated with 0.05 - 1 μM of inhibitors **1a**-**d** for 2 hrs, after which residual proteasome activity was labeled with 1 μM MV151 for 1 hr. Labeled proteins were resolved by 12.5% SDS-PAGE with fluorescent readout followed by coomassie brilliant blue staining. Proteasome β-subunits are designated on the basis of reported labeling by MV151.[32] 'M': protein marker.

similar potency. This indicates that the epoxomicin derivatives, like epoxomicin itself, are covalent and irreversible inhibitors of the catalytically active proteasome β-subunits. Complete inhibition was observed at inhibitor concentrations of 0.5-1 µM and higher.

As a first evaluation of the applicability of the synthesized probes in Diels-Alder ligation procedures, the Diels-Alder reaction of diene-derivatized probe **1c** with 1 equivalent of tagged maleimide **3** was performed in the absence of proteins. The reaction was monitored by LC/MS analysis at various time points (Figure 3.4), which demonstrated the formation of the predicted Diels-Alder adduct over time. Although significant product formation wasobserved after 24 hrs, the reaction did not reach complete conversion in 3 days. Considering the potential degradation of proteins in cell extracts when left for an extended period of time and in view of practical convenience, it was decided to use an overnight incubation for the ensuing Diels-Alder two-step labeling experiments *in vitro* with an excess of the dienophile to further promote product formation.

The feasibility of the Diels-Alder ligation strategy for two-step profiling of enzymatic activity was demonstrated next. Cell extracts were exposed for 1 hr to ABP **1c** using a concentration at which it completely blocks the active proteasome β-subunits (1 µM) and subsequently exposed to varying concentrations of Bodipy-maleimide **3** (1 - 50 µM) overnight (Figure 3.5A). Since maleimide **3** is a Michael acceptor that reacts readily with (cysteine) thiol groups and may thereby cause a substantial amount of non-specific background labeling, the proteins were denaturated and cysteine residues were masked with Ellman's reagent (5,5'-dithiobis-(2-nitrobenzoic acid), DTNB) after incubation with **1c** and prior to addition of **3**. In this protocol, a chloroform/methanol precipitation step is necessary to remove remaining thiol-containing reagents before the ligation reaction, which

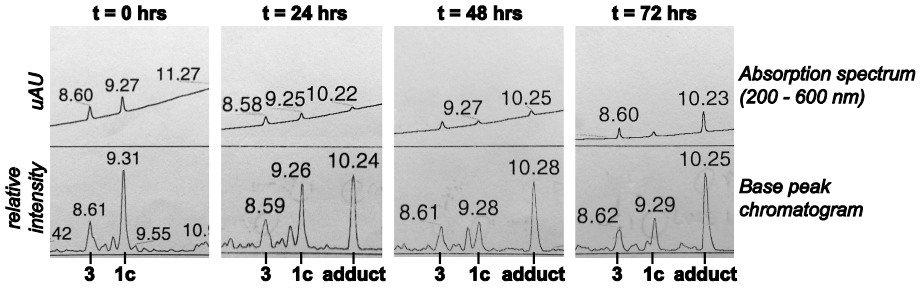

Figure 3.4. LC/MS analysis of Diels-Alder reaction of Bodipy-maleimide **3** with ABP **1c** (ratio 1:1) at selected time points (t = 0, 24, 48, 72 hrs). Fragments of obtained spectra with peaks corresponding to both reagents and Diels-Alder adduct are shown.

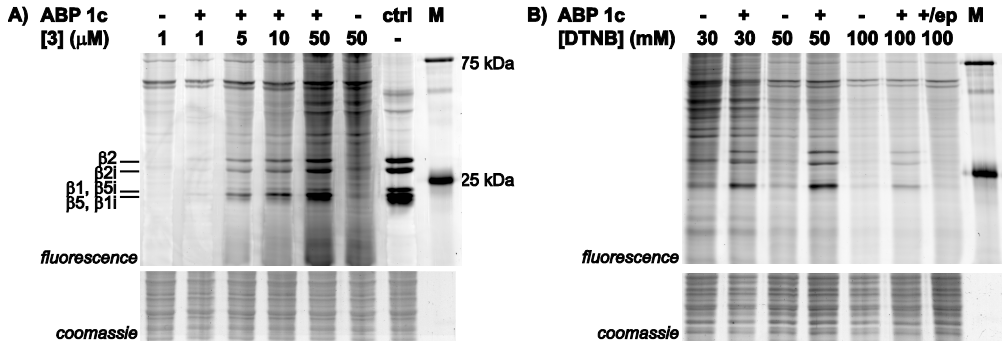

Figure 3.5. Labeling of proteasome activity in cell extracts by Diels-Alder ligation. A) Labeling in EL-4 cell extracts by exposure to 1 μM of ABP **1c** for 1 hr, denaturation, masking of cysteine residues and reaction with 1 - 50 μM of Bodipy-maleimide **3** overnight. B) Optimization of cysteine capping conditions by varying DTNB concentration (using 25 μM of **3**). Gels are 12.5% SDS-PAGE with fluorescent readout followed by coomassie brilliant blue staining as a loading control. 'ctrl': control sample labeled with 1 μM MV151. 'ep': 100 μM epoxomicin added to incubation with **1c**. 'M': protein marker.

simultaneously provides the opportunity to redissolve the sample in a buffer optimal for Diels-Alder ligation (pH 6).[26,27] A second precipitation step was used to quench the reaction and remove the excess of maleimide-tag **3**. Analysis of the labeled proteins on gel (Figure 3.5A) reveals, despite a considerable degree of background fluorescence, the specific fluorescent labeling of a number of bands which correspond to the proteasome β-subunits as labeled by MV151. Background fluorescence was not affected by the presence or absence of **1c**, confirming that it results from non-specific reactions of the maleimide-functionalized tag (**3**) rather than the inhibitor. In line with this observation, the concentration of cysteine capping reagent (DTNB) proved to be of crucial importance for the amount of background labeling, with an optimum around 50 mM (Figure 3.5B). The observed reduction in specific labeling when using a higher DTNB concentration is possibly due to an insufficient removal of the excess of reagent by a single precipitation step, causing it to interfere with the subsequent ligation reaction.

Next, the efficiency of the Diels-Alder ligation with the different dienes was assessed by performing the two-step labeling procedure in cell extracts with ABPs **1a**-**d** (Figure 3.6). Specific labeling with Bodipy-maleimide **3** (25 μM) was observed for diene-derivatized epoxomicin analogues **1c**, **1a** and **1b** but not for anthracenyl-derivative **1d**, which is apparently not able to undergo efficient Diels-Alder ligation with maleimide **3** under these conditions. The specific fluorescent signals were completely blocked by adding an excess of the selective proteasome inhibitor epoxomicin, demonstrating that the observed bands

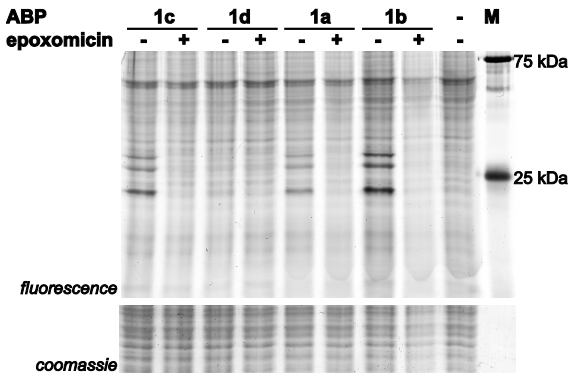

Figure 3.6. Diels-Alder based proteasome labeling in cell extracts using ABPs **1a**-**d**. EL-4 cell lysates were exposed to 1 µM of **1a-d** in the presence or absence of 100 µM epoxomicin for 1 hr, followed by denaturation, masking of cysteine residues and labeling with 25 µM Bodipy-maleimide **3** overnight. Labeled proteins were resolved by 12.5% SDS-PAGE with fluorescent readout followed by coomassie brilliant blue staining. 'M': protein marker.

indeed reflect labeling of the catalytically active proteasome β-subunits. The ligation reaction proceeded most efficiently with the non-cyclic dienes in **1c** and especially **1b**. The lower efficiency of furyl-derivative **1a** is somewhat surprising as this diene is fixed in the *cis*-configuration which these reactants need to adopt for the Diels-Alder cycloaddition.

Using the most reactive heptadienoyl-functionalized ABP **1b**, efforts were then made to further improve the efficiency of the Diels-Alder ligation by varying the concentration of dienophile (Figure 3.7A) and the reaction time of the ligation step (Figure 3.7B). Maleimide concentrations between 10 and 25 µM appeared to give the best results in terms of signal intensity and ratio of specific to background fluorescence. Both non-specific and specific labeling were also dependent on the reaction time, giving the best results when Diels-Alder ligation was performed with 25 µM of maleimide **3** for 4 - 20 hrs. After overnight incubation the signal intensity of proteasome labeling was similar to that obtained by direct labeling with fluorescent ABP MV151. Hence, a reaction time of 20 hrs and a dienophile concentration of 25 µM were selected for the following labeling experiments.

In a next experiment, the Diels-Alder approach was applied to the labeling of proteasome activity *in situ*. The cell-permeability of diene-functionalized probe **1b** was first demonstrated by treating cultured EL-4 cells with increasing concentrations of the probe followed by cell lysis and labeling of residual proteasome activity with MV151 (Figure 3.8A). Having shown the ability of the diene-functionalized ABP to inhibit the active proteasome β-subunits *in situ*, lysates from cells that had been treated with ABP **1b** (5 µM) were then

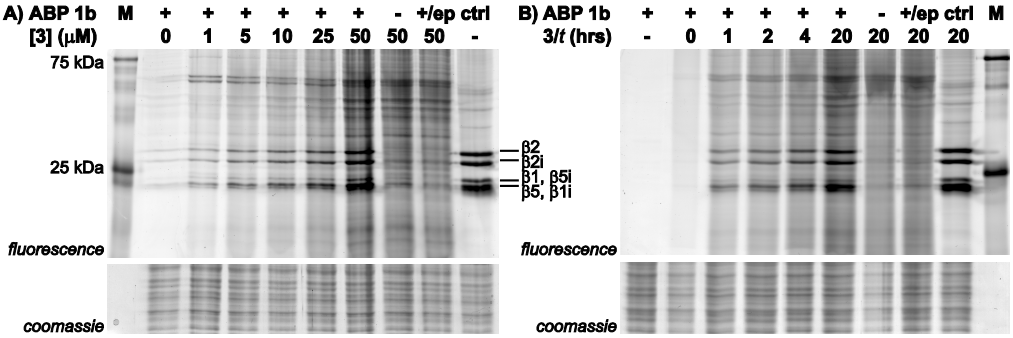

Figure 3.7. Optimization of Diels-Alder labeling procedure in EL-4 cell extracts by exposure to 1 μM of ABP **1b** for 1 hr, denaturation, masking of cysteine residues and reaction with A) 1 - 50 μM of reagent **3** overnight, or B) 25 μM **3** for 1 - 20 hrs. Gels are 12.5% SDS-PAGE with fluorescent readout followed by coomassie brilliant blue staining. 'ctrl': control sample labeled with 1 μM MV151. 'ep': 100 μM epoxomicin added to incubation with **1b**. 'M': protein marker.

subjected to the Diels-Alder labeling procedure with maleimide **3** (Figure 3.8B). Analysis of the fluorescent labeling on gel revealed the specific labeling of several bands that are not present in lysates from untreated cells and correspond to the proteasome β-subunits labeled by MV151. These results demonstrate that the Diels-Alder method can be applied to monitor enzymatic activity in living cells by *in situ* targeting with a diene-functionalized ABP and post-lysis labeling with a tagged maleimide reagent.

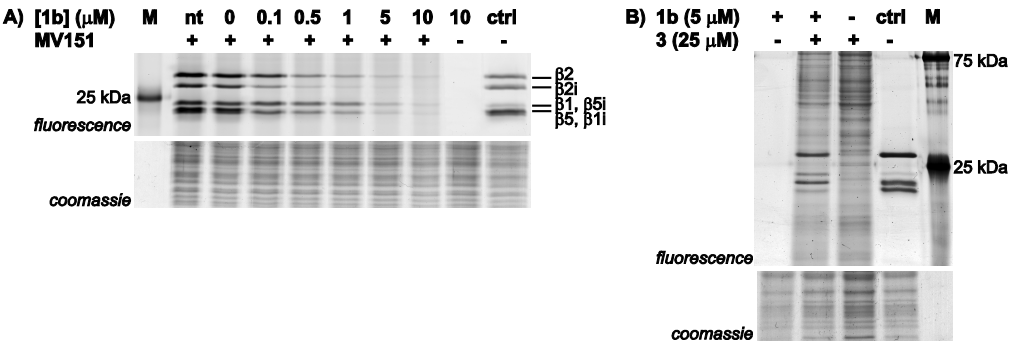

Figure 3.8. Targeting of proteasome activity *in situ* by ABP **1b**. Cultured EL-4 cells were exposed for 2 hrs to 0.1 - 10 μM of probe **1b** or 1 μM MV151 as a control ('ctrl') and then lysed. A) Residual proteasome activity in lysates was labeled with 1 μM MV151 for 1 hr. B) Lysates were subjected to denaturation, masking of cysteine residues and Diels-Alder ligation with 25 μM Bodipy-maleimide **3** overnight. Labeled proteins were resolved by 12.5% SDS-PAGE with fluorescent readout followed by coomassie brilliant blue staining. 'nt': non-treated control cells. 'M': protein marker.

Having established the applicability of the Diels-Alder strategy for two-step labeling of proteasome activity, attention was focused on using the approach to label a class of less abundant enzymes, cysteine proteases of the papain family (cathepsins). For this purpose a heptadienoyl-functionalized derivative of the irreversible cathepsin inhibitor DCG-04[37] was synthesized (**2b**, Scheme 3.1). Standard solid-phase peptide chemistry was employed to obtain resin-bound peptide **4**. The epoxysuccinate warhead **9** was synthesized from D-(-)-diethyl tartrate (**7**) by using a slightly modified literature procedure.[42] Briefly, the *cis*-diol was converted to a racemic mixture of *trans*-β-chloro alcohols which was then treated with DBU for epoxide formation (**8**), after which selective saponification of one of the ethyl esters afforded epoxysuccinate **9**. Next, deprotection of the *N*-terminal amine in peptide **4** followed by condensation with **9** and cleavage from the resin with concomitant deprotection provided ethyl ester **5** as well as a side product in which the ester was hydrolyzed (**6**). The obtained mixture of peptides was not readily separable due to the presence of a free amine in both of the compounds and was therefore used as such for the final step, reaction of the lysine ε-amine in peptides **5** and **6** with succinimidyl ester **10**.[38] The two products could then easily be separated to provide diene-derivatized DCG-04 analogue **2b**.

Scheme 3.1 Synthesis of diene-functionalized DCG-04 derivative **2b**

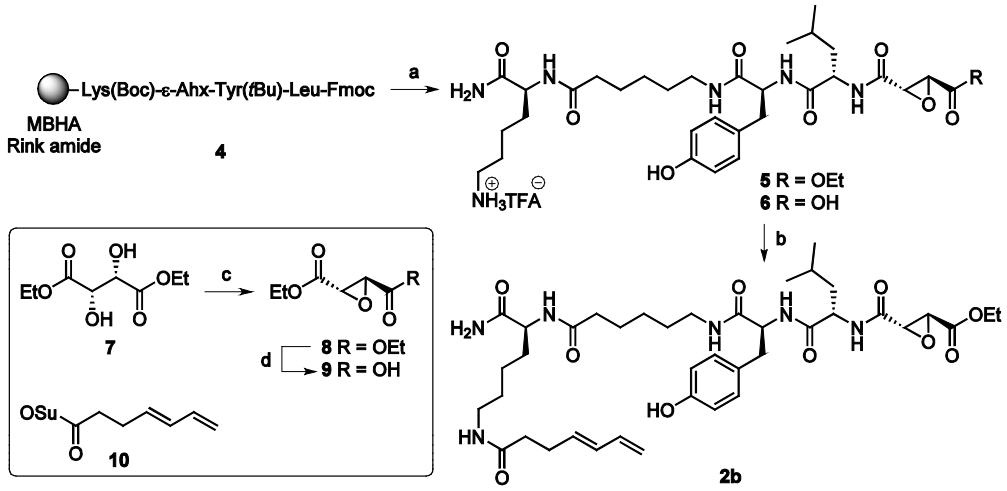

Reagents and conditions: a) *i*) piperidine/NMP (1/4, v/v), rt, 30 min, *ii*) **9**, DiPEA, BOP, NMP, rt, overnight, *iii*) TFA/TIS/H_2O (95/2.5/2.5, v/v/v), rt, 2 hrs, **5** 67%, **6** 33%; b) **10**, DiPEA, DCE/DMF, rt, overnight, 76% from **5**; c) *i*) 33% HBr in AcOH, 0 °C → rt, overnight, *ii*) AcCl, EtOH, reflux, 3.5 hrs, *iii*) DBU, Et_2O, 0 °C, 4.5 hrs, 56%; d) KOH, EtOH, 0 °C, 3 hrs, then rt, 2 hrs, 86%.

The ability of the diene-functionalized DCG-04 derivative (**2b**) to irreversibly inhibit cathepsin activity was demonstrated by performing a competition assay against the fluorescent cysteine protease ABP N_3-Bodipy(TMR)-DCG-04[43] in RAW cell extracts (Figure 3.9A). Subsequently, two-step labeling of cathepsin activity was realized by treatment of cell extracts with ABP **2b**, using a concentration at which it completely blocked fluorescent labeling by N_3-Bodipy(TMR)-DCG-04, followed by Diels-Alder ligation with Bodipy-tagged maleimide **3** (Figure 3.9B). Despite the lower intensity of specific signals as compared to background fluorescence than was observed for the two-step labeling of proteasome activity, two bands are visible only in ABP-treated samples which thus represent proteins that are specifically labeled by means of the two-step Diels-Alder ligation procedure. These bands correspond to the proteins that are labeled by N_3-Bodipy(TMR)-DCG-04. Moreover, the fluorescent labeling was blocked by adding an excess of DCG-04, which confirms the specific labeling of catalytically active cathepsins. On the basis of the apparent molecular weights and a previously reported DCG-04 labeling profile in RAW cell extracts,[44] the labeled proteases are tentatively assigned cathepsin Z and cathepsin B.

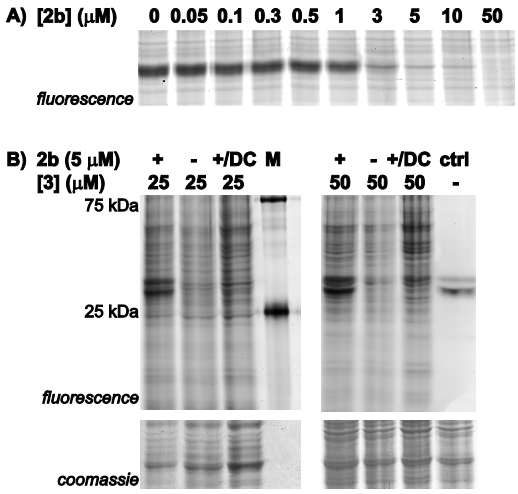

Figure 3.9. Diels-Alder based labeling of active cathepsins in cell extracts. RAW cell lysates were exposed to 0.05 - 50 μM of diene-derivatized ABP **2b** for 1 hr and then A) exposed to N_3-Bodipy(TMR)-DCG-04 (0.5 μM) for 1 hr to label residual cathepsin activity, or B) subjected to denaturation, masking of cysteine residues and Diels-Alder ligation with 25 or 50 μM Bodipy-maleimide **3** overnight. Gels are 12.5% SDS-PAGE with fluorescent readout (A, B) followed by coomassie brilliant blue staining (B). 'ctrl': control sample labeled with 0.5 μM N_3-Bodipy (TMR)-DCG-04. 'DC': exposure to **2b** in the presence of 25 μM DCG-04. 'M': protein marker.

In a final experiment the possibility was investigated to monitor different proteolytic activities in a single sample by combining Diels-Alder two-step labeling with the Staudinger-Bertozzi ligation, another widely used bioorthogonal ligation reaction. For this purpose, the azide-derivatized proteasome probe **11**[45] was employed, which selectively targets the β1 proteasome subunits and enables labeling via Staudinger-Bertozzi ligation with biotin-tagged phosphine **12**[46] (Figure 3.10). At the same time the β2 and β5 subunits can then be labeled by Diels-Alder ligation. The dual labeling procedure was performed in HEK cell extracts, which contain only the three constitutive active proteasome subunits β1, β2 and β5. Cell extracts were first exposed to azide-modified ABP **11** using a concentration at which it completely blocks β1 activity, and then to diene-equipped probe **1b** to target the non-occupied subunits β2 and β5. Next, Staudinger-Bertozzi ligation was effected by treatment with biotin-phosphine **12**, after which denaturation, cysteine masking and Diels-Alder reaction with fluorescent maleimide **3** were performed as before. As shown in Figure 3.10, ligation with maleimide **3** in samples treated with both **1b** and **11** resulted in the exclusive fluorescent labeling of the diene-modified subunits β2 and β5, while Staudinger ligation with phosphine **12** gave selective labeling of the β1 subunit on Western blot. Importantly, no cross-reactivity was observed and the labeling efficiency obtained by combining both ligation methods in the same sample was comparable to that of the separate ligation reactions. This experiment shows that the Diels-Alder ligation and Staudinger-Bertozzi ligation are mutually orthogonal and can be combined in the same sample to monitor different enzymatic activities.

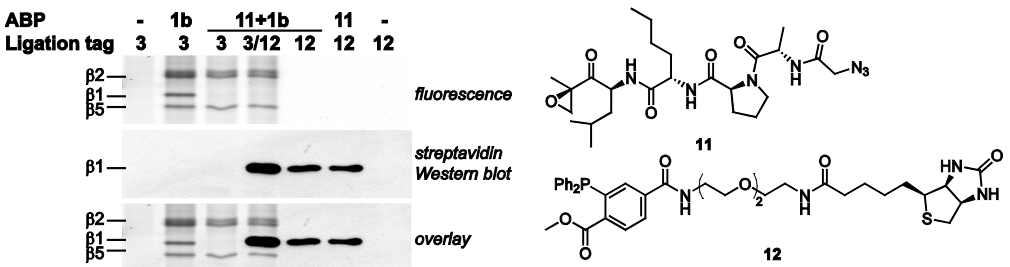

Figure 3.10. Dual ligation strategy using Diels-Alder and Staudinger-Bertozzi ligation in the same sample. HEK cell extracts were exposed successively to azide-functionalized β1-selective proteasome probe **11** (5 μM) for 1 hr, diene-derivatized probe **1b** (5 μM) for 1 hr, and biotin-phosphine **12** (100 μM) for 1 hr. After protein denaturation and masking of cysteine residues, Diels-Alder ligation was performed with Bodipy-maleimide **3** (25 μM) overnight. The labeled proteins were resolved by 12.5% SDS-PAGE with fluorescent readout followed by streptavidin Western blotting. Proteasome β-subunits are designated on the basis of previously reported labeling profiles.[45,47]

3.3 Conclusion

The Diels-Alder [4+2] cycloaddition was used as a ligation reaction for two-step ABPP by incorporation of a conjugated diene into an ABP and subsequent labeling with a fluorescently tagged maleimide. The Diels-Alder method was applied to monitor the activity of endogenously expressed proteasome β-subunits and cathepsins in cellular extracts and forms a useful complement to Staudinger-Bertozzi and click ligation strategies. From the panel of four tested dienes, the heptadienoyl moiety in **1b** proved to react most efficiently with maleimide **3** for proteasome labeling *in vitro*. The Diels-Alder approach is fully orthogonal with respect to the Staudinger-Bertozzi ligation and both reactions can be performed in the same sample, providing the possibility to modify two different biomolecules, for example two enzymatic activities or metabolites, with different labels to study them simultaneously. Limitations of the Diels-Alder procedure are the need to mask cysteine residues prior to dienophile addition which precludes *in vivo* applications, and significant background labeling by the maleimide reagent which might hamper the detection of proteins with low abundance or endogenous activity. The broad use of the Diels-Alder reaction as a bioorthogonal ligation method therefore requires a dienophile that is unreactive towards cysteine residues and other functionalities present in biological samples. During the completion of the labeling experiments described in this chapter, several related studies were reported on the *in situ* and *in vivo* imaging of small molecules by inverse-electron-demand Diels-Alder reaction.[48,49] The use of tetrazine as a diene and a strained alkene as a dienophile afforded very fast and selective labeling reactions and allowed the ligations to be performed in living cells. The application of a tetrazine ligation strategy for the profiling of endogenous enzymatic activities is described in Chapter 4.

Experimental procedures

A. Synthesis

General

All reagents were commercial grade and were used as received unless stated otherwise. MeOH and NMP were obtained from Biosolve. Toluene, EtOAc and PetEt (Riedel-de Haën) used for column chromatography were of technical grade and distilled before use. DCE, DCM, DMF, THF and dioxane (Biosolve) were of analytical grade and when used under anhydrous conditions stored over flame-dried 4 Å molecular sieves. Reactions were monitored by TLC-analysis using DC-alufolien (Merck, Kieselgel60, F254) with detection by UV-absorption (254/366 nm), spraying with a solution of $(NH_4)_6Mo_7O_{24}{\cdot}4H_2O$ (25 g/L) and $(NH_4)_4Ce(SO_4)_4{\cdot}2H_2O$ (10 g/L) in 10% aqueous sulfuric acid followed by charring at ~150 °C or spraying with an aqueous solution of $KMnO_4$ (7%) and K_2CO_3 (2%). Column chromatography was performed on silica gel (Screening Devices BV, 0.040 - 0.063 mm, 60 Å). LC/MS analysis was performed on an LCQ Adventage Max (Thermo Finnigan) ion-trap spectrometer (ESI+) coupled to a Surveyor HPLC

system (Thermo Finnigan) equipped with a C18 column (Gemini, 4.6 mm x 50 mm, 5µm particle size, Phenomenex). The applied buffers were A: H_2O, B: ACN and C: 1 % aqueous TFA. Reported gradients represent the percentage of buffer B in buffer A with 10% buffer C. HRMS analysis was performed on an LTQ Orbitrap (Thermo Finnigan) mass spectrometer equipped with an electronspray ion source in positive mode (source voltage 3.5 kV, sheath gas flow 10 mL min−1, capillary temperature 250 °C) with resolution R = 60000 at m/z 400 (mass range m/z = 150 - 2000) and dioctylphtalate (m/z = 391.28428) as a "lock mass". The high resolution mass spectrometer was calibrated prior to measurements with a calibration mixture (Thermo Finnigan). ^{1}H- and ^{13}C-APT-NMR spectra were recorded on a Jeol JNM-FX-200 (200/50) or Bruker AV-400 (400/100 MHz). Chemical shifts are given in ppm (δ) relative to the solvent peak or to tetramethylsilane as internal standard. Coupling constants (*J*) are given in Hz. All presented ^{13}C-APT spectra are proton decoupled. Peak assignments are based on 2D ^{1}H-COSY and ^{13}C-HSQC NMR experiments. Compounds **1a**-**d**, **3** and **10** were described previously.[38]

(2*S*,3*S*)-diethyl oxirane-2,3-dicarboxylate (8)

D-(-)-diethyl tartrate (**7**) (29 g, 0.14 mol) was cooled to 0 °C, before a solution of 33% HBr in acetic acid (120 mL) was added dropwise over 45 min. After complete addition, the reaction mixture was stirred at 0 °C for 15 min and then at room temperature overnight. Next, the mixture was poored onto crushed ice/H_2O (300 mL) and extracted with Et_2O (3x). The combined organics were washed with H_2O (3x), dried over anhydrous $MgSO_4$, filtered and concentrated *in vacuo*. Remaining solvents were concentrated in the presence of toluene. The crude oil was dissolved in EtOH and acetyl chloride (5.1 mL, 70 mmol, 0.5 eq.) was added. The reaction mixture was stirred under reflux for 3.5 hrs, before being concentrated at a temperature of 30 °C. The remaining yellowish oil was dissolved in Et_2O (175 mL), cooled to 0 °C and put under argon atmosphere. A solution of DBU (21 mL, 0.14 mol, 1.0 eq.) in Et_2O (90 mL) was added dropwise over 100 min. The reaction mixture was then stirred at 0 °C for 1 hr, more DBU (2.1 mL, 14 mmol, 0.1 eq.) was added and the reaction mixture was stirred for an additional 2 hrs, before being quenched with H_2O. The mixture was washed with 1M $KHSO_4$ solution and H_2O and the organic layer was dried over anhydrous $MgSO_4$, filtered and concentrated *in vacuo*. Purification by column chromatography (PetEt → 15% EtOAc in PetEt) yielded title compound **8** (15 g, 79 mmol, 56% over 3 steps). ^{1}H NMR (400 MHz, $CDCl_3$): δ (ppm) 4.32-4.22 (m, 4H), 3.66 (s, 2H), 1.32 (t, *J* = 7.15, 7.15 Hz, 6H). ^{13}C NMR (100 MHz, $CDCl_3$): δ (ppm) 166.69, 62.14, 51.96, 13.96.

(2*S*,3*S*)-3-(ethoxycarbonyl)oxirane-2-carboxylic acid (9)

A solution of compound **8** (14 g, 76 mmol) in absolute EtOH (200 mL) was cooled to 0 °C and a solution of KOH (5.0 g, 76 mmol, 1.0 eq.) in absolute EtOH (100 mL) was added dropwise over 20 min. Next, the reaction mixture was stirred at 0 °C for 3 hrs and then at room temperature for 2 hrs, before being concentrated *in vacuo*. H_2O (200 mL) was added to the residue and the basic aqueous mixture was washed with DCM (1x 30 mL). The aqueous layer was then acidified with concentrated HCl (7.0 mL), NaCl (60 g) was added and the mixture was extracted with EtOAc (4x 200 mL). The combined organics were dried over anhydrous $MgSO_4$, filtered and concentrated *in vacuo* to give title compound **9** (11 g, 66 mmol, 86%). ^{1}H NMR (400 MHz, $CDCl_3$): δ (ppm) 6.24 (bs, 1H), 4.33-4.20 (m, 2H), 3.74-3.61 (m, 2H), 1.32 (t, *J* = 7.10, 7.10 Hz, 3H). ^{13}C NMR (100 MHz, $CDCl_3$): δ (ppm) 168.54, 166.92, 61.95, 51.49, 51.42, 13.38.

MBHA-Rink amide-Lys(Boc)-Ahx-Tyr(*t*Bu)-Leu(Fmoc) (4)

4-methylbenzhydrylamine (MBHA) functionalized Rink amide resin (3.2 g, 0.64 mmol/g, 2.1 mmol) was washed with DCM and deprotected with 20% piperidine in NMP for 20 min. After washing with NMP (2x) and DCM (2x), the resin was coupled to Fmoc-Lys(Boc)-OH (2.4 g, 5.2 mmol, 2.5 eq.) in the presence of BOP (2.3 g, 5.2 mmol, 2.5 eq.) and DiPEA (1.1 mL, 6.2 mmol, 3.0 eq.) in NMP; the reaction mixture was shaken overnight, followed by washing with NMP (2x) and DCM (2x). The remaining free amines were capped with acetic anhydride (0.98 mL, 10 mmol, 5.0 eq.)

in the presence of DiPEA (3.6 mL, 21 mmol, 10 eq.) in DCM for 30 min. The resin was then washed with Et_2O, dried *in vacuo* overnight and the loading of the resin was determined to be 0.30 mmol/g by spectrophotometric analysis (3.7 g, 1.1 mmol, 53%). The obtained resin (3.0 g, 0.90 mmol) was submitted to three cycles of standard Fmoc-based solid phase peptide synthesis as follows: after deprotection with 20% piperidine in NMP for 30 min, the resin was washed with NMP (2x) and DCM (3x) and coupled to ε-Ahx-Fmoc (0.80 g, 2.3 mmol, 2.5 eq.) in the presence of BOP (1.0 g, 2.3 mmol, 2.5 eq.) and DiPEA (0.45 mL, 2.7 mmol, 3.0 eq.) in NMP for 3 days, followed by washing with NMP (3x) and DCM (3x). The second and third cycles were done in the same way, coupling to Fmoc-Tyr(*t*Bu)-OH (1.0 g, 2.3 mmol, 2.5 eq.) for 5 hrs and Fmoc-Leu-OH (0.80 g, 2.3 mmol, 2.5 eq.) overnight, respectively. Couplings were monitored for completion by the Kaiser test. Washing with Et_2O and drying *in vacuo* overnight yielded resin-bound compound **4**.

(2*S*,3*S*)-3-(ethoxycarbonyl)oxirane-2-carboxyl-Leu-Tyr-Ahx-Lys.TFA (5)

Resin-bound compound **4** (~0.90 mmol) was deprotected with 20% piperidine in NMP for 30 min. The resin was washed with NMP (2x) and DCM (3x) before being subjected to a condensation cycle with free acid **9** (0.36 g, 2.3 mmol, 2.5 eq.) in the presence of BOP (1.0 g, 2.3 mmol, 2.5 eq.) and DiPEA (0.45 mL, 2.7 mmol, 3.0 eq.) in NMP; the reaction mixture was shaken overnight, followed by washing with NMP (3x) and DCM (3x). The condensation cycle was repeated after which the Kaiser test indicated complete coupling. Cleavage from the resin was then accomplished by treatment with TFA/TIS/H_2O (95/2.5/2.5, v/v/v) for 2 hrs at room temperature. After filtration and concentration *in vacuo* in the presence of toluene, the residue was recrystallized first from acetone/MeOH/EtOAc and then from MeOH/Et_2O, yielding a 2:1 mixture of fully deprotected ester **5** and free acid **6** (total yield 0.73 g, 0.93 mmol, quant.) according to NMR analysis. LC/MS analysis: R_t 5.0 min (linear gradient 10 → 90% B in 15 min), m/z 677.4 $[M+H]^+$, 1353.2 $[2M+H]^+$. ^1H NMR (400 MHz, MeOD): δ (ppm) 6.98 (d, *J* = 7.87 Hz, 2H), 6.66 (d, *J* = 7.76 Hz, 2H), 4.44 (t, *J* = 7.23, 7.23 Hz, 1H), 4.37 (dd, *J* = 7.59, 5.82 Hz, 1H), 4.30 (dd, *J* = 7.96, 5.15 Hz, 1H), 4.26-4.16 (m, 1H), 3.79-3.61 (m, 1H), 3.61-3.46 (m, 1H), 3.17-3.07 (m, 2H), 3.06-2.98 (m, 2H), 2.98-2.91 (m, 2H), 2.91-2.73 (m, 2H), 2.20 (t, *J* = 6.87, 6.87 Hz, 2H), 1.66-1.63 (m, 2H), 1.59-1.31 (m, 9H), 1.26 (t, *J* = 6.99, 6.99 Hz, 3H), 1.23-1.13 (m, 2H), 0.88 (d, *J* = 5.77 Hz, 3H), 0.84 (d, *J* = 5.75 Hz, 3H).

(2*S*,3*S*)-3-(ethoxycarbonyl)oxirane-2-carboxyl-Leu-Tyr-Ahx-((*N*)-(*E*)-hepta-4,6-dienoyl)Lys-H_2N (2b)

A mixture of **5** and **6** (0.31 g, 0.39 mmol, non-hydrolyzed/hydrolyzed 2/1) was dissolved in DCE/DMF under argon atmosphere and made basic (pH 8.5) using DiPEA (0.13 mL, 0.78 mmol, 2.0 eq.), before a solution of OSu-ester **10** (0.23 g, 1.0 mmol, 2.6 eq.) in DCE/DMF was added. After stirring overnight at room temperature under argon atmosphere, the reaction mixture was concentrated *in vacuo*. The residue was taken up in MeOH/acetone and the soluble fraction was purified by column chromatography ($CHCl_3$ → 10% MeOH in $CHCl_3$), yielding diene-modified title compound **2b** (0.16 g, 0.20 mmol, 76% from non-hydrolyzed starting material **7**). ^1H NMR (400 MHz, dmso-*d*6): δ (ppm) 8.54 (d, *J* = 8.19 Hz, 1H), 8.11 (d, *J* = 8.24 Hz, 1H), 7.82-7.74 (m, 2H), 7.30 (s, 1H), 6.96 (d, *J* = 8.40 Hz, 2H), 6.61 (d, *J* = 8.32 Hz, 2H), 6.28 (td, *J* = 17.03, 10.26, 10.26 Hz, 1H), 6.04 (dd, *J* = 15.16, 10.53 Hz, 1H), 5.74-5.64 (m, 1H), 5.02 (dd, *J* = 50.10, 13.54 Hz, 2H), 4.37-4.28 (m, 2H), 4.23-4.08 (m, 3H), 3.73-3.69 (m, 1H), 3.62-3.57 (m, 1H), 3.07-2.88 (m, 4H), 2.82 (dd, *J* = 13.69, 5.57 Hz, 1H), 2.67 (dd, *J* = 13.64, 8.85 Hz, 1H), 2.26 (dd, *J* = 14.23, 7.06 Hz, 2H), 2.17-2.05 (m, 4H), 1.59 (td, *J* = 9.47, 6.89, 6.89 Hz, 1H), 1.54-1.26 (m, 12H), 1.23 (t, *J* = 7.10, 7.10 Hz, 3H), 1.20-1.12 (m, 2H), 0.83 (dd, *J* = 14.79, 6.46 Hz, 6H).

Diels-Alder reaction of maleimide-tag 3 with diene-functionalized probe 1c

Fluorescent maleimide **3** (5 mM) was reacted with diene-derivatized probe **1c** (5 mM) in a 1/1 (v/v) mixture of H_2O and DMSO at room temperature. The reactions were monitored by LC/MS analysis at various time points (t = 0, 24, 48, 72 hrs). LC/MS analysis (linear gradient 10 → 90% B in 15 min): Bodipy-maleimide **3**: R_t 8.6 min, m/z 589.3 [M-

F]$^+$, 631.4 [M+Na]$^+$, 1217.0 [2M+H]$^+$; Probe **1c**: R_t 9.3 min (linear gradient 10 → 90% B in 15 min), m/z 637.2 [M+H]$^+$, 1295.1 [2M+Na]$^+$; Diels-Alder adduct [**3** + **1c**]: R_t 10.2 min (linear gradient 10 → 90% B in 15 min), m/z 1245.3 [M+H]$^+$.

B. Biochemistry

General

EL-4 and HEK-293T cells were cultured in DMEM supplemented with 10% (v/v) FCS, 10 units/mL penicillin and 10 µg/mL streptomycin in a 5% CO_2 humidified incubator at 37 °C. Cells were harvested, washed with PBS (2x) and lysed in digitonin lysis buffer (50 mM Tris pH 7.5, 250 mM sucrose, 5 mM $MgCl_2$, 1 mM DTT, 2 mM ATP, 0.025% digitonin) for 30 min on ice followed by sonication on ice for 3x 10 s. After centrifugation of the cells at 16,100 g for 15 min at 4 °C, the supernatants were collected and the protein concentration was determined by Bradford assay. RAW cell lysates were prepared by incubating harvested RAW cells in MES lysis buffer (50 mM MES pH 5.5, 50 mM NaCl, 5 mM DTT, 0.013% digitonin) for 30 min on ice followed by sonication and centrifugation. Precipitation of proteins was done using a chloroform/methanol (c/m) precipitation protocol.[50] SDS-PAGE analysis: in-gel fluorescence was measured on a Typhoon Variable Mode Imager (Amersham Biosciences) using Cy3/TAMRA settings (excitation wavelength 532 nm, emission wavelength 580 nm). As a loading control gels were stained with Coomassie Brilliant Blue. For Western blotting, the proteins were transferred onto a PVDF membrane using a Bio-Rad Trans-Blot cell system. Membranes were blocked with 1% BSA in TBS-t(+) (0.1% Tween 20) for 1 hr at room temperature, hybridized with Streptavidin-HRP for 45 min at room temperature (1:10,000 in blocking buffer) (Molecular Probes, Life Technologies), washed with TBS-t(+) and TBS and then visualized using an ECL+ Western blotting detection kit (Amersham Biosciences). Markers used were Precision Plus Dual Color protein standard (Bio-Rad) and Biotinylated protein marker (Bio-Rad). MV151[32], N_3-Bodipy(TMR)-DCG-04[43], DCG-04[37], **11**[45] and **12**[46] are described in literature.

***In vitro* competition assay versus MV151**

EL-4 cell lysates (10 µg total protein per experiment) in lysis buffer (9 µL) were exposed to the indicated concentrations of **1a**, **1b**, **1c** or **1d** (1 µL 10x solution in DMSO) for 2 hrs at 37 °C, after which the lysates were incubated with 1 µM MV151 (1 µL 10 µM in DMSO) for 1 hr at 37 °C. The reaction mixtures were then heated to 55 °C for 20 minutes with 4 µL 4x Laemmli's sample buffer containing 2-mercaptoethanol and resolved on 12.5% SDS-PAGE. In-gel visualization of the fluorescent labeling was performed in the wet gel slabs directly.

***In vitro* competition assay versus N_3-Bodipy(TMR)-DCG-04**

RAW cell lysates (50 µg total protein per experiment) in MES lysis buffer (9 µL) were exposed to the indicated concentrations of **2b** (1 µL 10x solution in DMSO) for 1 hr at 37 °C, prior to incubation with 0.5 µM N_3-Bodipy(TMR)-DCG-04 (1 µL 5 µM in DMSO) for 1 hr at 37 °C. The reaction mixtures were boiled for 3 minutes with 4 µL 4x Laemmli's sample buffer containing 2-mercaptoethanol and resolved on 12.5% SDS-PAGE. In-gel visualization of the fluorescent labeling was performed in the wet gel slabs directly.

Diels-Alder based proteasome labeling *in vitro*

In a typical experiment, EL-4 cell lysates (50 µg total protein per experiment) in lysis buffer (9 µL) were exposed to 1 µM **1a**, **1b**, **1c** or **1d** (1 µL 10 µM DMSO) for 1 hr at 37 °C in the presence or absence of 100 µM epoxomicin (1 µL 1 mM in DMSO). Control samples were labeled with 1 µM MV151. The proteins were then denatured for 15 min at room temperature in 8 M urea (80 µL 9 M in H_2O), after which cysteine residues were reduced with 5 mM DTT (5 µL 100 mM in H_2O) for 30 min at 55 °C and capped with 50 mM DTNB (5 µL 1 M in DMSO) for 3.5 hrs at room temperature. Next, the mixtures were subjected to c/m precipitation and the proteins were taken up in 5 µL Diels-

Alder buffer (5 mM NaH_2PO_4, 20 mM NaCl, 0.2 mM $MgCl_2$, pH 6.0) containing 6 M urea, diluted to 2 M urea by addition of 10 µL Diels-Alder buffer and then exposed to the indicated concentrations of Bodipy-maleimide **3** (1.7 µL 10x solution in DMSO) overnight at 37 °C. Where indicated, reaction times were reduced to 1, 2 or 4 hrs. After quenching by c/m precipitation, proteins were taken up in 10 µL Laemmli's sample buffer containing 2-mercaptoethanol, heated to 55 °C for 15 minutes and resolved on 12.5% SDS-PAGE. In-gel visualization of the fluorescent labeling was performed in the wet gel slabs directly.

Diels-Alder based cathepsin labeling *in vitro*

RAW cell lysates (50 µg total protein per experiment) in MES lysis buffer (9 µL) were exposed to 5 µM of ABP **2b** (0.5 µL 100 µM DMSO) for 1 hr at 37 °C in the presence or absence of 25 µM DCG-04 (1.3 µL 200 µM in DMSO). Control samples were labeled with 0.5 µM N_3-Bodipy(TMR)-DCG-04. Then the proteins were subjected to denaturation, cysteine capping and Diels-Alder ligation with Bodipy-maleimide **3** (25 or 50 µM) using the same procedure as described for Diels-Alder based proteasome labeling.

Diels-Alder based proteasome labeling *in situ*

Some $1*10^6$ EL-4 cells per experiment were grown overnight in 5.5 mL of medium and exposed to the indicated concentrations of **1b** for 2 hrs at 37 °C in a total volume of 6 mL medium containing 0.25% DMSO. As a control, cells were exposed to 1 µM MV151, 0 µM probe (DMSO control) or no compound at all (non-treated control). The cells were then harvested, washed with PBS (2x) and lysed in digitonin lysis buffer.

Competition experiment. Lysates (10 µg total protein per experiment in 9 µL lysis buffer) were incubated with 1 µM MV151 (1 µL 10 µM in DMSO) for 1 hr at 37 °C. The reaction mixtures were then heated to 55 °C for 20 minutes with 4 µL 4x Laemmli's sample buffer containing 2-mercaptoethanol and resolved on 12.5% SDS-PAGE. In-gel visualization of the fluorescent labeling was performed in the wet gel slabs directly.

Diels-Alder ligation. Lysates from cells treated with 5 µM **1b** (20 µg total protein per experiment in 10 µL lysis buffer) were subjected to denaturation, cysteine capping and Diels-Alder ligation with 25 µM Bodipy-maleimide **3** using the same procedure as described for *in vitro* Diels-Alder based proteasome labeling.

Combined Diels-Alder and Staudinger ligation for labeling of proteasome β-subunits

HEK cell lysates (50 µg total protein per experiment) in lysis buffer (9 µL) were exposed to 5 µM **11** (1 µL 50 µM DMSO) for 1 hr at 37 °C, followed by exposure to 5 µM **1b** (1 µL 50 µM DMSO) for 1 hr at 37 °C. Next, 100 µM of biotin-phosphine **12** was added (1.2 µL 1 mM in DMF) and the lysates were again incubated for 1 hr at 37 °C. The proteins were then denatured for 15 min at room temperature in 8 M urea (80 µL 9 M in H_2O), after which cysteine residues were reduced with 5 mM DTT (5 µL 100 mM in H_2O) for 30 min at 55 °C and capped with 50 mM DTNB (5 µL 1 M in DMSO) for 3.5 hrs at room temperature. Next, the mixtures were subjected to c/m precipitation and the proteins were taken up in 5 µL Diels-Alder buffer (5 mM NaH_2PO_4, 20 mM NaCl, 0.2 mM $MgCl_2$, pH 6.0) containing 6 M urea, diluted to 2 M urea by addition of 10 µL Diels-Alder buffer and then exposed to 25 µM Bodipy-maleimide **3** (1.7 µL 250 µM in DMSO) overnight at 37 °C. After quenching by c/m precipitation, the proteins were taken up in 10 µL Laemmli's sample buffer containing 2-mercaptoethanol, heated to 55 °C for 15 minutes and resolved on 12.5% SDS-PAGE. In-gel visualization of the fluorescent labeling was performed in the wet gel slabs directly, after which biotinylated proteins were detected by streptavidin Western blotting.

References

1. Mahal, L. K.; Yarema, K. J.; Bertozzi, C. R. *Science* **1997**, *276*, 1125.
2. Saxon, E.; Bertozzi, C. R. *Science* **2000**, *287*, 2007.
3. Prescher, J. A.; Dube, D. H.; Bertozzi, C. R. *Nature* **2004**, *430*, 873.
4. Rostovtsev, V. V. ; Green, L. G.; Fokin, V. V.; Sharpless, K. B. *Angew. Chem. Int. Ed.* **2002**, *41*, 2596.
5. Wang, Q.; Chan, T. R.; Hilgraf, R.; Fokin, V. V.; Sharpless, K. B.; Finn, M. G. *J. Am. Chem. Soc.* **2003**, *125*, 3192.
6. Heal, W. P.; Tate, E. W. *Org. Biomol. Chem.* **2010**, *8*, 731.
7. Vocadlo, D. J.; Hang, H. C.; Kim, E. J.; Hanover, J. A.; Bertozzi, C. R. *Proc. Natl. Acad. Sci. USA* **2003**, *100*, 9116.
8. Kho, Y.; Kim, S. C.; Jiang, C.; Barma, D.; Kwon, S. W.; Cheng, J.; Jaunbergs, J.; Weinbaum, C.; Tamanoi, F.; Falck, J.; Zhao, Y. *USA* **2004**, *101*, 12479.
9. Hang, H. C.; Geutjes, E. J.; Grotenbreg, G.; Pollington, A. M.; Bijlmakers, M. J.; Ploegh, H. L. *J. Am. Chem. Soc.* **2007**, *129*, 2744.
10. Ban, H.; Gavrilyuk, J.; Barbas 3rd, C. F. *J. Am. Chem. Soc.* **2010**, *132*, 1523.
11. Speers, A. E.; Adam, G. C.; Cravatt, B. F. *J. Am. Chem. Soc.* **2003**, *125*, 4686.
12. Ovaa, H.; van Swieten, P. F.; Kessler, B. M.; Leeuwenburgh, M. A.; Fiebiger, E.; van den Nieuwendijk, A. M. C. H.; Galardy, P. J.; van der Marel, G. A.; Ploegh, H. L.; Overkleeft, H. S. *Angew. Chem. Int. Ed.* **2003**, *42*, 3626.
13. van Swieten, P. F.; Samuel, E.; Hernández, R. O.; van den Nieuwendijk, A. M. C. H.; Leeuwenburgh, M. A.; van der Marel, G. A.; Kessler, B. M.; Overkleeft, H. S.; Kisselev, A. F. *Bioorg. Med. Chem. Lett.* **2007**, *17*, 3402.
14. Seelig, B.; Jäschke, A. *Tetrahedron Lett.* **1997**, *38*, 7729.
15. Hill, K. W.; Taunton-Rigby, J.; Carter, J. D.; Kropp, E.; Vagle, K.; Pieken, W.; McGee, D. P. C.; Husar, G. M.; Leuck, M.; Anziano, D. J.; Sebesta, D. P. *J. Org. Chem.* **2001**, *66*, 5352.
16. Graham, D.; Grondin, A.; McHugh, C.; Fruk, L.; Smith, W. E. *Tetrahedron Lett.* **2002**, *43*, 4785.
17. Fruk, L.; Grondin, A.; Smith, W. E.; Graham, D. *Chem. Commun.* **2002**, 2100.
18. Tona, R.; Häner, R. *Chem. Commun.* **2004**, 1908.
19. Tona, R. Häner, R. *Bioconjugate Chem.* **2005**, *16*, 837.
20. Marchán, V.; Ortega, S.; Pulido, D.; Pedroso, E.; Grandas, A. *Nucleic Acids Res.* **2006**, *34*, e24.
21. Borsenberger, V.; Howorka, S. *Nucleic Acids Res.* **2009**, *37*, 1477.
22. Husar, G. M.; Anziano, D. J.; Leuck, M.; Sebesta, D. P. *Nucleosides Nucleotides Nucleic Acids* **2001**, *20*, 559.
23. Latham-Timmons, H. A.; Wolter, A.; Roach, J. S.; Giare, R.; Leuck, M. *Nucleosides Nucleotides Nucleic Acids* **2003**, *22*, 1495.
24. Pozsgay, V.; Vieira, N. E.; Yergey, A. *Org. Lett.* **2002**, *4*, 3191.
25. Berkin, A.; Coxon, B.; Pozsgay, V. *Chem. Eur. J.* **2002**, *8*, 4424-4433.
26. De Araújo, A. D.; Palomo, J. M.; Cramer, J.; Köhn, M.; Schröder, H.; Wacker, R.; Niemeyer, C.; Alexandrov, K.; Waldmann, H. *Angew. Chem. Int. Ed.* **2005**, *45*, 296.
27. De Araújo, A. D.; Palomo, J. M.; Cramer, J.; Seitz, O.; Alexandrov, K.; Waldmann, H. *Chem. Eur. J.* **2006**, *12*, 6095.
28. Blackman, M. L.; Royzen, M.; Fox, J. M. *J. Am. Chem. Soc.* **2008**, *130*, 13518.
29. Devaraj, N. K.; Weissleder, R.; Hilderbrand, S. A. *Bioconjugate Chem.* **2008**, *19*, 2297.
30. Devaraj, N. K.; Upadhyay, R.; Haun, J. B.; Hilderbrand, S. A.; Weissleder, R. *Angew. Chem. Int. Ed.* **2009**, *48*, 7013.
31. Verdoes, M.; Florea, B. I.; van der Marel, G. A.; Overkleeft, H. S. *Eur. J. Org. Chem.* **2009**, *2009*, 3301.
32. Verdoes, M.; Florea, B. I.; Menendez-Benito, V.; Maynard, C. J.; Witte, M. D.; van der Linden, W. A.; van den Nieuwendijk, A. M. C. H.; Hofmann, T.; Berkers, C. R.; van Leeuwen, F. W.; Groothuis, T. A.; Leeuwenburgh, M. A.; Ovaa, H.; Neefjes, J. J.; Filippov, D. V.; van der Marel, G. A.; Dantuma, N. P.; Overkleeft, H. S. *Chem. Biol.* **2006**, *13*, 1217.

33. Sharma, L. K.; Lee, N.-R.; Jang, E. R.; Lei, B.; Zhan, C.-G.; Lee, W.; Kim, K.-B. *ChemBioChem* **2012**, *13*, 1899.
34. Verdoes, M.; Willems, L. I.; van der Linden, W. A.; Duivenvoorden, B. A.; van der Marel, G. A.; Florea B. I.; Kisselev, A. F.; Overkleeft, H. S. *Org. Biomol. Chem.* **2010**, *8*, 2719.
35. Hanada, M.; Sugawara, K.; Kaneta, K.; Toda, S.; Nishiyama, Y.; Tomita, K.; Yamamoto, H.; Konishi, M.; Oki, T. *J. Antibiot*. **1992**, *45*, 1746.
36. Sin, N.; Kim, K. B.; Elofsson, M.; Meng, L.; Auth, H.; Kwok, B. H. B.; Crews, C. M. *Bioorg. Med. Chem. Lett.* **1999**, *9*, 2283.
37. Greenbaum, D.; Medzihradszky, K. F.; Burlingame, A.; Bogyo, M. *Chem. Biol.* **2000**, *7*, 569.
38. Verdoes, M. Thesis entitled *Chemical Tools To Probe The Proteasome*, Leiden University **2008**, Chapter 7, p. 127-138.
39. Aki, M.; Shimbara, N.; Takashina, M.; Akiyama, K.; Kagawa, S.; Tamura, T.; Tanahashi, N.; Yoshimura, T.; Tanaka, K.; Ichihara, A. *J. Biochem.* **1994**, *115*, 257.
40. Rock, K. L.; Goldberg, A. L. *Annu. Rev. Immunol.* ***1999****, 17*, 739.
41. Kloetzel, P. M.; Ossendorp, F. *Curr. Opin. Immunol.* **2004**, *16*, 76.
42. Bogyo, M.; Verhelst, S.; Bellingard-Dubouchaud, V.; Toba, S.; Greenbaum, D. *Chem. Biol.* **2000**, *7*, 27.
43. Hillaert, U.; Verdoes, M.; Florea, B. I.; Saragliadis, A.; Habets, K. L.; Kuiper, J.; van Calenbergh, S.; Ossendorp, F.; van der Marel, G. A.; Driessen, C.; Overkleeft, H. S. *Angew. Chem. Int. Ed.* **2009**, *48*, 1629.
44. Lennon-Duménil, A.-M.; Bakker, A. H.; Maehr, R.; Fiebiger, E.; Overkleeft, H. S.; Rosemblatt, M.; Ploegh, H. L.; Lagaudrière-Gesbert, C. *J. Exp. Med.* **2002**, *196*, 529.
45. Britton, M.; Lucas, M. M.; Downey, S. L.; Screen, M.; Pletnev, A. A.; Verdoes, M.; Tokhunts, R. A.; Amir, O.; Goddard, A. L.; Pelphrey, P. M.; Wright, D. L.; Overkleeft, H. S.; Kisselev, A. F. *Chem. Biol.* **2009**, *16*, 1278.
46. Verdoes, M.; Florea, B. I.; Hillaert, U.; Willems, L. I.; van der Linden, W. A.; Sae-Heng, M.; Filippov, D. V.; Kisselev, A. F.; van der Marel, G. A.; Overkleeft, H. S. *ChemBioChem* **2008**, *9*, 1735.
47. Kessler, B. M.; Tortorella, D.; Altun, M.; Kisselev, A. F.; Fiebinger, E.; Hekking, B. G.; Ploegh, H. L.; Overkleeft, H. S.; *Chem. Biol.* **2001**, *8*, 913.
48. Devaraj, N. K.; Hilderbrand, S.; Upadhyay, R.; Mazitschek, R.; Weissleder, R. *Angew. Chem. Int. Ed.* **2010**, *49*, 2869.
49. Rossin, R.; Verkerk, P. R.; van den Bosch, S. M.; Vulders, R. C. M.; Verel, I.; Lub, J.; Robillard, M. S. *Angew. Chem. Int. Ed.* **2010**, *49*, 3375.
50. Wessel, D.; Flügge, U. I. *Anal. Biochem.* **1984**, *138*, 141.

4

Triple bioorthogonal ligation strategy for simultaneous labeling of multiple enzymatic activities

Lianne I. Willems, Nan Li, Bogdan I. Florea, Mark Ruben, Gijsbert A. van der Marel, Herman S. Overkleeft, Angew. Chem. Int. Ed. ***2012****, 51, 4431-4434.*

4.1 Introduction

Bioorthogonal chemistry plays an important role in chemical biology research by creating the means to carry out selective chemical transformations in complex biological samples. A ligation reaction classifies as being bioorthogonal when it can be performed in a biological sample in a chemoselective manner without any interference with the biological system. Initially applied to the labeling of cell-surface glycoproteins,[1-3] nowadays bioorthogonal reactions are being used to study a wide variety of biological processes, for example those involving post-translational modifications.[4] The most widely used bioorthogonal ligation strategies include the Staudinger-Bertozzi ligaton, in which an azide is reacted with a phosphine reagent,[1,2] the azide-alkyne Huisgen [2+3] cycloaddition (also termed 'click' reaction), either catalyzed by copper(I)[5-7] or driven by ring strain,[8] and the inverse-electron-demand Diels-Alder reaction of tetrazine with a strained alkene.[9,10] Continuing efforts are being made to develop ligations that are more selective and efficient than existing methods. At the same time the high complexity of biological processes often requires the study of

multiple targets simultaneously, creating a need for ligation reactions that are orthogonal with respect to each other and can thus be used concurrently in a single experiment. Over the past decade, a number of tandem ligation strategies for use in bioconjugation has been described in literature.[11-17] In addition it has been demonstrated that the ligation of ketones with hydrazides can be performed together with the Staudinger-Bertozzi ligation for the simultaneous imaging of two different types of glycans on cell surfaces.[18] The first reported use of a tandem bioorthogonal ligation procedure in complex biological samples (cell lysates) is outlined in Chapter 3.[19] This strategy, which involves ensuing Staudinger-Bertozzi ligation and Diels-Alder [4+2] cycloaddition, utilizes mutually orthogonal reagents but suffers from the need to mask free thiols prior to the ligation step in order to avoid non-specific labeling. More recently it was reported that the copper-free azide-cyclooctyne cycloaddition can be used concurrently with an inverse-electron-demand Diels-Alder reaction between tetrazine and *trans*-cyclooctene for the simultaneous labeling of two different receptors on cell surfaces, provided that the proper reagents are carefully selected so that cross-reactivity is minimized.[20]

In this chapter a triple ligation strategy is described that employs the tetrazine ligation, Staudinger-Bertozzi ligation and copper(I)-catalyzed click reaction for the selective and simultaneous labeling of three different targets in a single experiment. To demonstrate the feasibility of this approach the triple ligation is applied to two-step activity-based protein profiling (ABPP), an area of research in which bioorthogonal chemistry is used to introduce a reporter group onto an enzyme active-site directed chemical probe (or activity-based probe, ABP) after binding of the probe to a target enzyme (Figure 4.1). The temporal separation of the ABP and the reporter entity which is thereby achieved is of particular interest when the presence of the tag interferes with selectivity, affinity, cell-permeability or bioavailability of the probe. A further advantage of two-step ABPP strategies as compared to direct labeling by a tagged ABP is the option to use different reporter groups depending on the experimental settings and the desired method of analysis while using a single ABP. Several examples of two-step ABPP strategies based on click chemistry[21] and Staudinger-Bertozzi ligation[22] have been described previously. The tetrazine ligation, however, has thus far not been used for this purpose.

The first part of this chapter describes the development of a tetrazine ligation strategy for two-step ABPP, in which an ABP functionalized with norbornene as a ligation handle is used to target a specific enzymatic activity after which reaction with a tetrazine reagent conjugated to a reporter group enables detection and analysis of the labeled proteins (Figure 4.1A). Similar to the development of the Diels-Alder ligation method described in

Chapter 3, the 20S proteasome is used as a model system. The 20S proteasome is a multi-subunit protein complex containing three catalytically active subunits (β1, β2 and β5) that have different substrate preferences and can be targeted by either broad-spectrum or subunit-specific ABPs.[23-27] Based on previously reported mechanism-based inhibitors, two proteasome ABPs were designed that are functionalized with norbornene as a ligation handle (**1** and **2**, Figure 4.2). ABP **1** is derived from the pan-reactive proteasome inhibitor epoxomicin[28,29] while ABP **2** has a different scaffold based on a β5 subunit-selective proteasome inhibitor.[27] In addition, three tetrazine reagents were designed that are functionalized with different fluorescent tags, BodipyTMR (**3a**) and BodipyFL (**3b**), or a biotin tag (**3c**). With these probes, the use of the tetrazine ligation for the profiling of endogenous proteasome activity in cell extracts and cultured cells is demonstrated. In the second part of this chapter the developed tetrazine labeling procedure is combined with two established ligation methods in a tandem ligation strategy for the simultaneous labeling of three different enzymatic activities in the same sample (Figure 4.1B).

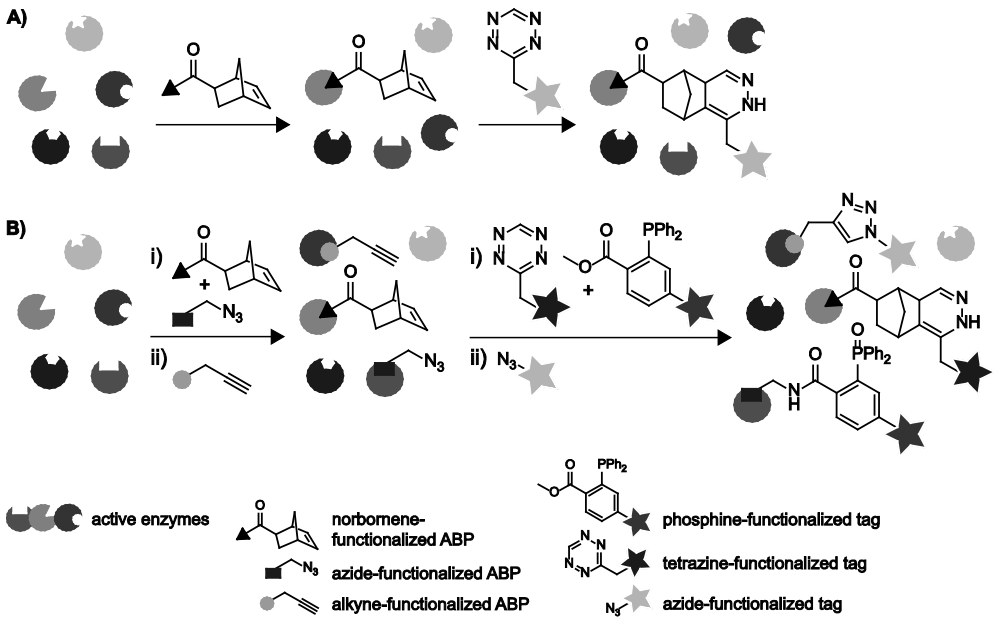

Figure 4.1. The tetrazine ligation in activity-based protein profiling. A) Schematic representation of a two-step labeling strategy based on the tetrazine-norbornene cycloaddition. B) Schematic representation of a triple bioorthogonal ligation strategy involving tetrazine ligation, Staudinger-Bertozzi ligation and copper(I)-catalyzed click reaction for simultaneous labeling of multiple enzymatic activities. ABP: activity-based probe.

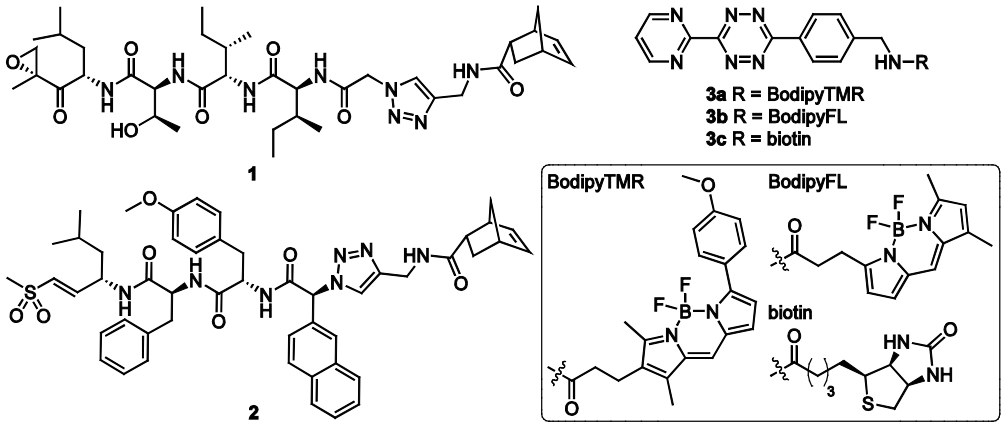

Figure 4.2. Structures of target compounds: norbornene-functionalized proteasome ABPs **1** and **2** and tetrazines derivatized with two different Bodipy fluorophores (**3a**, **3b**) or a biotin tag (**3c**).

4.2 Results and discussion

The synthetic routes towards norbornene-functionalized epoxomicin derivative **1** and vinyl sulfone **2** are depicted in Schemes 4.1 and 4.2, respectively. It was envisioned that an alkyne-functionalized norbornene moiety would enable facile coupling of the ligation handle to the respective azide-functionalized inhibitors by copper(I)-catalyzed click reaction. Hence, the synthetic strategy commenced with the conversion of commercially available norbornene-carboxylic acid **4** into succinimidyl ester **5** (Scheme 4.1). The endo and exo isomers of the acid (**4**) and the OSu ester (**5**) could not be separated. However, reaction of **5** with propargylamine resulted in a mixture of alkyne-functionalized products **6** (endo) and **7** (exo) that proved to be easily separable by column chromatography. The major isomer, endo-norbornene-alkyne **6**, was then used for a copper(I)-catalyzed click reaction with previously reported azide-modified inhibitor **9**,[30] which was in turn obtained from tetrapeptide epoxyketone **8**,[31] to provide ABP **1**. As a starting point for the synthesis of putative β5-selective proteasome ABP **2** the previously described tripeptide vinyl sulfone **12** was used (Scheme 4.2).[27] Norbornene-alkyne **6** was first coupled via a copper(I)-catalyzed click reaction to azido-naphthalenyl-acetic acid **10**,[32] after which the resulting norbornene building block **11** was condensed with the deprotected vinyl sulfone tripeptide to give norbornene-functionalized probe **2**. It should be noted that compound **6** consists of two enantiomers so that norbornene-equipped probes **1** and **2** are both obtained as a mixture of two diastereomers. No attempts were made to separate these isomers as it was assumed that the stereochemistry at this position would not profoundly affect the inhibitory potency of the probes or the ligation efficiency with tetrazine.

Scheme 4.1 Synthesis of norbornene-functionalized proteasome ABP **1**

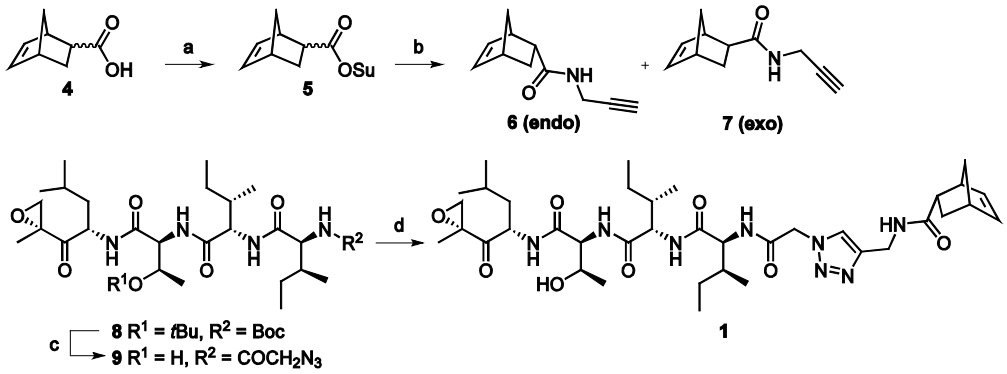

Reagents and conditions: a) *N*-HOSu, EDC.HCl, DCE, rt, overnight, 74%; b) propargyl amine, DiPEA, DCE, rt, 3 hrs, **6** 65%, **7** 13%; c) *i*) TFA, rt, 30 min, *ii*) 2-azidoacetyl-OSu, DiPEA, DCE, rt, 4 hrs, 88 %; d) **6**, $CuSO_4.H_2O$, sodium ascorbate, *t*BuOH/H_2O/toluene (1/1/1, v/v/v), 80 °C, overnight, 47%.

The key step in the route towards tetrazine reagents **3a**-**c** is the generation of the 1,2,4,5-tetrazine moiety. The synthesis of asymmetrically substituted tetrazines can be accomplished by reaction of two appropriately substituted nitriles with hydrazine, resulting in the formation of a dihydrotetrazine intermediate via several condensation and elimination steps, followed by oxidation with sodium nitrite in acetic acid to afford the tetrazine product.[33,34] Generally the yield of these reactions is rather low, which is at least

Scheme 4.2 Synthesis of norbornene-functionalized proteasome ABP **2**

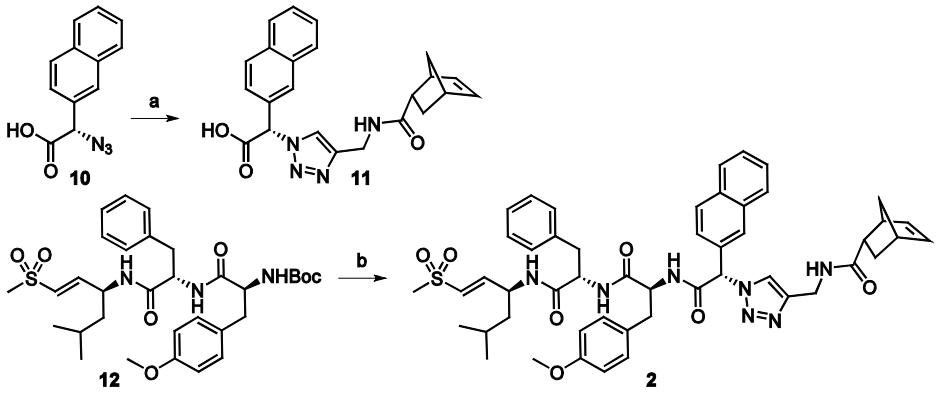

Reagents and conditions: a) **6**, $CuSO_4.H_2O$, sodium ascorbate, DMF, 80 °C, overnight, 59%; b) *i*) TFA/DCM (1/1, v/v), rt, 30 min, *ii*) **11**, HCTU, DiPEA, DMF, rt, 5 hrs, 60%.

partly due to the formation of symmetrically substituted byproducts. In a first attempt to synthesize tetrazines **3a**-**c**, a mixture of 4-aminomethylbenzonitrile (**13**) and 2-cyanopyrimidine (**14**) was refluxed with hydrazine hydrate in ethanol and then oxidized by careful addition of sodium nitrite in aqueous acetic acid (Scheme 4.3). Instead of compound **15**, however, an unexpected product was isolated in which the primary amine had been converted into a hydroxyl group (**16**). A possible explanation for this conversion is that the primary amine, upon addition of the acidic solution of sodium nitrite to the dihydrotetrazine intermediate, reacts with NO^+ and forms a diazonium species which is then susceptible to nucleophilic attack by a water molecule. In line with this hypothesis, other tetrazine products isolated after this reaction included the symmetrical dihydroxy tetrazine as well as acetyloxy-substituted tetrazine products resulting from reaction of the diazonium species with acetic acid. It was found that these side reactions could be prevented by first dissolving the dihydrotetrazine intermediate in acetic acid before addition of the oxidizing reagent, in which case alcohol **16** was not detected and amine-functionalized tetrazine **15** was formed instead. In order to further minimize side reactions and also facilitate purification procedures, the primary amine in **13** was protected with a Boc group (**17**) prior to tetrazine formation. Reaction of **17** with **14** and an excess of hydrazine hydrate followed by oxidation with sodium nitrite in acetic acid provided Boc-protected tetrazine **18**. After deprotection, the free amine was reacted with BodipyTMR-OSu,[25] BodipyFL-OSu[35] or biotin-OSu to afford the tagged tetrazines **3a**-**c**.

Scheme 4.3 Synthesis of Bodipy-tagged tetrazines **3a** and **3b** and biotinylated tetrazine **3c**

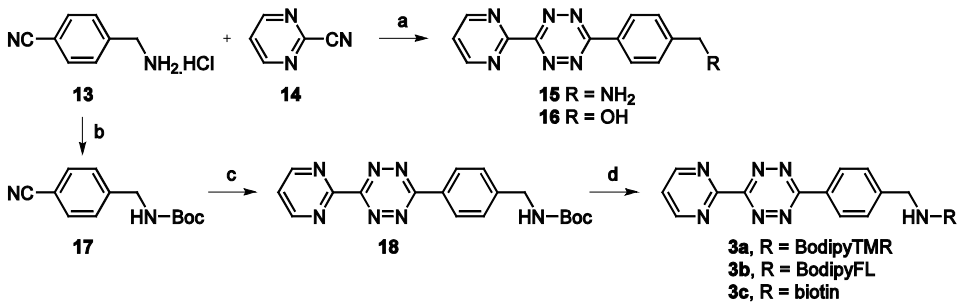

Reagents and conditions: a) *i*) $H_2NNH_2.H_2O$, EtOH, 80 °C, overnight, *ii*) $NaNO_2$, AcOH/H_2O (1/1, v/v), 0 °C, 15 min, **15** 0%, **16** 5%; b) Boc_2O, Et_3N, DCM, rt, overnight, quant.; c) *i*) **14**, $H_2NNH_2.H_2O$, EtOH, 70 °C, 24 hrs, *ii*) AcOH, then $NaNO_2$, H_2O, 0 °C, 15 min, 11%; d) *i*) TFA/DCM (1/1, v/v), rt, 15 min, *ii*) BodipyTMR-OSu (**a**), BodipyFL-OSu (**b**) or biotin-OSu (**c**), DiPEA, DCE/DMF, rt, overnight, **3a** 79%, **3b** 63%, **3c** 49%.

Before using the synthesized probes in two-step labeling experiments, the ability of the norbornene-functionalized ABPs **1** and **2** to inhibit the activity of the 20S proteasome in cell extracts and cultured cells was evaluated. HEK cell extracts were exposed to increasing concentrations of probes **1** and **2**, after which the residual proteasome activity was labeled with MV151,[25] a fluorescently labeled ABP that targets the catalytically active proteasome β-subunits β1, β2 and β5 (Figure 4.3A). The fluorescent labeling was completely abolished by preincubation with 1 μM of ABP **1**, revealing that this probe is an irreversible inhibitor of all three proteolytically active proteasome β-subunits. ABP **2**, on the other hand, only blocked the fluorescent labeling of a single band corresponding to β5, which indicates that this probe is a β5-subunit selective proteasome inhibitor. Similar results were obtained by treatment of cultured HEK cells with **1** or **2** followed by cell lysis and labeling with MV151 (Figure 4.3B). Both norbornene-functionalized probes were able to inhibit proteasome activity *in situ* and are thus cell-permeable. As before, ABP **1** reduced the fluorescent labeling of all three catalytically active proteasome β-subunits, although no complete inhibition was reached up to a concentration of 50 μM. ABP **2** appeared to inhibit β5 completely at the lowest concentration tested (1 μM) and did not affect the labeling of the other proteasome β-subunits.

Having established the inhibitory potency of the norbornene-derivatized ABPs, the applicability of the tetrazine ligation for two-step labeling of endogenous proteasome activity *in vitro* and *in situ* was examined. HEK cell extracts were treated with norbornene-functionalized ABP **1** at a concentration at which it completely inhibits proteasome activity, and subsequently reacted with varying concentrations of one of the tetrazine reagents **3a**-**c** for 1 hr at 37 °C (Figures 4.4A-C). Ligation with all three tetrazine reagents resulted in the

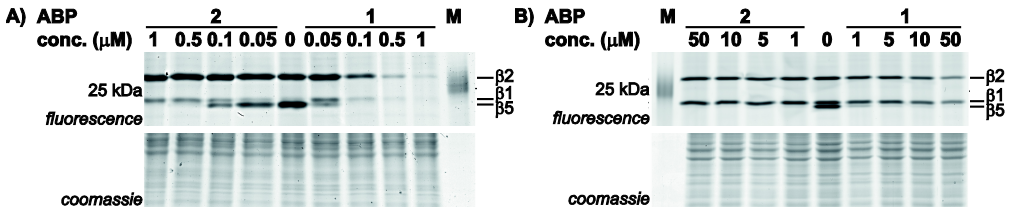

Figure 4.3. Inhibition of proteasome activity by probes **1** and **2**. A) HEK cell lysates labeled with 1 μM MV151 for 1 hr after preincubation with 0.05 - 1 μM of compounds **1** or **2** for 1 hr. B) Cultured HEK cells were treated with 1 - 50 μM of compounds **1** or **2** for 4 hrs. After cell lysis residual proteasome activity was labeled with 1 μM MV151 for 1 hr. Gels are 12.5% SDS-PAGE with fluorescent readout followed by coomassie brilliant blue staining. Proteasome β-subunits are designated on the basis of reported labeling by MV151.[25] 'conc.': probe concentration. 'M': protein marker.

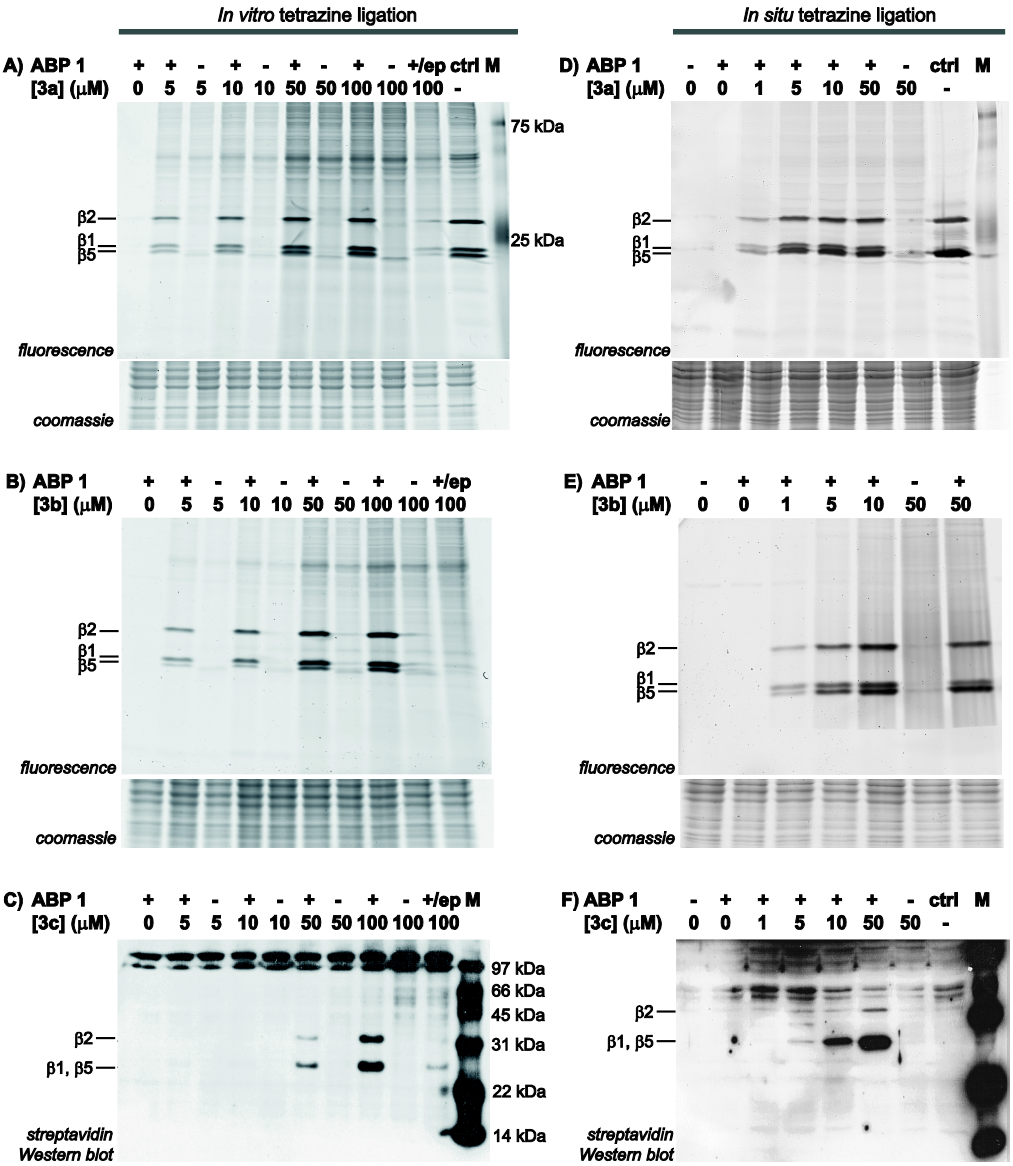

Figure 4.4. *In vitro* and *in situ* labeling of proteasome activity by tetrazine ligation. A-C) HEK cell extracts were exposed to 1 μM of ABP **1** for 1 hr and then incubated with 5 - 100 μM of tetrazines **3a**-**c** for 1 hr. D-F) Cultured HEK cells were exposed to 10 μM of ABP **1** for 3 hrs, incubated with 1 - 50 μM of tetrazines **3a**-**c** for 1 hr and lysed. Proteins were resolved by 12.5% SDS-PAGE and detected by in-gel fluorescent readout in Cy3 (**3a**, panels A and D) and Cy2 (**3b**, panels B and E) channels or by streptavidin Western blotting (**3c**, panels C and F). Coomassie brilliant blue staining was used as a loading control (A, B, D, E). 'ctrl': control extracts or cells labeled with 1 μM MV151. 'ep': 100 μM epoxomicin added to incubation with ABP **1**. 'M': protein marker.

labeling of the three catalytically active proteasome β-subunits in a concentration-dependent manner.[36] The high selectivity and specificity of the ligation reaction is apparent from the absence of proteasome labeling and low degree of background labeling in the absence of the norbornene-functionalized ABP (**1**) and when proteasome activity is inhibited by an excess of epoxomicin. Comparison of the labeling intensity in samples treated with tetrazine **3a** to that obtained by direct labeling with the fluorescent ABP MV151, which contains the same Bodipy(TMR) tag as **3a**, revealed that under these conditions the ligation reaction appears to reach completion at a tetrazine concentration of 50 μM and higher (Figure 4.4A). Ligation with tetrazine-BodipyFL **3b** appeared to proceed with similar efficiency as with **3a** (Figure 4.4B). In case of biotinylated tetrazine **3c**, however, the relatively low labeling intensity after treatment with 50 μM of the probe as compared to reaction with 100 μM of the reagent indicates that this reagent reacts less efficiently than the fluorescently labeled tetrazines (Figure 4.4C).

Next, the efficacy of the tetrazine ligation inside living cells was evaluated. Cultured HEK cells were incubated with ABP **1**, washed and subsequently exposed to varying concentrations of tetrazines **3a**-**c** for 1 hr. After cell lysis the labeled proteins were analyzed by SDS-PAGE (Figures 4.4D-F). *In situ* tetrazine ligation with fluorescently labeled tetrazines **3a** and **3b** resulted in efficient labeling of the active proteasome β-subunits, with labeling visible at tetrazine concentrations as low as 1 μM. This demonstrates that the tetrazine probes are cell-permeable and that the ligation reaction can be performed successfully inside living cells. Furthermore, the ligation proceeded with very high selectivity and even less non-specific labeling than in cell lysates. A reduced cell-permeability of the biotin-functionalized tetrazine reagent (**3c**) as compared to the fluorescently labeled tetrazines is presumably at the basis of its lower labeling efficiency.

In an attempt to further improve the tetrazine-mediated labeling in cell extracts, the reaction time and temperature of the ligation step were varied (Figures 4.5A and 4.5C). In addition, the compatibility of the tetrazine ligation with buffers of various pH values ranging from pH 4 to pH 8 was tested (Figure 4.5B). When using 50 μM of tetrazine **3a**, labeling of the active proteasome β-subunits was visible within 30 minutes and appeared to be complete within 1-2 hrs. No marked effects of pH on reaction efficiency or selectivity were found. Similarly, no profound differences were detected when performing the reaction at room temperature instead of 37 °C. However, at higher temperature (50 °C) or a prolonged reaction time (overnight) an enhanced degree of non-specific labeling was observed. Therefore, all ensuing tetrazine ligation reactions were carried out at 37 °C for 1 hr.

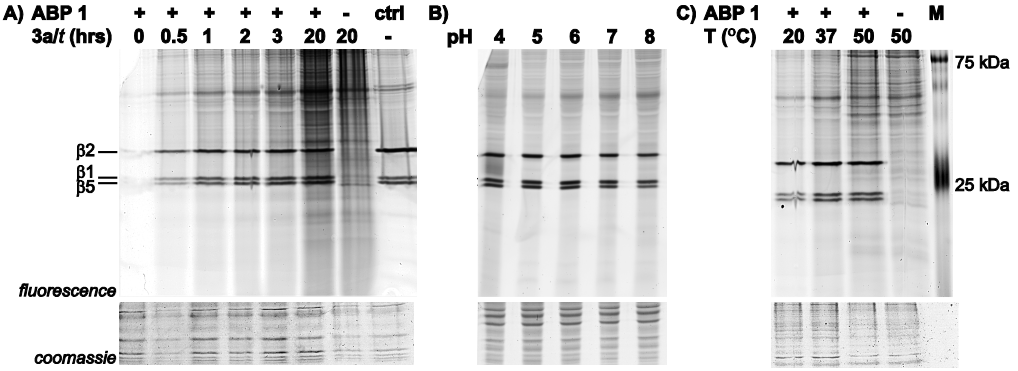

Figure 4.5. Optimization of *in vitro* tetrazine ligation conditions. Labeling in HEK cell extracts using 1 µM of ABP **1** followed by reaction with A) 50 µM of tetrazine **3a** for 0.5 - 20 hrs (37 °C, pH 7.5), B) 10 µM **3a** for 1 hr in buffers of varying pH (37 °C), or C) 50 µM **3a** for 1 hr at 20 - 50 °C (pH 7.5). Gels are 12.5% SDS-PAGE with fluorescent readout followed by coomassie brilliant blue staining. 'ctrl': control sample labeled with 1 µM MV151. 'M': protein marker.

In a next set of experiments the tetrazine ligation was compared to three other commonly used ligation methods, the Staudinger-Bertozzi ligation, the copper(I)-catalyzed click reaction and the strain-promoted click reaction, by applying the four different ligation reactions to the two-step labeling of proteasome activity in cell extracts. For this purpose two epoxomicin derivatives were designed that are similar to norbornene-functionalized ABP **1** but are equipped with either an azide or an alkyne as the ligation handle (compounds **9** and **19**, respectively, Figure 4.6). Azide-modified ABP **9** is a known inhibitor of the three

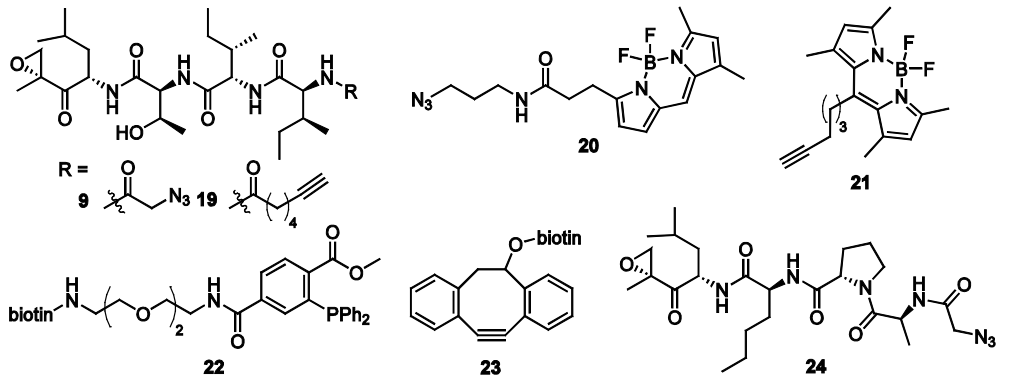

Figure 4.6. Structures of azide- and alkyne-functionalized proteasome ABPs **9** and **19**, Bodipy-tagged azide (**20**) and alkyne (**21**) reagents for copper(I)-catalyzed click reaction, biotin-phosphine **22** for Staudinger-Bertozzi ligation, biotin-dibenzocyclooctyne **23** for strain-promoted click reaction, and azide-derivatized β1-selective proteasome ABP **24**.

Scheme 4.4 Synthesis of alkyne-functionalized proteasome ABP **19** and azido-BodipyFL **20**

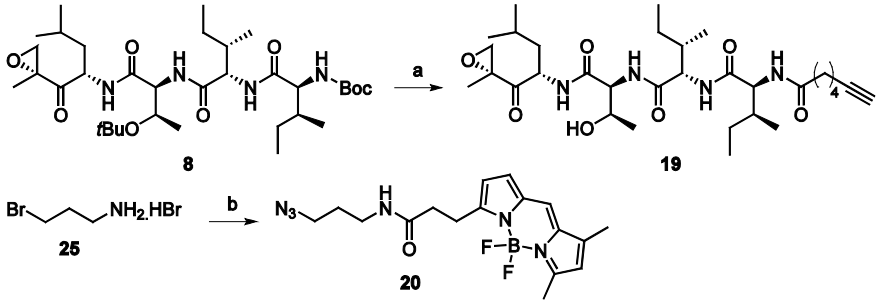

Reagents and conditions: a) *i*) TFA, rt, 30 min, *ii*) 6-heptynoyl-OSu, DiPEA, DCE, rt, overnight, 87%; b) *i*) NaN_3, DMF, rt, overnight, *ii*) BodipyFL-OSu, DiPEA, DCE/DMF, rt, 5 hrs, 99%.

proteolytically active proteasome β-subunits[30] and was generated in the synthetic route towards ABP **1** (see Scheme 4.1). Alkyne-functionalized ABP **19** was synthesized from tetrapeptide epoxyketone **8** by deprotection and subsequent reaction of the primary amine with the succinimidyl ester of 6-heptynoic acid[37] (Scheme 4.4). A competition experiment confirming the ability of ABP **19** to inhibit the catalytically active proteasome β-subunits in HEK cell extracts is shown in Figure 4.7. In addition to the ABPs, a number of Bodipy- and biotin-tagged reagents was selected to enable two-step labeling via the various ligation reactions (**20**-**23**, Figure 4.6). Reagents **21**,[30] **22**[38] and **23**[39] have been reported previously. Azido-BodipyFL **20** was synthesized in two steps from 3-bromopropanamine (**25**) in near quantitative yield (Scheme 4.4).

With all probes in hand, two-step labeling experiments were carried out by exposure of cell extracts to ABPs **1**, **9** or **19** followed by reaction with one of the ligation reagents **3b**-**c** or **20**-**23** (Figure 4.8). Labeling via tetrazine ligation with norbornene-derivatized ABP **1** and biotinylated tetrazine **3c** gave similar results in terms of selectivity and efficiency to

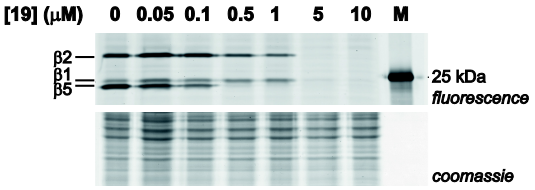

Figure 4.7. Inhibition of proteasome activity by probe **19**. HEK cell lysates were treated with 0.05 - 10 μM of compound **19** for 1 hr and then labeled with 1 μM MV151 for 1 hr. Proteins were resolved by 12.5% SDS-PAGE and detected by in-gel fluorescent readout followed by coomassie brilliant blue staining. 'M': protein marker.

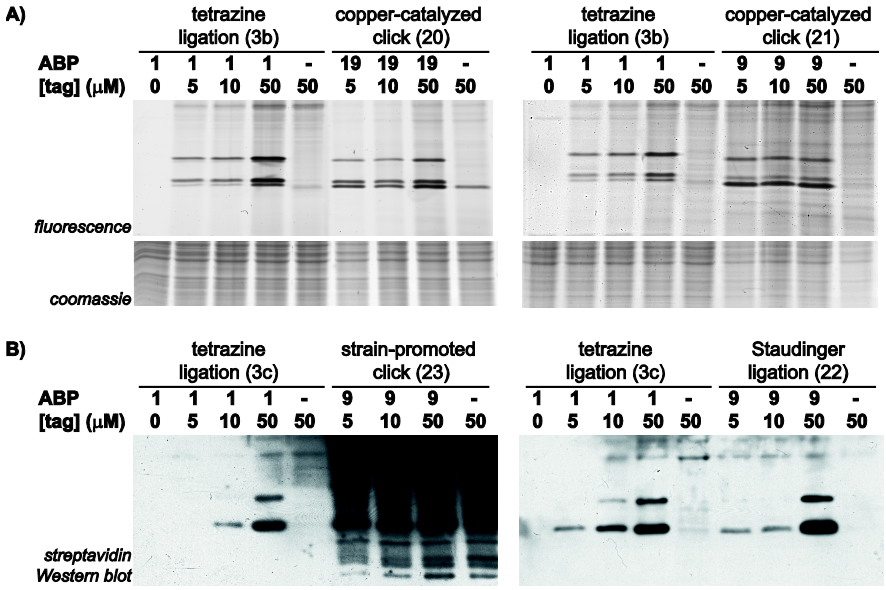

Figure 4.8. Comparison of various ligation strategies. HEK cell extracts were exposed to 1 μM of ABPs **1**, **9** or **19** for 1 hr and then reacted with 5 - 50 μM of tetrazines **3b** or **3c**, Bodipy-azide **20**, Bodipy-alkyne **21**, biotin-phosphine **22**, or biotin-dibenzocyclooctyne **23** for 1 hr. Copper(I)-catalyzed click reactions with **20** and **21** were performed in the presence of 1 mM $CuSO_4$, 1 mM TCEP and 100 μM TBTA. Proteins were resolved by 12.5% SDS-PAGE and detected by A) in-gel fluorescent readout (**3b**, **20**, **21**) followed by coomassie brilliant blue staining or B) streptavidin Western blotting (**3c**, **22**, **23**).

Staudinger-Bertozzi ligation with azide-functionalized ABP **9** and biotin-phosphine **22**. Additionally, tetrazine ligation with Bodipy(FL)-tetrazine **3b** appeared to proceed with comparable efficiency to the copper(I)-catalyzed click procedures with either ABP **9** and Bodipy-alkyne **21** or ABP **19** and Bodipy-azide **20**. A remarkable difference between the two copper-catalyzed click reactions is the degree of background fluorescence, as the combination of azide-functionalized ABP **9** and alkyne-Bodipy **21** gave more background labeling than the click procedure using alkyne-ABP **19** and azido-Bodipy **20**. Attempts to label proteasome activity via strain-promoted click reaction with biotinylated dibenzocyclooctyne **23** resulted in a very high amount of background labeling in which specific signals were not detectable. This result confirms previous findings that strain-promoted click procedures are poorly compatible with cell extracts.[40]

Having established the utility of the tetrazine ligation strategy for two-step profiling of endogenous proteasome activity, the final part of this chapter focuses on the development of a triple ligation strategy. First, the orthogonality of the tetrazine ligation with respect to the Staudinger-Bertozzi ligation and the copper(I)-catalyzed click reaction was

demonstrated. Potential cross-reactivity between norbornene-, azide- and alkyne-tagged proteasome ABPs (**1**, **9** and **19**, respectively) and azide, alkyne, phosphine and tetrazine reagents (**20**, **21**, **22** and **3b**, respectively) was evaluated by performing two-step proteasome labeling experiments in cell extracts with different combinations of the probes (Figure 4.9A). As before, labeling of the catalytically active proteasome β-subunits was obtained by exposure of cell extracts to ABP **1** followed by reaction with **3b**, as well as by making use of probes **19** and **20**, **9** and **21** or **9** and **22**. No cross-reactivity could be detected when any of the other probe combinations was used, which opens up the possibility to perform all three ligation reactions simultaneously. However, it was found that background fluorescence caused by the fluorescently labeled tetrazine reagent is drastically increased when it is mixed with the click cocktail for copper(I)-catalyzed click reactions, to such an extent that specific labeling is no longer detectable (Figure 4.9B). An investigation of the compatibility of tetrazine labeling with the separate click reagents revealed that the high degree of background fluorescence is caused by the presence of copper sulfate. As a result, the tetrazine ligation and the copper(I)-catalyzed click reaction can not be performed at the same time. Nevertheless a triple ligation experiment can be designed in which these two reactions are carried out consecutively so that the copper catalyst does not interfere with labeling by the tetrazine reagent.

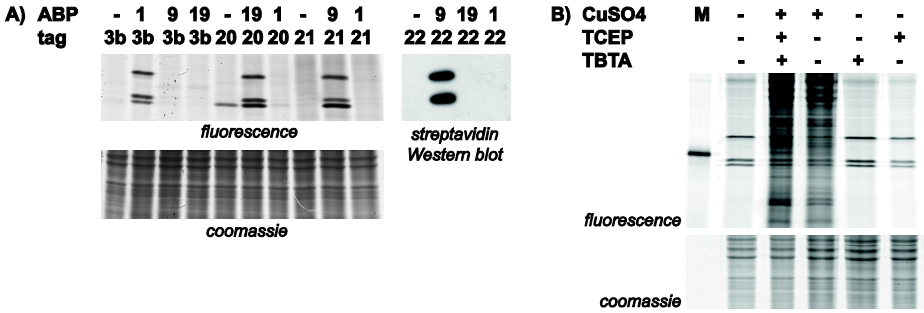

Figure 4.9. Orthogonality of tetrazine ligation, Staudinger-Bertozzi ligation and copper(I)-catalyzed click reaction. A) Labeling in HEK cell extracts using 1 µM of ABPs **1**, **9** or **19** followed by reaction with 50 µM of tetrazine **3b**, azide **20**, alkyne **21** or phosphine **22** for 1 hr. Click reactions with **20** and **21** were performed in the presence of 1 mM $CuSO_4$, 1 mM TCEP and 100 µM TBTA. B) Tetrazine ligation in HEK cell extracts using 1 µM of ABP **1** followed by reaction with 50 µM of tetrazine **3a** in the presence of 1 mM $CuSO_4$, 1 mM TCEP and/or 100 µM TBTA. Labeled proteins were resolved by 12.5% SDS-PAGE and detected by in-gel fluorescent readout in Cy3 (**3a**) and Cy2 (**3b**, **20**, **21**) channels or by streptavidin Western blotting (**22**). Coomassie brilliant blue staining was used as a loading control. 'M': protein marker.

In a seminal experiment, a triple ligation strategy that combines the tetrazine ligation, the Staudinger-Bertozzi ligation and the copper(I)-catalyzed click reaction was used to label the three proteolytically active proteasome β-subunits each with a different tag via one of the different ligation reactions. In order to enable separate labeling of the β-subunits, the β5-subunit selective norbornene-functionalized ABP **2** was used together with the β1-selective azide-functionalized proteasome probe **24**[32] (Figure 4.6). After exposure of cell extracts to probes **2** and **24**, alkyne-derivatized ABP **19** was added which could then only bind to the non-occupied proteasome β2-subunits. This sequence of addition should lead to the selective tagging of β1-subunits with an azide, β2-subunits with an alkyne and β5-subunits with a norbornene moiety. Next, the lysates were exposed to tetrazine-BodipyTMR **3a** and biotin-phosphine **22** for 1 hr, after which the excess of the reagents was removed by buffer exchange and lastly copper(I)-catalyzed click ligation was performed with azido-BodipyFL **20** for 1 hr. In this procedure, the washing step in between the ligation reactions is necessary to remove both the excess of tetrazine before addition of the copper catalyst as well as the excess of phosphine which might otherwise react with the azido-Bodipy reagent and thereby interfere with the click reaction. The use of two different Bodipy fluorophores and a biotin tag enables the separate visualization of the proteins labeled by each of the ligation reactions by using in-gel fluorescence scanning with two different scanner settings followed by streptavidin Western blotting. As shown in Figure 4.10, the three ligation reactions each resulted in the selective labeling of a single proteasome subunit. Tetrazine-BodipyTMR **3a** selectively labeled the proteasome β5-subunits by reaction with norbornene-ABP **2**, while β1-subunits were labeled by Staudinger-Bertozzi ligation of azido-ABP **24** with biotin-phosphine **22** and β2-subunits were labeled by copper(I)-catalyzed click reaction of alkyne-ABP **19** and azido-Bodipy **20**. The results obtained by performing all ligation reactions in the same sample were similar to those of the separate ligation reactions, demonstrating the value of the tandem labeling strategy for the selective labeling of three different catalytic activities in a single experiment.

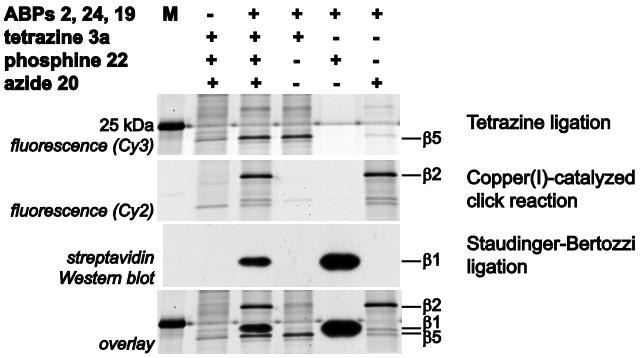

Figure 4.10. Triple ligation strategy. HEK cell extracts were exposed to 1 µM of β5-selective proteasome ABP **2** and 5 µM of β1-selective ABP **24** followed by 1 µM of ABP **19**, treated with 25 µM of tetrazine **3a** and 100 µM of phosphine **22** and subsequently reacted with 25 µM of azide **20** in the presence of 1 mM $CuSO_4$, 1 mM TCEP, and 100 µM TBTA. Proteins were resolved by 12.5% SDS-PAGE with fluorescent readout in Cy3 (**3a**) and Cy2 (**20**) channels followed by streptavidin Western blotting (**22**). 'M': protein marker.

4.3 Conclusion

A two-step ABPP strategy was developed that is based on the inverse-electron-demand Diels-Alder reaction of tetrazine with norbornene. Incorporation of norbornene into an ABP that targets the catalytically active proteasome β-subunits enabled the labeling of endogenous proteasome activity by reaction with fluorescently labeled or biotin-tagged tetrazines. The tetrazine ligation proceeds with high selectivity in cell extracts and inside living cells and forms a valuable complement to existing two-step ABPP methods. The reagents used for the tetrazine ligation were shown to be orthogonal to those used in Staudinger-Bertozzi ligation and copper(I)-catalyzed click reactions. Although tetrazines are not directly compatible with copper-catalyzed click chemistry, this drawback can easily be overcome by a simple washing step between the two ligation reactions which allows their consecutive use in the same experiment. A triple ligation strategy combining the tetrazine ligation, the Staudinger-Bertozzi ligation and the copper(I)-catalyzed click reaction was used for the simultaneous labeling of three enzymatic activities with different tags in a single experiment. This tandem ligation strategy will not only be useful for application in ABPP but also for the study of other biological processes such as post-translational modifications, enabling the selective monitoring of multiple targets at the same time in complex biological samples. Moreover, the possibility to perform both tetrazine and Staudinger-Bertozzi ligations inside living cells[22,41] and in living animals[3,42] should enable the use of tandem labeling procedures *in vivo*.[43]

Experimental procedures

A. Synthesis

General

All reagents were commercial grade and were used as received unless stated otherwise. MeOH was obtained from Biosolve. Toluene, EtOAc and PetEt (Riedel-de Haën) used for column chromatography were of technical grade and distilled before use. DCE, DCM, DMF, and THF (Biosolve) were of analytical grade and when used under anhydrous conditions stored over flame-dried 4 Å molecular sieves. Reactions were monitored by TLC-analysis using DC-alufolien (Merck, Kieselgel60, F254) with detection by UV-absorption (254/366 nm), spraying with a solution of 20% H_2SO_4 in EtOH or a solution of $(NH_4)_6Mo_7O_{24}{\cdot}4H_2O$ (25 g/L) and $(NH_4)_4Ce(SO_4)_4{\cdot}2H_2O$ (10 g/L) in 10% aqueous sulfuric acid followed by charring at ~150 °C or by spraying with an aqueous solution of $KMnO_4$ (7%) and K_2CO_3 (2%). Column chromatography was performed on silica gel (Screening Devices BV, 0.040 - 0.063 mm, 60 Å). LC/MS analysis was performed on an LCQ Adventage Max (Thermo Finnigan) ion-trap spectrometer (ESI+) coupled to a Surveyor HPLC system (Thermo Finnigan) equipped with a C18 column (Gemini, 4.6 mm x 50 mm, 5µm particle size, Phenomenex). The applied buffers were A: H_2O, B: ACN and C: 1 % aqueous TFA. Reported gradients represent the percentage of buffer B in buffer A with 10% buffer C. HRMS analysis was performed on an LTQ Orbitrap (Thermo Finnigan) mass spectrometer equipped with an electronspray ion source in positive mode (source voltage 3.5 kV, sheath gas flow 10 mL min−1, capillary temperature 250 °C) with resolution R = 60000 at m/z 400 (mass range m/z = 150 - 2000) and dioctylphtalate (m/z = 391.28428) as a "lock mass". The high resolution mass spectrometer was calibrated prior to measurements with a calibration mixture (Thermo Finnigan). ^{1}H- and ^{13}C-APT-NMR spectra were recorded on a Brüker AV-400 (400/100MHz) or a Bruker DMX600 (600/150 MHz) instrument with a cryoprobe. Chemical shifts are given in ppm (δ) relative to the solvent peak or to tetramethylsilane as internal standard. Coupling constants (*J*) are given in Hz. All presented ^{13}C-APT spectra are proton decoupled. Peak assignments are based on 2D ^{1}H-COSY and ^{13}C-HSQC NMR experiments.

5-Norbornene-2-carboxylic acid succinimidyl ester (5)

To a solution of 5-norbornene-2-carboxylic acid **4** (mixture of endo and exo, predominantly endo) (10 mmol, 1.25 mL) in DCE under argon atmosphere was added EDC.HCl (40 mmol, 7.7 g, 4.0 eq.) and *N*-HOSu (40 mmol, 4.6 g, 4.0 eq.). The reaction mixture was stirred overnight at room temperature, washed with 1 M HCl (3x), dried over anhydrous MgSO4, filtered and concentrated *in vacuo*. The crude product was purified by column chromatography (PetEt → PetEt/EtOAc 2/1 (v/v)), yielding succinimidyl ester **5** (mixture of endo and exo) as a white powder (1.75 g, 7.4 mmol, 74%). R_f 0.4 (PetEt/EtOAc 2/1). ^{1}H NMR (400 MHz, $CDCl_3$): δ (ppm) 6.26-6.20 (m, 1H), 6.16-6.12 (m, 1H), 3.42-3.40 (m, 1H), 3.27-3.23 (m, 1H), 3.00-2.98 (m, 1H), 2.84-2.81 (m, 4H), 2.07-1.99 (m, 1H), 1.56-1.44 (m, 2H), 1.36-1.33 (m, 1H). ^{13}C NMR (100 MHz, $CDCl_3$): δ (ppm) 169.91, 169.29, 138.48, 138.07, 135.20, 132.09, 49.58, 47.06, 46.37, 46.33, 42.44, 41.70, 40.53, 40.21, 30.90, 29.49, 25.54, 25.51.

***N*-(2-propynyl)-5-norbornene-2-carboxamide (6 and 7)**

To a solution of norbornene-OSu **5** (mixture of endo and exo) (2.0 mmol, 0.47 g) in DCE under argon atmosphere was added propargyl amine (2.0 mmol, 0.11 g, 1.0 eq.) and DiPEA (5.0 mmol, 0.87 mL, 2.5 eq.). The reaction mixture was stirred at room temperature for 3 hrs before being concentrated *in vacuo*. The crude product was purified by column chromatography (PetEt → 15% EtOAc in PetEt), followed by recrystallization from EtOAc/PetEt to give **6** and **7** separately as white crystals. Based on the endo/exo ratio in the starting material, the larger product batch was designated the endo product **6** (0.24 g, 1.3 mmol, 65%) and the smaller batch the exo product **7** (43 mg, 0.25 mmol, 13%). R_f **6** 0.25/**7** 0.4 (PetEt/EtOAc 4/1). ^{1}H NMR (400 MHz, $CDCl_3$) **6**: δ (ppm) 6.25-6.23 (m, 1H), 6.00-5.98 (m, 2H),

4.00 (dd, *J* = 5.2, 2.4 Hz, 2H), 3.17-3.16 (m, 1H), 2.92-2.88 (m, 2H), 2.22 (t, *J* = 2.4 Hz, 1H), 1.97-1.90 (m, 1H), 1.47-1.44 (m, 1H), 1.40-1.36 (m, 1H), 1.31-1.29 (m, 1H). ^{1}H NMR (400 MHz, $CDCl_3$) **7**: δ (ppm) 6.16-6.14 (m, 1H), 6.11-6.09 (m, 1H), 5.88 (s, 1H), 4.07 (dd, *J* = 5.2, 2.4 Hz, 2H), 2.96-2.93 (m, 2H), 2.24 (t, *J* = 2.4 Hz, 1H), 2.05-2.01 (m, 1H), 1.95-1.90 (m, 1H), 1.72-1.70 (m, 1H), 1.37-1.31 (m, 2H). ^{13}C NMR (100 MHz, $CDCl_3$) **6**: δ (ppm) 173.96, 137.72, 132.00, 79.81, 71.13, 49.86, 46.09, 44.44, 42.58, 29.59, 28.96. ^{13}C NMR (100 MHz, CDCl3) **7**: δ (ppm) 175.28, 138.28, 135.85, 79.75, 71.44, 47.03, 46.28, 44.41, 41.50, 30.41, 29.25. LC/MS analysis: **6**: R_t 5.0 min (linear gradient 10 → 90% B in 15 min), m/z 176.0 $[M+H]^+$, 350.8 $[2M+H]^+$; **7**: R_t 5.7 min (linear gradient 10 → 90% B in 15 min), m/z 175.9 $[M+H]^+$. HRMS: calcd. for $[C_{12}H_{14}NO]^+$ 176.10699, found **6** 176.10684, **7** 176.10682.

***N*-(2-azidoacetyl)-Ile-Ile-Thr-leucinyl-2-methyloxirane (9)**

Tetrapeptide epoxyketone **8**[31] (0.33 g, 0.50 mmol) was deprotected with TFA for 30 min at room temperature before being concentrated in the presence of toluene. The TFA salt of the deprotected compound was redissolved in DCE under argon atmosphere and DiPEA (0.17 mL, 1.0 mmol, 2.0 eq.) and 2-azidoacetyl-OSu (0.10 g, 0.50 mmol, 1.0 eq.) were added. The reaction mixture was stirred at room temperature for 4 hrs, concentrated *in vacuo* and the crude product was purified by column chromatography (DCM → 4% MeOH in DCM) to yield azide-modified epoxyketone **9** (0.26 g, 0.44 mmol, 88%). ^{1}H NMR (400 MHz, $CDCl_3$/CD_3OD): δ (ppm) 7.80 (d, *J* = 8.4 Hz, 1H), 7.53 (d, *J* = 7.6 Hz, 1H), 7.49 (d, *J* = 8.4 Hz, 1H), 7.32 (d, *J* = 8.8 Hz, 1H), 4.39-4.35 (m, 1H), 4.26-4.18 (m, 2H), 4.14-4.10 (m, 1H), 3.92-3.88 (m, 1H), 3.83 (s, 2H), 3.13 (d, *J* = 4.8 Hz, 1H), 2.75 (d, *J* = 4.8 Hz, 1H), 1.67-1.61 (m, 2H), 1.51-1.47 (m, 1H), 1.36 (s, 3H), 1.41-1.30 (m, 3H), 1.19-1.08 (m, 2H), 0.98-0.94 (m, 5H), 0.81-0.70 (m, 18H). ^{13}C NMR (100 MHz, $CDCl_3$/CD_3OD): δ (ppm) 207.52, 174.63, 171.38, 171.12, 167.36, 66.81, 59.03, 57.94, 57.29, 52.24, 51.90, 50.59, 50.50, 39.14, 37.13, 36.62, 24.95, 24.74, 24.60, 22.99, 20.78, 17.85, 16.52, 14.92, 10.76, 10.69. LC/MS analysis: R_t 8.0 min (linear gradient 10 → 90% B in 15 min), m/z 582.1 $[M+H]^+$, 1185.0 $[2M+Na]^+$.

***N*-((4-(*N*-(5-norbornene-2-carbonyl)aminomethyl)-1H-1,2,3-triazol-1-yl)acetyl)-Ile-Ile-Thr-leucinyl-2-methyloxirane (1)**

Azide-functionalized probe **9** (60 µmol, 35 mg) and alkyne **6** (60 µmol, 10 mg, 1.0 eq.) were dissolved in a mixture of *t*BuOH/toluene/H_2O (2/2/1, v/v/v) (2 mL). After adding $CuSO_4.H_2O$ (6 µmol, 0.5 mL 12 mM in H_2O, 10 mol%) and sodium ascorbate (9 µmol, 0.5 mL 18 mM in H_2O, 15 mol%), the mixture was stirred at 80 °C overnight before being concentrated *in vacuo*. Purification by column chromatography (2x; DCM → 6% MeOH in DCM, then EtOAc → 15% MeOH in EtOAc) yielded norbornene-functionalized peptide epoxyketone **1** (21 mg, 28 µmol, 47%) as a racemic mixture of diastereomers. R_f 0.3 (10% MeOH in DCM). ^{1}H NMR (600 MHz, CD_3OD): δ (ppm) 8.25-8.23 (m, 1H), 8.19-8.16 (m, 2H), 7.98-7.96 (m, 1H), 7.84 (s, 1H), 6.18-6.17 (m, 1H), 5.91-5.89 (m, 1H), 5.22 (2xd, *J* = 16 Hz, 2H), 4.60-4.57 (m, 1H), 4.42-4.41 (m, 2H), 4.37-4.27 (m, 3H), 4.07-4.06 (m, 1H), 3.28 (d, *J* = 4.8 Hz, 1H), 3.18-3.17 (m, 1H), 2.96-2.93 (m, 2H), 2.90-2.89 (m, 1H), 1.89-1.85 (m, 3H), 1.75-1.72 (m, 1H), 1.58-1.50 (m, 3H), 1.49 (s, 3H), 1.42-1.31 (m, 5H), 1.21-1.20 (m, 1H), 1.18 (d, *J* = 6.0 Hz, 3H), 0.97-0.89 (m, 18H). ^{13}C NMR (150 MHz, CD_3OD): δ (ppm) 207.37, 174.87, 171.53, 170.17, 165.76, 145.00, 136.42, 130.95, 123.70, 66.53, 57.96, 57.76, 57.43, 57.35, 50.94, 50.76, 49.77, 48.66, 45.47, 43.21, 41.86, 38.25, 36.12, 35.83, 33.67, 27.80, 27.79, 24.09, 23.89, 23.79, 21.63, 19.36, 17.90, 14.89, 13.80, 8.50. LC/MS analysis: R_t 7.8 min (linear gradient 10 → 90% B in 15 min), m/z 757.3 $[M+H]^+$, 1513.3 $[2M+H]^+$. HRMS: calcd. for $[C_{39}H_{61}N_8O_8]^+$ 757.46069, found 757.46120; calcd. for $[C_{39}H_{60}N_8O_8Na]^+$ 779.44263, found 779.44285.

(S)-2-(4-(*N*-(5-norbornene-2-carbonyl)aminomethyl)-1H-1,2,3-triazol-1-yl)-2-(naphthalen-2-yl)acetic acid (11)

(S)-2-azido-2-(naphthalen-2-yl)acetic acid (**10**)[32] (1.0 mmol, 0.23 g) and alkyne **6** (1.0 mmol, 0.18 g, 1.0 eq.) were dissolved in DMF. After adding $CuSO_4.H_2O$ (0.1 mmol, 0.1 mL 1 M in H_2O, 10 mol%) and sodium ascorbate (0.15 mmol, 0.15 mL 1 M in H_2O, 15 mol%), the mixture was stirred at 80 °C overnight before being concentrated *in*

vacuo. The crude product was purified by column chromatography (DCM → 10% MeOH in DCM with 1% AcOH), then recrystallized from DCM and finally resuspended in 1 M HCl after which the norbornene-functionalized acid **11** was collected as white crystals (0.24 g, 0.59 mmol, 59%). R_f 0.3 (10% MeOH in DCM with 1% AcOH). ^{1}H NMR (400 MHz, DMSO-d_6): δ (ppm) 8.11-7.94 (m, 5H), 7.81 (d, *J* = 5.6 Hz, 1H), 7.60-7.56 (m, 3H), 6.90 (s, 1H), 5.99-5.94 (m, 1H), 5.69-5.58 (m, 1H), 4.29-4.16 (m, 2H), 3.09-3.06 (m, 1H), 2.79-2.76 (m, 2H), 1.71-1.65 (m, 1H), 1.28-1.20 (m, 3H). ^{13}C NMR (100 MHz, DMSO-d_6): δ (ppm) 172.90, 169.18, 145.43, 136.79, 132.81, 132.61, 132.08, 131.98, 131.82, 128.71, 128.10, 127.63, 127.06, 126.81, 125.99, 122.73, 65.43, 49.35, 45.57, 43.19, 42.06, 34.27, 28.27. LC/MS analysis: R_t 7.9 min (linear gradient 0 → 90% B in 15 min), m/z 403.2 $[M+H]^+$, 805.1 $[2M+H]^+$, 827.3 $[2M+Na]^+$. HRMS: calcd. for $[C_{23}H_{23}N_4O_3]^+$ 403.17647, found 403.17587; calcd. for $[C_{23}H_{22}N_4O_3Na]^+$ 425.15841, found 425.15763.

_N_-((S)-2-(4-(_N_-(5-norbornene-2-carbonyl)aminomethyl)-1H-1,2,3-triazol-1-yl)-2-(naphthalen-2-yl)acetyl)-Tyr(Me)-Phe-((S)-(1-(methylsulfonyl)-5-methyl-hexen-3-yl))amide (2)

Boc-protected vinyl sulfone **12**[27] (0.10 mmol, 62 mg) was treated with TFA/DCM (1/1, v/v) for 30 min and then concentrated *in vacuo* in the presence of toluene. The residue was dissolved in DMF under argon atmosphere and DiPEA (0.20 mmol, 35 µL, 2.0 eq.), acid **11** (0.10 mmol, 40 mg, 1.0 eq.) and HCTU (0.15 mmol, 62 mg, 1.5 eq.) were added. The reaction mixture was stirred for 5 hrs at room temperature before DCM was added and the mixture was washed with H_2O. The aqueous layer was extracted with DCM and the combined organic layers were dried over $MgSO_4$, filtered and concentrated *in vacuo*. The crude product was purified by column chromatography (2x; DCM → 3% MeOH in DCM, then toluene → toluene/acetone 2/1 (v/v)), yielding the norbornene-functionalized peptide vinyl sulfone **2** (54 mg, 60 µmol, 60%) as a racemic mixture of diastereomers. R_f 0.4 (5% MeOH in DCM). ^{1}H NMR (400 MHz, CD_3OD): δ (ppm) 7.87-7.66 (m, 5H), 7.55-7.47 (m, 2H), 7.26-7.14 (m, 6.5H), 7.00 (d, *J* = 8.4 Hz, 0.5H), 6.86-6.84 (m, 1.5H), 6.67-6.57 (m, 1.5H), 6.41 (d, *J* = 7.6 Hz, 1H), 5.99-5.93 (m, 2H), 5.74-5.56 (m, 1H), 4.89-4.85 (m, 1H), 4.64-4.59 (m, 2H), 4.37-4.31 (m, 2H), 3.75-3.67 (2xs, 1.5H), 3.50 (s, 1.5H), 3.05-2.96 (m, 4H), 2.87 (s, 3H), 2.84-2.72 (m, 3H), 1.81-1.73 (m, 1H), 1.66-1.52 (m, 1H), 1.35-1.20 (m, 5H), 0.92-0.79 (m, 6H). ^{13}C NMR (100 MHz, CD_3OD): δ (ppm) 170.78, 170.58, 170.47, 170.40, 166.43, 166.25, 158.02, 157.71, 146.20, 146.09, 144.43, 136.41, 136.34, 135.58, 135.53, 132.61, 132.29, 130.83, 130.78, 130.55, 130.33, 130.31, 129.36, 129.19, 128.32, 128.21, 128.16, 128.08, 127.40, 127.36, 127.28, 127.25, 126.80, 126.77, 126.65, 126.59, 125.77, 125.74, 123.95, 123.85, 122.22, 122.14, 113.07, 112.84, 65.40, 54.21, 53.94, 53.70, 53.65, 48.72, 48.66, 47.08, 45.39, 45.33, 45.30, 43.11, 41.74, 41.25, 41.15, 37.13, 37.03, 36.94, 36.21, 33.67, 33.62, 29.61, 27.78, 27.73, 21.36, 21.29, 20.17, 20.11. LC/MS analysis: R_t 9.3 min (linear gradient 10 → 90% B in 15 min), m/z 900.4 $[M+H]^+$, 1800.3 $[2M+H]^+$.

4-(6-(2-pyrimidinyl)-1,2,4,5-tetrazin-3-yl)benzylhydroxide (16)

To a solution of 4-(aminomethyl)benzonitrile.HCl (**13**) (12 mmol, 2.0 g) and 2-cyanopyrimidine (**14**) (15 mmol, 1.6 g, 1.3 eq.) in EtOH was added $H_2NNH_2.H_2O$ (150 mmol, 7.3 mL, 12.5 eq.) and the reaction mixture was stirred under reflux (80 °C) overnight. Then, more $H_2NNH_2.H_2O$ (10 eq.) was added and the reaction mixture was stirred for an additional 4 hrs at 80 °C, after which it was allowed to cool to temperature and concentrated *in vacuo*. A solution of $NaNO_2$ (150 mmol, 10 g, 12.5 eq.) in H_2O/AcOH 1/1 (v/v, 30 mL) was then added slowly to the residue at 0 °C. The resulting pink mixture was stirred for 15 min at 0 °C, diluted with H_2O and extracted with DCM (3x) until the water layer was colourless. The combined organic layers were dried over anhydrous $MgSO_4$, filtered and concentrated *in vacuo*. The crude product was purified by column chromatography (2x; toluene → 25% acetone in toluene, then DCM → 12% MeOH in DCM), followed by trituration with a mixture of toluene and acetone to give tetrazine **16** as a purple solid (0.15 g, 0.55 mmol, 5%). R_f 0.3 (acetone/DCM 1/1). ^{1}H NMR (400 MHz, CD_3OD): δ (ppm) 9.14 (d, *J* = 4.8 Hz, 2H), 8.69 (d, *J* = 8.0 Hz, 2H), 7.78 (t, *J* = 4.8 Hz, 1H), 7.67 (d, *J* = 8.4 Hz, 2H), 4.76 (d, *J* = 8.0 Hz, 2H). ^{13}C NMR (100

MHz, CD_3OD): δ (ppm) 163.93, 159.70, 159.20, 149.01, 129.72, 129.22, 128.58, 128.05, 124.40, 64.59. HRMS: calcd. for $[C_{13}H_{11}N_6O]^+$ 267.09834, found 267.09945.

4-(Boc-aminomethyl)benzonitrile (17)

4-(Aminomethyl)benzonitrile.HCl (**13**) (30 mmol, 5.0 g) was coevaporated with toluene (3x) and dissolved in DCM under argon atmosphere. After addition of Et_3N (75 mmol, 11 mL, 2.5 eq.) and Boc_2O (33 mmol, 7.4 g, 1.1 eq.) the reaction mixture was stirred at room temperature overnight before being concentrated *in vacuo*. The crude product was purified by column chromatography (PetEt → 20% EtOAc in PetEt), followed by recrystallization from EtOAc/PetEt to yield Boc-protected benzonitrile **17** as a white solid (7.0 g, 30 mmol, quant.). R_f 0.9 (10% MeOH in DCM). ^{1}H NMR (400 MHz, $CDCl_3$): δ (ppm) 7.62 (d, *J* = 8.0 Hz, 2H), 7.39 (d, *J* = 8.0 Hz, 2H), 5.06 (s, 1H), 4.37 (d, *J* = 6.0 Hz, 2H), 1.46 (s, 9H). ^{13}C NMR (100 MHz, $CDCl_3$): δ (ppm) 155.79, 144.61, 132.33, 127.71, 118.74, 110.97, 79.99, 44.10, 28.28. LC/MS analysis: R_t 7.7 min (linear gradient 10 → 90% B in 15 min), m/z 132.9 $[M\text{-}Boc+H]^+$, 232.9 $[M+H]^+$.

Boc-4-(6-(2-pyrimidinyl)-1,2,4,5-tetrazin-3-yl)benzylamine (18)

To a solution of 4-(*N*-Boc-aminomethyl)benzonitrile **17** (30 mmol, 7.0 g) and 2-cyanopyrimidine **14** (60 mmol, 6.3 g, 2.0 eq.) in EtOH was added $H_2NNH_2.H_2O$ (300 mmol, 15 mL, 10 eq.) and the reaction mixture was stirred under reflux (70 °C) overnight. Then, more 2-cyanopyrimidine **14** (1.5 eq.) and $H_2NNH_2.H_2O$ (5.0 eq.) were added and the reaction mixture was stirred for an additional 7 hrs at 70 °C, after which it was allowed to cool to temperature and concentrated *in vacuo*. The residue was dissolved in AcOH (100 mL) and cooled to 0 °C before a solution of $NaNO_2$ (300 mmol, 21 g, 10 eq.) in H_2O (50 mL) was added dropwise. The pink mixture was stirred for 15 min at 0 °C, diluted with H_2O and extracted with DCM (3x). The combined organic layers were dried over anhydrous $MgSO_4$, filtered and concentrated *in vacuo*. The crude product was purified by column chromatography (2x; EtOAc, then DCM → 10% acetone in DCM), followed by recrystallization from EtOAc/PetEt to yield Boc-protected tetrazine **18** as purple crystals (1.3 g, 3.4 mmol, 11%). R_f 0.6 (25% acetone in DCM). ^{1}H NMR (400 MHz, $CDCl_3$): δ (ppm) 9.14 (d, *J* = 4.8 Hz, 2H), 8.70 (d, *J* = 8.0 Hz, 2H), 7.60 (t, *J* = 4.8 Hz, 1H), 7.55 (d, *J* = 8.4 Hz, 2H), 5.11 (s, 1H), 4.47 (d, *J* = 6.0 Hz, 2H), 1.49 (s, 9H). ^{13}C NMR (100 MHz, $CDCl_3$): δ (ppm) 164.30, 163.01, 159.51, 158.39, 155.91, 144.98, 130.19, 129.07, 128.12, 122.45, 79.83, 44.34, 28.36. LC/MS analysis: R_t 7.1 min (linear gradient 10 → 90% B in 15 min), m/z 366.1 $[M+H]^+$, 730.9 $[2M+H]^+$. HRMS: calcd. for $[C_{18}H_{20}N_7O_2]^+$ 366.16730, found 366.16728.

***N*-BodipyTMR-4-(6-(2-pyrimidinyl)-1,2,4,5-tetrazin-3-yl)benzylamine (3a)**

Boc-protected tetrazine **18** (0.1 mmol, 37 mg) was treated with TFA/DCM (1/1, v/v) for 15 min and then concentrated *in vacuo* in the presence of toluene. The residue was dissolved in DCE/DMF under argon atmosphere and DiPEA (0.2 mmol, 35 µL, 2.0 eq.) and BodipyTMR-OSu[25] (0.1 mmol, 50 mg, 1.0 eq.) were added. The reaction mixture was stirred at room temperature overnight before being concentrated *in vacuo*. The crude product was purified by column chromatography (DCM → 2% MeOH in DCM), followed by recrystallization from DCM/n-hexane to yield BodipyTMR-tetrazine **3a** as dark purple crystals (51 mg, 79 µmol, 79%). R_f 0.7 (10% MeOH in DCM). ^{1}H NMR (400 MHz, $CDCl_3$): δ (ppm) 9.12 (d, *J* = 4.8 Hz, 2H), 8.57 (d, *J* = 8.4 Hz, 2H), 7.88 (d, *J* = 8.8 Hz, 2H), 7.58 (t, *J* = 4.8 Hz, 1H), 7.40 (d, *J* = 8.0 Hz, 2H), 7.05 (s, 1H), 6.96 (d, *J* = 8.8 Hz, 2H), 6.94 (d, *J* = 4.4 Hz, 1H), 6.53 (d, *J* = 4.4 Hz, 1H), 6.08 (t, *J* = 5.6 Hz, 1H), 4.49 (d, *J* = 5.6 Hz, 2H), 3.85 (s, 3H), 2.80 (t, *J* = 7.2 Hz, 2H), 2.52 (s, 3H), 2.37 (t, *J* = 7.2 Hz, 2H), 2.15 (s, 3H). ^{13}C NMR (100 MHz, $CDCl_3$): δ (ppm) 171.69, 164.21, 162.98, 160.36, 159.50, 158.86, 158.37, 155.82, 144.00, 139.77, 134.98, 134.50, 130.69, 130.65, 130.29, 129.07, 128.47, 128.12, 125.37, 122.89, 122.49, 118.49, 113.69, 55.25, 43.25, 36.29, 19.99, 13.15, 9.58. LC/MS analysis: R_t 8.6 min (linear gradient 10 → 90% B in 15 min), m/z 624.2 $[M\text{-}F]^+$, 668.2 $[M+Na]^+$, 1291.0 $[2M+H]^+$, 1313.1 $[2M+Na]^+$. HRMS: calcd. for $[C_{34}H_{30}BF_2N_9O_2Na]^+$ 668.24758, found 668.24816.

***N*-BodipyFL-4-(6-(2-pyrimidinyl)-1,2,4,5-tetrazin-3-yl)benzylamine (3b)**

Boc-protected tetrazine **18** (0.1 mmol, 37 mg) was treated with TFA/DCM (1/1, v/v) for 15 min and then concentrated *in vacuo* in the presence of toluene. The residue was dissolved in DCE/DMF under argon atmosphere and DiPEA (0.2 mmol, 35 µL, 2.0 eq.) and BodipyFL-OSu[35] (0.1 mmol, 39 mg, 1.0 eq.) were added. The reaction mixture was stirred at room temperature overnight before being concentrated *in vacuo*. The crude product was purified by column chromatography (DCM → 2% MeOH in DCM), followed by recrystallization from DCM/n-hexane to yield BodipyFL-tetrazine **3b** as purple crystals (34 mg, 63 µmol, 63%). R_f 0.8 (10% MeOH in DCM). ^{1}H NMR (400 MHz, $CDCl_3$): δ (ppm) 9.13 (d, *J* = 4.8 Hz, 2H), 8.58 (d, *J* = 8.0 Hz, 2H), 7.59 (t, *J* = 4.8 Hz, 1H), 7.36 (d, *J* = 8.4 Hz, 2H), 7.10 (s, 1H), 6.89 (d, *J* = 4.0 Hz, 1H), 6.36 (s, 1H), 6.32 (d, *J* = 4.0 Hz, 1H), 6.06 (s, 1H), 4.52 (d, *J* = 5.6 Hz, 2H), 3.32 (t, *J* = 7.2 Hz, 2H), 2.78 (t, *J* = 7.2 Hz, 2H), 2.52 (s, 3H), 2.23 (s, 3H). ^{13}C NMR (100 MHz, $CDCl_3$): δ (ppm) 171.56, 164.31, 163.05, 160.55, 159.59, 158.39, 156.69, 144.31, 144.21, 135.35, 134.10, 130.04, 128.94, 128.41, 128.20, 123.81, 122.45, 120.50, 117.58, 43.12, 35.89, 24.77, 14.91, 11.32. LC/MS analysis: R_t 7.9 min (linear gradient 10 → 90% B in 15 min), m/z 520.2 $[M-F]^+$, 1079.1 $[2M+H]^+$. HRMS: calcd. for $[C_{27}H_{24}BFN_9O]^+$ 520.21754, found 520.21767.

***N*-biotin-4-(6-(2-pyrimidinyl)-1,2,4,5-tetrazin-3-yl)benzylamine (3c)**

Boc-protected tetrazine **18** (0.1 mmol, 37 mg) was treated with TFA/DCM (1/1, v/v) for 15 min and then concentrated *in vacuo* in the presence of toluene. The residue was dissolved in DCE/DMF under argon atmosphere and DiPEA (0.2 mmol, 35 µL, 2.0 eq.) and biotin-OSu (0.1 mmol, 34 mg, 1.0 eq.) were added. The reaction mixture was stirred at room temperature overnight before being concentrated *in vacuo*. The crude product was purified by column chromatography (DCM → 10% MeOH in DCM), followed by recrystallization from a mixture of DCM/MeOH (1/1, v/v) and n-hexane to yield biotin-tetrazine **3c** as purple crystals (24 mg, 49 µmol, 49%). R_f 0.7 (20% MeOH in DCM). ^{1}H NMR (400 MHz, CD_3OD): δ (ppm) 9.14 (d, *J* = 4.8 Hz, 2H), 8.69 (d, *J* = 8.0 Hz, 2H), 7.67 (t, *J* = 4.8 Hz, 1H), 7.57 (d, *J* = 8.4 Hz, 2H), 4.59-4.49 (m, 3H), 4.32-4.29 (m, 1H), 3.20-3.15 (m, 1H), 2.93 (dd, *J* = 13.0, 4.8 Hz, 1H), 2.74 (d, *J* = 12.8 Hz, 1H), 2.31 (t, *J* = 7.2 Hz, 2H), 1.78-1.63 (m, 4H), 1.51-1.44 (m, 2H). ^{13}C NMR (100 MHz, CD_3OD): δ (ppm) 173.90, 164.33, 163.87, 162.52, 158.93, 158.27, 144.50, 129.93, 128.87, 128.33, 122.66, 61.72, 59.93, 55.32, 42.80, 40.14, 35.43, 28.15, 27.86, 25.27. LC/MS analysis: R_t 5.2 min (linear gradient 10 → 90% B in 15 min), m/z 492.2 $[M+H]^+$, 983.1 $[2M+H]^+$, 1473.9 $[3M+H]^+$. HRMS: calcd. for $[C_{23}H_{26}N_9O_2S]^+$ 492.19247, found 492.19228; calcd. for $[C_{23}H_{25}N_9O_2SNa]^+$ 514.17441, found 514.17417.

***N*-(6-heptynoyl)-Ile-Ile-Thr-leucinyl-2-methyloxirane (19)**

Fully protected peptide epoxyketone **8**[31] (15 µmol, 10 mg) was treated with TFA for 30 min and then concentrated *in vacuo* in the presence of toluene. The residue was dissolved in DCE under argon atmosphere and DiPEA (45 µmol, 8.0 µL, 3.0 eq.) and 6-heptynoic acid succinimidyl ester[37] (15 µmol, 3.3 mg, 1.0 eq.) were added. The reaction mixture was stirred overnight at room temperature before being concentrated *in vacuo*. The crude product was purified by column chromatography (DCM → 2% MeOH in DCM) and then redissolved in DCM and washed with H_2O (3x), dried over $MgSO_4$, filtered and concentrated *in vacuo* to give alkyne-functionalized peptide epoxyketone **19** as a white powder (8.0 mg, 13 µmol, 87%). R_f 0.4 (5% MeOH in DCM). ^{1}H NMR (400 MHz, $CDCl_3$): δ (ppm) 8.37 (bs, 1H), 7.89 (bs, 1H), 7.77 (bs, 1H), 7.12 (bs, 1H), 4.75-4.71 (m, 2H), 4.61-4.59 (m, 2H), 4.12-4.11 (m, 1H), 3.30 (s, 1H), 2.91 (s, 1H), 2.36-2.19 (m, 4H), 1.94 (s, 1H), 1.77-1.69 (m, 6H), 1.60-1.53 (m, 8H), 1.41-1.30 (m, 1H), 1.11 (d, *J* = 4.8 Hz, 3H), 1.10-1.03 (m, 1H), 0.92-0.83 (m, 18H).^{13}C NMR (100 MHz, $CDCl_3$): δ (ppm) 208.19, 172.79, 171.96, 171.87, 170.63, 83.94, 68.60, 67.11, 59.19, 57.61, 57.27, 56.98, 52.36, 50.69, 39.27, 38.01, 37.64, 35.82, 27.88, 25.21, 25.15, 25.02, 24.85, 23.28, 21.17, 18.13, 17.30, 16.82, 15.29, 15.25, 11.42. LC/MS analysis: R_t 8.5 min (linear gradient 10 → 90% B in 15 min), m/z 607.5 $[M+H]^+$, 629.6 $[M+Na]^+$, 1213.5 $[2M+H]^+$, 1235.5 $[2M+Na]^+$.

***N*-BodipyFL-3-azidopropylamine (20)**

To a solution of 3-bromopropylamine.HBr (**25**) (1.0 mmol, 0.22 g) in DMF was added sodium azide (1.0 mmol, 65 mg, 1.0 eq.) and the mixture was stirred overnight at room temperature. Then, 1/20 part of this solution (50 µmol, 3.0 eq.) was added to a solution of BodipyFL-OSu[35] (17 µmol, 6.6 mg, 1.0 eq.) and DiPEA (100 µmol, 17 µL, 6.0 eq.) in DCE under argon atmosphere. The reaction mixture was stirred at room temperature for 5 hrs before DCM was added and the mixture was washed with a saturated aqueous $NaHCO_3$ solution and 1 M HCl (3x). The combined aqueous layers were extracted with DCM and all organic layers were combined, dried over anhydrous $MgSO_4$, filtered and concentrated *in vacuo*. The crude product was purified by column chromatography (chloroform) yielding azido-BodipyFL **20** (6.3 mg, 17 µmol, 99%). R_f 0.7 (5% MeOH in DCM). ^{1}H NMR (400 MHz, CD_3OD): δ (ppm) 7.43 (s, 1H), 7.00 (s, 1H), 6.32 (s, 1H), 6.21 (s, 1H), 3.31-3.20 (m, 6H), 2.61 (t, *J* = 7.2 Hz, 2H), 2.51 (s, 3H), 2.28 (s, 3H), 1.74-1.71 (m, 2H). ^{13}C NMR (100 MHz, CD_3OD): δ (ppm) 174.75, 161.40, 158.37, 145.88, 136.56, 134.87, 129.55, 125.78, 121.36, 117.68, 49.99, 37.69, 36.05, 29.66, 25.62, 14.86, 11.17. LC/MS analysis: R_t 8.2 min (linear gradient 10 → 90% B in 15 min), m/z 355.3 $[M-F]^+$, 375.0 $[M+H]^+$, 397.1 $[M+Na]^+$, 749.1 $[2M+H]^+$, 771.1 $[2M+Na]^+$.

B. Biochemistry

General

HEK-293T cells were cultured in DMEM supplemented with 10% (v/v) FCS, 10 units/mL penicillin and 10 µg/mL streptomycin in a 5% CO_2 humidified incubator at 37 °C. Cells were harvested, washed with PBS (2x) and lysed in digitonin lysis buffer (50 mM Tris pH 7.5, 250 mM sucrose, 5 mM $MgCl_2$, 1 mM DTT, 2 mM ATP, 0.025% digitonin) for 30 min on ice. After centrifugation of the cells at 16,100 g for 20 min at 4 °C, the supernatants were collected and the protein concentration was determined by Bradford assay. Precipitation of proteins was done using a chloroform/methanol (c/m) precipitation protocol.[44] SDS-PAGE analysis: in-gel fluorescence was measured on a Typhoon Variable Mode Imager (Amersham Biosciences) using Cy3/TAMRA settings (excitation wavelength 532 nm, emission wavelength 580 nm) or Cy2/Blue FAM settings (excitation wavelength 488 nm, emission wavelength 520 nm). As a loading control gels were stained with Coomassie Brilliant Blue. For Western blotting, the proteins were transferred onto a PVDF membrane using a Bio-Rad Trans-Blot cell system. Membranes were blocked with 1% BSA in TBS-t(+) (0.1% Tween 20) overnight at room temperature, hybridized with Streptavidin-HRP for 1 hr at room temperature (1:10,000 in blocking buffer) (Molecular Probes, Life Technologies), washed with TBS-t(+) and TBS and then visualized using an ECL+ Western blotting detection kit (Amersham Biosciences). Markers used were Precision Plus Dual Color protein standard (Bio-Rad) and Biotinylated protein marker (Bio-Rad). MV151[25], **21**[30], **22**[38], **23**[39] and **24**[32] are described in literature.

***In vitro* competition assay versus MV151**

HEK cell lysates (20 µg total protein per experiment) in lysis buffer (9 µL) were exposed to the indicated concentrations of ABP **1**, **2** or **19** (1 µL 10x solution in DMSO) for 1 hr at 37 °C, after which the lysates were incubated with 1 µM MV151 (1.1 µL 10 µM in DMSO) for 1 hr at 37 °C. The reaction mixtures were then boiled for 5 min at 100 °C with 4 µL 4x Laemmli's sample buffer containing 2-mercaptoethanol and resolved on 12.5% SDS-PAGE. In-gel visualization of the fluorescent labeling was performed in the wet gel slabs directly using Cy3/TAMRA settings.

***In situ* competition assay versus MV151**

HEK cells (~1x10^6 cells per experiment) were seeded in 6 cm petri dishes and grown overnight, after which the medium was removed and the cells were exposed to the indicated concentrations of ABP **1** or **2** (2 µL 1000x solution in DMSO) in 2 mL fresh medium for 4 hrs at 37 °C. Next, the cells were harvested by scraping, centrifuged

for 5 min at 1200 rpm and washed with PBS (2x), before flash freezing the cell pellets in liquid nitrogen and cell lysis in 50 µL lysis buffer. The lysates (10 µg total protein per experiment) in lysis buffer (9 µL) were exposed to 1 µM MV151 (1 µL 10 µM in DMSO) for 1 hr at 37 °C, boiled for 5 min at 100 °C with 4 µL 4x Laemmli's sample buffer containing 2-mercaptoethanol and resolved on 12.5% SDSPAGE. In-gel visualization of the fluorescent labeling was performed in the wet gel slabs directly using Cy3/TAMRA settings.

General procedure for tetrazine ligation *in vitro*

HEK cell lysates (20 µg total protein per experiment) in lysis buffer (9 µL) were exposed to 1 µM ABP **1** or **2** (1 µL 10 µM in DMSO) for 1 hr at 37 °C in the presence or absence of 100 µM epoxomicin (1 µL 1 mM in DMSO), followed by addition of the indicated concentrations of tetrazine **3a**, **3b** or **3c** (1.1 µL 10x solution in DMSO) and incubation for 1 hr at 37 °C. Control samples were labeled with 1 µM MV151. After quenching by c/m precipitation, proteins were taken up in 10 µL Laemmli's sample buffer containing 2-mercaptoethanol, boiled for 5 min at 100 °C and resolved on 12.5% SDS-PAGE. Fluorescent labeling was visualized in the wet gel slabs directly using Cy3/TAMRA settings (**3a**, MV151) or Cy2/Blue FAM settings (**3b**). Biotinylated proteins (**3c**) were detected by streptavidin Western blotting.

Optimisation of tetrazine ligation conditions. Tetrazine ligation was performed for 0.5, 1, 2, 3 or 20 hrs at 37 °C or for 1 hr at 20, 37 or 50 °C. Alternatively, the pH of the reaction mixture was adjusted by addition of a citric acid/phosphate buffer (9 µL) (pH 4, 5, 6, 7, or 8) prior to addition of tetrazine **3a**.

Compatibility with click conditions. One or more of the following reagents were added to the tetrazine ligation reaction mixture: 1 mM $CuSO_4$ (1 µL 10 mM in H_2O), 1 mM TCEP (1 µL 10 mM in H_2O) and 100 µM TBTA (1 µL 1 mM in DMSO).

Cross-reactivity. ABPs **1**, **9** and **19** (1 µM) were used for reaction with tetrazine **3b** (50 µM).

General procedure for tetrazine ligation *in situ*

HEK cells (~$1x10^6$ cells per experiment) were seeded in 6 cm petri dishes and grown overnight, after which the medium was removed and the cells were exposed to 10 µM ABP **1** (2 µL 10 mM in DMSO) in 2 mL fresh medium for 3 hrs at 37 °C. Control cells were exposed to MV151 (1 µM) for 3 hrs at 37 °C. After removal of the medium, the cells were washed with 3 mL fresh medium for 30 min at 37 °C and then exposed to the indicated concentrations of tetrazine **3a**, **3b**, or **3c** (2 µL 1000x solution in DMSO) in 2 mL fresh medium for 1 hr at 37 °C. Next, the cells were harvested by scraping, centrifuged for 5 min at 1200 rpm and washed with PBS (2x), before flash freezing the cell pellets in liquid nitrogen and cell lysis in 50 µL lysis buffer. The lysates (20 µg total protein per experiment) were boiled for 5 min at 100 °C with Laemmli's sample buffer containing 2-mercaptoethanol and resolved on 12.5% SDS-PAGE. Fluorescent labeling was visualized in the wet gel slabs directly using Cy3/TAMRA settings (**3a**, MV151) or Cy2/Blue FAM settings (**3b**). Biotinylated proteins (**3c**) were detected by streptavidin Western blotting.

Staudinger-Bertozzi ligation and copper-free strain-promoted click ligation *in vitro*

HEK cell lysates (20 µg total protein per experiment) in lysis buffer (9 µL) were exposed to 1 µM ABP **9** (1 µL 10 µM in DMSO) for 1 hr at 37 °C, followed by addition of the indicated concentrations of phosphine **22** or dibenzocyclooctyn **23** (1.1 µL 10x solution in DMSO) and incubation for 1 hr at 37 °C. After quenching by c/m precipitation, proteins were taken up in 10 µL Laemmli's sample buffer containing 2-mercaptoethanol, boiled for 5 min at 100 °C and resolved on 12.5% SDS-PAGE. Biotinylated proteins were detected by streptavidin Western blotting.

Cross-reactivity. ABPs **1**, **9** and **19** (1 µM) were used for reaction with phosphine **22** (50 µM).

Copper(I)-catalyzed click ligation *in vitro*

HEK cell lysates (20 µg total protein per experiment) in lysis buffer (9 µL) were exposed to 1 µM ABP **9** or **19** (1 µL 10 µM in DMSO) for 1 hr at 37 °C. The mixtures were then diluted with an additional 9 µL lysis buffer containing 2 mM $CuSO_4$, 2 mM TCEP and 200 µM TBTA and exposed for 1 hr at 37 °C to the indicated concentrations of azide **20** (reaction with **19**) or alkyne **21** (reaction with **9**) (1 µL 20x solution in DMSO). After quenching by c/m precipitation, proteins were taken up in 10 µL Laemmli's sample buffer containing 2-mercaptoethanol, boiled for 5 min at 100 °C and resolved on 12.5% SDS-PAGE. Fluorescent labeling was visualized in the wet gel slabs directly using Cy2/Blue FAM settings.

Cross-reactivity. ABPs **1**, **9** and **19** (1 µM) were used for reaction with azide **20** and/or alkyne **21** (50 µM).

Triple ligation procedure *in vitro*

HEK cell lysates (30 µg total protein per experiment) in lysis buffer (9 µL) were exposed to 1 µM ABP **2** and 5 µM ABP **24** (0.5 µL 20x solution in DMSO each) for 1 hr at 37 °C, and then to 1 µM ABP **19** (0.5 µL 20 µM in DMSO) for 1 hr at 37 °C. After diluting the mixtures with an additional 9 µL lysis buffer, 25 µM BodipyTMR-tetrazine **3a** and 100 µM biotin-phosphine **22** (0.5 µL 40x solution in DMSO each) were added and the mixtures were incubated for 1 hr at 37 °C. Next, the excess of reagents was removed by a buffer exchange to 50 mM Tris pH 7.5 using Millipore Amicon centrifugal filters (3 kDa MWCO). Samples were washed twice with 300 µL Tris buffer and concentrated to a final volume of 40 µL per sample, prior to addition of 1 mM $CuSO_4$, 1 mM TCEP and 100 µM TBTA (0.6 µL 100x solution each). The mixtures were then reacted with 25 µM BodipyFL-azide **20** (1.5 µL 1 mM in DMSO) for 1 hr at 37 °C. After quenching by c/m precipitation, proteins were taken up in 10 µL Laemmli's sample buffer containing 2-mercaptoethanol, boiled for 5 min at 100 °C and resolved on 12.5% SDS-PAGE. Fluorescent labeling was visualized in the wet gel slabs directly using Cy3/TAMRA settings (**3a**) and Cy2/Blue FAM settings (**20**) after which biotinylated proteins (**22**) were detected by streptavidin Western blotting.

References and notes

1. Mahal, L. K.; Yarema, K. J.; Bertozzi, C. R. *Science* **1997**, *276*, 1125.
2. Saxon, E.; Bertozzi, C. R. *Science* **2000**, *287*, 2007.
3. Prescher, J. A.; Dube, D. H.; Bertozzi, C. R. *Nature* **2004**, *430*, 873.
4. For recent reviews see: a) Sletten, E. M.; Bertozzi, C. R. *Acc. Chem. Res.* **2011**, *44*, 666; b) Devaraj, N. K.; Weissleder, R. *Acc. Chem. Res.* **2011**, *44*, 816; c) Ngo, J. T.; Tirell, D. A. *Acc. Chem. Res.* **2011**, *44*, 677; d) Hao, Z.; Hong, S.; Chen, X.; Chen, P. R. *Acc. Chem. Res.* **2011**, *44*, 742; e) Heal, W. P.; Tate, E. W. *Org. Biomol. Chem.* **2010**, *8*, 731; f) Willems, L. I.; van der Linden, W. A.; Li, N.; Li, K.-Y.; Liu, N.; Hoogendoorn, S.; van der Marel, G. A.; Florea, B. I.; Overkleeft, H. S. *Acc. Chem. Res.* **2011**, *44*, 718; g) Lang, K.; Chin, J. W. *ACS Chem. Biol.* **2014**, *9*, 16; h) Ramil, C. P.; Lin, Q. *Chem. Commun.* **2013**, *49*, 11007.
5. Tornøe, C. W.; Christensen, C.; Meldal, M. *J. Org. Chem.* **2002**, *67*, 3057.
6. Rostovtsev, V. V. ; Green, L. G.; Fokin, V. V.; Sharpless, K. B. *Angew. Chem. Int. Ed.* **2002**, *41*, 2596.
7. Wang, Q.; Chan, T. R.; Hilgraf, R.; Fokin, V. V.; Sharpless, K. B.; Finn, M. G. *J. Am. Chem. Soc.* **2003**, *125*, 3192.
8. Agard, N. J.; Prescher, J. A.; Bertozzi, C. R. *J. Am. Chem. Soc.* **2004**, *126*, 15046.
9. Devaraj, N. K.; Weissleder, R.; Hilderbrand, S. A. *Bioconjugate Chem.* **2008**, *19*, 2297.
10. Blackman, M. L.; Royzen, M.; Fox, J. M. *J. A. Chem. Soc.* **2008**, *130*, 13518.
11. Aucagne, V.; Leigh, D. A. *Org. Lett.* **2006**, *8*, 4505.
12. Chang, P. V.; Prescher, J. A.; Hangauer, M. J.; Bertozzi, C. R. *J. Am. Chem. Soc.* **2007**, *129*, 8400.
13. Kele, P.; Mezo, G.; Achatz, D.; Wolfbeis, O. S. *Angew. Chem. Int. Ed.* **2009**, *48*, 344.

14. Nurmi, L.; Lindqvist, J.; Randev, R.; Syrett, J.; Haddleton, D. M. *Chem. Commun.* **2009**, 2727.
15. Sanders, B. C.; Friscourt, F.; Ledin, P. A.; Mbua, N. E.; Arumugam, S.; Guo, J.; Boltje, T. J.; Popik, V. V.; Boons, G.-J.; *J. Am. Chem. Soc.* **2011**, *133*, 949.
16. Sletten, E. M.; Bertozzi, C. R. *J. Am. Chem. Soc.* **2011**, *133*, 17570.
17. Beal, D. M.; Albrow, V. E.; Burslem, G.; Hitchen, L.; Fernandes, C.; Lapthorn, C.; Roberts, L. R.; Selby, M. D.; Jones, L. H. *Org. Biomol. Chem.* **2012**, *10*, 548.
18. Chang, P. V.; Prescher, J. A.; Hangauer, M. J.; Bertozzi, C. R. *J. Am. Chem. Soc.* **2007**, *129*, 8400.
19. Willems, L. I.; Verdoes, M.; Florea, B. I.; van der Marel, G. A.; Overkleeft, H. S. *ChemBioChem* **2010**, *11*, 1769.
20. Karver, M. R.; Weissleder, R.; Hilderbrand, S. A. *Angew. Chem. Int. Ed.* **2012**, *51*, 920.
21. Speers, A. E.; Adam, G. C.; Cravatt, B. F. *J. Am. Chem. Soc.* **2003**, *125*, 4686.
22. Ovaa, H.; van Swieten, P. F.; Kessler, B. M.; Leeuwenburgh, M. A.; Fiebiger, E.; van den Nieuwendijk, A. M. C. H.; Galardy, P. J.; van der Marel, G. A.; Ploegh, H. L.; Overkleeft, H. S. *Angew. Chem. Int. Ed.* **2003**, *42*, 3626.
23. van Swieten, P. F.; Samuel, E.; Hernández, R. O.; van den Nieuwendijk, A. M. C. H.; Leeuwenburgh, M. A.; van der Marel, G. A.; Kessler, B. M.; Overkleeft, H. S.; Kisselev, A. F. *Bioorg. Med. Chem. Lett.* **2007**, *17*, 3402.
24. Verdoes, M.; Florea, B. I.; van der Marel, G. A.; Overkleeft, H. S. *Eur. J. Org. Chem.* **2009**, *2009*, 3301.
25. Verdoes, M.; Florea, B. I.; Menendez-Benito, V.; Maynard, C. J.; Witte, M. D.; van der Linden, W. A.; van den Nieuwendijk, A. M. C. H.; Hofmann, T.; Berkers, C. R.; van Leeuwen, F. W.; Groothuis, T. A.; Leeuwenburgh, M. A.; Ovaa, H.; Neefjes, J. J.; Filippov, D. V.; van der Marel, G. A.; Dantuma, N. P.; Overkleeft, H. S. *Chem. Biol.* **2006**, *13*, 1217.
26. Sharma, L. K.; Lee, N.-R.; Jang, E. R.; Lei, B.; Zhan, C.-G.; Lee, W.; Kim, K.-B. *ChemBioChem* **2012**, *13*, 1899.
27. Verdoes, M.; Willems, L. I.; van der Linden, W. A.; Duivenvoorden, B. A.; van der Marel, G. A.; Florea B. I.; Kisselev, A. F.; Overkleeft, H. S. *Org. Biomol. Chem.* **2010**, *8*, 2719.
28. Hanada, M.; Sugawara, K.; Kaneta, K.; Toda, S.; Nishiyama, Y.; Tomita, K.; Yamamoto, H.; Konishi, M.; Oki, T. *J. Antibiot*. **1992**, *45*, 1746.
29. Sin, N.; Kim, K. B.; Elofsson, M.; Meng, L.; Auth, H.; Kwok, B. H. B.; Crews, C. M. *Bioorg. Med. Chem. Lett.* **1999**, *9*, 2283.
30. Verdoes, M.; Hillaert, U.; Florea, B. I.; Sae-Heng, M.; Risseeuw, M. D. P.; Filippov, D. V.; van der Marel, G. A.; Overkleeft, H. S. *Bioorg. Med. Chem. Lett.* **2007**, *17*, 6169.
31. Florea , B. I.; Verdoes, M.; Li, N.; van der Linden, W. A.; Geurink, P. P.; van den Elst, H.; Hofmann, T.; De Ru, A.; van Veelen, P. A.; Tanaka, K.; Sasaki, K.; Murata, S.; Den Dulk, H.; Brouwer, J.; Ossendorp, F. A.; Kisselev, A. F.; Overkleeft, H. S. *Chem. Biol.* **2010**, *17*, 795.
32. Britton, M.; Lucas, M. M.; Downey, S. L.; Screen, M.; Pletnev, A. A.; Verdoes, M.; Tokhunts, R. A.; Amir, O.; Goddard, A. L.; Pelphrey, P. M.; Wright, D. L.; Overkleeft, H. S.; Kisselev, A. F. *Chem. Biol.* **2009**, *16*, 1278.
33. Clavier, G.; Audebert, P. *Chem. Rev.* **2010**, *110*, 3299.
34. After the synthesis described in this chapter was finished, an improved method for metal-catalyzed tetrazine synthesis was published: Yang, J.; Karver, M. R.; Li, W.; Sahu, S.; Devaraj, N. K. *Angew. Chem. Int. Ed.* **2012**, *51*, 1.
35. Geurink, P. P.; Klein, T.; Prèly, L.; Paal, K.; Leeuwenburgh, M. A.; van der Marel, G. A.; Kauffman, H. F.; Overkleeft, H. S.; Bischoff, R. *Eur. J. Org. Chem.* **2010**, *11*, 2100.
36. It should be noted that proteasome subunits β1 and β5, which have close to identical molecular weights, sometimes overlay on an SDS PAGE gel, especially when visualized by Western blotting. However, by tuning the conditions of the gel (e.g. running time and composition) they can be separated well.
37. Speers, A. E.; Adam, G. C.; Cravatt, B. F. *J. Am. Chem. Soc.* **2003**, *125*, 4686.
38. Verdoes, M.; Florea, B. I.; Hillaert, U.; Willems, L. I.; van der Linden, W. A.; Sae-Heng, M.; Filippov, D. V.; Kisselev, A. F.; van der Marel, G. A.; Overkleeft, H. S. *ChemBioChem* **2008**, *9*, 1735.

39. Ning, X.; Guo, J.; Wolfert, M. A.; Boons, G.-J. *Angew. Chem. Int. Ed.* **2008**, *47*, 2253.
40. van der Linden, W. A.; Li, N.; Hoogendoorn, S.; Ruben, M.; Verdoes, M.; Guo, J.; Boons, G. J.; van der Marel, G. A.; Florea, B. I.; Overkleeft, H. S. *Bioorg. Med. Chem.* **2012**, *20*, 662.
41. Devaraj, N. K.; Hilderbrand, S.; Upadhyay, R.; Mazitschek, R.; Weissleder, R. *Angew. Chem. Int. Ed.* **2010**, *49*, 2869.
42. Rossin, R.; Renart Verkerk, P.; van den Bosch, S. M.; Vulders, R. C. M.; Verel, I.; Lub, J.; Robillard, M. S. *Angew. Chem. Int. Ed.* **2010**, *49*, 3375.
43. After the work described in this chapter was published, a number of other reports appeared describing tandem ligation strategies for *in vivo* imaging of cell-surface glycosylation: a) Neves, A. A.; Stöckmann, H.; Wainman, Y. A.; Kuo, J. C.-H.; Fawcett, S.; Leeper, F. J.; Brindle, K. M. *Bioconjugate Chem.* **2013**, *24*, 934; b) Cole, C. M.; Yang, J.; Seckute, J.; Devaraj, N. K. *ChemBioChem* **2013**, *14*, 205; c) Niederwieser, A.; Späte, A.-K.; Nguyen, L. D.; Jüngst, C.; Reutter, W.; Wittmann, V. *Angew. Chem. Int. Ed.* **2013**, *52*, 4265; d) Späte, A.-K.; Busskamp, H.; Niederwieser, A.; Schart, V. F.; Marx, A.; Wittmann, V. *Bioconjugate Chem.* **2014**, *25*, 147. Another study detailed the dual labeling of live cells by using two different unnatural amino acids: Nikić, I.; Plass, T.; Schraidt, O.; Szymański, J.; Briggs, J. A.; Schultz, C.; Lemke, E. A. *Angew. Chem. Int. Ed.* **2014**, *53*, 2245.
44. Wessel, D.; Flügge, U. I. *Anal. Biochem.* **1984**, *138*, 141.

5

Synthesis of epoxide- and aziridine-based probes to target retaining galactosidases

5.1 Introduction

Glycosidases are hydrolytic enzymes responsible for the hydrolysis of glycosidic bonds in (oligo)saccharides and glycoconjugates and are crucial for the breakdown of glyco(sphingo)lipids in lysosomes. They can be classified according to the nature of their substrate and the mechanism of substrate hydrolysis, which generally involves cleavage with either retention or inversion of anomeric stereochemistry. For example, retaining β-glucosidases recognize β-linked glucoside substrates and hydrolyze the glycosidic bond with retention of stereochemistry at the anomeric position. The catalytic mechanism of retaining glycosidases is a two-step process that generally involves a double displacement mechanism as depicted schematically in Figure 5.1A.[1] In the first step the catalytic nucleophile, usually an aspartic or glutamic acid residue, attacks the anomeric center to cleave the glycosidic bond with inversion of configuration and thereby creates a covalent enzyme-substrate intermediate. Cleavage of the substrate aglycon is assisted by another glutamic or aspartic acid residue that acts as a general acid and protonates the leaving group. In the next step this residue, now acting as a general base, deprotonates a water molecule that hydrolyzes the glycosyl-enzyme intermediate, thereby releasing the glycoside from the active site. The configuration is again inverted, resulting in a net retention of anomeric stereochemistry. An

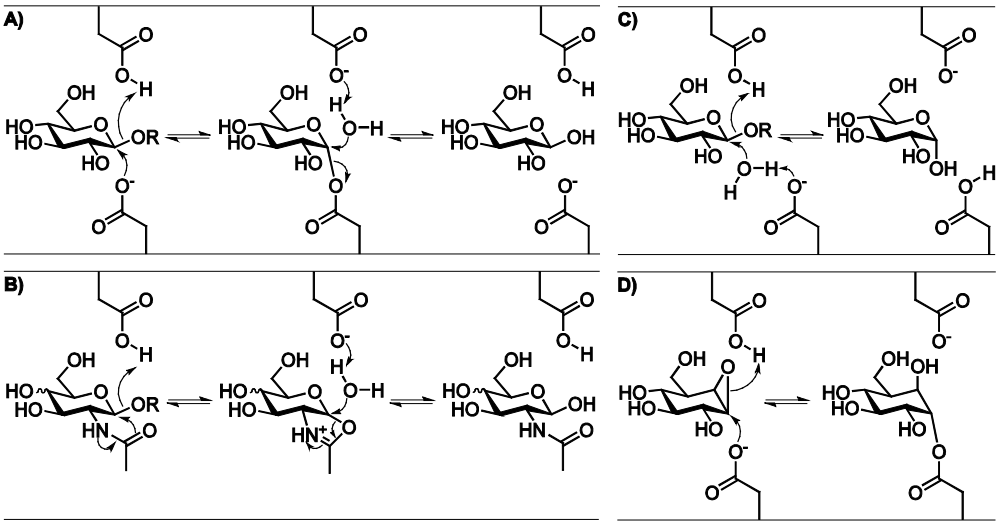

Figure 5.1. Mechanism of substrate hydrolysis by retaining β-glucosidases (A), *N*-acetylhexosaminidases (B) and inverting β-glucosidases (C). D) Proposed mechanism of cyclophellitol binding to retaining β-glucosidases.

alternative mechanism for hydrolysis with retention of configuration can occur when the substrate carries an acetamide substituent at C2 that assists in the cleavage of the glycosidic bond by acting as a nucleophile. This mechanism, for example used by *N*-acetylhexosaminidases, does not involve a covalent substrate-enzyme intermediate (Figure 5.1B).[2] The same holds true for the class of inverting glycosidases. These enzymes employ a one-step mechanism involving two carboxylic acid residues in the active site that act as a general base and a general acid.[1] The first carboxylic acid residue deprotonates a water molecule during its attack on the anomeric center, while the second residue protonates the leaving aglycon (Figure 5.1C).

Many covalent and irreversible mechanism-based glycosidase inhibitors have been described in literature.[3] These can generally be divided into two types: compounds that release a reactive aglycon after hydrolytic cleavage which then reacts with another residue in the active site, and inhibitors that contain a reactive electrophile that is attacked by the active site nucleophile to create a stable covalent bond. The latter class includes epoxide- and aziridine-based inhibitors as well as glycosides that are functionalized with one or more fluorine substituents at C2 and/or C5.[4-14] Of these, especially the fluorosugars have received considerable attention. Drawbacks of these inhibitors are their modest potency and the reversibility of binding, although the covalent enzyme-probe intermediate is usually sufficiently stable to enable analysis of the adducts. In contrast, the epoxide based inhibitors

have proven to enable very potent and selective irreversible inhibition of specific glycosidases. Cyclophellitol (**1**) is a naturally occurring β-glucosidase inhibitor that was first isolated in 1990 from the mushroom *Phellinus* sp. (Figure 5.2A).[5,6] In a follow-up study it was demonstrated that cyclophellitol is a selective and potent mechanism-based irreversible inhibitor of several retaining β-glucosidases.[7] The β-glucopyranose-configured inhibitor is thought to bind in the active site by mimicking a β-linked glucoside substrate and to enable covalent bond formation through reaction of the epoxide with the catalytic nucleophile (Figure 5.1D). In later studies, the α-epoxide stereoisomers (1*R*,6*S*)- and (1*R*,2*S*,6*S*)-cyclophellitol (**2** and **3**, Figure 5.2A) were shown to be irreversible inhibitors of retaining α-glucosidases and α-mannosidases, respectively,[8,9] while the β-epoxide isomer of inhibitor **3** was synthesized as a putative β-mannosidase inhibitor.[10] Conduritol B epoxide (**5**), although structurally related to cyclophellitol, is less potent and also less selective as a result of its structural symmetry, resulting in the inhibition of both retaining β- and α-glucosidases.[11,12] Two galactopyranose-configured isomers, conduritol C epoxides **6** and **7**, have been identified as irreversible inhibitors of several retaining α- and β-galactosidases, respectively.[13] In addition to the epoxide-based inhibitors, a few aziridine derivatives have been synthesized. For example, the aziridine analogue of cyclophellitol (**4**) is an inhibitor of

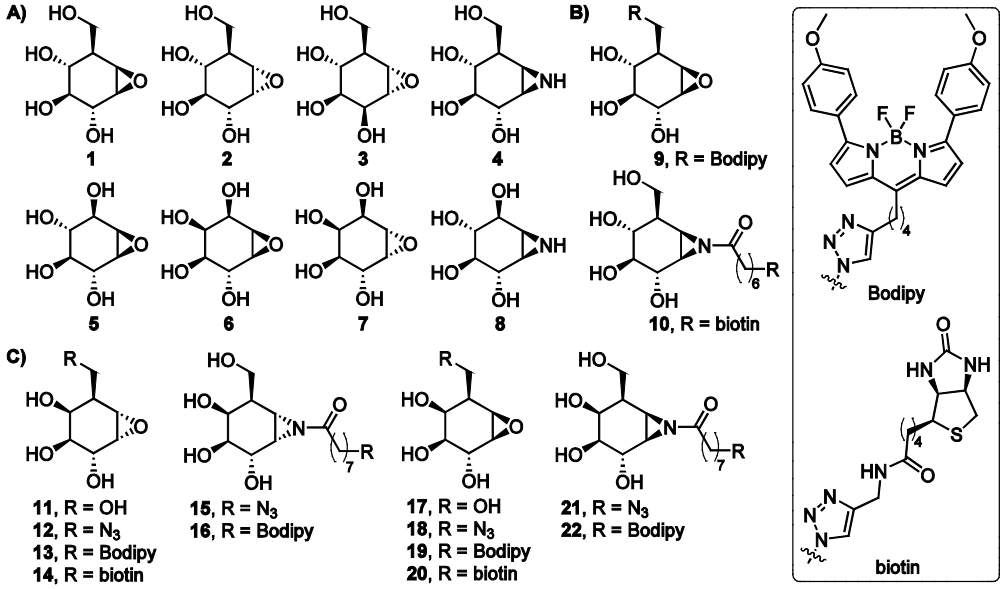

Figure 5.2. A) Irreversible glycosidase inhibitors (**1-8**). B) ABPs for retaining β-exoglucosidases (**9-10**). C) Target compounds: inhibitors and ABPs for retaining α-galactosidases (**11-16**) and β-galactosidases (**17-22**).

retaining β-glucosidases[9] and conduritol B aziridine (**8**) inhibits a number of retaining α- and β-glucosidases.[14] The remarkable selectivity and potency of cyclophellitol, in combination with the highly conserved catalytic mechanism of this class of enzymes, opens up the potential to develop selective inhibitors for different retaining glycosidases by altering the configuration of the inhibitor to that of the natural substrates of the target enzyme. For example, galactopyranose-configured epoxides may enable specific targeting of catalytically active retaining galactosidases. In the same line, the structure of these inhibitors can be exploited for the design of ABPs that target a specific class of glycosidases. Cyclophellitol has already served as a basis to develop a number of epoxide- and aziridine-based probes for retaining β-exoglucosidases (e.g. **9** and **10**, Figure 5.2B).[15,16] Surprisingly, other than the glucosidase and mannosidase inhibitors described above, no differently configured isomers of cyclophellitol or ABPs **9** and **10** have been reported. It would therefore be desirable to develop new synthetic strategies that enable the synthesis of such compounds. This chapter describes the synthesis of two series of galactopyranose-configured ABPs (**12-16** and **18-22**, Figure 5.2C) for retaining α- and β-galactosidases, respectively, with the electrophilic aziridine and epoxide moieties in either an α- or a β-configuration[17] to allow attack by the respective catalytic nucleophiles. The ABPs are functionalized with a fluorescent Bodipy tag, a biotin tag or an azide that can be used for two-step labeling. In addition, the epoxide-based inhibitors **11** and **17** are synthesized as α- and β-galactopyranose-configured cyclophellitol isomers.

5.2 Results and discussion

All target compounds were synthesized from a single precursor, dibenzylated compound **27**, that was prepared in 3 steps from aldehyde **24**[18] following conditions similar to those described in literature (Scheme 5.1).[19] Dibutylboryl triflate mediated reaction of **24** with oxazolidinone **23**[20] resulted in the stereoselective formation of *syn*-aldol adduct **25**, which after removal of the Evans template (**26**) was subjected to ring-closing metathesis to provide cyclohexene **27**. The synthetic route towards α- and β-epoxides **11** and **17** and their azide-modified derivatives **12** and **18** is depicted in Scheme 5.2. The azide moiety was installed at C6 (carbohydrate numbering) by selective tosylation of the primary alcohol in **27** followed by substitution with sodium azide to give **28**. Next, the benzyl groups were removed with BCl_3 and the free hydroxyl groups benzoylated (**29**) in order to enable facile deprotection after formation of the epoxide. Epoxidation was performed with *m*CPBA to give the α- and β-epoxides (**30**) in a ratio of approximately 4:1. After final deprotection with sodium methoxide the isomers could be separated by column chromatography to give

Scheme 5.1 Synthesis of dibenzylated cyclohexene **27**

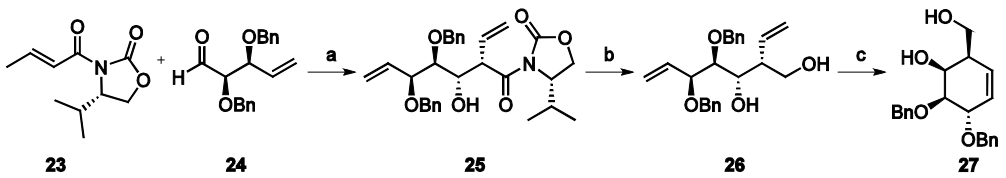

Reagents and conditions: a) $Bu_2BSO_3CF_3$, Et_3N, DCM, -78 °C → -15 °C, 3.5 hrs, 63%; b) $LiBH_4$, THF/H_2O, 0 °C → rt, 2 hrs, 85%; c) Grubbs II, DCM, 40 °C, overnight, 78%.

enantiomerically pure azide-functionalized α- and β-epoxides **12** and **18**. The same strategy of deprotection, benzoylation and epoxidation was used to synthesize the non-tagged epoxide inhibitors **11** and **17**. In this case it proved impossible to separate the mixture of α- and β-epoxides (ratio 1:1) in the protected (**32**) or deprotected (**33**) stage. However, acetylation of **33** was found to give a separable mixture of mainly tri-acetylated β-epoxide **34β1**, a small amount of fully acetylated β-epoxide **34β2**, and fully acetylated α-epoxide **34α**. After separation of the isomers by column chromatography, deprotection yielded the enantiomerically pure α- and β-epoxides **11** and **17**. In order to synthesize the Bodipy- and

Scheme 5.2 Synthesis of α- and β-galactopyranose-configured epoxides (**11**, **17**) and azide-modified derivatives (**12**, **18**)

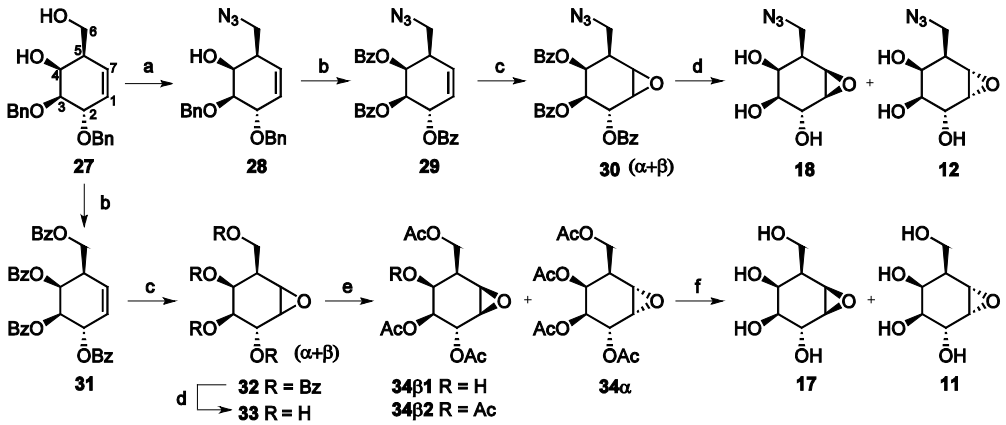

Reagents and conditions: a) *i*) *p*TsCl, Et_3N, DCM, rt, 4 days, *ii*) NaN_3, DMF, 60 °C, overnight, 63%; b) *i*) BCl_3, DCM, -78 °C, 4 hrs, *ii*) BzCl, pyridine, rt, overnight, **29** 85%, **31** 76%; c) *m*CPBA, DCM, rt, 4-8 days, **30** 53%, **32** 62%; d) NaOMe, MeOH, rt, 1.5 hrs, **18** 8% + **12** 42%, **33** 76%; e) Ac_2O, pyridine, rt, 4 hrs, **34α** 38% + **34β1** 20% + **34β2** 2%; f) NaOMe, MeOH, rt, 2 hrs, **11** 94%, **17** 84%.

biotin-tagged epoxide ABPs, their azide-functionalized precursors **12** and **18** were subjected to copper(I)-catalyzed azide-alkyne cycloadditions ('click' reactions) with Bodipy-alkyne **35**[21] or biotin-alkyne **36**[22] (Scheme 5.3). The click reactions proceeded smoothly to provide the fluorescently labeled α-epoxide **13** and biotinylated probe **14** as well as their β-epoxide isomers **19** and **20**.

The strategy towards β-aziridine ABPs **21** and **22** is based on the previously reported procedure to synthesize β-glucosidase probe **10** and relies on the stereocontrolled formation of a β-aziridine with the aid of the primary alcohol at C6 (Scheme 5.4).[16] Briefly, the primary hydroxyl in **27** was selectively transformed into the trichloroacetimidate which was then subjected to iodocyclization. Acidic hydrolysis of the intermediate imidate was followed by the addition of base to effect nucleophilic displacement of the iodine by the amine, providing aziridine **39**. In case of the α-aziridine ABPs **15** and **16** it might be possible to apply a similar procedure by creating an imidate with the hydroxyl group at C2 in order to achieve iodocyclization below the plane of the cyclohexane ring. However, such a strategy would require a number of additional protection and deprotection steps in order to selectively unmask this hydroxyl group. Therefore another route was evaluated to synthesize the α-aziridine probes, commencing with the formation of fully benzylated β-epoxide **42**. Although an α/β mixture was formed by *m*CPBA-mediated epoxidation of **41**, the most prevalent product was β-epoxide **42** with only a small amount of the corresponding α epoxide (ratio 6:1). Moreover, the two isomers could easily be separated by column chromatography. Next, the β-epoxide was opened with sodium azide and lithium perchlorate as a Lewis acid to give a mixture of azido-alcohols (**43**).[23] Treatment of **43** with

Scheme 5.3 Synthesis of biotin- and Bodipy-functionalized epoxide ABPs (**13**, **14**, **19**, **20**) and Bodipy-spacer **38**

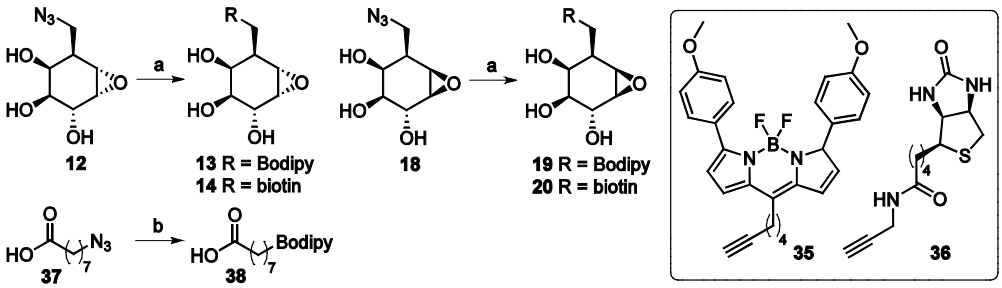

Reagents and conditions: a) Bodipy-alkyne **35** or biotin-alkyne **36**, $CuSO_4.5H_2O$, sodium ascorbate, DMF, rt, overnight, **13** 88%, **14** 68%, **19** 90%, **20** 68%; b) Bodipy-alkyne **35**, $CuSO_4.5H_2O$, sodium ascorbate, DMF, 80 °C, 4.5 hrs, 87%.

Scheme 5.4 Synthesis of α- and β-galactopyranose-configured aziridine ABPs (**15**, **16**, **21**)

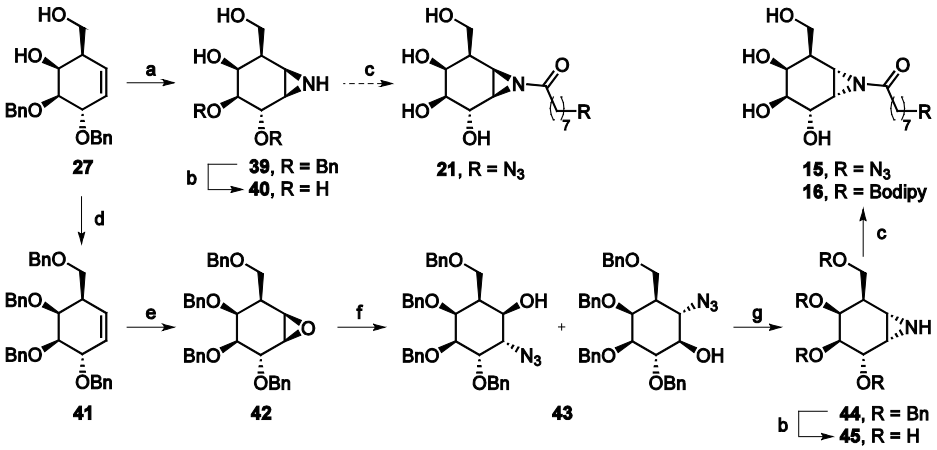

Reagents and conditions: a) *i*) CCl_3CN, DBU, DCM, 0 °C, 1.5 hrs, *ii*) I_2, $NaHCO_3$, H_2O, rt, overnight, *iii*) HCl, MeOH, rt, 3.5 hrs, *iv*) HCl, dioxane, 60 °C, 1 hr, *v*) $NaHCO_3$, MeOH, rt, 4 days, 52%; b) Li, NH_3 (l), THF, -60 °C, 45 min; c) **37** or **38**, EEDQ, DMF, 0 °C, 90 min, **15** 14%, **16** 15%; d) NaH, BnBr, TBAI, DMF, rt, overnight, 85%; e) *m*CPBA, DCM, rt, overnight, 63%; f) NaN_3, $LiClO_4$, ACN, 80 °C, overnight, 73%; g) Ph_3P, ACN, 80 °C, 2 hrs, 26%.

triphenylphosphine led to the formation of the α-aziridine moiety (**44**) via an intramolecular Staudinger-like ring closure.[24] The yield of this reaction was rather low, partly due to the fact that it proved difficult to remove the formed triphenylphosphine oxide. In addition, it might be possible that the intramolecular rearrangement of the iminophosphorane intermediate is hindered by steric factors or ring strain, resulting in reduction of the azide to an amine during workup. Nonetheless, the α-aziridine **44** could be obtained in enantiomerically pure form in four steps starting from **27**. It proved impossible to synthesize β-aziridine **39** using the same strategy since no product was formed by opening of the benzylated epoxide (the α-isomer of **42**) under the same conditions as described above, nor under acidic 'nonchelating' conditions (NaN_3, MeOH/1.2 M NH_4Cl (4:1), 80 °C)[23] or with the use of phase transfer conditions (NaN_3, Bu_4NCl, ACN/H_2O, 80 °C).

The final stage in the synthetic route towards the aziridine ABPs involved deprotection of the benzyl groups in **39** and **44** by Birch reduction and acylation of the aziridine nitrogen with an azide- or Bodipy-functionalized spacer (**37**, **38**) using EEDQ as the coupling reagent (Scheme 5.4).[16] In case of the α-aziridine **44**, deprotection and subsequent acylation followed by HPLC purification provided the azide- and Bodipy-tagged products **15** and **16**. After deprotection of the β-aziridine **39**, however, some byproduct formation was observed by ^{1}H NMR analysis. Furthermore, attempts to acylate the crude product **40** with azido-

spacer **37** were unsuccessful since ^{1}H NMR analysis indicated significant degradation and almost complete disappearance of the aziridine proton peaks after HPLC purification and ensuing lyophilization. Further analysis by LC/MS revealed that the aziridine was opened with HCl, despite the fact that no acids were used during purification. Instability of the acylated aziridine moiety is a recurring problem during the synthesis of such ABPs and opening of the aziridine was also repeatedly observed with the α-galactosidase ABPs and the β-glucosidase ABPs described previously.[16] Hence, care has to be taken that the acylation reaction as well as ensuing HPLC purification and lyophilization are performed in the absolute absence of any traces of acid. It appears that the β-aziridine moiety is very unstable even under these conditions and consequently the β-aziridine ABP **21** could not be isolated.

The diastereomeric configuration of the α- and β-epoxides **11** and **17** was determined by ^{1}H NMR analysis and was supported by a comparison of the experimental coupling constants with the corresponding values obtained from DFT calculations (Table 5.1). The optimized structures obtained by these calculations are shown in Figure 5.3. The assignment of the diastereomeric configuration of epoxides **12**, **18** and **42** could be deduced from epoxides **11** and **17**. In all cases a characteristic configuration-dependent pattern of epoxide proton peaks was observed in which the H1 and H7 peaks (carbohydrate numbering) of the β-epoxides are consistently closer together than those of the α-epoxides. Moreover, the H1-H2 coupling is smaller and the H5-H7 coupling larger for the β-isomers than the α-isomers. The correct configuration of β-epoxide **42** was further supported by the fact that it leads to α-aziridine **44**, which can in turn be confirmed by comparison with β-aziridine **39** of which the configuration is known.

Table 5.1. Comparison of experimental and calculated coupling constants for epoxides **11** and **17**

α-epoxide **11**	*J* exp. (Hz)	*J* calc. (Hz)	β-epoxide **17**	*J* exp. (Hz)	*J* calc. (Hz)
H1-H7	4.0	3.7	H1-H7	3.7	3.4
H1-H2	2.5	2.2	H1-H2	n.d. (a)	0.04
H2-H3	8.6	6.9	H2-H3	8.6	6.6
H3-H4	1.9	1.8	H3-H4	n.d. (b)	2.7
H4-H5	3.6	4.0	H4-H5	4.0	3.5
H5-H7	n.d. (a)	0.04	H5-H7	1.7	1.5
H4-H7	1.8	1.1	H4-H7	n.d. (a)	0.8

Coupling constants obtained from DFT calculations ('calc.') as compared to experimental data from ^{1}H NMR analysis ('exp.'). n.d.: values were not determined because of a) very small coupling constants (J < 1 Hz) or b) peak overlap.

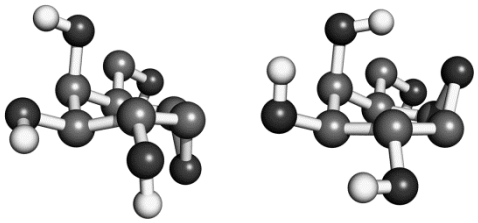

Figure 5.3. Optimized structures of α-epoxide **11** (left) and β-epoxide **17** (right) obtained by DFT calculations.

In the synthetic strategies described here, the formation of both α- and β-epoxides by *m*CPBA-mediated epoxidation is favorable, as long as the two isomers can be separated at some point in the route of synthesis. In other cases, however, it may be desirable to obtain only one isomer and for that purpose other oxidation methods should be evaluated. It is worth noting that the fully benzoylated compound **31** gives a 1:1 ratio of α- and β-epoxides whereas an α:β ratio of 4:1 was obtained with the C6-azide-functionalized analogue **29**. Full benzylation (**41**) on the other hand leads to more β-selectivity during epoxidation (α:β 1:6). These results indicate that formation of the β-epoxide is favored in the absence of chelating effects and that the presence of a benzoyl group at either the allylic (C2) or homoallylic (C6) position can enhance α- or β-selectivity, respectively. As expected, deprotection of either **29** or **31** prior to epoxidation led to the formation of mainly the α-epoxide (α:β > 15:1) due to strong coordination of the allylic OH to *m*CPBA.

5.3 Conclusion

Two sets of galactopyranose-configured glycosidase probes were synthesized that are equipped with an electrophilic α- or β-configured epoxide moiety in order to enable targeting of retaining α- and β-galactosidases, respectively. Each set consists of a non-tagged inhibitor (**11**, **17**), an ABP for two-step labeling with an azide as a ligation handle (**12**, **18**), and two ABPs that are functionalized with a fluorescent Bodipy tag (**13**, **19**) or a biotin tag (**14**, **20**). Next to the epoxide-based ABPs, efforts were undertaken to synthesize analogous probes with an aziridine as the electrophile in which an azide or Bodipy tag is installed via acylation of the aziridine moiety. Whereas the α-aziridine ABPs **15** and **16** were successfully obtained, it proved impossible to isolate β-aziridine probe **21** since even the use of a completely acid-free purification procedure resulted in opening of the labile acylated aziridine. Hence, other methods or a different probe design will be necessary to realize the synthesis of aziridine-based β-galactosidase ABPs. Evaluation of the inhibitory potency of the synthesized α- and β-configured probes as well as their application for the labeling of human retaining α- and β-galactosidases is described in Chapters 6 and 7, respectively.

Experimental procedures

General

All reagents were commercial grade and were used as received unless stated otherwise. DCM, DCE, DMF and THF (Biosolve) were of analytical grade and when used under anhydrous conditions stored over flame-dried 3 Å molecular sieves. EtOAc (Riedel-de Haën) used for column chromatography was of technical grade and distilled before use. Reactions were monitored by TLC-analysis using DC-alufolien (Merck, Kieselgel60, F254) with detection by UV-absorption (254/366 nm), spraying with 20% H_2SO_4 in ethanol or a solution of $(NH_4)_6Mo_7O_{24}.4H_2O$ (25 g/L) and $(NH_4)_4Ce(SO_4)_4.2H_2O$ (10 g/L) in 10% aqueous sulfuric acid followed by charring at ~150 °C or by spraying with an aqueous solution of $KMnO_4$ (7%) and K_2CO_3 (2%). Column chromatography was performed on silica gel (Screening Devices BV, 0.040 - 0.063 mm, 60 Å). LC/MS analysis was performed on an LCQ Adventage Max (Thermo Finnigan) ion-trap spectrometer (ESI+) coupled to a Surveyor HPLC system (Thermo Finnigan) equipped with a C18 column (Gemini, 4.6 mm x 50 mm, 5µm particle size, Phenomenex). The applied buffers were A: H_2O, B: ACN and C: 1 % aqueous TFA. Reported gradients represent the percentage of buffer B in buffer A with 10% buffer C. Alternatively, where indicated LC/MS analysis was performed using an API 3000 ESI (Q1) mass spectrometer (Applied Biosystems) coupled to a Jasco (900 series) HPLC system. The applied buffers were A: H_2O, B: ACN and C: 100 mM NH_4OAc in H_2O. Reported gradients represent the percentage of buffer B in buffer A with 10% buffer C. HRMS analysis was performed on an LTQ Orbitrap (Thermo Finnigan) mass spectrometer equipped with an electronspray ion source in positive mode (source voltage 3.5 kV, sheath gas flow 10 mL min−1, capillary temperature 250 °C) with resolution R = 60000 at m/z 400 (mass range m/z = 150 - 2000) and dioctylphtalate (m/z = 391.28428) as a "lock mass". The high resolution mass spectrometer was calibrated prior to measurements with a calibration mixture (Thermo Finnigan). For reversed-phase HPLC purification an automated HPLC system equipped with a C18 semiprep column (Gemini C18, 250 mm x 10 mm, 5µm particle size, 110 Å pore size, Phenomenex) was used. ^{1}H- and ^{13}C-APT-NMR spectra were recorded on a Brüker AV-400 (400/100MHz) or a Bruker DMX600 (600/150 MHz) instrument with a cryoprobe. Chemical shifts are given in ppm (δ) relative to the solvent peak or to tetramethylsilane as internal standard. Coupling constants (*J*) are given in Hz. All presented ^{13}C-APT spectra are proton decoupled. Peak assignments are based on 2D ^{1}H-COSY and ^{13}C-HSQC NMR experiments.

(S)-3-((2S,3S,4S,5S)-4,5-bis(benzyloxy)-3-hydroxy-2-vinylhept-6-enoyl)-4-isopropyloxazolidin-2-one (25)

Note: Solutions of aldehyde **24**[18] and oxazolidinone **23**[20] in DCM were put under argon atmosphere and dried over activated 4Å molsieves for at least 1 hr prior to use. Et_3N was distilled over CaH_2 and stored on activated 4Å molsieves under argon atmosphere.

A solution of oxazolidinone **23** (32 mmol, 6.3 g, 2.0 eq.) in DCM under argon atmosphere was cooled to -78 °C with the use of a cryostate before addition of $Bu_2BSO_3CF_3$ (32 mmol, 32 mL 1 M in DCM, 2.0 eq.) and Et_3N (35 mmol, 4.9 mL, 2.2 eq.). The reaction mixture was stirred at -78 °C for 1 hr, then at 0 °C (ice bath) for 15 min and subsequently cooled back to -78 °C. A solution of aldehyde **24** (16 mmol, 4.7 g, 1.0 eq.) in DCM under argon atmosphere was added via canula after which the temperature was allowed to rise to -20 °C over 2 hrs and maintained at -15 °C for 1.5 hrs. Next, the mixture was removed from the cold bath and put in an ice bath of -5 °C. After quenching with PBS (20 mL), H_2O_2 (30% aqueous solution) was added dropwise while keeping the temperature of the mixture below 5 °C, until no more rise in temperature was observed. At this point the mixture was stirred for another 45 min while slowly warming to room temperature after which aqueous saturated $NaHCO_3$ was added and the aqueous layer was extracted with DCM (3x). The combined organic layers were dried over $MgSO_4$, filtered and concentrated *in vacuo*. The crude product was purified by column chromatography (pentane → 10% EtOAc in pentane) to afford the aldol adduct **25** (4.9 g, 10 mmol, 63%). ^{1}H NMR (400 MHz, $CDCl_3$): δ (ppm) 7.39-7.25 (m, 10H), 6.06 (ddd, *J* = 18.5, 9.7, 7.1

Hz, 1H), 5.92 (ddd, *J* = 17.3, 10.1, 8.8 Hz, 1H), 5.45-5.37 (m, 3H), 5.29 (dd, *J* = 10.2, 1.6 Hz, 1H), 5.02 (dd, *J* = 9.0, 7.2 Hz, 1H), 4.69 (dd, *J* = 11.5, 4.0 Hz, 2H), 4.55-4.40 (m, 3H), 4.29 (dd, *J* = 7.3, 3.9 Hz, 1H), 4.03 (dt, *J* = 8.6, 3.5 Hz, 1H), 3.84 (dd, *J* = 9.0, 3.0 Hz, 1H), 3.58 (dd, *J* = 8.3, 3.9 Hz, 1H), 3.39 (bs, 1H), 3.26 (t, *J* = 8.8 Hz, 1H), 2.26-2.14 (m, 1H), 0.75 (dd, *J* = 18.8, 7.0 Hz, 6H). ^{13}C NMR (100 MHz, $CDCl_3$): δ (ppm) 172.53, 153.53, 138.01, 137.76, 134.55, 133.56, 128.17, 128.00, 127.64, 127.53, 127.32, 127.09, 120.43, 119.14, 81.78, 79.90, 73.04, 71.12, 70.66, 62.38, 57.94, 50.06, 27.96, 17.75, 14.41.

(2R,3S,4S,5S)-4,5-bis(benzyloxy)-2-vinylhept-6-ene-1,3-diol (26)

Oxazolidinone **25** (13.8 mmol, 6.8 g) was dissolved in THF (100 mL) at 0 °C after which H_2O (8 mL) and $LiBH_4$ (35 mmol, 17.5 mL 2 M in THF, 2.5 eq.) were added. The reaction mixture was stirred at 0 °C for 1 hr and then at room temperature for 1 hr, before being quenched with 2 M NaOH. The resulting mixture was extracted with Et_2O (2x) and the combined organic layers were washed with aqueous saturated $NaHCO_3$ and Brine, dried over $MgSO_4$ and concentrated *in vacuo*. Purification by column chromatography (pentane → 40% EtOAc in pentane) yielded alcohol **26** as a white solid (4.3 g, 12 mmol, 85%).^{1}H NMR (400 MHz, $CDCl_3$): δ (ppm) 7.45-7.21 (m, 10H), 6.14-5.94 (m, 2H), 5.49-5.33 (m, 2H), 5.26 (dd, *J* = 10.4, 2.1 Hz, 1H), 5.13 (dd, *J* = 17.5, 2.2 Hz, 1H), 4.67 (d, *J* = 11.8 Hz, 1H), 4.57 (d, *J* = 11.1 Hz, 1H), 4.48 (d, *J* = 11.1 Hz, 1H), 4.39 (d, *J* = 11.8 Hz, 1H), 4.21 (dd, *J* = 7.0, 3.8 Hz, 1H), 4.05 (d, *J* = 9.1 Hz, 1H), 3.77-3.64 (m, 2H), 3.51 (dd, *J* = 9.1, 3.7 Hz, 1H), 3.39 (bs, 1H), 2.58 (ddt, *J* = 7.9, 5.7, 2.9 Hz, 1H), 2.20 (bs, 1H). ^{13}C NMR (100 MHz, $CDCl_3$): δ (ppm) 137.75, 137.26, 135.28, 133.85, 128.55, 128.36, 127.93, 127.86, 127.80, 119.51, 119.05, 79.58, 78.97, 73.08, 72.53, 70.97, 65.58, 47.33.

(3S,4S,5S,6R)-6-(hydroxymethyl)-3,4-dibenzyloxy-5-hydroxy-cyclohex-1-ene (27)

To a solution of **26** (7.8 mmol, 2.9 g) in DCM under argon atmosphere was added second generation Grubbs catalyst (0.4 mmol, 0.34 g, 5 mol%). The reaction mixture was stirred at 40 °C in the dark for 20 hrs, DMSO (40 mmol, 2.8 mL, 100 eq. with respect to catalyst) was added and the mixture was stirred overnight at room temperature before being concentrated *in vacuo*. Purification by column chromatography (pentane → pentane/EtOAc 1/1 (v/v)) gave cyclohexene **27** (7.2 mmol, 2.5 g, 92%). ^{1}H NMR (400 MHz, $CDCl_3$): δ (ppm) 7.38-7.28 (m, 10 H), 5.84 (d, *J* = 10.4 Hz, 1H), 5.55 (d, *J* = 10.1 Hz, 1H), 4.71 (d, *J* = 8.5 Hz, 4H), 4.33-4.31 (m, 2H), 3.82-3.80 (m, 2H), 3.65 (d, *J* = 7.4 Hz, 1H), 2.95 (bs, 2H), 2.45 (d, *J* = 6.1 Hz, 1H). ^{13}C NMR (100 MHz, $CDCl_3$): δ (ppm) 138.45, 137.93, 128.45, 128.32, 127.85, 127.75, 127.57, 127.43, 126.75, 81.80, 77.31, 76.58, 72.15, 41.87.

(3S,4S,5S,6R)-6-(azidomethyl)-3,4-dibenzyloxy-5-hydroxy-cyclohex-1-ene (28)

A solution of (3S,4S,5S,6R)-6-(hydroxymethyl)-3,4-dibenzyloxy-5-hydroxy-cyclohex-1-ene (**27**) (0.76 mmol, 0.26 g) in DCM under argon atmosphere was cooled to 0 °C before *p*TsCl (0.84 mmol, 0.16 g, 1.1 eq.) and Et_3N (1.4 mmol, 0.19 mL, 1.8 eq.) were added. The reaction mixture was stirred overnight at room temperature, after which TLC analysis indicated incomplete reaction. Therefore another 0.5 eq. of *p*TsCl (75 mg) and 1.8 eq. of Et_3N (0.19 mL) were added after 24 hrs and again after 48 hrs. The mixture was stirred for a total of 4 days, after which 1 M aqueous HCl was added and the aqueous layer was extracted with Et_2O (3x). The combined organic layers were dried over $MgSO_4$, filtered and concentrated *in vacuo*. The crude tosylated product was then redissolved in DMF under argon atmosphere and NaN_3 (7.6 mmol, 0.50 g, 10 eq.) was added. The reaction mixture was heated to 60 °C, stirred overnight and concentrated *in vacuo*. The residue was then redissolved in EtOAc and washed with 1 M aqueous HCl (1x), aqueous saturated $NaHCO_3$ (1x) and Brine (1x), dried over $MgSO_4$, filtered and concentrated *in vacuo.* Purification by column chromatography (pentane → 12% EtOAc in pentane in steps of 2%) gave the dibenzylated azide **28** (0.17 g, 0.48 mmol, 63% over two steps). ^{1}H NMR (400 MHz, $CDCl_3$): δ (ppm) 7.46-7.31 (m, 10H), 5.86 (dt, *J* = 10.2, 2.6 Hz, 1H), 5.48 (dd, *J* = 9.6, 1.6 Hz, 1H), 4.81-4.73 (m, 4H), 4.40-4.27 (m, 2H), 3.70 (dd, *J* = 7.8, 2.2 Hz, 1H), 3.60 (dd, *J* = 11.9, 9.3 Hz, 1H), 3.40 (dd, *J* = 11.9, 6.5 Hz, 1H), 2.56 (dt, *J* = 6.3, 3.1 Hz, 1H), 2.50-2,47

(m, 1H). ^{13}C NMR (100 MHz, $CDCl_3$): δ (ppm) 138.51, 138.03, 128.56, 128.44, 127.96, 127.92, 127.86, 127.70, 125.50, 82.12, 76.80, 72.42, 72.26, 67.58, 51.77, 40.63. HRMS: calcd. for $[C_{21}H_{24}O_3N_3]^+$ 366.18122, found 366.18143; calcd. for $[C_{21}H_{23}O_3N_3Na]^+$ 388.16316, found 388.16322. $[\alpha]D^{20}$ (c = 0.1, $CHCl_3$): +118°.

(3S,4R,5S,6R)-6-(azidomethyl)-3,4,5-tribenzoyloxy-cyclohex-1-ene (29)

A solution of dibenzylated azide **28** (0.47 mmol, 0.17 g) in DCM was cooled to -78 °C under argon atmosphere before addition of BCl_3 (4.8 mmol, 4.8 mL 1 M in DCM, 10 eq.). The reaction mixture was stirred at -78 °C for 4 hrs, quenched with MeOH, concentrated *in vacuo* and coevaporated with toluene (3x). The deprotected product was then dissolved in pyridine, BzCl was added (4.7 mmol, 0.55 mL, 10 eq.) and the mixture was stirred overnight at room temperature. After quenching with aqueous saturated $NaHCO_3$ the mixture was extracted with DCM (3x) and the combined organic layers were dried over $MgSO_4$, filtered and concentrated *in vacuo*. The product was purified by column chromatography (pentane → 7.5% EtOAc in pentane) to yield the tribenzoylated product **29** (0.20 g, 0.40 mmol, 85% over two steps). ^{1}H NMR (400 MHz, $CDCl_3$): δ (ppm) 8.19-7.86 (m, 6H), 7.66-7.28 (m, 9H), 6.21-6.12 (m, 1H), 6.12-6.07 (m, 1H), 6.03 (dt, *J* = 10.3, 2.7 Hz, 1H), 5.89-5.82 (m, 1H), 5.71 (dd, *J* = 8.6, 2.3 Hz, 1H), 3.52 (dd, *J* = 12.1, 7.7 Hz, 1H), 3.42 (dd, *J* = 12.1, 7.8 Hz, 1H), 3.10-3.08 (m, 1H). ^{13}C NMR (100 MHz, $CDCl_3$): δ (ppm) 166.11, 165.84, 165.51, 133.75, 133.55, 133.28, 133.21, 130.17, 129.78, 129.76, 129.72, 129.46, 129.20, 129.17, 128.66, 128.46, 128.40, 128.31, 127.48, 126.55, 73.14, 70.49, 69.85, 51.46, 39.87. HRMS: calcd. for $[C_{28}H_{23}O_6N_3Na]^+$ 520.14791, found 520.14724. $[\alpha]D^{20}$ (c = 0.2, $CHCl_3$): +265°.

(2S,3S,4S,5S)-5-(azidomethyl)-2,3,4-tribenzoyloxy-7-oxabicyclo[4.1.0]heptane (30)

Tribenzoylated azide **29** (0.40 mmol, 0.20 g) was dissolved in DCM under argon atmosphere and 3-chloroperoxybenzoic acid (1.2 mmol, 0.27 g, 3.0 eq.) was added. The reaction mixture was stirred at room temperature for a total of 4 days, concentrated *in vacuo* and purified by column chromatography (pentane → 10% EtOAc in pentane) giving the azido-epoxide **30** as a mixture of α- and β-isomers (ratio 4:1) (0.11 g, 0.21 mmol, 53%). ^{1}H NMR (400 MHz, $CDCl_3$): δ (ppm) 8.12-7.81 (m, 6H α + 6H β), 7.68-7.25 (m, 9H α + 9H β), 6.04 (dd, *J* = 9.3, 2.3 Hz, 1H α), 5.93-5.86 (m, 1H α + 1H β), 5.75 (d, *J* = 9.4 Hz, 1H β), 5.60 (dd, *J* = 9.3, 1.9 Hz, 1H α), 5.53 (dd, *J* = 9.3, 2.6 Hz, 1H β), 3.88 (dd, *J* = 3.9, 2.3 Hz, 1H α), 3.68-3.42 (m, 2H α + 4H β), 3.35 (dd, *J* = 3.9, 1.7 Hz, 1H α), 2.80-2.74 (m, 1H α + 1H β). ^{13}C NMR (100 MHz, $CDCl_3$): δ (ppm) 166.25, 165.68, 165.65, 165.54, 165.47, 165.26, 134.59, 133.66, 133.62, 133.53, 133.48, 133.36, 133.30, 130.88, 129.80, 129.79, 129.76, 129.73, 129.71, 129.64, 129.01, 128.96, 128.92, 128.89, 128.83, 128.67, 128.64, 128.58, 128.56, 128.49, 128.43, 128.33, 128.32, 72.17, 70.85, 70.32, 70.18, 68.47, 66.77, 54.44, 54.14, 53.67, 52.04, 49.77, 49.75, 39.01, 38.27. LC/MS analysis: R_t 9.3 min (linear gradient 10 → 90% B in 15 min), m/z 514.1 $[M+H]^+$, 1026.7 $[2M+H]^+$. HRMS: calcd. for $[C_{28}H_{24}O_7N_3]^+$ 514.16088, found 514.16066; calcd. for $[C_{28}H_{23}O_7N_3Na]^+$ 536.14282, found 536.14242. $[\alpha]D^{20}$ (c = 0.2, $CHCl_3$): +189°.

(2R,3S,4S,5R)-5-(azidomethyl)-2,3,4-trihydroxy-7-oxabicyclo[4.1.0]heptane: α-epoxide 12 and β-epoxide 18

Epoxide **30** (0.19 mmol, 96 mg) was dissolved in MeOH (2.5 mL) and deprotected with NaOMe (38 µmol, 6.8 µL 5.6 M in MeOH, 20 mol%) for 1.5 hrs at room temperature. The reaction mixture was then quenched by addition of Amberlite-H^+ IR-200, filtered and concentrated *in vacuo*. The product was purified by multiple rounds of column chromatography (DCM → 3% MeOH in DCM in steps of 0.5%) to separate the α-epoxide **12** (16 mg, 80 µmol, 42%) and β-epoxide **18** (3.0 mg, 15 µmol, 8%) (yield of mixed α/β product 7.0 mg, 35 µmol, 18%). ^{1}H NMR (600 MHz, MeOD) α-epoxide **12**: δ (ppm) 4.07 (dd, *J* = 8.6, 2.5 Hz, 1H), 3.78 (dd, *J* = 3.4, 1.8 Hz, 1H), 3.59 (dd, *J* = 12.2, 8.0 Hz, 1H), 3.48 (dd, *J* = 12.3, 8.3 Hz, 1H), 3.39 (dd, *J* = 8.5, 1.9 Hz, 1H), 3.32 (dd, *J* = 3.9, 2.4 Hz, 1H), 2.97 (dd, *J* = 3.9, 1.8 Hz, 1H), 2.09 (td, *J* = 8.2, 3.5 Hz, 1H). ^{13}C NMR (150 MHz, MeOD) α-epoxide **12**: δ (ppm) 73.56, 72.15, 70.53, 58.08, 55.29, 51.73, 41.83. ^{1}H NMR (600 MHz, MeOD) β-epoxide **18**: δ (ppm) 3.92 (dd, *J* = 8.7, 0.7 Hz, 1H), 3.82 (ddd, *J* = 4.1, 2.5, 1.3 Hz, 1H), 3.70 (dd, *J* = 12.1, 8.2 Hz, 1H), 3.63 (dd, *J* = 12.1, 7.2 Hz, 1H), 3.33 (dd, *J* = 8.6, 2.6 Hz, 1H), 3.26-

3.22 (m, 1H), 3.17 (d, *J* = 3.7 Hz, 1H), 2.28 (dddd, *J* = 8.2, 7.2, 4.1, 1.8 Hz, 1H). ^{13}C NMR (150 MHz, MeOD) β-epoxide **18**: δ (ppm) 76.39, 70.36, 69.50, 58.03, 55.21, 51.58, 40.43. [α]D^{20} (c = 0.1 (β)/0.3 (α), MeOH): **12** +81°, **18** +64°.

(3S,4R,5S,6R)-6-(benzoyloxymethyl)-3,4,5-tribenzoyloxy-cyclohex-1-ene (31)

A solution of (3S,4S,5S,6R)-6-(hydroxymethyl)-3,4-dibenzyloxy-5-hydroxy-cyclohex-1-ene (**27**) (0.5 mmol, 0.17 g) in DCM under argon atmosphere was cooled to -78 °C before BCl_3 was added (5 mmol, 5 mL 1M in DCM, 10 eq.). The reaction mixture was stirred under argon at -78 °C for 4 hrs and then quenched with MeOH, concentrated *in vacuo* and coevaporated with toluene (3x). Purification by column chromatography (10% MeOH in EtOAc → 20% MeOH in EtOAc) afforded the fully deprotected compound, which was redissolved in pyridine and cooled to 0 °C. Next, benzoyl chloride was added (5 mmol, 0.6 mL, 10 eq.) and the mixture was stirred overnight at room temperature before being quenched with a saturated aqueous $NaHCO_3$ solution. The aqueous layer was extracted with DCM (3x) and the combined organic layers were dried over $MgSO_4$, filtered and concentrated *in vacuo*. Purification by column chromatography (pentane → 10% EtOAc in pentane) yielded the fully benzoylated product **31** (0.22 g, 0.38 mmol, 76% over two steps). ^{1}H NMR (400 MHz, $CDCl_3$): δ (ppm) 8.00-7.88 (m, 8H), 7.62-7.30 (m, 12H), 6.23-6.18 (m, 2H), 6.09-6.06 (m, 1H), 5.88 (dd, *J* = 1.2, 10.4 Hz, 1H), 5.78 (dd, *J* = 2.2, 8.6 Hz, 1H), 4.59 (dd, *J* = 6.4, 10.8 Hz, 1H), 4.32 (dd, *J* = 8.8, 10.8 Hz, 1H), 3.44-3.40 (m, 1H). ^{13}C NMR (100 MHz, $CDCl_3$): δ (ppm) 166.23, 166.14, 165.87, 165.51, 133.71, 133.42, 133.26, 133.20, 133.13, 129.80, 129.77, 129.74, 129.68, 129.51, 129.35, 129.24, 128.60, 128.47, 128.39, 128.31, 126.86, 126.81, 73.10, 70.60, 69.30, 63.05, 39.47. LC/MS analysis: R_t 10.1 min (linear gradient 10 → 90% B in 15 min), m/z 599.1 $[M+Na]^+$, 1174.9 $[2M+Na]^+$. HRMS: calcd. for $[C_{35}H_{29}O_8]^+$ 577.18569, found 577.18602; calcd. for $[C_{35}H_{28}O_8Na]^+$ 599.16764, found 599.16727. [α]D^{20} (c = 0.1, $CHCl_3$): +250°.

(2R,3S,4S,5R)-5-(benzoyloxymethyl)-2,3,4-tribenzoyloxy-7-oxabicyclo[4.1.0]heptane (32)

To a solution of **31** (0.42 mmol, 0.24 g) in DCM was added 3-chloroperoxybenzoic acid (1.1 mmol, 0.24 g, 2.5 eq.) and the reaction mixture was stirred for 4 days at room temperature. Then, an additional 1 eq. of 3-chloroperoxybenzoic acid was added and the reaction mixture was stirred again for 4 days at room temperature, before being concentrated *in vacuo*. Purification by column chromatography (pentane → 15% EtOAc in pentane) yielded a mixture of the α- and β-epoxides **32** in a 1:1 ratio (0.15 g, 0.26 mmol, 62%). ^{1}H NMR (400 MHz, $CDCl_3$): δ (ppm) 8.19-7.76 (m, 8H α + 8H β), 7.68-7.20 (m, 12H α + 12H β), 6.14-5.98 (m, 2H α + 1H β), 5.78 (d, *J* = 9.4 Hz, 1H β), 5.68 (dd, *J* = 1.8, 9.2 Hz, 1H α), 5.61 (dd, *J* = 2.6, 9.4 Hz, 1H β), 4.78 (dd, *J* = 6.7, 11.1 Hz, 1H β), 4.70-4.62 (m, 1H α), 4.52-4.46 (m, 1H α + 1H β), 3.92 (dd, *J* = 2.3, 3.7 Hz, 1H α), 3.50 (s, 2H β), 3.43 (dd, *J* = 1.5, 3.8 Hz, 1H α), 3.21-3.01 (m, 1H α + 1H β). ^{13}C NMR (100 MHz, $CDCl_3$): δ (ppm) 166.28, 165.69, 165.58, 133.59, 133.50, 133.44, 133.25, 133.20, 133.16, 130.00, 129.86, 129.77, 129.68, 129.12, 129.08, 129.01, 128.68, 128.58, 128.47, 128.40, 128.28, 72.13, 70.85, 70.30, 69.87, 68.71, 66.25, 61.92, 61.79, 54.17, 53.98, 53.42, 51.73, 38.59, 37.75. LC/MS analysis: R_t 9.7 min (linear gradient 10 → 90% B in 15 min), m/z 593.1 $[M+H]^+$, 1206.9 $[2M+Na]^+$. HRMS: calcd. for $[C_{35}H_{29}O_9]^+$ 593.18061, found 593.18073; calcd. for $[C_{35}H_{28}O_9Na]^+$ 615.16255, found 615.16184. [α]D^{20} (c = 0.1, $CHCl_3$): +130°.

(2R,3S,4S,5R)-5-(hydroxymethyl)-7-oxabicyclo[4.1.0]heptane-2,3,4-triol: mix of α- and β-epoxide (33)

A solution of tetrabenzoylated epoxides **32** (α- and β-epoxides in 1:1 ratio) (0.30 mmol, 180 mg) in MeOH was treated with sodium methoxide (0.12 mmol, 21 µL 5.6 M in MeOH, 0.4 eq.) at room temperature for 1.5 hrs. After neutralization with Amberlite-H^+ IR-200 the reaction mixture was filtered and concentrated *in vacuo*. Purification by column chromatography (10% MeOH in DCM → 15% MeOH in DCM) yielded the fully deprotected product **33** (α- and β-epoxides in 1.5:1 ratio) (40 mg, 0.23 mmol, 76%). ^{1}H NMR (400 MHz, $CDCl_3$): δ (ppm) 4.07 (dd, *J* = 2.4, 8.4 Hz, 1H α), 3.91 (d, *J* = 8.4 Hz, 1H β), 3.87-3.82 (m, 3H α + 3H β), 3.38 (dd, *J* = 1.6, 8.4 Hz, 1H α), 3.32-3.29 (m, 1H α + 2H β), 3.15 (d, *J* = 4.0 Hz, 1H β), 3.08 (dd, *J* = 1.6, 4.0 Hz, 1H α), 2.18-2.16 (m, 1H β), 2.05-2.00 (m, 1H α).

Separation of α- and β-epoxides by acetylation-deacetylation (11 + 17)

An α/β mixture of deprotected epoxides **33** (0.26 mmol, 45 mg) was coevaporated with toluene before being dissolved in pyridine under argon atmosphere. After addition of acetic anhydride (10 mmol, 0.9 mL, 38 eq.) the mixture was stirred at room temperature for 4 hrs, then concentrated *in vacuo* and coevaporated with toluene (3x). After purification by column chromatography (DCM → 0.6% MeOH in DCM in steps of 0.1%) three different products were isolated: the tetra-acetylated form of the α-isomer **34α** (0.10 mmol, 35 mg, 38%), a small amount of tetra-acetylated β-isomer **34β2** (4.4 µmol, 1.5 mg, 2%) and tri-acetylated β-isomer **34β1** (53 µmol, 16 mg, 20%). ^{1}H NMR (400 MHz, $CDCl_3$) **34α**: δ (ppm) 5.52-5.41 (m, 2H), 5.00 (dd, *J* = 9.6, 1.8 Hz, 1H), 4.24-4.07 (m, 2H), 3.59 (dd, *J* = 4.0, 2.4 Hz, 1H), 3.10 (dd, *J* = 4.0, 1.6 Hz, 1H), 2.68 (td, *J* = 8.1, 3.7 Hz, 1H), 2.13 (s, 3H), 2.10 (s, 3H), 2.06 (s, 3H), 2.00 (s, 3H). ^{1}H NMR (400 MHz, $CDCl_3$) **34β2**: δ (ppm) 5.52-5.45 (m, 1H), 5.26 (d, *J* = 9.4 Hz, 1H), 4.95 (dd, *J* = 9.6, 2.0 Hz, 1H), 4.35-4.20 (m, 2H), 3.26-3.17 (m, 2H), 2.78-2.74 (m, 1H), 2.12 (s, 3H), 2.09 (s, 3H), 2.05 (s, 3H), 1.96 (s, 3H). ^{1}H NMR (400 MHz, $CDCl_3$) **34β1**: δ (ppm) 5.35 (d, *J* = 9.1 Hz, 1H), 4.90 (dd, *J* = 9.1, 2.6 Hz, 1H), 4.46-4.38 (m, 2H), 3.99 (d, *J* = 9.3 Hz, 1H), 3.44-3.37 (m, 1H), 3.30 (d, *J* = 3.6 Hz, 1H), 2.54 (tdd, *J* = 7.6, 3.5, 1.3 Hz, 1H), 2.46 (d, *J* = 11.0 Hz, 1H), 2.13 (s, 3H), 2.12 (s, 3H), 2.10 (s, 3H). The β-isomers **34β1** and **34β2** were then combined and deprotected separately from **34α** by treatment with sodium methoxide (30 µmol, 5 µL 5.6 M in MeOH, 0.3 eq. for **34α** and 17 µmol, 3 µL 5.6 M in MeOH, 0.3 eq. for **34β**) in MeOH at room temperature for 2 hrs. The mixtures were neutralized with Amberlite-H^+ IR-200, filtered and concentrated *in vacuo*. The crude products were finally purified by column chromatography (10% MeOH in DCM → 15% MeOH in DCM) to give α-epoxide **11** (17 mg, 94 µmol, 94%) and β-epoxide **17** (8.5 mg, 48 µmol, 84%). ^{1}H NMR (600 MHz, MeOD) α-isomer **11**: δ (ppm) 4.09 (dd, *J* = 8.5, 2.5 Hz, 1H), 3.85 (ddd, *J* = 3.6, 1.8, 1.8 Hz, 1H), 3.78 (dd, *J* = 11.0, 6.6 Hz, 1H), 3.74 (dd, *J* = 11.0, 8.0 Hz, 1H), 3.41 (dd, *J* = 8.6, 1.9 Hz, 1H), 3.33 (dd, *J* = 4.0, 2.5 Hz, 1H), 3.10 (dd, *J* = 4.0, 1.7 Hz, 1H), 2.04 (ddd, *J* = 8.0, 6.6, 3.5 Hz, 1H). ^{13}C NMR (150 MHz, MeOD) α-epoxide **11**: δ (ppm) 73.76, 72.77, 70.79, 62.28, 58.10, 55.46, 44.34. ^{1}H NMR (600 MHz, MeOD) β-isomer **17**: δ (ppm) 3.93 (d, *J* = 8.6 Hz, 1H), 3.88-3.82 (m, 3H), 3.33-3.31 (m, 2H), 3.17 (d, *J* = 3.7 Hz, 1H), 2.18 (tdd, *J* = 7.3, 4.0, 1.7 Hz, 1H). ^{13}C NMR (150 MHz, MeOD) β-epoxide **17**: δ (ppm) 76.72, 70.76, 69.96, 61.87, 57.76, 55.36, 42.82. $[\alpha]D^{20}$ (c = 0.2, MeOH): **11** +85°, **17** +67°.

(1R,2R,3S,4S,5R,6S)-5-((Bodipy-triazolyl)methyl)-2,3,4-trihydroxy-7-oxabicyclo[4.1.0]heptane (13)

Azido-epoxide **12** (25 µmol, 5.0 mg) and Bodipy-alkyne **35**[21] (25 µmol, 12 mg, 1.0 eq.) were dissolved in DMF (0.5 mL) under argon atmosphere. After addition of copper(II)sulfate pentahydrate (5 µmol, 5 µL 1 M in H_2O, 0.2 eq.) and sodium ascorbate (10 µmol, 10 µL 1 M in H_2O, 0.4 eq.) the reaction mixture was stirred at room temperature overnight. The mixture was then concentrated *in vacuo* and purified by column chromatography (DCM → 3% MeOH in DCM) to yield Bodipy-epoxide **13** as a purple solid (15 mg, 22 µmol, 88%). ^{1}H NMR (400 MHz, MeOD): δ (ppm) 7.89-7.82 (m, 4H), 7.78 (s, 1H), 7.43 (d, *J* = 4.4 Hz, 2H), 7.01-6.94 (m, 4H), 6.70 (d, *J* = 4.3 Hz, 2H), 4.60-4.53 (m, 2H), 4.13 (dd, *J* = 8.5, 2.4 Hz, 1H), 3.85 (s, 6H), 3.66-3.61 (m, 1H), 3.42 (dd, *J* = 8.5, 1.8 Hz, 1H), 3.37-3.34 (m, 1H), 3.07-3.02 (m, 2H), 2.97 (dd, *J* = 3.9, 1.8 Hz, 1H), 2.79-2.75 (m, 2H), 2.55 (td, *J* = 8.2, 3.5 Hz, 1H), 1.88-1.83 (m, 4H). ^{13}C NMR (100 MHz, MeOD): δ (ppm) 160.77, 157.39, 145.31, 136.08, 130.71, 127.03, 125.10, 119.66, 115.98, 113.22, 72.03, 70.53, 69.06, 56.67, 54.41, 53.30, 49.13, 41.27, 32.86, 29.58, 29.00, 24.48. LC/MS analysis: R_t 10.4 min (linear gradient 10 → 50% B in 15 min), m/z 666.3 $[M-F]^+$, 685.9 $[M+H]^+$, 1371.0 $[2M+H]^+$. HRMS: calcd. for $[C_{36}H_{39}O_6N_5BF_2]^+$ 686.29560, found 686.29599; calcd. for $[C_{36}H_{38}O_6N_5BF_2Na]^+$ 708.27754, found 708.27719.

(1R,2R,3S,4S,5R,6S)-5-((biotin-triazolyl)methyl)-2,3,4-trihydroxy-7-oxabicyclo[4.1.0]heptane (14)

Azido-epoxide **12** (25 µmol, 5.0 mg) and biotin-alkyne **36**[22] (25 µmol, 7.0 mg, 1.0 eq.) were dissolved in DMF (0.5 mL) under argon atmosphere. After addition of copper(II)sulfate pentahydrate (5 µmol, 5 µL 1 M in H_2O, 0.2 eq.) and sodium ascorbate (10 µmol, 10 µL 1 M in H_2O, 0.4 eq.) the reaction mixture was stirred at room temperature overnight. The mixture was then concentrated *in vacuo* and purified by column chromatography (DCM → 30%

MeOH in DCM) to yield biotin-epoxide **14** as a white solid (8.0 mg, 17 µmol, 68%). ^{1}H NMR (400 MHz, MeOD): δ (ppm) 7.97 (s, 1H), 4.65-4.60 (m, 2H), 4.52 (ddd, *J* = 8.0, 5.0, 1.0 Hz, 1H), 4.47 (s, 2H), 4.32 (dd, *J* = 7.9, 4.5 Hz, 1H), 4.14 (dd, *J* = 8.6, 2.4 Hz, 1H), 3.66 (dt, *J* = 3.7, 1.8 Hz, 1H), 3.43 (dd, *J* = 8.6, 1.8 Hz, 1H), 3.37-3.36 (m, 1H), 3.22 (ddd, *J* = 8.9, 5.9, 4.4 Hz, 1H), 3.02 (dd, *J* = 4.0, 1.8 Hz, 1H), 2.96 (dd, *J* = 12.8, 5.0 Hz, 1H), 2.74 (d, *J* = 12.7 Hz, 1H), 2.58 (td, *J* = 8.1, 3.5 Hz, 1H), 2.27 (t, *J* = 7.3 Hz, 2H), 1.78-1.57 (m, 4H), 1.48-1.42 (m, 2H). ^{13}C NMR (100 MHz, MeOD): δ (ppm) 174.63, 145.05, 123.62, 72.00, 70.51, 69.03, 61.95, 60.23, 56.70, 55.59, 53.32, 49.23, 41.34, 39.66, 35.14, 34.20, 28.28, 28.05, 25.29. LC/MS analysis: R_t 3.6 min (linear gradient 10 → 50% B in 15 min), m/z 483.3 $[M+H]^+$, 965.1 $[2M+H]^+$, 1446.9 $[3M+H]^+$. HRMS: calcd. for $[C_{20}H_{31}O_6N_6S]^+$ 483.20203, found 483.20176; calcd. for $[C_{20}H_{30}O_6N_6SNa]^+$ 505.18397, found 505.18347. $[\alpha]D^{20}$ (c = 0.1, MeOH): +48°.

(1R,2R,3S,4S,5R,6S)-5-((Bodipy-triazolyl)methyl)-2,3,4-trihydroxy-7-oxabicyclo[4.1.0]heptane (19)

Azido-epoxide **18** (25 µmol, 5.0 mg) and Bodipy-alkyne **35**[21] (25 µmol, 12 mg, 1.0 eq.) were dissolved in DMF (0.5 mL) under argon atmosphere. After addition of copper(II)sulfate pentahydrate (5 µmol, 5 µL 1 M in H_2O, 0.2 eq.) and sodium ascorbate (10 µmol, 10 µL 1 M in H_2O, 0.4 eq.) the reaction mixture was stirred at room temperature overnight. The mixture was then concentrated *in vacuo* and purified by column chromatography (DCM → 3% MeOH in DCM) to yield Bodipy-epoxide **19** as a purple solid (15 mg, 22 µmol, 90%). ^{1}H NMR (400 MHz, MeOD): δ (ppm) 1.91-7.82 (m, 4H), 7.77 (s, 1H), 7.44 (d, *J* = 4.4 Hz, 2H), 7.03-6.93 (m, 4H), 6.70 (d, *J* = 4.3 Hz, 2H), 4.70 (d, *J* = 7.8 Hz, 2H), 3.97 (d, *J* = 8.5 Hz, 1H), 3.86 (s, 6H), 3.66-3.58 (m, 1H), 3.42-3.40 (m, 1H), 3.18 (d, *J* = 3.7 Hz, 1H), 3.11-2.97 (m, 3H), 2.86-2.76 (m, 2H), 2.73 (ddt, *J* = 7.6, 4.3, 2.2 Hz, 1H), 1.91-1.82 (m, 4H). ^{13}C NMR (100 MHz, MeOD): δ (ppm) 160.78, 157.38, 136.09, 130.79, 127.03, 125.11, 123.06, 119.63, 113.22, 74.73, 68.51, 67.89, 56.77, 54.41, 53.27, 48.74, 39.84, 32.86, 29.59, 29.02, 24.46. LC/MS analysis: R_t 10.5 min (linear gradient 10 → 50% B in 15 min), m/z 666.3 $[M-F]^+$, 686.0 $[M+H]^+$, 1371.0 $[2M+H]^+$. HRMS: calcd. for $[C_{36}H_{39}O_6N_5BF_2]^+$ 686.29560, found 686.29615; calcd. for $[C_{36}H_{38}O_6N_5BF_2Na]^+$ 708.27754, found 708.27725.

(1R,2R,3S,4S,5R,6S)-5-((biotin-triazolyl)methyl)-2,3,4-trihydroxy-7-oxabicyclo[4.1.0]heptane (20)

Azido-epoxide **18** (25 µmol, 5.0 mg) and biotin-alkyne **36**[22] (25 µmol, 7.0 mg, 1.0 eq.) were dissolved in DMF (0.5 mL) under argon atmosphere. After addition of copper(II)sulfate pentahydrate (5 µmol, 5 µL 1 M in H_2O, 0.2 eq.) and sodium ascorbate (10 µmol, 10 µL 1 M in H_2O, 0.4 eq.) the reaction mixture was stirred at room temperature overnight. The mixture was then concentrated *in vacuo* and purified by column chromatography (DCM → 30% MeOH in DCM) to yield biotin-epoxide **20** as a white solid (8.0 mg, 17 µmol, 68%). ^{1}H NMR (400 MHz, MeOD): δ (ppm) 7.93 (s, 1H), 4.75 (d, *J* = 7.7 Hz, 2H), 4.52 (ddd, *J* = 8.0, 5.0, 0.9 Hz, 1H), 4.46 (s, 2H), 4.32 (dd, *J* = 7.9, 4.5 Hz, 1H), 3.98 (d, *J* = 8.5 Hz, 1H), 3.63 (ddd, *J* = 4.1, 2.7, 1.2 Hz, 1H), 3.38-3.36 (m, 1H), 3.25-3.22 (m, 1H), 3.21 (d, *J* = 3.8 Hz, 1H), 3.14-3.08 (m, 1H), 2.96 (dd, *J* = 12.7, 5.0 Hz, 1H), 2.78 (ddt, *J* = 7.7, 5.4, 2.7 Hz, 1H), 2.73 (d, *J* = 12.8 Hz, 1H), 2.27 (t, *J* = 7.3 Hz, 2H), 1.81-1.55 (m, 4H), 1.50-1.38 (m, 2H). ^{13}C NMR (100 MHz, MeOD): δ (ppm) 174.62, 144.82, 123.89, 74.73, 68.46, 67.88, 61.95, 60.23, 56.79, 55.59, 53.25, 48.86, 39.87, 39.65, 35.14, 34.22, 28.29, 28.04, 25.30. LC/MS analysis: R_t 3.7 min (linear gradient 10 → 50% B in 15 min), m/z 483.3 $[M+H]^+$, 965.0 $[2M+H]^+$, 1447.1 $[3M+H]^+$. HRMS: calcd. for $[C_{20}H_{31}O_6N_6S]^+$ 483.20203, found 483.20179; calcd. for $[C_{20}H_{30}O_6N_6SNa]^+$ 505.18397, found 505.18357. $[\alpha]D^{20}$ (c = 0.1, MeOH): +36°.

8-(Bodipy-triazole)-octanoic acid 38

8-Azidooctanoic acid **37**[25] (0.50 mmol, 93 mg) and Bodipy-alkyne **35**[21] (0.50 mmol, 0.24 g, 1.0 eq.) were dissolved in DMF under argon atmosphere. After addition of copper(II)sulfate pentahydrate (100 µmol, 100 µL 1 M in H_2O, 0.2 eq.) and sodium ascorbate (200 µmol, 200 µL 1 M in H_2O, 0.4 eq.) the reaction mixture was heated to 80 °C and stirred for 4.5 hrs. The mixture was then concentrated *in vacuo* and purified by column chromatography (DCM → 2% MeOH in DCM) to yield Bodipy-acid **38** as a purple solid (0.29 g, 0.43 mmol, 87%). ^{1}H NMR (400 MHz, $CDCl_3$): δ

(ppm) 7.83 (d, *J* = 8.8 Hz, 4H), 7.27-7.26 (m, 2H), 7.18 (s, 1H), 6.92 (d, *J* = 8.8 Hz, 4H), 6.58 (d, *J* = 3.2 Hz, 2H), 4.30-4.28 (m, 2H), 3.83 (s, 6H), 2.96-2.95 (m, 2H), 2.79-2.77 (m, 2H), 2.32 (t, *J* = 7.2 Hz, 2H), 1.90-1.83 (m, 6H), 1.62-1.58 (m, 2H), 1.32-1.25 (m, 6H). ^{13}C NMR (100 MHz, $CDCl_3$): δ (ppm) 178.12, 160.29, 157.15, 144.67, 135.88, 130.71, 126.73, 124.89, 119.73, 113.47, 55.00, 53.33, 33.77, 32.72, 30.02, 29.78, 29.05, 28.49, 28.30, 25.95, 24.71, 24.31.

(3S,4R,5S,6R)-6-(benzyloxymethyl)-3,4,5-tribenzyloxy-cyclohex-1-ene (41)

A solution of (3S,4S,5S,6R)-6-(hydroxymethyl)-3,4-dibenzyloxy-5-hydroxy-cyclohex-1-ene (**27**) (3.5 mmol, 1.2 g) in DMF under argon atmosphere was cooled to 0 °C before tetrabutylammonium iodide (35 µmol, 13 mg, 1 mol%), benzyl bromide (8.4 mmol, 1.0 mL, 2.4 eq.) and sodium hydride (8.4 mmol, 0.33 g (60% in mineral oil), 2.4 eq.) were added. The reaction mixture was stirred overnight at room temperature and subsequently quenched with MeOH. Next, H_2O was added and the resulting mixture was extracted with EtOAc (3x). The combined organic layers were washed with H_2O (1x) and Brine (1x), dried over $MgSO_4$, filtered and concentrated *in vacuo*, yielding a mixture of products having 3 or 4 benzyl groups. These were separated by column chromatography (pentane → 5% EtOAc in pentane → 20% EtOAc in pentane) after which the tribenzylated products were again subjected to the benzylation reaction as before. After work-up and column chromatography purification (pentane → 5% EtOAc in pentane) the fully benzylated product **41** was obtained (total yield 1.5 g, 3.0 mmol, 85%). ^{1}H NMR (400 MHz, $CDCl_3$): δ (ppm) 7.39-7.23 (m, 20H), 5.80-5.76 (m, 1H), 5.48 (d, *J* = 10.4 Hz, 1H), 4.93 (d, *J* = 11.6 Hz, 1H), 4.78-4.68 (m, 4H), 4.64 (d, *J* = 11.6 Hz, 1H), 4.50-4.43 (m, 3H), 4.20 (dd, *J* = 1.6, 1.6 Hz, 1H), 3.75 (dd, *J* = 1.6, 8.0 Hz, 1H), 3.62-3.46 (m, 2H), 2.72-2.68 (m, 1H). ^{13}C NMR (100 MHz, $CDCl_3$): δ (ppm) 139.03, 138.77, 138.70, 138.15, 128.40, 128.32, 128.30, 128.17, 127.87, 127.81, 127.79, 127.67, 127.49, 127.47, 127.44, 127.38, 126.66, 83.20, 77.66, 75.12, 74.03, 73.28, 72.37, 72.16, 70.17, 41.92. LC/MS analysis: R_t 10.8 min (linear gradient 10 → 90% B in 15 min), m/z 521.1 $[M+H]^+$, 543.3 $[M+Na]^+$. HRMS: calcd. for $[C_{35}H_{37}O_4]^+$ 521.26864, found 521.26864; calcd. for $[C_{35}H_{36}O_4Na]^+$ 543.25058, found 543.24988. $[\alpha]D^{20}$ (c = 0.1, $CHCl_3$): +105°.

(2R,3S,4S,5R)-5-(benzyloxymethyl)-2,3,4-tribenzyloxy-7-oxabicyclo[4.1.0]heptane: β-epoxide (42)

To a solution of **41** (0.70 mmol, 0.36 g) in DCM under argon atmosphere was added 3-chloroperoxybenzoic acid (1.7 mmol, 0.30 g, 2.5 eq.). After stirring overnight, the reaction mixture was quenched with saturated aqueous Na_2SO_3 and extracted with DCM (2x). The combined organic layers were washed with saturated aqueous NaHCO3 (1x), dried over MgSO4, filtered and concentrated *in vacuo*. The crude products were purified and separated by column chromatography (pentane → 10% EtOAc in pentane) to afford α-epoxide isomer of **42** (37 mg, 70 µmol, 10%) and β-epoxide **42** (0.24 g, 0.43 mmol, 63%). ^{1}H NMR (400 MHz, $CDCl_3$) α-epoxide: δ (ppm) 7.41-7.22 (m, 20H), 4.90-4.79 (m, 3H), 4.70 (dd, *J* = 11.8, 17.8 Hz, 2H), 4.53-4.45 (m, 3H), 4.25 (dd, *J* = 2.4, 8.4 Hz, 1H), 3.93-3.92 (m, 1H), 3.62 (dd, *J* = 8.6, 1.0 Hz, 1H), 3.58 (d, *J* = 8.0 Hz, 2H), 3.37 (dd, *J* = 2.4, 4.0 Hz, 1H), 2.96 (dd, *J* = 1.4, 4.0 Hz, 1H), 2.32-2.28 (m, 1H). ^{13}C NMR (100 MHz, $CDCl_3$) α-epoxide: δ (ppm) 138.68, 138.60, 138.58, 137.89, 128.40, 128.31, 128.26, 128.21, 128.10, 127.97, 127.88, 127.85, 127.75, 127.73, 127.67, 127.52, 127.45, 81.10, 76.73, 75.68, 74.23, 73.68, 73.35, 73.04, 68.53, 55.20, 54.35, 40.89. ^{1}H NMR (400 MHz, $CDCl_3$) β-epoxide **42**: δ (ppm) 7.38-7.20 (m, 20H), 4.86 (d, *J* = 12.0 Hz, 1H), 4.81-4.66 (m, 4H), 4.56 (d, *J* = 12.0 Hz, 1H), 4.49-4.42 (m, 2H), 4.14 (d, *J* = 8.8 Hz, 1H), 3.94 (dd, *J* = 4.0, 2.0 Hz, 1H), 3.73-3.62 (m, 2H), 3.45 (dd, *J* = 2.0, 8.8 Hz, 1H), 3.23 (d, *J* = 4.0 Hz, 1H), 3.16-3.15 (m, 1H), 2.32-2.30 (m, 1H). ^{13}C NMR (100 MHz, $CDCl_3$) β-epoxide **42**: δ (ppm) 138.80, 138.44, 137.96, 128.36, 128.33, 128.25, 128.05, 127.81, 127.77, 127.71, 127.68, 127.63, 127.44, 127.42, 127.21, 82.47, 76.11, 74.27, 73.38, 73.15, 72.79, 72.62, 68.79, 54.37, 52.38, 40.19. LC/MS analysis: α-epoxide: R_t 10.3 min (linear gradient 10 → 90% B in 15 min), m/z 537.0 $[M+H]^+$, 559.3 $[M+Na]^+$; **42**: R_t 10.3 min (linear gradient 10 → 90% B in 15 min), m/z 537.1 $[M+H]^+$, 559.3 $[M+Na]^+$. HRMS: calcd. for $[C_{35}H_{37}O_5]^+$ 537.26355, found for α-epoxide 537.26385, for **42** 537.26391; calcd. for $[C_{35}H_{36}O_5Na]^+$ 559.24550, found for α-epoxide 559.24515, for **42** 559.24491. $[\alpha]D^{20}$ (c = 0.1, $CHCl_3$): α-epoxide +30°, **42** +66°.

(1R,2S,3R,4S,5S,6S)-2-azido-3-(benzyloxymethyl)-4,5,6-tribenzyloxy-cyclohexanol and (1R,2S,3S,4S,5S,6S)-2-azido-6-(benzyloxymethyl)-3,4,5-tribenzyloxy-cyclohexanol (43)

A solution of β-epoxide **42** (0.48 mmol, 0.26 g) in ACN under argon atmosphere was heated to 80 °C before addition of sodium azide (24 mmol, 1.6 g, 50 eq.) and lithium perchlorate (4.8 mmol, 0.51 g, 10 eq.). After stirring under reflux overnight, the reaction mixture was allowed to cool to room temperature, quenched with H_2O and extracted with DCM (3x). The combined organic layers were dried over $MgSO_4$, filtered and concentrated *in vacuo*. Purification by column chromatography (pentane → 10% EtOAc in pentane) yielded a mixture of two azido alcohols **43** in a ratio of 1:1.3 (0.20 g, 0.35 mmol, 73%). ^{1}H NMR (400 MHz, $CDCl_3$): δ (ppm) 7.39-7.18 (m, 20H isomer 1 + 20H isomer 2), 5.02-4.67 (m, 5H isomer 1 + 5H isomer 2), 4.51-4.40 (m, 3H isomer 1 + 3H isomer 2), 4.30-4.26 (m, 2H isomer 1 + 1H isomer 2), 4.11-4.09 (m, 1H isomer 1), 3.91-3.87 (m, 1H isomer 1 + 1H isomer 2), 3.79-3.77 (m, 2H isomer 1 + 1H isomer 2), 3.69-3.41 (m, 2H isomer 1 + 5H isomer 2), 2.05-2.02 (m, 1H isomer 1), 1.68-1.62 (m, 1H isomer 2). ^{13}C NMR (100 MHz, $CDCl_3$): δ (ppm) 138.14, 138.04, 137.99, 137.85, 137.80, 128.59, 128.45, 128.43, 128.41, 128.35, 128.23, 128.05, 127.94, 127.90, 127.81, 127.78, 127.75, 127.70, 127.66, 127.59, 127.51, 127.44, 127.42, 83.58, 81.21, 80.68, 78.25, 76.93, 76.60, 75.86, 75.59, 75.02, 73.54, 73.43, 73.39, 73.32, 73.28, 72.50, 71.55, 67.71, 64.75, 61.58, 42.31, 38.59. LC/MS analysis: R_t 10.4 min (linear gradient 10 → 90% B in 15 min), m/z 579.9 $[M+H]^+$; and R_t 10.6 min, m/z 580.0 $[M+H]^+$. HRMS: calcd. for $[C_{35}H_{38}N_3O_5]^+$ 580.28060, found 580.28078; calcd. for $[C_{35}H_{37}N_3O_5Na]^+$ 602.26254, found 602.26211. $[\alpha]D^{20}$ (c = 0.1, $CHCl_3$): -2°.

(1S,2S,3S,4S,5R,6S)-5-(benzyloxymethyl)-2,3,4-tribenzyloxy-7-azabicyclo[4.1.0]heptane (44)

A mixture of azido alcohols **43** (0.50 mmol, 0.29 g) was dissolved in ACN under argon atmosphere. After addition of triphenylphosphine (0.65 mmol, 0.17 g, 1.3 eq.), the reaction mixture was heated to 80 °C and stirred under reflux for 2 hrs. The mixture was then allowed to cool to room temperature and concentrated *in vacuo*. The crude product was purified by column chromatography (DCM → 0.8% MeOH in DCM) to give α-aziridine **44** (pure yield 70 mg, 0.13 mmol, 26%; and an additional 77 mg product containing triphenylphosphine oxide). ^{1}H NMR (400 MHz, $CDCl_3$): δ (ppm) 7.47-7.22 (m, 20H), 4.89-4.79 (m, 3H), 4.70 (dd, *J* = 11.6, 22.8 Hz, 2H), 4.55-4.43 (m, 3H), 4.23 (dd, *J* = 4.0, 8.4 Hz, 1H), 3.88-3.87 (m, 1H), 3.61-3.55 (m, 3H), 2.55-2.52 (m, 1H), 2.19-2.15 (m, 1H), 2.02 (d, *J* = 6.0 Hz, 1H). ^{13}C NMR (100 MHz, $CDCl_3$): δ (ppm) 139.09, 138.92, 138.84, 138.06, 132.03, 131.93, 128.47, 128.35, 128.32, 128.25, 128.20, 128.13, 128.11, 127.85, 127.79, 127.72, 127.65, 127.60, 127.36, 127.31, 127.27, 81.88, 76.87, 76.25, 73.99, 73.10, 72.91, 72.35, 69.81, 41.89, 34.15, 32.08. LC/MS analysis: R_t 7.7 min (linear gradient 10 → 90% B in 15 min), m/z 536.1 $[M+H]^+$, 1071.2 $[2M+H]^+$. HRMS: calcd. for $[C_{35}H_{38}NO_4]^+$ 536.27954, found 536.27943. $[\alpha]D^{20}$ (c = 0.1, MeOH): +56°.

(1S,2S,3S,4S,5R,6S)-5-(hydroxymethyl)-2,3,4-trihydroxy-7-azabicyclo[4.1.0]heptane (45)

Ammonia was condensed at -60 °C (~5 mL) under argon flow using Birch equipment. Lithium (50 mg) was added and the solution was stirred for 30 min at -60 °C, before a solution of α-aziridine **44** (0.10 mmol, 36 mg) in THF (5 mL) was added. The reaction mixture was stirred at -60 °C under argon for 45 min, quenched with MilliQ (2 mL) and allowed to warm to room temperature. After all ammonia had evaporated, the mixture was further concentrated *in vacuo* and redissolved in MilliQ. Neutralization with Amberlite-H^+ resulted in resin-bound product, which was filtered, washed with MilliQ and then eluted using a 1M aqueous NH_4OH solution (10x 1 mL). After evaporation *in vacuo* the product was redissolved in MilliQ and Amberlite-$NH4^+$ was added. Product was eluted from the resin by filtration and washing with MilliQ until the pH of the eluted solution was neutral (pH 7). The combined eluates were concentrated *in vacuo* to yield the crude deprotected α-aziridine **45**, which was used without further purification. ^{1}H NMR (400 MHz, D_2O): δ (ppm) 4.01 (dd, *J* = 4.2, 9.0 Hz, 1H), 3.78 (s, 1H), 3.68-3.64 (m, 2H), 3.28 (d, *J* = 8.8 Hz, 1H), 2.54-2.51 (m, 1H), 2.08 (d, *J* = 6.4 Hz, 1H), 1.90-1.86 (m, 1H).

(1S,2S,3S,4S,5R,6S)-5-(hydroxymethyl)-2,3,4-trihydroxy-*N*-(8-azidooctanoyl)-7-azabicyclo[4.1.0]heptane (15)

8-Azidooctanoic acid **37**[25] (0.40 mmol, 78 mg) was preactivated with EEDQ (0.40 mmol, 99 mg, 1.0 eq.) in DMF (0.4 mL) under argon for 2 hours at room temperature. Deprotected aziridine **45** (65 µmol) was dissolved in DMF (1 mL) under argon and cooled to 0 °C, after which 33 µL of the activated ester solution was added (33 µmol, 0.5 eq.) and the mixture was stirred at 0 °C for 30 min. Then another 0.5 eq. of the activated ester was added and the reaction mixture was stirred at 0 °C for another 60 min. After quenching with MeOH, the mixture was concentrated *in vacuo*, purified by HPLC under neutral conditions using a gradient of 22 → 28% ACN in H_2O in 12 min, and lyophilized to yield aziridine **15** as a white powder (3.0 mg, 9.0 µmol, 14%). ^{1}H NMR (600 MHz, MeOD): δ (ppm) 4.08 (dd, *J* = 4.2, 9.0 Hz, 1H), 3.87-3.86 (m, 1H), 3.82-3.75 (m, 2H), 3.37 (dd, *J* = 1.8, 8.4 Hz, 1H), 3.30-3.27 (m, 2H), 2.97 (dd, *J* = 4.2, 6.0 Hz, 1H), 2.61 (d, *J* = 6.0 Hz, 1H), 2.56-2.44 (m, 2H), 2.02 (td, *J* = 7.8, 7.2, 3.6 Hz, 1H), 1.66-1.57 (m, 4H), 1.39-1.34 (m, 6H). ^{13}C NMR (150 MHz, MeOD): δ (ppm) 188.72, 74.36, 73.13, 69.15, 62.84, 52.44, 44.54, 43.27, 39.44, 37.12, 30.17, 29.94, 27.68, 27.66, 25.90. LC/MS analysis (ammonium acetate): R_t 7.5 min (linear gradient 0 → 50% B in 15 min), m/z 343.4 $[M+H]^+$, 360.5 $[M+NH_4]^+$. HRMS: calcd. for $[C_{15}H_{27}N_4O_5]^+$ 343.19760, found 343.19757; calcd. for $[C_{15}H_{27}N_4O_5Na]^+$ 365.17954, found 365.17939.

(1S,2S,3S,4S,5R,6S)-5-(hydroxymethyl)-2,3,4-trihydroxy-*N*-(8-(Bodipy-triazole)-octanoyl)-7-azabicyclo[4.1.0]heptane (16)

Bodipy acid **38** (0.10 mmol, 67 mg) was preactivated with EEDQ (0.10 mmol, 25 mg, 1.0 eq.) in DMF (1 mL) under argon for 2 hours at room temperature. Deprotected aziridine **45** (60 µmol) was dissolved in DMF (0.5 mL) under argon and cooled to 0 °C, after which 0.3 mL of the activated ester solution was added (30 µmol, 0.5 eq.) and the mixture was stirred at 0 °C for 30 min. Then another 0.5 eq. of the activated ester was added and the reaction mixture was stirred at 0 °C for another 60 min. After quenching with MeOH, the mixture was concentrated *in vacuo*, purified by HPLC under neutral conditions using a gradient of 48 → 51% ACN in H_2O in 12 min, and lyophilized to yield aziridine **16** as a purple powder (7.4 mg, 9.0 µmol, 15%). ^{1}H NMR (400 MHz, MeOD): δ (ppm) 7.87 (d, *J* = 8.8 Hz, 4H), 7.72 (s, 1H), 7.46 (d, *J* = 4.3 Hz, 2H), 7.00 (d, *J* = 9.2 Hz, 4H), 6.72 (d, *J* = 4.3 Hz, 2H), 4.36 (t, *J* = 7.0 Hz, 2H), 4.10 (dd, *J* = 8.6, 4.0 Hz, 1H), 3.88 (s, 6H), 3.87-3.80 (m, 1H), 3.79 (dd, *J* = 7.4, 4.3 Hz, 2H), 3.38 (dd, *J* = 8.6, 1.8 Hz, 1H), 3.12-3.06 (m, 2H), 2.96 (dd, *J* = 6.0, 4.0 Hz, 1H), 2.82-2.78 (m, 2H), 2.62-2.58 (m, 1H), 2.55-2.35 (m, 2H), 2.03 (td, *J* = 7.8, 7.3, 3.6 Hz, 1H), 1.94-1.82 (m, 6H), 1.63-1.52 (m, 2H), 1.32-1.21 (m, 6H). LC/MS analysis: R_t 7.4 min (linear gradient 10 → 90% B in 15 min), m/z 827.07 $[M+H]^+$, 807.47 $[M-F]^+$, 1653.40 $[2M+H]^+$. Of note, under these acidic LC/MS conditions the aziridine is partially opened to give a second peak at R_t 7.2 min (linear gradient 10 → 90% B in 15 min), m/z 845.07 $[(M+H_2O)+H]^+$, 825.40 $[(M+H_2O)-F]^+$, 1689.13 $[2(M+H_2O)+H]^+$. HRMS: calcd. for $[C_{44}H_{54}BF_2N_6O_7]^+$ 827.41096, found 827.41180.

(1R,2S,3S,4S,5R,6R)-5-(hydroxymethyl)-2,3-dibenzyloxy-4-hydroxy-7-azabicyclo[4.1.0]heptane (39)

Cyclohexene **27** (0.50 mmol, 0.17 g) was coevaporated with toluene before being dissolved in DCM (10 mL) at 0 °C under argon atmosphere. Next, CCl_3CCN (0.50 mmol, 51 µL, 1.0 eq.) and DBU (25 µmol, 2.0 µL, 0.05 eq.) were added and the reaction mixture was stirred at 0 °C for 1.5 hrs. The mixture was removed from the ice bath before H_2O (1.5 mL), $NaHCO_3$ (5.0 mmol, 0.40 g, 10 eq.) and I_2 (1.5 mmol, 0.38 g, 3.0 eq.) were added. After stirring at room temperature overnight, the reaction was quenched with 10% aqueous $Na_2S_2O_3$ and the aqueous layer was extracted with EtOAc (2x). The combined organics were dried over $MgSO_4$, filtered and concentrated *in vacuo*. The residue was redissolved in MeOH, cooled to 0 °C and concentrated HCl (6.3 mmol, 0.6 mL, 13 eq.) was added after which the reaction mixture was stirred at room temperature for 3.5 hrs. Next, the mixture was concentrated *in vacuo*, the residue was redissolved in dioxane and again concentrated HCl (16 mmol, 1.5 mL, 32 eq.) was added. The mixture was stirred at 60 °C for 1 hr, concentrated *in vacuo* and coevaporated with toluene (3x). The residue was redissolved in MeOH, $NaHCO_3$ (10 mmol, 0.8 g, 20 eq.) was added and the reaction mixture was stirred at room

temperature for 4 days. After addition of H_2O the aqueous layer was extracted with EtOAc and the organic layer was dried over $MgSO_4$, filtered and concentrated *in vacuo*. The crude product was purified by column chromatography (DCM → 6% MeOH in DCM) to afford dibenzylated β-aziridine **39** (92 mg, 0.26 mmol, 52%). ^{1}H NMR (400 MHz, $CDCl_3$): δ (ppm) 7.46-7.22 (m, 10H), 4.83-4.61 (m, 4H), 4.13-4.04 (m, 2H), 3.99 (dd, *J* = 10.9, 7.5 Hz, 1H), 3.90 (dd, *J* = 10.9, 6.2 Hz, 1H), 3.39 (dd, *J* = 7.9, 2.3 Hz, 1H), 2.50-2.32 (m, 2H), 2.06-1.96 (m, 1H). ^{13}C NMR (100 MHz, $CDCl_3$): δ (ppm) 138.31, 138.17, 128.62, 128.58, 128.54, 128.49, 128.46, 128.43, 128.35, 128.29, 128.17, 128.15, 128.02, 127.96, 127.93, 127.90, 127.87, 127.85, 127.80, 127.78, 127.63, 83.29, 78.57, 73.10, 71.69, 67.42, 62.40, 39.47, 32.63, 32.53. LC/MS analysis: R_t 5.4 min (linear gradient 10 → 90% B in 15 min), m/z 356.1 $[M+H]^+$, 711.1 $[2M+H]^+$.

(1R,2S,3S,4S,5R,6R)-5-(hydroxymethyl)-2,3,4-trihydroxy-7-azabicyclo[4.1.0]heptane (40)

The β-aziridine **39** (0.10 mmol, 36 mg) was deprotected using the same procedure as described for α-aziridine **45** to give β-aziridine **40**. ^{1}H NMR (400 MHz, D_2O): δ (ppm) 4.10 (d, *J* = 8.0 Hz, 1H), 3.87-3.78 (m, 3H), 3.43 (d, *J* = 8.0 Hz, 1H), 2.44 (bs, 1H), 2.34-2.33 (m, 1H), 2.04 (bs, 1H).

(1R,2S,3S,4S,5R,6R)-5-(hydroxymethyl)-2,3,4-trihydroxy-N-(8-azidooctanoyl)-7-azabicyclo[4.1.0]heptane (21)

Deprotected β-aziridine **40** (0.10 mmol) was acylated with azido-spacer **37**[25] using the same procedure as described for α-aziridine **15** to give β-aziridine **21**. After HPLC purification and lyophilization, however, NMR analysis revealed that no aziridine proton peaks were present, indicating that the product had degraded by opening of the aziridine.

DFT calculations

The calculated ^{1}H NMR coupling constants were obtained by first finding the lowest energy conformation of both epoxide isomers, for which a library of gas phase conformations was generated using the conformer distribution option included in the Spartan 04[26] program employing DFT/B3LYP 6-31G(d). All conformers were further optimized by Gaussion 03[27] at DFT/B3LYP 6-311G(d,p), their zero-point energies were calculated and the energies corrected for solvent by another optimization step employing a Polarizable Continuum Model set for water. The energies of these conformers, corrected for their zero-point energies, were compared and of the lowest energy conformer an NMR calculation was performed using the Gauge-Independent Atomic Orbital (GIAO) method with added spin-spin coupling calculation.

References

1. Zechel, D. L.; Withers, S. G. *Acc. Chem. Res.* **2000**, *33*, 11.
2. Mark, B. L.; Vocadlo, D. J.; Knapp, S.; Triggs-Raine, B. L.; Withers, S. G.; James, M. N. G. *J. Biol. Chem.* **2001**, *276*, 10330.
3. For a review, see: Rempel, B. P.; Withers, S. G. *Glycobiology* **2008**, *18*, 570.
4. Withers, S. G.; Rupitz, K.; Street, I. P. *J. Biol. Chem.* **1988**, *263*, 7929.
5. Tatsuta, K.; Niwata, Y.; Umezawa, K.; Toshima, K.; Nakata, M. *Tetrahedron Lett.* **1990**, *31*, 1171.
6. Atsumi, S.; Umezawa, K.; Iinuma, H.; Naganawa, H.; Nakamura, H.; Iitaka, Y.; Takeuchi, T. *J. Antibiot.* **1990**, *43*, 49.
7. Withers, S. G.; Umezawa, K. *Biochem. Biophys. Res. Commun.* **1991**, *177*, 532.
8. Tatsuta, K.; Niwata, Y.; Umezawa, K.; Toshima, K.; Nakata, M. *J. Antibiot.* **1991**, *44*, 456.
9. Tatsuta, K.; Niwata, Y.; Umezawa, K.; Toshima, K.; Nakata, M. *J. Antibiot.* **1991**, *44*, 912.
10. Shing, T. K. M.; Tai, V. W.-F. *J. Chem. Soc., Chem Commun,* **1993**, 995-997.
11. Legler, G. *Adv. Carbohydr. Chem. Biochem.* **1990**, *48*, 319.

12. Hermans, M. M. P.; Kroos, M. A.; van Beeumen, J.; Oostra, B. A.; Reuser, A. J. J. *J. Biol. Chem.* **1991**, *266*, 13507.
13. Legler, M.; Herrchen, M. *FEBS letters* **1981**, *135*, 139.
14. Caron, G.; Withers, S. G.; *Biochem. Biophys. Res. Commun.* **1989**, *163*, 495.
15. Witte, M. D.; Kallemeijn, W. W.; Aten, J.; Li, K.-Y.; Strijland, A.; Donker-Koopman, W. E.; van den Nieuwendijk, A. M. C. H.; Bleijlevens, B.; Kramer, G.; Florea, B. I.; Hooibrink, B.; Hollak, C. E. M.; Ottenhoff, R.; Boot, R. G.; van der Marel, G. A.; Overkleeft, H. S.; Aerts, J. M. F. G. *Nat. Chem. Biol.* **2010**, *6*, 907.
16. Kallemeijn, W. W.; Li, K.-Y.; Witte, M. D.; Marques, A. R. A.; Aten, J.; Scheij, S.; Jiang, J.; Willems, L. I.; Voorn-Brouwer, T. M.; van Roomen, C. P. A. A.; Ottenhoff, R.; Boot, R. G.; van den Elst, H.; Walvoort, M. T. C.; Florea, B. I.; Codée, J. D. C.; van der Marel, G. A.; Aerts, J. M. F. G.; Overkleeft, H. S. *Angew. Chem. Int. Ed.* **2012**, *51*, 12529.
17. The designation of the α-/β-stereochemistry of all galactopyranose-configured epoxides and aziridines is based on α-/β-galactopyranose nomenclature.
18. Hansen, F. G.; Bundgaard, E.; Madsen, R. *J. Org. Chem.* **2005**, *70*, 10139.
19. Harrak, Y.; Barra, C. M.; Delgado, A.; Castaño, A. R.; Llebaria, A. *J. Am. Chem. Soc.* **2011**, *133*, 12079.
20. Evans, D. A.; Sjogren, E. B.; Bartroli, J.; Dow, R. L. *Tetrahedron Lett.* **1986**, *27*, 4957.
21. Verdoes, M.; Hillaert, U.; Florea, B. I.; Sae-Heng, M.; Risseeuw, M. D. P.; Filippov, D. V.; van der Marel, G. A.; Overkleeft, H. S. *Bioorg. Med. Chem. Lett*. **2007**, *17*, 6169.
22. Verdoes, M.; Florea, B. I.; Hillaert, U.; Willems, L. I.; van der Linden, W. A.; Sae-Heng, M.; Filippov, D. V.; Kisselev, A. F.; van der Marel, G. A.; Overkleeft, H. S. *ChemBioChem* **2008**, *9*, 1735.
23. Serrano, P.; Llebaria, A.; Delgado, A. *J. Org. Chem.* **2005**, *70*, 7829.
24. Ritzen, B.; van Oers, M. C. M.; van Delft, F. L.; Rutjes, F. P. J. T. *J. Org. Chem.* **2009**, *74*, 7548.
25. David, O.; Meester, W. J. N.; Bieraügel, H.; Schoenmaker, H. E.; Hiemstra, H.; van Maarseveen, J. H. *Angew. Chem. Int. Ed.* **2003**, *42*, 4373.
26. Spartan'04, Wavefunction, Inc., Irvine, CA. Except for molecular mechanics and semi-empirical models, the calculation methods used in Spartan'04 have been documented in: Kong, J.; White, C.A.; Krylov, A.I.; Sherrill, C.D.; Adamson, R.D.; Furlani, T.R.; Lee, M.S.; Lee, A.M.; Gwaltney, S.R.; Adams, T.R.; Ochsenfeld, C.; Gilbert, A.T.B.; Kedziora, G.S.; Rassolov, V.A.; Maurice, D.R.; Nair, N.; Shao, Y.; Besley, N.A.; Maslen, P.E.; Dombroski, J.P.; Daschel, H.; Zhang, W.; Korambath, P.P.; Baker, J.; Byrd, E.F.C.; van Voorhis, T.; Oumi, M.; Hirata, S.; Hsu, C.-P.; Ishikawa, N.; Florian, J.; Warshel, A.; Johnson, B.G.; Gill, P.M.W.; Head-Gordon, M.; Pople, J.A. *J. Computational Chem.* **2000**, *21*, 1532.
27. Gaussian 03, Revision C.02, Frisch, M. J.; Trucks, G. W.; Schlegel, H. B.; Scuseria, G. E.; Robb, M. A.; Cheeseman, J. R.; Montgomery, Jr., J. A.; Vreven, T.; Kudin, K. N.; Burant, J. C.; Millam, J. M.; Iyengar, S. S.; Tomasi, J.; Barone, V.; Mennucci, B.; Cossi, M.; Scalmani, G.; Rega, N.; Petersson, G. A.; Nakatsuji, H.; Hada, M.; Ehara, M.; Toyota, K.; Fukuda, R.; Hasegawa, J.; Ishida, M.; Nakajima, T.; Honda, Y.; Kitao, O.; Nakai, H.; Klene, M.; Li, X.; Knox, J. E.; Hratchian, H. P.; Cross, J. B.; Bakken, V.; Adamo, C.; Jaramillo, J.; Gomperts, R.; Stratmann, R. E.; Yazyev, O.; Austin, A. J.; Cammi, R.; Pomelli, C.; Ochterski, J. W.; Ayala, P. Y.; Morokuma, K.; Voth, G. A.; Salvador, P.; Dannenberg, J. J.; Zakrzewski, V. G.; Dapprich, S.; Daniels, A. D.; Strain, M. C.; Farkas, O.; Malick, D. K.; Rabuck, A. D.; Raghavachari, K.; Foresman, J. B.; Ortiz, J. V.; Cui, Q.; Baboul, A. G.; Clifford, S.; Cioslowski, J.; Stefanov, B. B.; Liu, G.; Liashenko, A.; Piskorz, P.; Komaromi, I.; Martin, R. L.; Fox, D. J.; Keith, T.; Al-Laham, M. A.; Peng, C. Y.; Nanayakkara, A.; Challacombe, M.; Gill, P. M. W.; Johnson, B.; Chen, W.; Wong, M. W.; Gonzalez, C.; and Pople, J. A.; Gaussian, Inc., Wallingford CT, **2004**.

6

A potent and selective activity-based probe for human retaining α-galactosidases

6.1 Introduction

Lysosomal degradation of glycosphingolipids is mediated by the consecutive action of several glycosidases, each displaying a unique substrate specificity. A deficiency in one of the lysosomal glycosidases can cause accumulation of the corresponding substrates in lysosomes and consequently lead to a lysosomal storage disorder. Although the primary defects underlying such disorders are similar, they generally show a completely different disease progress, phenotype and clinical manifestation.[1] An attractive approach to study glycosidases and their involvement in disease is the use of activity-based probes (ABPs) that allow the visualization of active enzymes in their natural environment.[2,3] This method is especially useful for the class of retaining glycosidases, since these form a covalent enzyme-substrate intermediate during hydrolysis and are thus amenable to targeting by ABPs that react covalently with the catalytic nucleophile in the active site.

The human enzyme α-galactosidase A (αGal A) is a retaining glycosidase that resides in lysosomes and cleaves terminal α-linked galactosyl moieties from polysaccharides, glycolipids and glycoproteins.[4] It is one of only two human enzymes within the family of retaining α-galactosidases. The related lysosomal enzyme α-*N*-acetylgalactosaminidase, also termed α-galactosidase B (αGal B), hydrolyzes substrates with a terminal *N*-

acetylgalactosamine (NAGA) moiety.[5] The two proteins share 46% amino acid sequence identity and their active site differs only in two amino acid residues, which are responsible for the interaction with the substrate's C2-substituent.[6,7] Consequently, αGal B can accommodate the larger C2 substituent in NAGA as compared to α-galactose while it also tolerates a C2-hydroxyl substituent and is thus capable of hydrolyzing α-galactosides, though with lower efficiency than NAGA substrates. By replacing the two unique active site residues in either αGal A or αGalB with the corresponding residues from the other enzyme, the specificities of the two enzymes can be interchanged.[7] The hydrolysis of α-galactosides by both enzymes occurs through a double displacement mechanism resulting in cleavage of the glycosidic bond and the release of free galactose with overall retention of the α-anomeric configuration (Figure 6.1A). Two carboxylic acid residues are required in the active site to function as a nucleophile and a general acid/base. In human αGal A, these residues have been identified as the aspartic acid residues D170 and D231, respectively.[6] Furthermore it was found that the enzyme forms a homodimer with each monomer containing at least three distinct *N*-linked glycosylation sites that are essential for the lysosomal transport of αGal A mediated by the mannose-6-phosphate receptor.[6]

A deficiency in αGal A is at the basis of the lysosomal storage disorder Fabry disease, an X-linked recessive disorder characterized by the lysosomal accumulation of glycosphingolipids with terminal α-galactosyl moieties.[4,8] More than 400 mutations in the gene encoding αGal A (GLA) are known that lead to malfunctioning or absence of the enzyme. Symptoms of the classic manifestation of Fabry disease include skin lesions, chronic pain, corneal opacity, intolerance to heat, inability to sweat and micro-albuminuria. Moreover, non-specific complications can develop later in life including progressive kidney disease, cardiac symptoms and cerebrovascular disease. The primary storage lipid globotriaosylceramide is further metabolized to globotriaosylsphingosine, which is highly

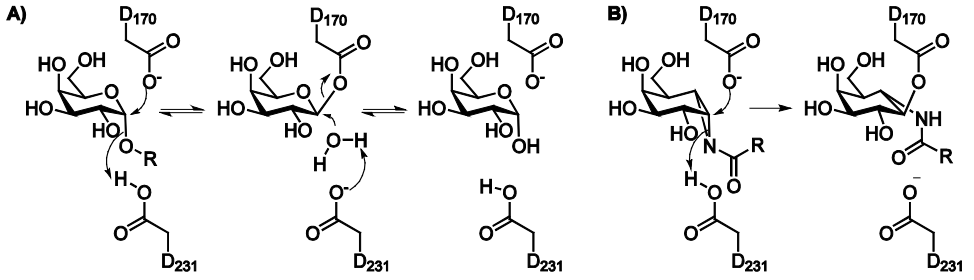

Figure 6.1. A) Mechanism of substrate hydrolysis by αGal A. B) Proposed mechanism by which ABPs **1** and **2** bind to αGal A.

elevated in plasma of Fabry patients and believed to be responsible for many of the symptoms.[9,10] However, there appears to be no clear correlation between the GLA mutation, residual αGal A activity, the amount of lipid storage and the nature or onset of clinical symptoms.[10] Diagnosis of Fabry disease is presently confirmed by demonstrating reduced αGal A activity using fluorogenic substrate assays. Additionally, elevated plasma levels of globotriaosylsphingosine can be used to confirm diagnosis of classic Fabry disease.[10,11] In atypical patients that usually display uncharacteristic symptoms in combination with relatively high residual αGal A activity, diagnosis is generally less straightforward than in classic patients. The currently applied treatment for Fabry disease is enzyme replacement therapy, in which patients receive recombinant human αGal A to restore enzyme function. Two recombinant protein products are currently available, Replagal produced by Shire and Fabrazyme produced by Genzyme.[12,13] These enzymes have an identical amino acid sequence but a different glycosylation pattern as a result of the different cell lines they are produced in, which causes a different tissue distribution and dose response.[14] Unfortunately, the effectiveness of enzyme replacement therapy for the treatment of Fabry disease appears to be limited.[10]

The development of specific ABPs that enable monitoring of endogenous levels of catalytically active retaining α-galactosidases will provide useful new research tools for the investigation of αGal A. The α-galactopyranose-configured probes synthesized as described in Chapter 5 might serve this purpose (**1**-**5**; Figure 6.2). These probes were designed to bind in the active site of retaining α-galactosidases by mimicking a galactopyranoside substrate

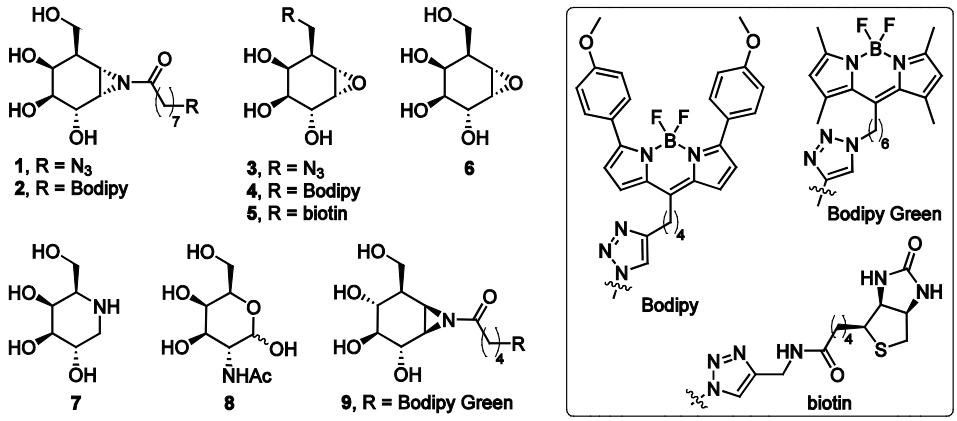

Figure 6.2. Structures of novel retaining α-galactosidase ABPs **1**-**5** and inhibitor **6**, known reversible inhibitors of αGal A (**7**) and αGal B (**7**, **8**), and retaining β-glucosidase ABP **9**.

and contain an α-configured electrophilic aziridine or epoxide moiety to allow attack by the catalytic nucleophile (Figure 6.1B). The ABPs are functionalized with a Bodipy fluorophore (**2**, **4**), a biotin tag (**5**) or an azide (**1**, **3**) as a ligation handle for two-step labeling. The azide-tagged ABPs may also be used as control probes and serve as α-galactosidase inhibitors. In addition, the non-tagged epoxide-based inhibitor **6** was synthesized as a galactopyranose-configured isomer of the known retaining β-glucosidase inhibitor cyclophellitol.[15-17] This chapter describes the biological evaluation of compounds **1**-**6** as retaining galactosidase inhibitors and the use of fluorescently labeled ABP **2** for the imaging of recombinant αGal A as well as endogenous activity of human retaining α-galactosidases in cell extracts.

6.2 Results and discussion

The inhibitory potential of compounds **1**-**6** on recombinant αGal A (Fabrazyme) was first assessed by measuring residual enzyme activity using the fluorogenic substrate 4-methylumbelliferyl α-D-galactoside (4-mu α-gal) after 30 min of preincubation with varying concentrations of the probes. The residual activity was plotted against the inhibitor concentration (Figure 6.3A) and these curves were used to calculate apparent IC_{50} values (Table 6.1). Aziridines **1** and **2** proved to be very potent inhibitors of αGal A with apparent IC_{50} values of 3.2 and 2.0 nM, respectively. Epoxide **6** inhibited the enzyme with 10,000-fold lower potency, and only reached full inhibition after a prolonged incubation time. Modification of the hydroxyl group at C6 by substitution with an azide (**3**) or functionalization with a tag (**4**, **5**) proved to be detrimental for inhibitory potency since no

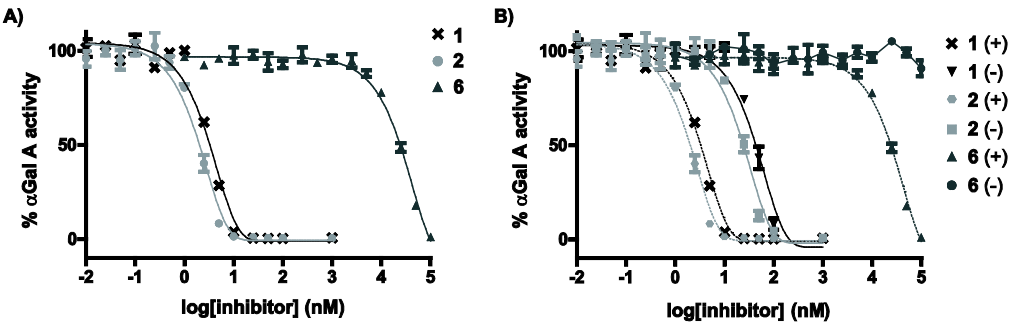

Figure 6.3. Inhibition of recombinant αGal A activity by **1**, **2** and **6**. A) Fabrazyme was treated for 30 min with the inhibitors after which residual activity was determined from hydrolysis of 4-mu α-gal. B) Effect of 30 min preincubation (+) (dotted lines) as compared to simultaneous addition of 4-mu α-gal and probes (-) (solid lines) on inhibition. The displayed inhibitor concentrations in both cases represent those without addition of the fluorogenic substrate solution.

Table 6.1. Inhibition of recombinant αGal A activity

Compound	Apparent IC_{50} (30 min preincubation)	% inhibition 30 min	% inhibition 6 hrs	Apparent IC_{50} without preincubation
Aziridine **1**	3.2 nM	100 (10 μM)	100 (10 μM)	44 nM
Bodipy-aziridine **2**	2.0 nM	100 (10 μM)	100 (10 μM)	24 nM
Epoxide **6**	30 μM	85 (100 μM)	100 (100 μM)	>100 μM
Azido-epoxide **3**	n.i.	0 (100 μM)	n.d.	n.d.
Bodipy-epoxide **4**	n.i.	0 (100 μM)	n.d	n.d
Biotin-epoxide **5**	n.i.	0 (100 μM)	n.d	n.d

Inhibition of Fabrazyme as determined from hydrolysis of 4-mu α-gal after preincubation for 30 min or 6 hrs with the indicated concentrations of **1**-**6**. Apparent IC_{50} values were calculated from plots of residual αGal A activity as a function of probe concentration with a preincubation time of 30 min (Figure 6.3A) or without preincubation (Figure 6.3B). n.i.: no inhibition observed up to 100 μM. n.d.: not determined.

inhibition was observed under these conditions using up to 100 μM of the probes. These findings are in contrast to previously reported data on the inhibition of retaining β-glucosidases using analogous C6-modified epoxide probes.[2] In order to confirm the non-reversible mode of binding by probes **1**, **2** and **6**, inhibition of αGal A activity after preincubation with the probes was compared to that obtained by simultaneous addition of the fluorogenic substrate and the ABPs (Figure 6.3B). The evident shifts in the plots of residual activity against probe concentration and the associated 10-fold lower IC_{50} values after preincubation as compared to simultaneous addition of inhibitors and fluorogenic substrate (Table 6.1) indicate that the binding of the probes is indeed irreversible.

In a next experiment the selectivity of compounds **1**-**6** was evaluated by measuring inhibition of recombinant galactocerebrosidase, a closely related retaining galactosidase that hydrolyzes β-linked instead of α-linked galactosyl moieties. Residual enzyme activity was measured using the fluorogenic substrate 4-methyl-umbelliferyl β-D-galactoside (4-mu β-gal) after 30 min of preincubation with the probes. The aziridines **1** and **2** were able to inhibit this enzyme but with 7,000-30,000 fold lower potency than αGal A (Figure 6.4A and Table 6.2). Interestingly, no evidence of irreversible binding could be obtained (Figure 6.4B). On the other hand, it was found that the non-tagged epoxide **6** inhibits galactocerebrosidase irreversibly and with similar potency to αGal A. The functionalized epoxides **3** and **4**, which do not inhibit αGal A activity, appeared to be weak inhibitors of galactocerebrosidase. Together these data demonstrate that the aziridines **1** and **2** should enable selective targeting of αGal A without affecting galactocerebrosidase, while epoxide **6** inhibits both enzymes.

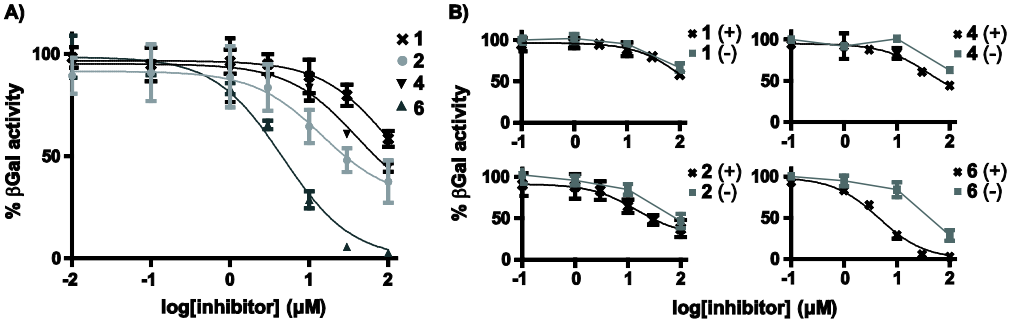

Figure 6.4. Inhibition of recombinant galactocerebrosidase activity by **1**, **2**, **4** and **6**. A) Recombinant galactocerebrosidase (βGal) was treated for 30 min with the inhibitors after which residual activity was determined from hydrolysis of 4-mu β-gal. B) Effect of 30 min preincubation (+) as compared to simultaneous addition of 4-mu β-gal and probes (-) on inhibition. The displayed inhibitor concentrations in both cases represent those without addition of the fluorogenic substrate solution.

Having established the inhibitory potential of the probes, aziridine ABPs **1** and **2** were next used to visualize recombinant αGal A on gel. Labeling of Fabrazyme with Bodipy-tagged ABP **2** for 1 hr resulted in fluorescent labeling of the enzyme in a concentration-dependent manner (Figure 6.5A). The smaller lower-running band most likely represents a non-glycosylated form of αGal A. The reaction appears to occur in a 1:1 ratio, since saturation is reached at 10 to 30 nM of probe when 20 nM of αGal A is used. Denaturation of the enzyme prior to labeling led to complete disappearance of the signal on gel, confirming that catalytically active enzyme is required for binding of the probe. Pretreatment of Fabrazyme with azide-tagged aziridine **1** resulted in concentration-dependent disappearance of the fluorescent labeling by ABP **2** (Figure 6.5B). In addition, it was shown that the enzyme can be

Table 6.2. Inhibition of recombinant galactocerebrosidase activity

Compound	Apparent IC_{50} (μM)	% inhibition	
		30 min	6 hrs
Aziridine **1**	106	42 (100 μM)	56 (100 μM)
Bodipy-aziridine **2**	14	63 (100 μM)	61 (100 μM)
Epoxide **6**	5	97 (100 μM)	98 (100 μM)
Azido-epoxide **3**	n.d.	20 (100 μM)	n.d.
Bodipy-epoxide **4**	40	56 (100 μM)	91 (100 μM)
Biotin-epoxide **5**	n.i.	0 (100 μM)	n.d

Inhibition of recombinant galactocerebrosidase as determined from hydrolysis of 4-mu β-gal after preincubation for 30 min or 6 hrs with probes **1**-**6**. Apparent IC_{50} values were calculated from plots of residual galactocerebrosidase activity as a function of probe concentration with a preincubation time of 30 min (Figure 6.4A). n.i.: no inhibition observed up to 100 μM. n.d.: not determined.

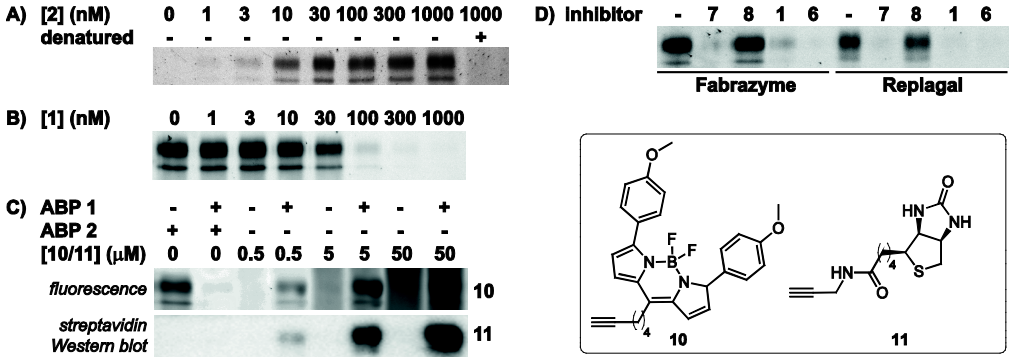

Figure 6.5. Labeling and inhibition of recombinant αGal A. A) Labeling of Fabrazyme (10 ng) with 1 nM - 1 μM of Bodipy-aziridine **2** for 1 hr; where indicated the enzyme was denatured prior to labeling. B) Fabrazyme (50 ng) labeled with 100 nM **2** after preincubation with 1 nM - 1 μM of aziridine **1** for 1 hr. C) Two-step labeling of Fabrazyme using 1 μM aziridine **1** followed by copper(I)-catalyzed click reaction with 0.5 - 50 μM of Bodipy-alkyne **10** or biotin-alkyne **11**; control samples were treated with 0.3 μM **2** instead of click reagents. D) Fabrazyme or Replagal labeled with 100 nM **2** after preincubation with inhibitors **7** (10 μM), **8** (100 mM), **6** (100 μM) or probe **1** (100 nM) for 1 hr. All gels are 10% SDS-PAGE with fluorescent readout or visualization by streptavidin Western blotting (C, lower panel).

visualized after targeting by ABP **1** by performing a copper(I)-catalyzed click reaction with Bodipy- and biotin-functionalized alkyne reagents **10**[18] and **11**[19] (Figure 6.5C). Replagal, the second recombinant enzyme that can be used for enzyme replacement therapy in Fabry disease, was also labeled effectively with probe **2** (Figure 6.5D). Labeling of either of the two enzymes was completely abolished by preincubation with aziridine probe **1** or epoxide inhibitor **6**. The labeling was also blocked by the competitive α-galactosidase inhibitor deoxygalactonojirimicin (**7**) but not by the selective αGal B inhibitor *N*-acetylgalactosamine (**8**) (see Figure 6.2).

The optimal pH for αGal A activity is around pH 4.6, consistent with the acidic pH of the lysosomal environment. By treating recombinant αGal A with ABP **2** in buffers of varying pH, it was revealed that the labeling is indeed pH-dependent with an optimum around pH 5 (Figure 6.6A). However, at high pH values (6 or 7) there was a discrepancy between the enzymatic activity as determined by fluorogenic substrate hydrolysis and the intensity of fluorescent labeling on gel (Figure 6.6C). This phenomenon is in agreement with previous findings on the labeling of retaining β-glucosidases by the corresponding aziridine probe **9**[20] (Figure 6.2) and may be explained by the fact that the aziridine moiety forms a better leaving group than the aglycon of the (fluorogenic) substrate and therefore allows for a more efficient reaction with the active site nucleophile at high pH. In order to confirm the

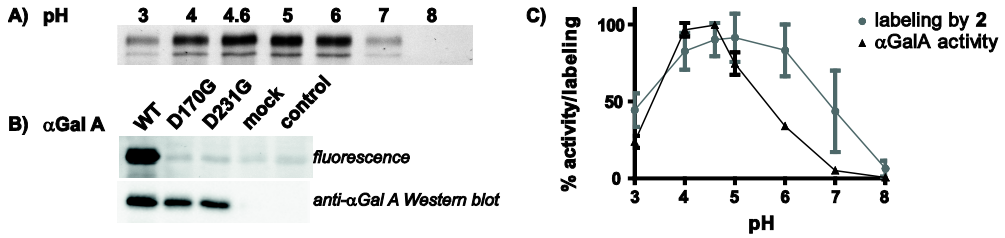

Figure 6.6. Dependence of probe binding on catalytic activity. A) Fabrazyme labeled with 50 nM **2** for 1 hr in buffers of varying pH. B) Labeling of recombinant wild-type αGal A (WT) and D170G or D231G mutants in lysates of transfected Cos-7 cells with 100 nM **2**; 'mock': mock-transfected cells; 'control': non-transfected cells. C) Quantification of gel bands in A (circles) as compared to Fabrazyme activity on 4-mu α-gal (triangles) at different pH values. Gels are 10% SDS-PAGE with fluorescent readout (A,B) followed by anti-αGal A Western blotting (B).

mechanism-based inhibition of αGal A by ABP **2**,mutants of αGal A lacking either the active site nucleophile (D170) or the general ac-id/base residue (D231) were generated. Reaction of the resulting recombinant enzymes with aziridine **2** demonstrated that absence of either of the aspartic acid residues leads to complete disappearance of the fluorescent signal on gel (Figure 6.6B). Hence, both residues are essential for labeling of the enzyme by the ABP which underscores the proposed binding mechanism as shown in Figure 6.1B.

Next, attention was focused on the labeling of endogenous α-galactosidases in cell extracts. Treatment of wild-type (WT) fibroblast extracts with Bodipy-aziridine **2** gave two fluorescently labeled proteins on gel (Figure 6.7A). In contrast, only one fluorescent signal, corresponding to the upper band in the WT fibroblasts, was visible in fibroblast extracts from αGal A deficient Fabry patients. This indicates that the lower signal, which is completely absent in Fabry cells, is αGal A. The identity of this protein can be further confirmed by the fact that the labeling in WT extracts was blocked by deoxygalactonojirimicin (**7**) but not by *N*-acetylgalactosamine (**8**). Likewise, competition of the upper signal by both inhibitors revealed that this protein is αGal B. The non-fluorescent aziridine ABP **1** was also able to bind both enzymes. Interestingly, epoxide inhibitor **6** selectively blocked labeling of αGal A without affecting αGal B. With the aim to determine whether Bodipy-aziridine **2** is more selective for αGal A or αGal B, the probe concentration and reaction time used for labeling in WT fibroblast lysates were reduced (Figure 6.7B). Although it proved impossible to obtain selective labeling of only one of the two enzymes, quantification of the fluorescent bands in Figure 6.7B revealed that the ratio of αGal A/αGal B labeling is higher after 2 min of labeling (1/0.9) than after 1 hr (1/2.1) which indicates that ABP **2** preferentially targets αGal A (Figure 6.7C).

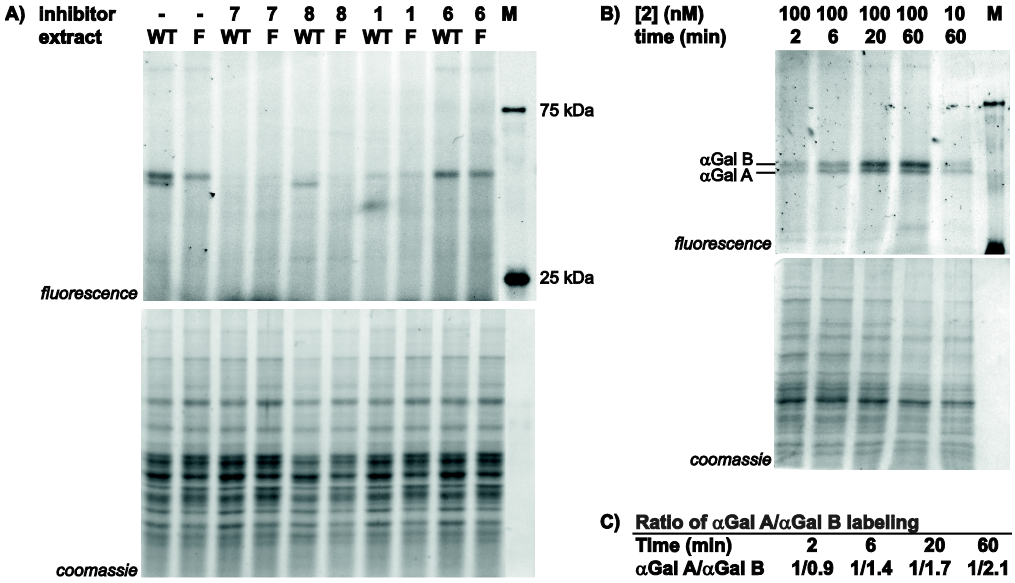

Figure 6.7. Labeling of endogenous α-galactosidases in cell extracts. A) Wild-type (WT) or Fabry (F) fibroblast extracts were treated with 100 nM **2** for 1 hr; where indicated extracts were preincubated for 1 hr with inhibitors **7** (10 μM), **8** (100 mM), **6** (100 μM) or probe **1** (1 μM). B) Labeling of WT fibroblast extracts with 10 or 100 nM **2** for 2 - 60 min. C) Ratio of αGal A/αGal B labeling as determined from quantification of gel bands in B. Gels are 10% SDS-PAGE with fluorescent readout followed by coomassie brilliant blue staining. 'M': protein marker.

In a final experiment the simultaneous labeling of retaining α-galactosidases and retaining β-glucosidases was examined by using α-galactosidase ABP **2** together with β-glucosidase ABP **9**[20], which is equipped with a different Bodipy fluorophore than **2** and can therefore be visualized using different scanner settings for in-gel fluorescent readout. Labeling of recombinant glucocerebrosidase (GBA1), a lysosomal retaining β-glucosidase, and αGal A with the two probes at the same time gave selective labeling of the anticipated enzymes without any observed cross-reactivity (Figure 6.8). Similarly, simultaneous treatment of fibroblast extracts with both ABPs enabled the selective labeling of endogenous αGal A and αGal B activity by aziridine **2** and GBA1 activity by probe **9**.

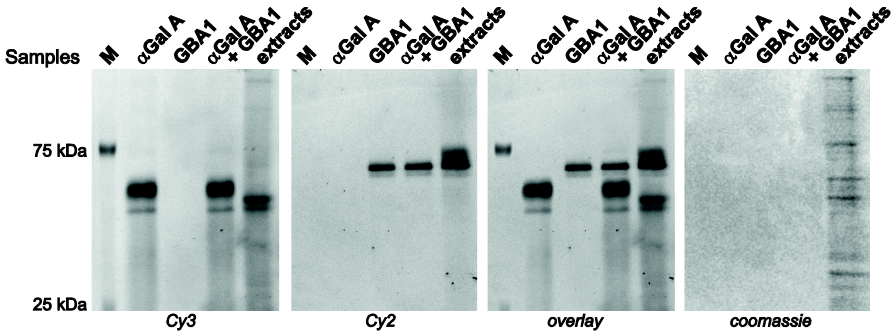

Figure 6.8. Simultaneous labeling of retaining α-galactosidases and β-glucosidases. Recombinant αGal A, recombinant GBA1 or WT fibroblast extracts were labeled with 100 nM **2** and 100 nM **9** and resolved by 10% SDS-PAGE with fluorescent readout in Cy3 (**2**) and Cy2 (**9**) channels followed by coomassie brilliant blue staining. 'M': protein marker.

6.3 Conclusion

A very potent aziridine-based fluorescent activity-based probe was identified (**2**) that enables profiling of endogenous αGal A and αGal B activity in cell extracts. The two enzymes can be separated on gel and are easily distinguished by competition with known inhibitors, which makes aziridine **2** a valuable probe to study the activity of human retaining α-galactosidases *in vitro*. Epoxide **6** is an irreversible inhibitor of αGal A that also inhibits galactocerebrosidase but not αGal B. Bodipy-aziridine **2** can be used in combination with the previously reported retaining β-glucosidase ABP **9** to study both enzyme classes simultaneously. A noteworthy difference between the two ABPs is the labeling of mutant enzymes lacking the active site nucleophile or general acid/base residue. While it was demonstrated that GBA1 labeling by aziridine **9** occurs in the absence of the acid/base residue,[20] aziridine **2** does not label either of the αGal A mutants and may thus be considered to be a 'true' activity-based probe that can report accurately on active enzyme levels. Bodipy-aziridine **2** may provide a useful new tool for studying human retaining α-galactosidases and their role in the development of Fabry disease, for evaluating the various phenotypic variants of the disease, and for diagnostic purposes and the assessment of the effects of therapeutic intervention. In addition, labeling of αGal B activity may turn out to be useful to study a related lysosomal storage disorder that is caused by αGal B deficiency, Schindler disease.[21]

Experimental procedures

General

Fibroblasts were obtained with consent from control donors and Fabry patients. Cell lines were cultured in DMEM/F-12 medium (Invitrogen) supplied with 10% (v/v) FBS in an incubator at 5% CO_2 and 37 °C. Recombinant α-galactosidase A was obtained from Genzyme (Fabrazyme) and Shire (Replagal), recombinant β-glucocerebrosidase (GBA1) was obtained from Genzyme (Cerezyme). For all *in vitro* assays, a 100 ng/μL stock solution of Fabrazyme or Replagal was prepared in McIlvaine pH 4.6/H_2O 1/1 (v/v), to which 100 ng/μL (0.1%) BSA was added for stabilization of the recombinant proteins. Cell lysates were prepared from cell pellets by resuspension in 50 mM potassium phosphate buffer (pH 6.0, 0.1% (v/v) Triton X-100) and sonication on ice for 3x 1 s with 1 min interval, after which the protein concentration was determined by BCA assay. SDS-PAGE analysis: in-gel fluorescence was measured on a Bio-Rad ChemiDoc MP scanner using Cy3 settings (Green Epi illumination, 605/50 Filter) or Cy2 settings (Blue Epi illumination, 530/28 Filter). As a loading control gels were stained with Coomassie Brilliant Blue. For Western blotting, the proteins were transferred onto a PVDF membrane (Bio-Rad Trans-Blot Turbo Transfer Pack) using a Bio-Rad Trans-Blot Turbo Transfer System. Membranes were blocked with 1% BSA in TBS-t(+) (0.1% Tween 20) for 1 hr at room temperature, hybridized with antibodies, washed with TBS-t(+) and TBS and then visualized using an ECL+ Western blotting detection kit (Amersham Biosciences). For detection of biotinylated proteins, membranes were hybridized with Streptavidin-HRP for 1 hr at room temperature (1:10,000 in blocking buffer) (Molecular Probes, Life Technologies). For detection of αGal A, membranes were hybridized with rabbit anti-GLA antibody at 4 °C overnight (1:500 in blocking buffer) followed by goat anti-rabbit-HRP antibody for 1 hr at room temperature (1:10,000 in blocking buffer) (Santa Cruz Biotechnology). The protein standard is a PageRuler Plus Prestained Protein Ladder (Thermo Scientific).

Fluorogenic substrate assay on recombinant αGal A

Fabrazyme (1 ng, 20 fmol per experiment) was diluted in McIlvaine buffer pH 4.6/H_2O 1/1 (v/v) containing 0.1% BSA (10 μL) and exposed to the indicated concentrations of compounds **1**-**6** (10 μL 2x solution in H_2O) for 30 min at 37 °C, before addition of 100 μL substrate mix (1.5 mg/mL 4-methylumbelliferyl-α-D-galactopyranoside in McIlvaine pH 4.6/H_2O 1/1 (v/v) + 0.1% BSA). After incubation at 37 °C for 20 min, the reaction was quenched with 2.5 mL 0.3 M glycine, pH 10.6 and fluorescence was measured with a fluorimeter LS55 (Perkin Elmer) using λ_{ex} 366 nm and λ_{em} 445 nm. For tests of irreversibility, the substrate mix was added simultaneously with the inhibitors to the enzyme (without any preincubation) and incubated for 20 min. All samples were corrected for background fluorescence (sample without enzyme) and residual enzyme activity was calculated as compared to a control sample incubated without inhibitors. Displayed values represent mean values from duplicate experiments and error bars indicate standard deviation (SD). Graphpad Prism 5 software was used to determine apparent IC_{50} values.

pH-dependent activity assay. Fabrazyme (1 ng, 20 fmol per experiment) in McIlvaine buffer pH 4.6/H_2O 1/1 (v/v) containing 0.1% BSA (10 μL) was mixed with 100 μL substrate mix of various pH values (1.5 mg/mL 4-methylumbelliferyl-α-D-galactopyranoside in McIlvaine pH 3 - pH 8/H_2O 1/1 (v/v) + 0.1% BSA). After incubation at 37 °C for 20 min, the reaction was quenched and fluorescence measured as described above. Displayed values represent mean values from 5 experiments and error bars indicate standard deviation (SD).

Fluorogenic substrate assay on recombinant galactocerebrosidase

Recombinant galactocerebrosidase was expressed in Cos-7 cells by transfection with cDNA encoding human galactocerebrosidase (gift from professor T. M. Cox, Cambridge). The culture medium containing the secreted recombinant protein was used directly for the fluorogenic substrate assay. Medium was diluted 2/1 (v/v) with

McIlvaine buffer pH 4.3 (10 µL total volume) and exposed to the indicated concentrations of compounds **1**-**6** (10 µL 2x solution in H_2O) for 30 min at 37 °C, before addition of 100 µL substrate mix (0.23 mg/mL 4-methylumbelliferyl-β-D-galactopyranoside in McIlvaine pH 4.3/H_2O 1/1 (v/v) with 0.2 M NaCl and 0.1% BSA). After incubation at 37 °C for 30 min, the reaction was quenched with 2.5 mL 0.3 M glycine, pH 10.6 and fluorescence was measured with a fluorimeter LS55 (Perkin Elmer) using λ_{ex} 366 nm and λ_{em} 445 nm. For tests of irreversibility, the substrate mix was added simultaneously with the inhibitors to the enzyme (without any preincubation) and incubated for 30 min. All samples were corrected for background fluorescence (sample without enzyme) and residual enzyme activity was calculated as compared to a control sample incubated in the same manner but without inhibitors. Displayed values represent mean values from triplicate experiments and error bars indicate standard deviation (SD). Graphpad Prism 5 software was used to determine apparent IC_{50} values.

***In vitro* labeling assays using recombinant αGal A**

In a typical experiment, Fabrazyme (10 ng, 0.20 pmol per experiment) was diluted in McIlvaine buffer pH 4.6/H_2O 1/1 (v/v) (9 µL total volume) and exposed to the indicated concentrations of ABP **2** (1 µL 10x solution in DMSO) for 1 hr at 37 °C. For denaturation of samples, Fabrazyme was heated to 100 °C for 5 min in McIlvaine buffer pH 4.6/H_2O 1/1 (v/v) containing 1% SDS (9 µL total volume) before addition of probe **2**. After labeling, the reaction mixtures were boiled for 5 min at 100 °C with 4 µL 4x Laemmli's sample buffer containing 2-mercaptoethanol and resolved on 10% SDS-PAGE. In-gel visualization of the fluorescent labeling was performed in the wet gel slabs directly using Cy3 settings.

Competition assays. Fabrazyme or Replagal (10 ng, 0.20 pmol per experiment) were first exposed for 1 hr at 37 °C to either 10 µM of **7**, 100 mM of **8**, 1 µM of **1**, or 100 µM of **6** (0.5 µL 20x solution in DMSO), before labeling with 100 nM **2** (0.5 µL 2 µM in DMSO) as described above.

pH-dependent labeling assay. Fabrazyme (50 ng, 1.0 pmol) was labeled with 50 nM of ABP **2** (1 µL 0.5 µM, 0.5 pmol, 0.5 eq.) as described above using McIlvaine buffers of pH 3 - pH 8. Gel bands were quantified using Image Lab 4.1 (Bio-Rad) software. Displayed values represent mean values from 5 independent experiments.

Copper(I)-catalyzed click reaction on recombinant αGal A

Fabrazyme (100 ng, 2.0 pmol per experiment, 1 µL 100 ng/µL) was mixed with 50 mM potassium phosphate buffer pH 4.6 (3.5 µL) and 1 µM of ABP **1** (0.5 µL 10 µM in DMSO, 5.0 pmol, 2.5 eq.). The reaction was incubated for 1 hr at 37 °C, before being diluted with 50 mM NaOAc containing 0.1% SDS (10 µL) for copper(I)-catalyzed click reaction using a slightly modified literature procedure.[22] After successive addition of 1 mM TBTA (2 µL 10 mM in DMSO), 2.5 mM DTT (0.5 µL 100 mM in H_2O) and 5 mM $CuSO_4$ (1 µL 100 mM in H_2O), the reaction mixtures were treated for 1 hr at 37 °C with 0.5, 5 or 50 µM of either Bodipy-alkyne **10**[18] or biotin-alkyne **11**[19] (1 µL 20x solution in DMSO; respectively 10, 100 and 1000 pmol; 5, 50 and 500 eq.). As a control, after exposure to ABP **1** the mixtures were diluted with 50 mM potassium phosphate buffer pH 4.6 (4 µL) and labeled with 0.3 µM ABP **2** (1 µL 3 µM in DMSO, 3.0 pmol, 1.5 eq.) for 1 hr at 37 °C instead of click reaction. The reaction mixtures were then boiled for 5 min at 100 °C with 7 µL 4x Laemmli's sample buffer containing 2-mercaptoethanol and resolved on 10% SDS-PAGE. In-gel visualization of the fluorescent labeling by ABP **2** and click reaction with **10** was performed in the wet gel slabs directly using Cy3 settings. Proteins labeled by click reaction with **11** were detected by streptavidin Western blotting.

Generation of αGal A mutants D170G and D231G

Molecular cloning and site-directed mutagenesis. Design of cloning primers and primers for mutation introduction were based on NCBI Reference sequence for human αGal A NM_000169.2 (GLA). The full-length αGal A wild-type

cDNA sequence was cloned from human mRNA (Hek293 cells) in pcDNA-DEST40 using the Gateway cloning system (Invitrogen). Full length cDNA was generated using the Pfx50 DNA polymerase (Invitrogen) and cloned in pDONR-221 with the following primers:
- forward: 5'-GGGGACAAGTTTGTACAAAAAAGCAGGCTACCACCATGCAGCTGAGGAACCCAGA-3'
- reverse: 5'- GGGGACCACTTTGTACAAGAAAGCTGGGTCTTAAAGTAAGTCTTTTAATGACATC-3'.

Site-directed mutagenesis was performed using the QuickChange II XL Site-Directed Mutagenesis Kit (Agilent Technologies) in order to change the nucleophilic (D170) and acid/base (D231) aspartic acid to glycine residues, using the following primers:
- nucleophile D170G: 5'-GATCTGCTAAAATTTGGTGGTTGTTACTGTGACAG-3'
- acid/base D231G: 5'- GGCGAAATTTTGCTGGCATTGATGATTCCTGGAAAAG-3'.

Recombinant protein expression. Cos-7 cells were cultured in HAMF12-DMEM (Invitrogen) supplied with 10% (v/v) FCS. Confluent cells were transfected with FuGENE (Roche) and either wild-type αGal A, D170G αGal A mutant, D231G αGal A mutant or chitotriosidase as a mock transfection control. The cells were harvested after 72 hours by scraping in 25 mM potassium phosphate buffer (pH 6.5, 0.1% (v/v) Triton X-100, protease inhibitor cocktail (Roche)). Control cells were not transfected.

Labeling of αGal A mutants

Cos-7 lysates (10 µg total protein per experiment) from cells transfected with either WT αGalA, D170G or D231G mutants, chitotriosidase or control cells were diluted in McIlvaine buffer pH 4.6 (9 µL total volume) and exposed to 100 nM of ABP **2** (1 µL 1 µM in DMSO) for 1 hr at 37 °C. The reaction mixtures were then boiled for 5 min at 100 °C with 4 µL 4x Laemmli's sample buffer containing 2-mercaptoethanol and resolved on 10% SDS-PAGE. In-gel visualization of the fluorescent labeling was performed in the wet gel slabs directly using Cy3 settings. Next, αGal A levels were detected by performing anti-GLA Western blotting.

***In vitro* labeling assay using cell lysates**

In a typical experiment, fibroblast lysates (20 µg total protein per experiment) were diluted in McIlvaine buffer pH 4.6 (9 µL total volume) and exposed to 100 nM of ABP **2** (1 µL 1 µM in DMSO) for 1 hr at 37 °C. Where indicated, a reduced reaction time or probe concentration was used. The reaction mixtures were then boiled for 5 min at 100 °C with 4 µL 4x Laemmli's sample buffer containing 2-mercaptoethanol and resolved on 10% SDS-PAGE. In-gel visualization of the fluorescent labeling was performed in the wet gel slabs directly using Cy3 settings. The gel bands in the fluorescence scan were quantified using Image Lab 4.1 (Bio-Rad) software to calculate the ratio of labeling between αGal A (lower signal) and αGal B (upper signal).

Competition assays. Fibroblast lysates (20 µg total protein per experiment) were first exposed for 1 hr at 37 °C to either 10 µM of **7**, 100 mM of **8**, 1 µM of **1**, or 100 µM of **6** (0.5 µL 20x solution in DMSO), before labeling with 100 nM **2** (0.5 µL 2 µM in DMSO) as described above.

Simultaneous labeling of retaining α-galactosidases and β-glucosidases

Wild-type fibroblast lysates (20 µg total protein), recombinant αGal A (Fabrazyme, 10 ng, 0.20 pmol), recombinant GBA1 (Cerezyme, 12 ng, 0.20 pmol) or a mixture of both recombinant proteins were diluted in McIlvaine buffer pH 4.6/H_2O 1/1 (v/v) (9 µL total volume) and labeled with 100 nM aziridine **2** plus 100 nM aziridine **9**[20] (each 0.5 µL 2 µM in DMSO, 1 pmol, 5 eq.) for 1 hr at 37 °C. The reaction mixtures were then boiled for 5 min at 100 °C with 4 µL 4x Laemmli's sample buffer containing 2-mercaptoethanol and resolved on 10% SDS-PAGE. In-gel visualization of the fluorescent labeling was performed in the wet gel slabs directly using Cy3 settings for probe **2** and Cy2 settings for probe **9**.

References

1. Gieselmann, V. *Biochim. Biophys. Acta* **1995**, *1270*, 103.
2. Witte, M. D.; Kallemeijn, W. W.; Aten, J.; Li, K.-Y.; Strijland, A.; Donker-Koopman, W. E.; van den Nieuwendijk, A. M. C. H.; Bleijlevens, B.; Kramer, G.; Florea, B. I.; Hooibrink, B.; Hollak, C. E. M.; Ottenhof R.; Boot, R. G.; van der Marel, G. A.; Overkleeft, H. S.; Aerts, J. M. F. G. *Nat. Chem. Biol.* **2010**, *6*, 907.
3. Stubbs, K. A. *Carbohydr. Res.* **2014**, *390*, 9.
4. Brady, R. O.; Gal, A. E.; Bradley, R. M.; Martensson, E.; Warshaw, A. L.; Laster, L. *N. Engl. J. Med.* **1967**, *276*, 1163.
5. Dean, K. J.; Sung, S. J.; Sweeley, C. C. *Biochem. Biophys. Res. Commun.* **1977**, *77*, 1411.
6. Garman, S. C.; Garboczi, D. N. *J. Mol. Biol.* **2004**, *337*, 319.
7. Tomasic, I. B.; Metcalf, M. C.; Guce, A. I.; Clark, N. E.; Garman, S. C. *J. Biol. Chem.* **2010**, *285*, 21560.
8. Schiffmann, R. *Pharmacol. Ther.* **2009**, *122*, 65.
9. Aerts, J. M.; Groener, J. E.; Kuiper, S.; Donker-Koopman, W. E.; Strijland, A.; Ottenhof, R.; van Roomen, C.; Mirzaian, M.; Wijburg, F. A.; Linthorst, G. E.; Vedder, A. C.; Rombach, S. M.; Cox-Brinkman, J.; Somerharju, P.; Boot, R. G.; Hollak, C. E.; Brady, R. O.; Poorthuis, B. J. *Proc. Natl. Acad. Sci. USA* **2008**, *105*, 2812.
10. Ferraz, M. J.; Kallemeijn, W. W.; Mirzaian, M.; Herrera Moro, D.; Marques, A.; Wisse, P.; Boot, R. G.; Willems, L. I.; Overkleeft, H. S.; Aerts, J. M. *Biochim. Biophys. Acta* **2014**, *1841*, 811.
11. Gold, H.; Mirzaian, M.; Dekker, N.; Ferraz, M. J.; Lugtenburg, J.; Codée, J. D. C.; van der Marel, G. A.; Overkleeft, H. S.; Linthorst, G. E.; Groener, J. E. M.; Aerts, J. M.; Poorthuis, B. J. H. M. *Clin. Chem.* **2013**, *59*, 547.
12. Schiffmann, R.; Kopp, J. B.; Austin III, H. A.; Sabnis S.; Moore, D. F.; Weibel, T.; Balow, J. E.; Brady, R. O. *JAMA.* **2001**, *285*, 2743.
13. Eng, C. M.; Guffon, N.; Wilcox, W. R.; Germain, D. P.; Lee, P.; Waldek, S.; Caplan, L.; Linthorst, G. E.; Desnick, R. J.; *N. Engl. J. Med.* **2001**, *345*, 9.
14. Lee, K.; Jin, X.; Zhang, K.; Copertino, L.; Andrews, L.; Baker-Malcolm, J.; Geagan, L.; Qiu, H.; Seiger, K.; Barngrover, D.; McPherson, J. M.; Edmunds, T. *Glycobiology* **2003**, *13*, 305.
15. Tatsuta, K.; Niwata, Y.; Umezawa, K.; Toshima, K.; Nakata, M. *Tetrahedron Lett.* **1990**, *31*, 1171.
16. Atsumi, S.; Umezawa, K.; Iinuma, H.; Naganawa, H.; Nakamura, H.; Iitaka, Y.; Takeuchi, T. *J. Antibiot.* **1990**, *43*, 49.
17. Withers, S. G.; Umezawa, K. *Biochem. Biophys. Res. Commun.* **1991**, *177*, 532.
18. Verdoes, M.; Hillaert, U.; Florea, B. I.; Sae-Heng, M.; Risseeuw, M. D. P.; Filippov, D. V.; van der Marel, G. A.; Overkleeft, H. S. *Bioorg. Med. Chem. Lett*. **2007**, *17*, 6169.
19. Verdoes, M.; Florea, B. I.; Hillaert, U.; Willems, L. I.; van der Linden, W. A.; Sae-Heng, M.; Filippov, D. V.; Kisselev, A. F.; van der Marel, G. A.; Overkleeft, H. S. *ChemBioChem* **2008**, *9*, 1735.
20. Kallemeijn, W. W.; Li, K.-Y.; Witte, M. D.; Marques, A. R. A.; Aten, J.; Scheij, S.; Jiang, J.; Willems, L. I.; Voorn-Brouwer, T. M.; van Roomen, C. P. A. A.; Ottenhoff, R.; Boot, R. G.; van den Elst, H.; Walvoort, M. T. C.; Florea, B. I.; Codée, J. D. C.; van der Marel, G. A.; Aerts, J. M. F. G.; Overkleeft, H. S. *Angew. Chem. Int. Ed.* **2012**, *51*, 12529.
21. Desnick, R. J.; Wang, A. M. *J. Inherit. Metab. Dis* **1990**, *13*, 549.
22. Witte, M. D.; Walvoort, M. T.; Li, K.-Y.; Kallemeijn, W. W.; Donker-Koopman, W. E.; Boot, R. G.; Aerts, J. M.; Codée, J. D.; van der Marel, G. A.; Overkleeft, H. S. *ChemBioChem* **2012**, *12*, 1263.

7

Activity-based profiling of human retaining β-galactosidases

7.1 Introduction

Glycosidases are responsible for the degradation of glycosphingolipids in lysosomes. When the activity of one of these hydrolases is deficient, accumulation of the corresponding substrates in lysosomes can occur which may lead to a lysosomal storage disorder. Despite the similarities in the primary cause of such disorders, they are usually very heterogeneous in clinical manifestation and course of the disease.[1] Two extreme examples are Morquio B syndrome and GM1 gangliosidosis, which are both caused by a deficiency in the lysosomal enzyme β-galactosidase but represent two completely different disease phenotypes.[2] Activity-based probes (ABPs) have shown promise as valuable research tools for the investigation of glycosidases and their involvement in disease.[3,4] The class of retaining glycosidases is especially susceptible to targeting by ABPs, since their catalytic mechanism involves the formation of a covalent enzyme-substrate intermediate which can be exploited for the design of novel ABPs.

At least three different retaining glycosidases that display β-galactosidase activity are known in humans. These include two lysosomal enzymes, galactocerebrosidase and β-galactosidase, and the membrane-bound non-lysosomal enzyme lactase, also known as lactase-phlorizin hydrolase, which is present in epithelial cells of the small intestine. Lactase

is responsible for cleaving lactose into galactose and glucose. With the exception of the majority of Northern Europeans, its activity rapidly declines after weaning which can cause lactose-intolerance in adults.[5,6] The lysosomal enzymes β-galactosidase and galactocerebrosidase both catalyze the hydrolysis of terminal β-linked galactosyl moieties. They have different substrate preferences, although there appears to be some overlap.[7,8] The substrates of β-galactosidase include glycosphingolipids (e.g. ganglioside GM1, lactosylceramide), glycoproteins and keratan sulfate-derived oligosaccharides.[2] Malfunctioning of β-galactosidase can result in two distinct lysosomal storage disorders, GM1 gangliosidosis and Morquio B syndrome. The former is a neurological disease characterized by ganglioside GM1 accumulation, whereas the primary storage lipid in Morquio B syndrome is keratin sulfate and main symptoms include dwarfism and skeletal abnormalities. These differences are likely caused by different effects of the various mutations in the gene encoding β-galactosidase on folding of the enzyme, substrate binding or binding of activator proteins that are necessary for GM1 ganglioside catabolism.[2,9]

Galactocerebrosidase is involved in the degradation of galactolipids such as galactosylceramide, galactosylsphingosine and monogalactosyldiglyceride.[10,11] It is an 80-kDa protein containing at least four *N*-linked glycosylation sites which are responsible for lysosomal trafficking via the mannose-6-phosphate receptor.[12] After entering the lysosomes, the enzyme is cleaved into 30- and 50-kDa subunits.[13] However, based on the crystal structure of the protein it is assumed that this cleavage does not result in dissociation of the subunits and has no effect on enzymatic activity.[12] Substrate hydrolysis by galactocerebrosidase occurs through a double displacement mechanism, similar to the mechanism described for retaining α-galactosidases in Chapter 6, with overall retention of the β-anomeric configuration (Figure 7.1A). The two carboxylic acid residues in the active site that function as a nucleophile and a general acid/base have been identified as the glutamic acid residues E258 and E182, respectively.[12,14]

A deficiency in galactocerebrosidase is at the basis of the autosomal recessive lysosomal storage disorder Krabbe disease, also named globoid cell leukodystrophy. More than 70 mutations in the gene encoding galactocerebrosidase have been implicated in the development of this disease.[12] The main pathological consequences are found in the peripheral and central nervous system, however the mechanism behind this neurodegenerative disorder has not yet been fully elucidated.[14] Reduced activity of galactocerebrosidase results in a reduced catabolism of galactosphingolipids including galactosylceramide. This forms the main lipid component of myelin, the protective sheath around neuron axons that is essential for correct functioning of the nervous system. The

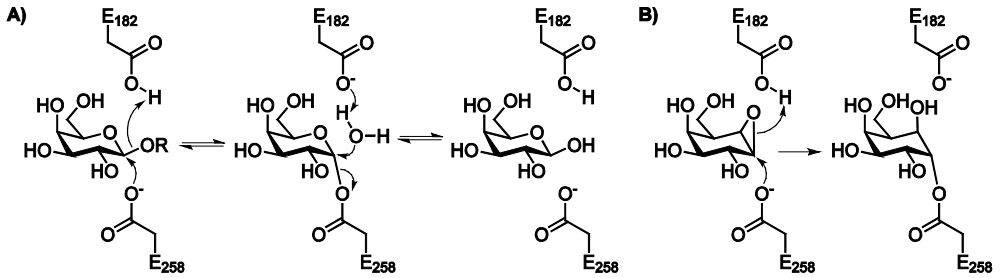

Figure 7.1. A) Mechanism of substrate hydrolysis by galactocerebrosidase. B) Proposed mechanism of galactocerebrosidase binding by inhibitor **5**.

accumulation of the toxic metabolite galactosylsphingosine eventually leads to the apoptosis of myelin-forming cells and consequently results in demyelination and neurodegeneration.[15,16] Infantile Krabbe disease is usually diagnosed before 1 year of age and lethal before the age of 2. Early symptoms include limb stiffness, developmental delay, and severe irritability. When diagnosed in adolescents or adults other symptoms may be observed such as seizures, feeding difficulties, slowing of mental and motor development, muscle weakness, spasticity, deafness, and blindness. The onset and severity of symptoms as well as the course of the disease in adult Krabbe patients is very variable, even in patients carrying the same mutation.[11,17] Diagnosis can be confirmed by measuring the residual galactocerebrosidase activity in leukocytes or cultured skin fibroblasts, which is usually 0-5% of normal levels. However, the amount of residual activity is not directly correlated to the clinical symptoms or course of the disease. Carriers may have as little as 10-20% of normal galactocerebrosidase activity without being affected. The only available treatment for Krabbe disease involves symptomatic treatment and physical therapy. Clinical trials with hematopoietic stem cell transplantation, which aims to restore galactocerebrosidase activity in the central nervous system and thereby prevent further demyelination, have shown that this therapy can slow the course of juvenile Krabbe disease when diagnosed at an early stage.[18,19]

Further investigations of galactocerebrosidase and its involvement in Krabbe disease would benefit from the availability of ABPs that specifically target this enzyme. In addition, a broad-spectrum ABP targeting all human retaining β-galactosidases may provide a valuable research tool to study these enzymes and the selectivity of new β-galactosidase inhibitors. Numerous fluorescent β-galactosidase probes have been reported in literature. However, most of these are reversible and can therefore not be used in, for example, gel-based assays. Examples include substrates consisting of a β-galactose moiety with a luminescent or

fluorogenic tag attached to the aglycon position that is released after cleavage by the enzyme[20-26] and fluorescently tagged competitive inhibitors.[27,28] A few ABPs that enable non-reversible mechanism-based labeling of retaining β-galactosidases have been reported (Figure 7.2A). Suicide substrates functionalized with a latent quinone methide precursor as the aglycon to which a fluorescent or fluorogenic tag is attached (**1**-**3**) were shown to act as covalent β-galactosidase probes.[29-32] Hydrolysis by the enzyme results in the release of a quinone methide which can then react covalently with a nearby nucleophilic amino acid residue. Of note, this type of probe also labels inverting galactosidases. Suicide substrates have found limited use for the specific labeling of glycosidases in cell extracts because the released quinone methide can diffuse out of the active site, making the labeling efficiency highly dependent on the presence and nature of nearby nucleophilic amino acid residues and also allowing the labeling of other proteins. Nonetheless, these probes were found to be useful for histological studies and fluorescence-activated cell sorting experiments, enabling the *in situ* fluorescent labeling of various cell types overexpressing bacterial or plant enzymes with β-galactosidase activity.[31,32] The second type of galactosidase ABPs is based on 2-fluorogalactoside inhibitors in which the hydroxyl group at C6 is substituted with an azide, which enables two-step labeling via Staudinger-Bertozzi ligation (**4**).[33] Although this ABP is not strictly irreversible, the covalent enzyme-probe intermediate is sufficiently stable to enable visualization of labeled proteins on gel. ABP **4** was used to label *Escherichia coli* β-galactosidase (LacZ) in cell extracts. To date, none of these probes has been used for the labeling of human retaining β-galactosidases.

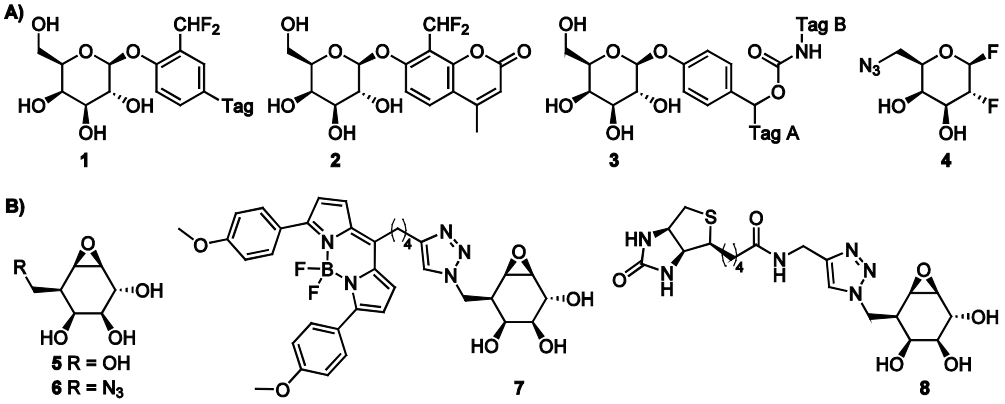

Figure 7.2. A) Structures of known β-galactosidase ABPs **1-4**. B) Structures of novel retaining β-galactosidase inhibitor **5** and ABPs **6-8**.

This chapter describes the evaluation of β-galactopyranose-configured epoxides **5**-**8** as inhibitors and ABPs for human galactocerebrosidase (Figure 7.2B). These probes, synthesized as described in Chapter 5, were designed such that they mimic the substrate's terminal galactosyl moiety and bind covalently to their target enzyme via a nucleophilic attack of the catalytic residue in the active site on the β-configured electrophilic epoxide moiety (Figure 7.1B). The non-tagged inhibitor **5** was synthesized as a galactose-configured isomer of the known retaining β-glucosidase inhibitor cyclophellitol.[34-36] In ABP **6** the primary hydroxyl group is substituted with an azide that can be used for two-step labeling via 'click' reaction or Staudinger-Bertozzi ligation. In addition, this probe may serve as a control probe and an inhibitor. ABPs **7** and **8** were obtained by functionalization of probe **6** with a Bodipy fluorophore and a biotin tag, respectively.

7.2 Results and discussion

The ability of compounds **5**-**8** to inhibit recombinant galactocerebrosidase was evaluated by measuring residual enzyme activity using the fluorogenic substrate 4-methylumbelliferyl β-D-galactoside (4-mu β-gal) after 30 min of preincubation with varying concentrations of the probes. The recombinant enzyme used for these assays was obtained by overexpression of human galactocerebrosidase in Cos-7 cells, resulting in excretion of the enzyme into the culture medium which was used without further purification.[37] Therefore the exact amount of enzyme is not known. Plots of residual activity against inhibitor concentration reveal a clear dose-dependent inhibition of galactocerebrosidase by all probes (Figure 7.3A). The apparent IC_{50} values calculated from these curves are shown in Table 7.1. The non-tagged epoxide **5** proved to be a very potent inhibitor of galactocerebrosidase with an apparent IC_{50} value of 38 nM. Substitution of the hydroxyl group at the C6 position with an azide (**6**), however, resulted in a dramatic loss of potency with an almost 2000-fold increase of the apparent IC_{50} value (70 μM). Probe **6** was found to reach full inhibition after a prolonged incubation time. Interestingly, the inhibitory potency was partially restored by incorporation of a Bodipy dye (**7**), but not a biotin tag (**8**), at the same position. Hence, it appears that the hydrophobic fluorophore leads to enhanced binding of the probe to its target enzyme and might be better tolerated in the active site of the enzyme than a small polar azide moiety. A similar result has been found previously for the inhibition of retaining β-glucosidases by analogous C6-modified probes, although the beneficial effect of the Bodipy dye was much larger in that case.[4] On the contrary, the findings described in Chapter 6 suggest that neither of the α-configured isomers of the C6-functionalized epoxide probes **6**-**8** appears to inhibit

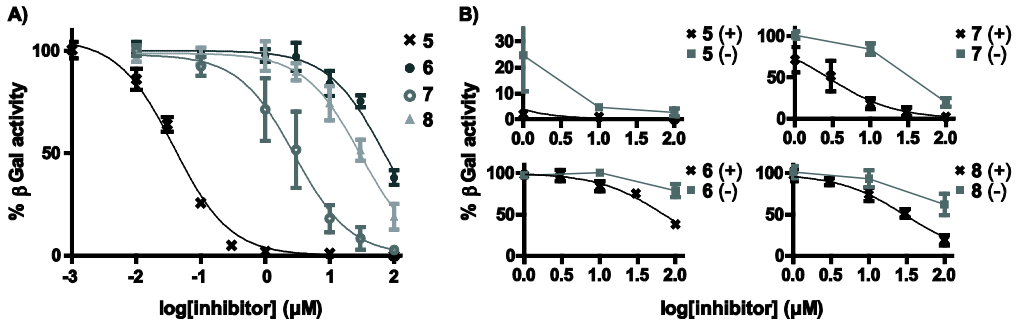

Figure 7.3. Inhibition of recombinant galactocerebrosidase activity. A) Recombinant galactocerebrosidase (βGal) was treated for 30 min with inhibitors **5**-**8** after which residual activity was determined from hydrolysis of 4-mu β-gal. B) Effect of 30 min preincubation (+) as compared to simultaneous addition of 4-mu β-gal and probes (-) on inhibition. The displayed inhibitor concentrations in both cases represent those without addition of the fluorogenic substrate solution.

retaining α-galactosidases, indicating that this phenomenon is dependent on the specific active site features and substrate tolerance of each individual glycosidase. The non-reversibility of galactocerebrosidase inhibition by epoxides **5**-**8** was demonstrated by testing the effect of preincubation on the amount of inhibition. Residual enzyme activity was measured as a function of probe concentration when the substrate and inhibitors were added simultaneously to the enzyme, and the obtained values were compared to those after preincubation of the enzyme with the inhibitors (Figure 7.3B). The evident shifts of the resulting curves confirm that preincubation leads to a higher percentage of inhibition and thereby indicate that the binding is irreversible. In order to assess the selectivity of inhibitors **5**-**8** for retaining β-galactosidases over the related class of retaining α-galactosidases, inhibition of recombinant α-galactosidase A (Fabrazyme) was determined by using a similar assay with the fluorogenic substrate 4-methylumbelliferyl α-D-galactoside. No inhibition was observed after 30 min of preincubation with up to 100 μM of the probes.

Table 7.1. Inhibition of recombinant galactocerebrosidase activity

Compound	**Apparent IC_{50} (μM)**	**% inhibition**	
		30 min	**6 hrs**
Epoxide **5**	0.038	98 (1 μM)	100 (1 μM)
Azido-epoxide **6**	70	62 (100 μM)	96 (100 μM)
Bodipy-epoxide **7**	2.8	97 (100 μM)	100 (100 μM)
Biotin-epoxide **8**	30	81 (100 μM)	97 (100 μM)

Inhibition of recombinant galactocerebrosidase as determined from hydrolysis of 4-mu β-gal after preincubation for 30 min or 6 hrs with probes **5**-**8**. Apparent IC_{50} values were calculated from plots of residual galactocerebrosidase activity as a function of probe concentration with a preincubation time of 30 min (Figure 7.3A).

Having shown that compounds **5**-**8** are able to irreversibly inhibit galactocerebrosidase, fluorescently labeled ABP **7** was used to visualize the recombinant enzyme on gel. As before, the non-purified enzyme in cell culture medium was used. Exposure to Bodipy-epoxide **7** for 1 hr resulted in concentration-dependent fluorescent labeling of a band around 80 kDa, corresponding to the molecular weight of galactocerebrosidase (Figure 7.4A). The labeling was completely abolished by denaturation of the enzyme prior to addition of the ABP, confirming the specific binding of the probe to catalytically active enzyme. In addition, a second fluorescently labeled band of approximately 60 kDa was visible at higher probe concentrations. This protein most likely represents serum albumin, a component of the cell culture medium. Unwanted labeling of albumin is a known problem with the use of Bodipy-functionalized probes and is caused by non-specific interactions of the hydrophobic dye with the protein. Evidence for the non-specific nature of these interactions is provided by the fact that denaturation of the protein by boiling in assay buffer prior to labeling with ABP **7** resulted in an even stronger fluorescent signal, which could only be eliminated by addition of the surfactant SDS. Moreover, pretreatment of samples with non-tagged inhibitor **5** led to complete disappearance of the fluorescent labeling of galactocerebrosidase by Bodipy-tagged epoxide **7**, while the labeling of albumin was unaffected (Figure 7.4B). Preincubation

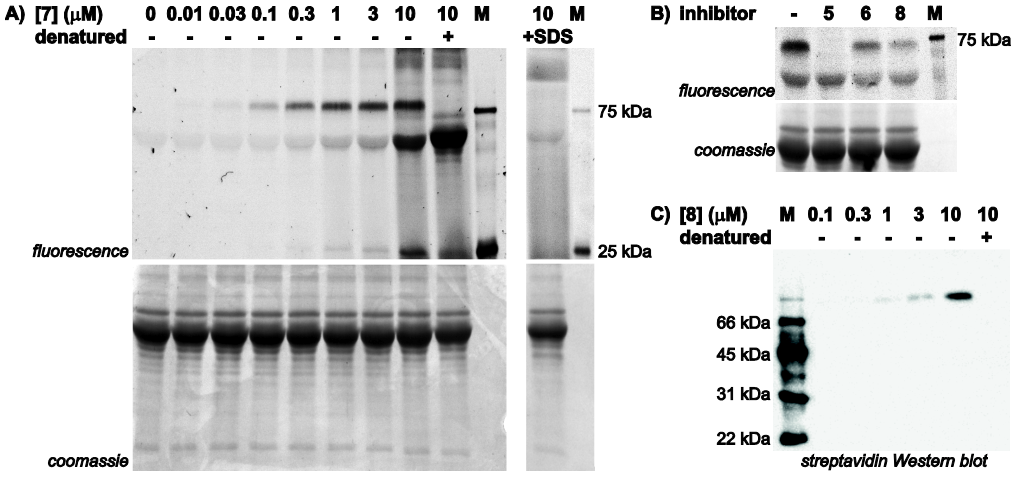

Figure 7.4. Labeling and inhibition of recombinant galactocerebrosidase. A) Labeling with 0.01 - 10 μM of Bodipy-epoxide **7** for 1 hr; where indicated enzyme was denatured prior to labeling by boiling at 100 °C for 3 min in assay buffer (+) or in buffer with 1% SDS (+SDS). B) Labeling with 0.2 μM **7** after preincubation with inhibitors **5** (0.2 μM), **6** (10 μM) or **8** (10 μM) for 1 hr. C) Labeling with 0.1 - 10 μM of biotin-epoxide **8** for 1 hr; where indicated enzyme was denatured prior to labeling by boiling at 100 °C for 3 min. All gels are 10% SDS-PAGE with fluorescent readout followed by coomassie brilliant blue staining (A, B) or streptavidin Western blotting (C). 'M': protein marker.

with azide- and biotin-tagged probes **6** and **8** resulted in partial blocking of the fluorescent labeling of galactocerebrosidase. Biotinylated ABP **8** also enables the visualization of galactocerebrosidase activity by streptavidin Western blotting (Figure 7.4C). In agreement with the higher IC_{50} value of this probe as compared to its fluorescently labeled analogue **7**, a relatively large amount of probe is required to (fully) label the enzyme. At the highest concentration tested (10 μM) a single biotin-labeled band was clearly visible that corresponds to catalytically active galactocerebrosidase.

Since galactocerebrosidase is a lysosomal enzyme, its activity is highest in a slightly acidic environment with an optimum around pH 4.3. The pH-dependence of galactocerebrosidase labeling by Bodipy-functionalized ABP **7** was examined by treating the recombinant enzyme with the probe in buffers of varying pH. As can be seen in Figure 7.5A, the intensity of fluorescent labeling of galactocerebrosidase is indeed highest at pH 4-5 while it is almost completely abolished at pH 3 and lower or pH 7 and higher. Quantification of the fluorescent gel bands revealed that the amount of labeling by ABP **7** overlaps perfectly with the enzymatic activity as determined by fluorogenic substrate hydrolysis (Figure 7.5B). These results indicate that binding of the probe occurs in an activity-based manner and support the proposed binding mechanism depicted in Figure 7.1B. However, the exact site of binding has yet to be confirmed.

In a final experiment the selective labeling of retaining β-galactosidases and retaining β-glucosidases by differently configured epoxide-based ABPs was tested. For this purpose, β-galactosidase ABP **7** and the previously reported β-glucosidase ABP **9**[3] (Figure 7.6) were used to label either recombinant galactocerebrosidase or recombinant glucocerebrosidase,

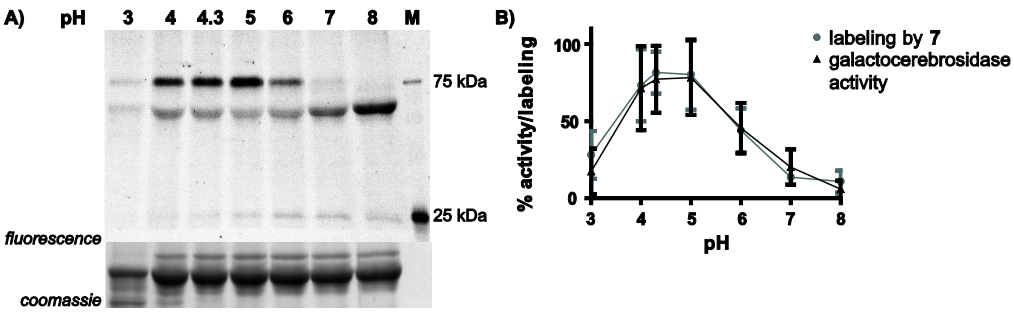

Figure 7.5. pH-dependence of galactocerebrosidase labeling. A) Recombinant galactocerebrosidase labeled with 0.5 μM **7** for 1 hr in buffers of varying pH; 10% SDS-PAGE with fluorescent readout followed by coomassie brilliant blue staining. B) Quantification of gel bands in A (circles) as compared to galactocerebrosidase activity on 4-mu β-gal (triangles) at different pH values. 'M': protein marker.

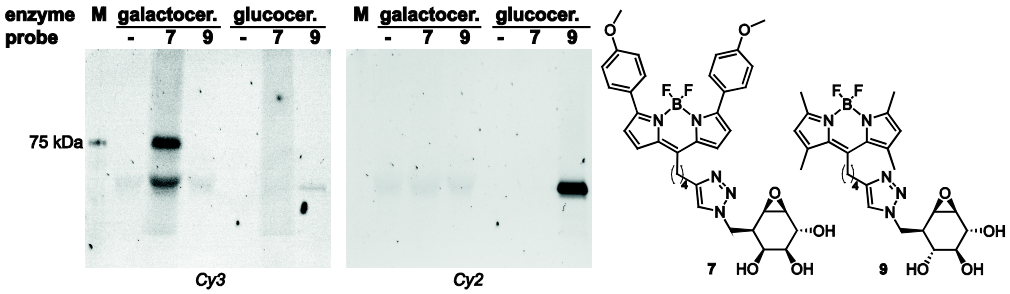

Figure 7.6. Selective labeling of retaining β-galactosidases and retaining β-glucosidases with differently configured epoxide ABPs. Recombinant galactocerebrosidase ('galactocer.') and glucocerebrosidase ('glucocer.') were labeled with 1 μM of ABP **7** or ABP **9** for 1 hr and labeled proteins were resolved by 7.5% SDS-PAGE with fluorescent readout in Cy2 (**9**) and Cy3 (**7**) channels. 'M': protein marker.

a lysosomal retaining β-glucosidase. The two ABPs are functionalized with different Bodipy fluorophores and can therefore be visualized using different scanner settings for in-gel fluorescent readout. While galactocerebrosidase was labeled exclusively by probe **7**, glucocerebrosidase was labeled by ABP **9** but not by its stereoisomer **7**. The absence of cross-reactivity demonstrates the selective targeting of each of these enzymes by the appropriately configured ABPs.

7.3 Conclusion

The β-galactopyranose-configured epoxide-based probes **5**-**8** were demonstrated to inhibit recombinant human galactocerebrosidase covalently and irreversibly. Of these probes, non-tagged epoxide inhibitor **5** is the most potent inhibitor. Substitution of the hydroxyl group at C6 with an azide (**6**) results in a dramatic loss of potency, whereas installment of a Bodipy tag at the same position (**7**) partially restores the inhibitory potency. Inhibition of other human retaining β-galactosidases, e.g. lysosomal β-galactosidase, by epoxides **5**-**8** remains to be determined but is not unlikely in view of their identical catalytic mechanism. Bodipy-functionalized ABP **7** and biotinylated ABP **8** enable the visualization of catalytically active galactocerebrosidase on gel. The epoxide probes label the enzyme in an activity-based manner and do not target the related glycosidase α-galactosidase A. Further experiments will have to reveal whether they can be used to label endogenously expressed β-galactosidases in cell extracts and living cells. In view of the positive results obtained with the α-galactopyranose- and β-glucopyranose-configured aziridine ABPs described in Chapter 6 and in literature,[38] efforts should also be made to expand the set of available β-galactosidase ABPs with aziridine-based probes. Finally, it should be noted that Bodipy-epoxide **7** differs only in the configuration of a single substituent from the previously

reported glucopyranose-configured stereoisomer **9** and yet the two probes enable selective targeting of galactocerebrosidase and glucocerebrosidase, respectively. These results demonstrate great potential for targeting different classes of retaining glycosidases by appropriate alterations in the probe configuration.

Experimental procedures

General

Recombinant galactocerebrosidase was expressed in Cos-7 cells by transfection with cDNA encoding human galactocerebrosidase.[37] The culture medium containing the secreted recombinant protein was used directly for fluorogenic substrate assays and labeling assays. Recombinant α-galactosidase A (Fabrazyme) and recombinant β-glucocerebrosidase (Cerezyme) were obtained from Genzyme. SDS-PAGE analysis: in-gel fluorescence was measured on a Bio-Rad ChemiDoc MP scanner using Cy3 settings (Green Epi illumination, 605/50 Filter) or Cy2 settings (Blue Epi illumination, 530/28 Filter). As a loading control gels were stained with Coomassie Brilliant Blue. For Western blotting, the proteins were transferred onto a PVDF membrane (Bio-Rad Trans-Blot Turbo Transfer Pack) using a Bio-Rad Trans-Blot Turbo Transfer System. Membranes were blocked with 1% BSA in TBS-t(+) (0.1% Tween 20) for 1 hr at room temperature, hybridized with Streptavidin-HRP for 1 hr at room temperature (1:10,000 in blocking buffer) (Molecular Probes, Life Technologies), washed with TBS-t(+) and TBS and then visualized using an ECL+ Western blotting detection kit (Amersham Biosciences). Protein standards are PageRuler Plus Prestained Protein Ladder (Thermo Scientific) and biotinylated protein marker (Bio-Rad).

Fluorogenic substrate assay on recombinant galactocerebrosidase

Culture medium containing recombinant galactocerebrosidase was diluted 2/1 (v/v) with McIlvaine buffer pH 4.3 (10 µL total volume) and exposed to the indicated concentrations of compounds **5**-**8** (10 µL 2x solution in H_2O) for 30 min at 37 °C, before addition of 100 µL substrate mix (0.23 mg/mL 4-methylumbelliferyl-β-D-galactopyranoside in McIlvaine pH 4.3/H_2O 1/1 (v/v) with 0.2 M NaCl and 0.1% BSA). After incubation at 37 °C for 30 min, the reaction was quenched with 2.5 mL 0.3 M glycine, pH 10.6 and fluorescence was measured with a fluorimeter LS55 (Perkin Elmer) using λ_{ex} 366 nm and λ_{em} 445 nm. For tests of irreversibility, the substrate mix was added simultaneously with the inhibitors to the enzyme (without any preincubation) and incubated for 30 min. All samples were corrected for background fluorescence (sample without enzyme) and residual enzyme activity was calculated as compared to a control sample incubated in the same manner but without inhibitors. Displayed values represent mean values from triplicate experiments and error bars indicate standard deviation (SD). Graphpad Prism 5 software was used to determine apparent IC_{50} values.

pH-dependent activity assay. Culture medium containing recombinant galactocerebrosidase was diluted 2/1 (v/v) with McIlvaine buffer pH 4.3 (10 µL total volume) and mixed with 100 µL substrate mix of various pH values (0.23 mg/mL 4-methylumbelliferyl-β-D-galactopyranoside in McIlvaine pH 3 - pH 8/H_2O 1/1 (v/v) with 0.2 M NaCl and 0.1% BSA). After incubation at 37 °C for 30 min, the reaction was quenched and fluorescence measured as described above. Displayed values represent mean values from 6 experiments and error bars indicate standard deviation (SD).

Fluorogenic substrate assay on recombinant αGal A

Fabrazyme was diluted to a concentration of 0.1 ng/µL in McIlvaine pH 4.6/H_2O 1/1 (v/v) containing 0.1% BSA for stabilization of the recombinant protein. A solution of Fabrazyme (1 ng, 20 fmol per experiment, 10 µL 0.1 ng/µL)

was exposed to the indicated concentrations of compounds **5**-**8** (10 µL 2x solution in H_2O) for 30 min at 37 °C, before addition of 100 µL substrate mix (1.5 mg/mL 4-methylumbelliferyl-α-D-galactopyranoside in McIlvaine pH 4.6/H_2O 1/1 (v/v) + 0.1% BSA). After incubation at 37 °C for 20 min, the reaction was quenched with 2.5 mL 0.3 M glycine, pH 10.6 and fluorescence was measured with a fluorimeter LS55 (Perkin Elmer) using λ_{ex} 366 nm and λ_{em} 445 nm. All samples were corrected for background fluorescence (sample without enzyme) and residual enzyme activity was calculated as compared to a control sample incubated in the same manner but without inhibitors.

***In vitro* labeling assays using recombinant galactocerebrosidase**

In a typical experiment, culture medium containing recombinant galactocerebrosidase (5 µL) was diluted with McIlvaine buffer pH 4.3/H_2O 2/1 (v/v) (14 µL) and exposed to the indicated concentrations of ABPs **7** or **8** (1 µL 20x solution in DMSO) for 1 hr at 37 °C. For denaturation of samples, the enzyme was heated to 100 °C for 3 min in buffer with or without 1% SDS (9 µL total volume) before addition of the probes. After labeling, the reaction mixtures were boiled for 5 min at 100 °C with 7 µL 4x Laemmli's sample buffer containing 2-mercaptoethanol and ½ of each sample was resolved on 10% SDS-PAGE. In-gel visualization of the fluorescent labeling by probe **7** was performed in the wet gel slabs directly using Cy3 settings. In case of probe **8**, biotinylated proteins were detected by performing streptavidin Western blotting.

Competition assays. Culture medium containing recombinant galactocerebrosidase (5 µL) in McIlvaine buffer pH 4.3/H_2O 2/1 (v/v) (14 µL) was first exposed for 1 hr at 37 °C to either 0.2 µM of **5**, 10 µM of **6** or 10 µM of **8** (1 µL 20x solution in DMSO), before labeling with 0.2 µM **7** (1 µL 4 µM in DMSO) as described above.

pH-dependent labeling assay. Culture medium containing recombinant galactocerebrosidase (5 µL) was diluted with McIlvaine buffers of pH 3 - pH 8/H_2O 2/1 (v/v) (14 µL) and labeled with 0.5 µM of ABP **7** (1 µL 10 µM in DMSO) for 1 hr at 37 °C. Gel bands were quantified using Image Lab 4.1 (Bio-Rad) software. Displayed values represent mean values from 4 independent experiments.

***In vitro* labeling assays using recombinant galactocerebrosidase and glucocerebrosidase**

Recombinant glucocerebrosidase (Cerezyme) in McIlvaine buffer pH 5.2/H_2O 1/1 (v/v) (9 µL 0.22 µM, 2.0 pmol, 0.12 µg per experiment) or culture medium containing recombinant galactocerebrosidase (2.5 µL) in McIlvaine buffer pH 4.3/H_2O 2/1 (v/v) (6.5 µL) were exposed to either 1 µM of epoxide **7** or 1 µM of epoxide **9**[4] (1 µL 10 µM in DMSO) for 1 hr at 37 °C. The reaction mixtures were then boiled for 5 min at 100 °C with 4 µL 4x Laemmli's sample buffer containing 2-mercaptoethanol and resolved on 7.5% SDS-PAGE. In-gel visualization of the fluorescent labeling was performed in the wet gel slabs directly using Cy3 settings for probe **7** and Cy2 settings for probe **9**.

References and notes

1. Gieselmann, V. *Biochim. Biophys. Acta* **1995**, *1270*, 103.
2. Callahan, J. W. *Biochim. Biophys. Acta* **1999**, *1455*, 85.
3. Stubbs, K. A. *Carbohydr. Res.* **2014**, *390*, 9.
4. Witte, M. D.; Kallemeijn, W. W.; Aten, J.; Li, K.-Y.; Strijland, A.; Donker-Koopman, W. E.; van den Nieuwendijk, A. M. C. H.; Bleijlevens, B.; Kramer, G.; Florea, B. I.; Hooibrink, B.; Hollak, C. E. M.; Ottenhof R.; Boot, R. G.; van der Marel, G. A.; Overkleeft, H. S.; Aerts, J. M. F. G. *Nat. Chem. Biol.* **2010**, *6*, 907.
5. Campbell, A. K.; Waud, J. P.; Matthews, S. B. *Sci. Prog.* **2009**, *92*, 241.
6. Potter, J.; Ho, M. W.; Bolton, H.; Furth, A. J.; Swallow, D. M.; Griffiths, B. *Biochem. Genet.* **1985**, *23*, 423.
7. Zschoche, A.; Fürst, W.; Schwarzmann, G.; Sanhoff, K. *Eur. J. Biochem.* **1994**, *222*, 83.
8. Tanaka, H.; Suzuki, K. *Brain Res.* **1977**, *122*, 325.

9. Ohto, U.; Usui, K.; Ochi, T.; Yuki, K.; Satow, Y.; Shimizu, T. *J. Biol. Chem.* **2012**, *287*, 1801.
10. D'Agostino, A. N.; Sayre, G. P.; Hayles, A. B. *Arch. Neurol.* **1963**, *8*, 82.
11. Wenger, D. A.; Rafi, M. A.; Luzi, P.; Datto, J.; Costantino-Ceccarini, E. *Mol. Genet. Metab.* **2000**, *70*, 1.
12. Deane, J. E.; Graham, S. C.; Kim, N. N.; Stein, P. E.; McNair, R.; Cachón-González, M. B.; Cox, T. M.; Read, R. J. *PNAS* **2011**, *108*, 15169.
13. Nagano, S.; Yamada, T.; Shinnoh, N.; Furuya, H.; Taniwaki, T.; Kira, J. *Clin. Chim. Acta* **1998,** *276*, 53.
14. Hill, C. H.; Graham, S. C.; Read, R. J.; Deane, J. E. *PNAS* **2013**, *110*, 20479.
15. Formichi, P.; Radi, E.; Battisti, C.; Pasqui, A.; Pompella, G.; Lazzerini, P. E.; Laghi-Pasini, F.; Leonini, A.; Di Stefano, A.; Federico, A. *J. Cell Physiol.* **2007,** *212*, 737.
16. Tanaka, K.; Nagara, H.; Kobayashi, T.; Goto, I. *Brain Res*. **1988**, *454*, 340.
17. Wenger, D.A.; Rafi, M. A.; Luzi, P. *Hum. Mutat.* **1997**, *10*, 268.
18. Krivit, W.; Shapiro, E. G.; Peters, C.; Wagner, J. E.; Cornu, G.; Kurtzberg, J.; Wenger, D.A.; Kolodny, E. H.; Vanier, M. T.; Loes, D. J.; Dusenbery. K.; Lockman, L. A. *New. Engl. J. Med.* **1998**, *338*, 1119.
19. Sakai, N. *Brain Dev*. **2009**, *31*, 485.
20. Wehrman, T. S.; Von Degenfeld, G.; Krutzik, P. ; Nolan, G. P.; Blau, H. M. *Nat. Methods* **2006**, *3*, 295.
21. Han, J.; Han, M. S.; Tung, C.-H. *Mol. BioSyst.* **2013**, *9*, 3001.
22. Kamiya, M.; Asanuma, D.; Kuranaga, E.; Takeishi, A.; Sakabe, M.; Miura, M.; Nagano T.; Urano, Y. *J. Am. Chem. Soc.* **2011**, *133*, 12960.
23. Urano, Y.; Kamiya, M.; Kanda, K.; Ueno, T.; Hirose K.; Nagano, T. *J. Am. Chem. Soc.* **2005**, *127*, 4888.
24. Tung, C. H.; Zeng, Q.; Shah, K.; Kim, D. E.; Schellingerhout D.; Weissleder, R. *Cancer Res*. **2004**, *64*, 1579.
25. Ho, N.-H.; Weissleder, R.; Tung, C.-H. *ChemBioChem* **2007**, *8*, 560.
26. Rotman, B.; Zderic J. A.; ;Edelstein, M.; *Proc. Natl. Acad. Sci. USA*, **1963**, *50*, 1.
27. Fröhlich, R. F. G.; Fantur, K.; Furneaux, R. H.; Paschke, E.; Stütz, A. E.; Wicki, J.; Withers, S. G.; Wrodnigg, T. M. *Bioorg. Med. Chem. Lett.* **2011**, *21*, 6872.
28. Greimel, P.; Häusler, H.; Lundt, I.; Rupitz, K.; Stütz, A. E.; Tarling, C. A.; Withers, S. G.; Wrodnigg, T. M. *Bioorg. Med. Chem. Lett.* **2006**, *16*, 2067.
29. Janda, K. D.; Lo, L. C.; Lo, C. H.; Sim, M. M.; Wang, R.; Wong, C. H.; Lerner, R. A. *Science* **1997**, *275*, 945.
30. Kurogochi, M.; Nishimura, S.-I.; Lee, Y. C. *J. Biol. Chem.* **2004**, *279*, 44704.
31. Kwan, D. H.; Chen, H.-M.; Ratananikom, K.; Hancock, S. M.; Watanabe, Y.; Kongsaeree, P. T.; Samuels, A. L.; Withers, S. G. *Angew. Chem. Int. Ed.* **2011**, *50*, 300.
32. Komatsu, T.; Kikuchi, K.; Takakusa, H.; Hanaoka, K.; Ueno, T.; Kamiya, M.; Urano, Y.; Nagano, T. *J. Am. Chem. Soc.* **2006**, *128*, 15946.
33. Vocadlo, D. J.; Bertozzi, C. R. *Angew. Chem. Int. Ed.* **2004**, *43*, 5338.
34. Tatsuta, K.; Niwata, Y.; Umezawa, K.; Toshima, K.; Nakata, M. *Tetrahedron Lett.* **1990**, *31*, 1171.
35. Atsumi, S.; Umezawa, K.; Iinuma, H.; Naganawa, H.; Nakamura, H.; Iitaka, Y.; Takeuchi, T. *J. Antibiot.* **1990**, *43*, 49.
36. Withers, S. G.; Umezawa, K. *Biochem. Biophys. Res. Commun.* **1991**, *177*, 532.
37. Recombinant galactocerebrosidase was generously provided by professor T. M. Cox, Cambridge.
38. Kallemeijn, W. W.; Li, K.-Y.; Witte, M. D.; Marques, A. R. A.; Aten, J.; Scheij, S.; Jiang, J.; Willems, L. I.; Voorn-Brouwer, T. M.; van Roomen, C. P. A. A.; Ottenhoff, R.; Boot, R. G.; van den Elst, H.; Walvoort, M. T. C.; Florea, B. I.; Codée, J. D. C.; van der Marel, G. A.; Aerts, J. M. F. G.; Overkleeft, H. S. *Angew. Chem. Int. Ed.* **2012**, *51*, 12529.

8

Summary and future prospects

The research described in this thesis involves the development of novel chemical tools and methods for the activity-based profiling of proteases and glycosidases. Activity-based protein profiling (ABPP) is a field of research that aims to obtain information on the activity of a protein or protein family within the context of a biological system. In order to enable the monitoring of enzymatic activity rather than protein expression levels, ABPP strategies make use of active-site directed chemical probes, termed activity-based probes (ABPs), that bind in a mechanism-based and irreversible manner to a specific target enzyme or multiple members of an enzyme family. An essential element of an ABP is a means to visualize, isolate, quantify and/or identify the labeled proteins. Depending on the nature of the detectable agent, ABPP experiments can involve either direct or two-step labeling strategies. Direct ABPs are functionalized with a reporter entity such as a fluorescent tag and/or an affinity tag. Alternatively, in two-step ABPs the reporter group is replaced by a small reactive moiety, referred to as 'ligation handle', that provides the option to introduce a tag after binding of the probe to a target enzyme. The attachment of a reporter group in two-step labeling strategies is realized by making use of bioorthogonal ligation reactions, which proceed with high selectivity and efficiency and are non-perturbing to the biological system at hand. In Chapter 1 the principles of ABPP and ABP design are discussed. Chapter 2 presents an overview of the various bioorthogonal ligation reactions that have been developed to date, with an emphasis on their use in two-step profiling of enzymatic activity.

The development of a two-step ABPP strategy based on the Diels-Alder cycloaddition is described in Chapter 3. Previously reported two-step ABPP methods all rely on the use of an alkyne or azide as a ligation handle for labeling of enzymatic activity via Staudinger-Bertozzi ligation or azide-alkyne cycloaddition ('click' reaction), which may either be catalyzed by copper(I) or driven by ring-strain. In contrast, the Diels-Alder approach makes use of ABPs that are functionalized with a conjugated diene to enable reaction with a tagged maleimide reagent as a dienophile. The Diels-Alder strategy was applied to label the activity of endogenously expressed proteasome β-subunits and cysteine proteases of the cathepsin family in cell extracts. Moreover, it was demonstrated that this ligation reaction can be performed in tandem with the Staudinger-Bertozzi ligation for the labeling of two different enzymatic activities in the same sample. Although the Diels-Alder method forms a useful complement to Staudinger-Bertozzi and click ligation strategies, its broad utility is limited by the need to mask cysteine residues prior to the addition of the dienophile, which precludes *in situ* and *in vivo* applications. In addition, a considerable amount of background labeling was observed that might hamper the detection of proteins with low endogenous activity.

To avoid non-specific reaction of the dienophile with cysteine residues, Chapter 4 details the development of a two-step ABPP strategy that is based on the inverse-electron-demand Diels-Alder reaction. By using tetrazine as a diene and norbornene as a dienophile, the selectivity and speed of the ligation reaction is drastically improved. A proteasome ABP functionalized with norbornene as a ligation handle enabled the efficient and selective labeling of endogenous proteasome activity in cell extracts and in cultured cells by reaction with fluorescently labeled or biotin-tagged tetrazine reagents. Furthermore, a triple ligation strategy was developed that combines the tetrazine ligation, Staudinger-Bertozzi ligation and copper(I)-catalyzed click reaction for the simultaneous labeling of three different enzymatic activities with different tags in the same sample. Despite the fact that tetrazines are not directly compatible with copper-catalyzed click chemistry, a simple washing step between these two ligation reactions allows their consecutive use in the same experiment.

The triple labeling procedure developed in Chapter 4 should not only be useful for ABPP applications but also for the simultaneous monitoring of other biomolecules, for instance modified cell surface glycans or post-translationally modified proteins, in complex biological samples. Furthermore, the fact that tetrazine and Staudinger-Bertozzi ligations can both be performed inside living cells[1,2] and in living animals[3,4] provides the possibility to develop tandem labeling procedures *in situ* and *in vivo*. *In situ* labeling via copper(I)-catalyzed click chemistry can be achieved without affecting cell viability by making use of specific ligands that accelerate the cycloaddition and sequester the copper-induced toxicity.[5,6]

Several reports have already described the metabolic incorporation of two differently tagged unnatural sugars for the simultaneous imaging of the corresponding glycan structures on live cell surfaces by strain-promoted click reaction and tetrazine ligation,[7-9] for example by making use of azide-modified *N*-acetylglucosamine derivative **1**[10] and cyclopropene-functionalized mannosamine **2**[7] (Figure 8.1A). The parallel labeling of additional cell surface glycans could be achieved by using alkyne-functionalized sugars, such as *N*-acetylneuraminic acid derivative **3**.[11] Alternatively, unnatural sugars that are tagged with a 3,3-disubstituted cyclopropene moiety, for instance *N*-acetylgalactosamine derivative **4**, may be used for bioorthogonal reaction with nitrile imines, which can be generated from tetrazoles *in situ* by exposure to UV light. In contrast to 1,3-disubstituted cyclopropenes, the 3,3-disubstituted cyclopropene moiety was demonstrated to show virtually no reactivity towards tetrazines, which enables the concurrent use of both ligation handles in a tandem labeling procedure.[12] Together, the ligation handles in compounds **1**-**4** should enable the parallel labeling of up to four different cell surface glycans or, for example, enzymatic activities (Figure 8.1B). Such a tandem ligation strategy would entail a number of steps starting with the inverse-electron-demand Diels-Alder reaction of the 1,3-disubstituted cyclopropene with a tetrazine and the (simultaneous) elaboration of the azide ligation handle via Staudinger-Bertozzi ligation with a phosphine, or alternatively via strain-

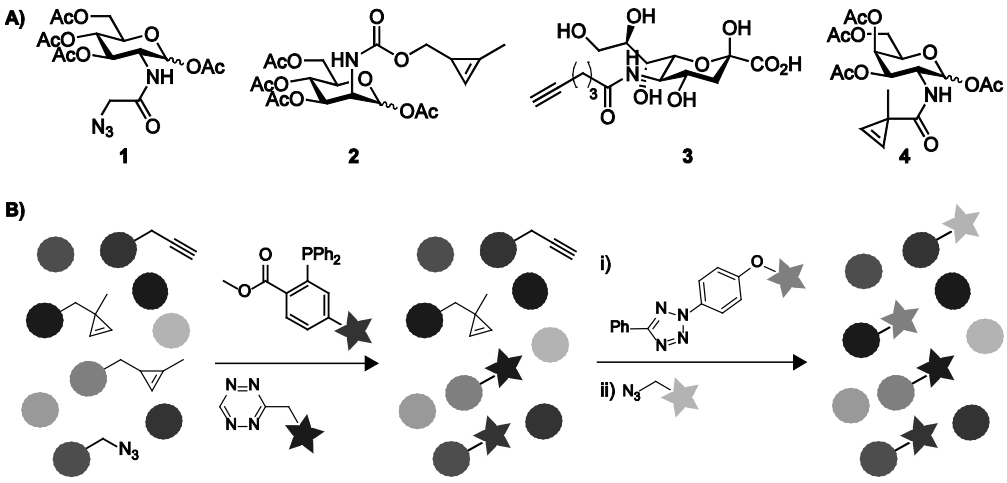

Figure 8.1. A) Peracetylated *N*-azidoacetyl glucosamine (**1**), cyclopropene-functionalized mannosamine derivative (**2**), alkyne-equipped neuraminic acid analogue (**3**) and *N*-acetyl galactosamine derivative with a 3,3-disubstituted cyclopropene (**4**) for bioorthogonal labeling of cell surface glycans. B) Tandem bioorthogonal labeling strategy involving four different ligation reactions.

promoted click reaction with a cyclooctyne. Subsequently, light-induced 1,3-dipolar cycloaddition of the 3,3-disubstituted cyclopropene with a nitrile imine can be performed, followed by copper(I)-catalyzed click reaction of the terminal alkyne with an azide.

The analysis of labeled proteins by mass spectrometry is an important method to identify target proteins and/or active-site peptides and to determine the exact site and mechanism of ABP binding. For this purpose, proteins are usually labeled with a biotin-tagged ABP and subsequently enriched by affinity-purification using streptavidin beads. Since the release of captured proteins from the beads requires harsh conditions and may result in contamination of the purified sample with endogenously biotinylated proteins, these methods benefit greatly from the use of cleavable linker systems. These may be incorporated in a direct ABP or in a bioorthogonal ligation reagent and enable the mild and chemoselective release of target proteins.

With the aim to make the developed tetrazine-based ABPP method suitable for such selective enrichment experiments, a tetrazine reagent was designed in which a hydrazine-cleavable linker separates the biotin tag from the tetrazine moiety (**11**, Figure 8.2).[13] A short polyethylene glycol (PEG) spacer was included to enhance water-solubility of the probe. The synthesis of biotin-cleavable linker-tetrazine **11** commenced with reduction of the azide in PEG spacer **14**[14] to an amine followed by reaction with the acid chloride generated from 6-heptynoic acid to give **15** (Scheme 8.1). After Boc-deprotection and reaction with biotin-OSu, the resulting alkyne-modified compound (**16**) was subjected to copper(I)-catalyzed click reaction with azide-functionalized levulinoyl derivative **18**[13] to give biotinylated cleavable linker **17**. The second building block was synthesized from tetrazine **12** (see Chapter 4), which was extended with an aminohexanoic acid spacer (**13**) to minimize potential steric

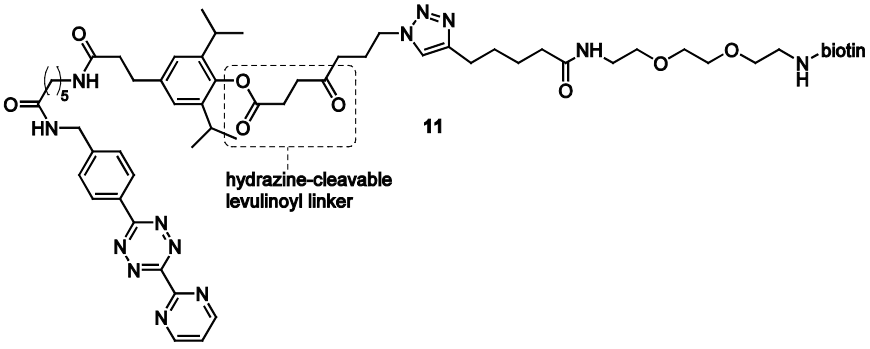

Figure 8.2. Biotinylated hydrazine-cleavable tetrazine reagent **11**.

Scheme 8.1 Synthesis of biotin-cleavable linker-tetrazine **11**

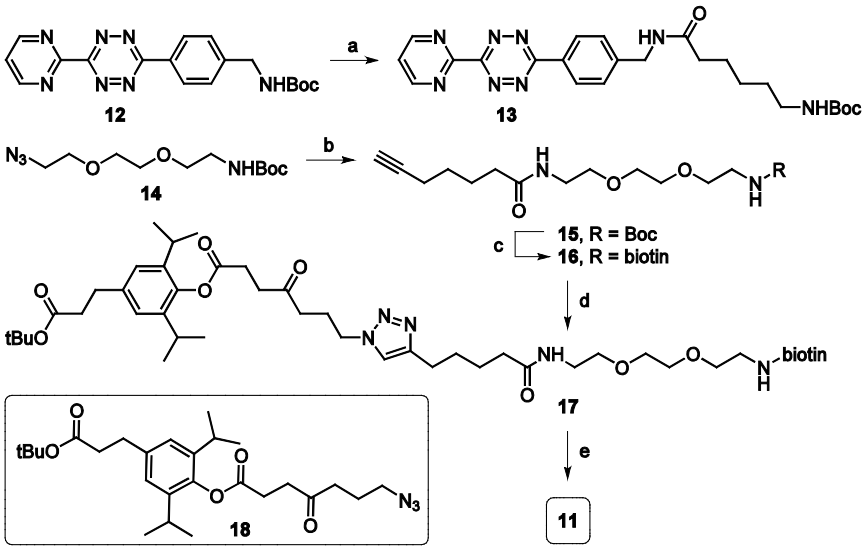

Reagents and conditions: a) *i*) TFA/DCM 1/1 (v/v), rt, 15 min, *ii*) Boc-Ahx-OSu, DiPEA, DCE/DMF, rt, overnight, 88%; b) *i*) PPh_3, THF/H_2O, rt, overnight, *ii*) [6-heptynoic acid preactivated with $(COCl)_2$, DMF, toluene, rt, 3 hrs], DiPEA, DCE, rt, overnight, 54%; c) *i*) TFA/DCM 1/1 (v/v), rt, 20 min, *ii*) biotin-OSu, DiPEA, DCE/DMF, rt, overnight, 87%; d) **18**, $CuSO_4$, sodium ascorbate, *t*BuOH/toluene/H_2O/DMF 1/1/1/1 (v/v/v/v), 80 °C, overnight, 60%; e) *i*) TFA/DCM 1/1 (v/v), rt, 30 min, *ii*) [**13** deprotected with TFA/DCM 1/1 (v/v), rt, 20 min], HCTU, DiPEA, DCM/DMF, rt, overnight, 70%.

hindrance of the linker system during the ligation reaction. Removal of the *t*Bu and Boc protecting groups in **17** and **13**, respectively, enabled HCTU-mediated coupling to afford the biotinylated hydrazine-cleavable tetrazine reagent **11**.

Two-step labeling experiments with norbornene-functionalized proteasome ABP **19** (see Chapter 4) and tetrazine reagent **11** demonstrated the selective labeling of the catalytically active proteasome β-subunits (β1, β2, β5) in cell extracts (Figure 8.3). Subsequent treatment with an excess of hydrazine resulted in disappearance of the specifically labeled protein bands on Western blot, indicating that the biotin tag was separated from the probe and thus that cleavage of the levulinoyl linker had occurred. Furthermore, preliminary enrichment experiments have revealed that the catalytically active proteasome β-subunits labeled by ABP **19** and biotin-cleavable linker-tetrazine **11** could be isolated from cell extracts using streptavidin beads and subsequently selectively released by treatment with hydrazine.

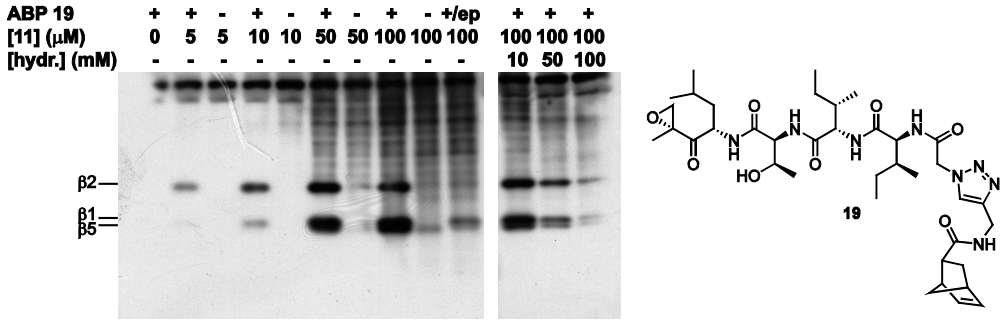

Figure 8.3. Labeling of proteasome activity in HEK cell extracts by 1 μM of ABP **19** for 1 hr followed by 5 - 100 μM of tetrazine **11** for 1 hr. Right panel: after the ligation reaction, samples were treated with 10, 50 or 100 mM hydrazine ('hydr.') overnight to cleave the levulinoyl linker. Proteins were resolved by 12.5% SDS-PAGE and detected by streptavidin Western blotting. 'ep': 100 μM epoxomicin added to compete for proteasome labeling by **19**.

The second part of this thesis describes the synthesis and biological evaluation of novel glycosidase ABPs. Glycosidases are hydrolytic enzymes responsible for the hydrolysis of glycosidic bonds in (oligo)saccharides and glycoconjugates such as glycosphingolipids in lysosomes. A deficiency in one of the lysosomal glycosidases can cause accumulation of the corresponding substrates in lysosomes, which may consequently lead to a lysosomal storage disorder. Despite the similarities in their primary defects, these disorders generally show a completely different disease progress, phenotype and clinical manifestation.[15] ABPP forms an attractive approach to study glycosidases and their involvement in disease.[16,17] At present a limited number of glycosidase ABPs has been developed, which is likely due to the tight substrate preference and the lack of covalent interactions with the substrate in the catalytic mechanism of many of these enzymes. Most of the retaining type of glycosidases, however form a covalent enzyme-substrate intermediate and are therefore amenable to targeting by ABPs that react covalently with the catalytic nucleophile in the active site.

Chapter 5 describes the design and synthesis of two series of irreversible inhibitors and ABPs for retaining α- and β-galactosidases. These probes are equipped with an electrophilic epoxide or aziridine moiety as the warhead in either an α- or a β-configuration to allow attack by the respective active site nucleophiles. The α- and β-galactopyranose-configured epoxide-based compounds include a non-tagged inhibitor as well as three ABPs in which the hydroxyl group at C6 (carbohydrate numbering) is substituted with an azide, a Bodipy fluorophore or a biotin tag. In addition, two aziridine-based α-galactosidase ABPs were synthesized in which an azide or Bodipy tag is installed via acylation of the aziridine nitrogen. Unfortunately, efforts to isolate the β-galactopyranose-configured isomers of these aziridine probes have so far proven unsuccessful, since even the use of a completely acid-free

procedure for HPLC purification and ensuing lyophilization resulted in opening of the acylated aziridine.

The inhibitory potency of the α-configured probes as well as their application for the labeling of human retaining α-galactosidases is described in Chapter 6. The aziridine-based ABPs proved to be very potent inhibitors of the human enzyme α-galactosidase A (αGal A), the deficiency of which is at the basis of the lysosomal storage disorder Fabry disease. The non-tagged epoxide inhibitor displayed a more than 10,000 fold lower potency towards αGal A than the aziridine probes, whereas none of the C6-modified epoxide ABPs showed any inhibition at all, revealing that the primary hydroxyl group is essential for binding of the probes to their target enzyme. Interestingly, the non-tagged epoxide proved to be an equally potent inhibitor of galactocerebrosidase, a human retaining β-galactosidase, while the aziridine ABPs did not inhibit this enzyme. The exact binding mechanism of the α-galactosidase probes to αGal A has yet to be confirmed by mass spectrometry analysis of the labeled active site peptides and/or crystallization of the recombinant enzyme with the probes covalently bound in the active site. The Bodipy-tagged aziridine ABP was demonstrated to enable the fluorescent labeling of endogenous αGal A activity in wild-type fibroblast cell extracts. Besides αGal A, the probe also labeled *N*-acetyl-galactosaminidase (αGal B), a related human enzyme displaying retaining α-galactosidase activity. In addition, the fluorescently labeled ABP was used to directly compare α-galactosidase activity in extracts from wild-type cells with those obtained from classic Fabry patients, which lack αGal A activity and accordingly showed only labeling of αGal B. An interesting application of the ABP would be to profile retaining α-galactosidase activity in samples from Fabry patients that have different mutations in αGal A and/or different phenotypic variants of the disease.

Preliminary *in situ* labeling experiments with the Bodipy-tagged aziridine ABP in fibroblast cell cultures revealed that no specific fluorescent signals could be detected on gel, despite the fact that inhibition of αGal A activity could clearly be demonstrated in extracts of probe-treated cells by measuring residual enzyme activity with the fluorogenic substrate 4-methylumbelliferyl α-D-galactoside (Figure 8.4). A possible explanation for the lack of fluorescent labeling is that the levels of enzymatic activity might be very low and thereby make it difficult to detect the labeled proteins, and/or that the ester bond formed between the enzyme and the probe is labile under the conditions used for SDS-PAGE analysis. The *in situ* inhibition of αGal A and αGal B activity by either tagged or non-tagged aziridine probes (**20** and **21**), regardless of their ability to enable visualization on gel, can be used to provide insight into the nature and extent of glyco(sphingo)lipid accumulation that results from reduced α-galactosidase activity by using mass spectrometry analysis.[18,19]

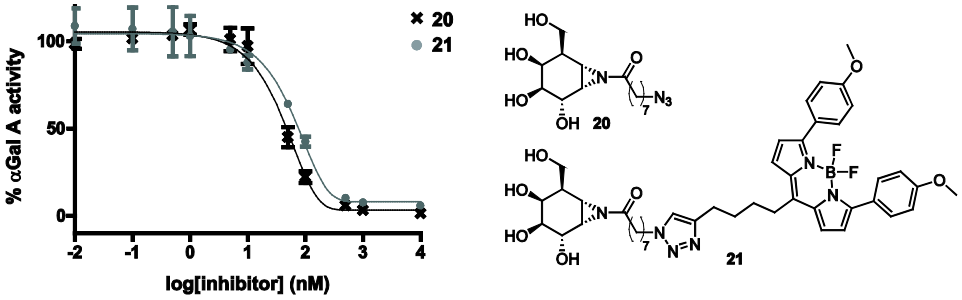

Figure 8.4. Inhibition of αGal A activity in wild-type fibroblast cells by treatment with 0.01 nM - 10 µM of ABPs **20** and **21** for 2 hrs. After cell lysis residual activity was determined from hydrolysis of 4-methylumbelliferyl α-D-galactoside.

In order to enable the visualization of enzymatic activity *in situ* and *in vivo*, it might be useful to improve the intensity and/or signal-to-background ratio of the fluorescent labeling. More sensitive detection of the labeled proteins could for example be realized by using an aziridine that is functionalized with a different (near-infrared) fluorophore such as Cy5 (**22**, Figure 8.5). Alternatively, the background labeling may be strongly reduced by performing two-step labeling with a cyclopropene-modified ABP (**25**) in combination with a quenched tetrazine reagent which only becomes fluorescent after reaction with the dienophile (e.g. **26**[20]). Biotin-tagged aziridines (**23** and **24**) would also form a useful complement to the set of available α-galactosidase ABPs by providing the option to enrich the labeled proteins in order to facilitate subsequent detection on Western blot and/or identification by mass spectrometry. Efforts have been undertaken to synthesize biotin-aziridine **24**, however the

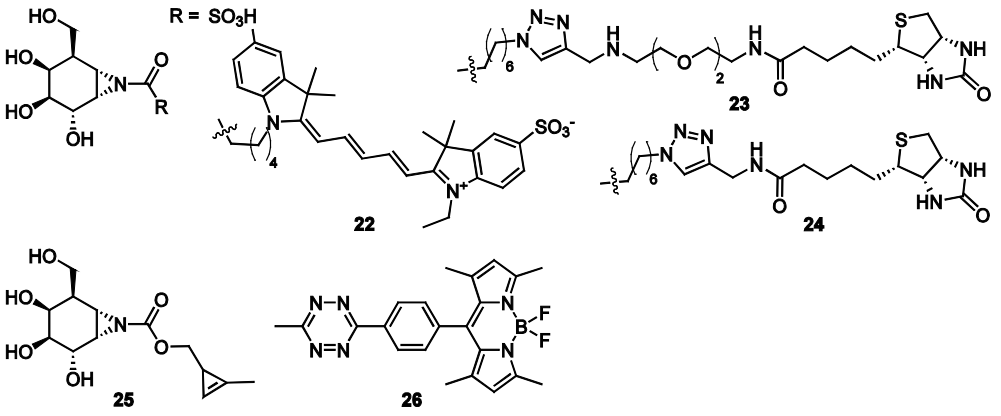

Figure 8.5. Putative aziridine-based retaining α-galactosidase ABPs functionalized with a Cy5 fluorophore (**22**), a biotin tag (**23** and **24**) or a cyclopropene ligation handle (**25**), and quenched Bodipy-tagged tetrazine **26**.

isolation of this compound proved difficult due to solubility issues and opening of the aziridine. It appears that these problems are at least partly due to the low solubility of the biotin spacer, and therefore the introduction of a PEG-spacer such as in probe **23** might offer a more practical alternative.

Chapter 7 describes the evaluation of the β-galactopyranose-configured epoxide probes for their ability to inhibit and label recombinant galactocerebrosidase, a human retaining β-galactosidase. The non-tagged epoxide proved to be the most potent inhibitor of this enzyme. While the inhibitory potency was almost 2,000-fold decreased for the ABP with an azide at C6, the installment of a Bodipy tag at the same position partially restored the inhibitory potency. A similar trend has been reported for the inhibition of retaining β-glucosidases by C6-modified β-glucopyranose-configured epoxide probes, although the beneficial effect of the Bodipy dye was much larger in that case.[16] In contrast, neither of the C6-functionalized α-galactopyranose-configured epoxide isomers (Chapter 6) appeared to inhibit retaining α-galactosidases, indicating that the substrate tolerance and restrictions in the active site of each individual glycosidase play an important role for the successful targeting with epoxide-based ABPs. The Bodipy- and biotin-functionalized β-galactosidase ABPs were shown to enable the visualization of catalytically active recombinant galactocerebrosidase on gel. It remains to be determined whether these probes also target other human retaining β-galactosidases, for instance lysosomal β-galactosidase, and whether they can be used to label endogenously expressed β-galactosidases in cell extracts and living cells. In addition, the exact binding mechanism of the ABPs to the active site of their target enzyme(s) has yet to be confirmed. Notably, the epoxide probes selectively labeled galactocerebrosidase without affecting the related enzymes α-galactosidase A and glucocerebrosidase. The fact that this latter enzyme can be targeted selectively by ABPs that differ only in the configuration of a single hydroxyl substituent from the β-galactosidase probes described here[16] demonstrates the potential to target different classes of retaining (exo)glycosidases by using similar ABPs that are modified in such a way that they mimic the natural substrate of the target enzyme.

Considering the results obtained with the α-galactopyranose- and β-glucopyranose-configured aziridine-based ABPs (see above), the synthesis of aziridine-based probes for β-galactosidases will likely provide ABPs with higher reactivity and/or altered selectivity than the epoxide-based probes. The availability of broad-spectrum as well as specific fluorescently labeled β-galactosidase ABPs would be useful to analyze differences in substrate preference of the different retaining β-galactosidases and to monitor enzymatic activity in the various lysosomal storage disorders that are associated with β-galactosidase

deficiency. A deficiency in galactocerebrosidase is at the basis of Krabbe disease while a deficiency in lysosomal β-galactosidase can lead to either Morquio B syndrome or GM1 gangliosidosis. The potential overlap in substrate preferences and the interplay between these enzymes have not yet been fully elucidated, and in this respect a set of β-galactosidase probes with different selectivity profiles might provide useful research tools. In addition, the (non-tagged) epoxide inhibitor may also be a valuable tool to study the accumulation of glyco(sphingo)lipids that occurs after inhibition of retaining β-galactosidase activity.

The instability of acylated aziridines is a recurring problem during the synthesis of aziridine-based ABPs and is mainly due to the electron-withdrawing nature of the carbonyl group, which activates the aziridine towards nucleophilic ring-opening. At the same time this property is probably also responsible for the superior reactivity of aziridine probes as compared to their epoxide analogues (Chapter 6).[16,21] An optimal balance between synthetic access and reactivity of an aziridine-based ABP may be realized by changing the nature of the functional group added to the aziridine nitrogen, for example by alkylation or sulfonylation as in probes **27** and **28** (Figure 8.6). Moreover, since the high reactivity of acylated aziridine probes was demonstrated to be accompanied by a loss in selectivity,[21] the synthesis of other substituted aziridines with varying reactivity may provide the option to tune their selectivity and thereby develop both highly specific and broad-spectrum ABPs. A non-substituted aziridine has a ring strain similar to an epoxide but is in principle less electrophilic due to its lower electronegativity,[22] so that the intrinsic reactivity of a non-activated aziridine (**27**) is likely lower than that of an epoxide. However, the aziridine-based ABPs have the advantage that the hydroxyl substituents are not used for the attachment of a tag and are therefore all available for making interactions with the active site of their target enzymes, potentially resulting in more tight binding and an increase in potency. In addition, it seems likely that the aziridine nitrogen will be protonated by the general acid/base residue in the active site, thereby strongly activating the aziridine towards nucleophilic ring-opening. Alkylated β-aziridine **27** can be derived from α-epoxide **29** (see Chapter 5) by opening of the epoxide with azido-PEG-amine **30**, mesylation of the resulting hydroxyl group and subsequent treatment with base to achieve aziridine formation.[23] A fluorophore or an affinity tag can then be introduced by copper(I)-catalyzed click reaction of the azide in **27** with an alkyne-functionalized tag. Sulfonylated aziridine **28** may be synthesized from deprotected aziridine **31** in a manner similar to the acylated aziridines described in Chapter 5 by selective reaction of the aziridine nitrogen with an activated ester of sulfonic acid **32** (e.g. an *N*-hydroxybenzotriazole ester).[24]

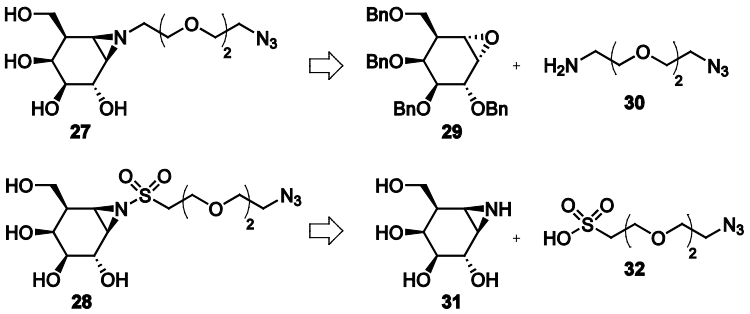

Figure 8.6. Alkylated (**27**) and sulfonylated (**28**) β-galactopyranose-configured aziridines.

Recently, a new method has been reported for the direct and mild conversion of olefins to *N*-H aziridines via a rhodium-catalyzed reaction with *O*-(2,4-dinitrophenyl) hydroxylamine (DPH) in trifluoroethanol.[25] This reaction can be performed in the presence of various functional groups, including unprotected alcohols, and may offer a useful alternative strategy to synthesize aziridine-based glycosidase ABPs. For example, galactopyranose- and glucopyranose-configured aziridines **34**-**35** and **37**-**38** can be obtained in a single step from the appropriately substituted cyclohexene precursors (**33** and **36**, respectively) (Scheme 8.2). This method would eliminate the need to first synthesize an epoxide or to form the aziridine with the aid of the primary hydroxyl group, procedures that were applied in Chapter 5. Although in general both diastereomeric aziridine products are formed, it seems likely that directing effects by the unprotected hydroxyl groups will affect the stereochemical outcome of the reaction. Hence, protection of one or more hydroxyl groups may be necessary to achieve formation of the desired α- and/or β-configured aziridines.

Scheme 8.2 Proposed new strategy for aziridine formation during the synthesis of glycosidase ABPs

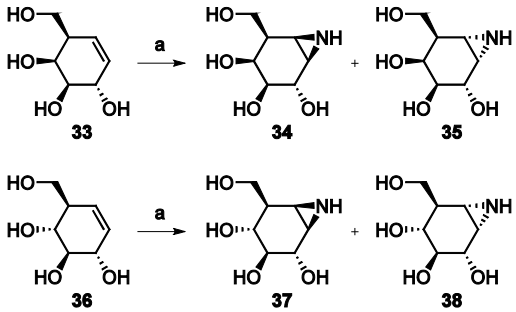

Reagents and conditions: a) DPH, $Rh_2(esp)_2$ (Du Bois' catalyst), CF_3CH_2OH.

The synthetic strategy towards the galactosidase probes that was developed in this thesis can also be applied to the synthesis of a number of differently configured probes. For example, α-*N*-acetylgalactopyranose-configured probes (**39** and **40**, Figure 8.7) may enable the selective targeting of α-*N*-acetylgalactosaminidase (αGal B), the deficiency of which is at the basis of the lysosomal storage disorder Schindler disease. Although this enzyme was targeted by the aziridine-based α-galactosidase probes described in Chapter 6, the labeling was not selective. In fact, it was demonstrated that these probes label αGal A more efficiently than αGal B. Since this latter enzyme binds α-linked *N*-acetylgalactosamine substrates with much higher efficiency than α-galactosides, it is likely that substitution of the hydroxyl group at C2 (carbohydrate numbering) in the ABPs with an acetylated amine will increase their selectivity for αGal B and might even completely abolish the labeling of αGal A. A proposed strategy towards the synthesis of these probes is depicted in Scheme 8.3 and involves the same synthetic route as was used for the galactosidase probes but starts from a differently configured and orthogonally protected aldehyde (**43**). This compound may be obtained by procedures similar to those described in literature,[26] using D-ribose as the starting material to achieve the required stereochemistry.[27] Aldol condensation with oxazolidinone **44**, removal of the Evans template and ring-closing metathesis as described in Chapter 5 will lead to compound **45**. Next, several protective group manipulations are necessary to selectively unmask the hydroxyl group at C2 (**46**), which can then be activated with triflic anhydride and substituted with TMS azide to yield compound **47**. Reduction of the azide to an amine and subsequent acetylation may provide compound **48**, from which the epoxide- and aziridine-based probes **39** and **40** can be synthesized.

Other compounds that can be synthesized via a similar synthetic strategy are α-L-fucopyranose-configured probes (**41**, Figure 8.7), which might enable the labeling of human retaining α-L-fucosidases. Epoxide-based inhibitors are also an option (**42**), but since the natural substrates of these enzymes lack a substituent at C6 the attachment of a tag at this position will likely not be tolerated, so that the tag would need to be introduced at a less straightforward position. The synthesis of probes **41** and **42** requires the use of the enantiomers of the starting materials that were used in Chapter 5, i.e. oxazolidinone **50**

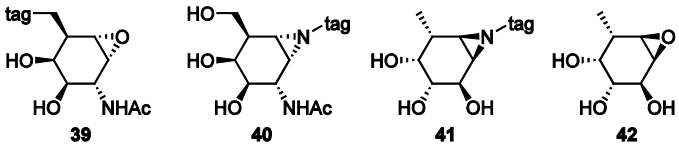

Figure 8.7. Putative inhibitors and ABPs to target α-*N*-acetylgalactosaminidase (**39**, **40**) and α-L-fucosidase (**41**, **42**).

Scheme 8.3 Proposed route of synthesis towards building blocks **48** and **54**

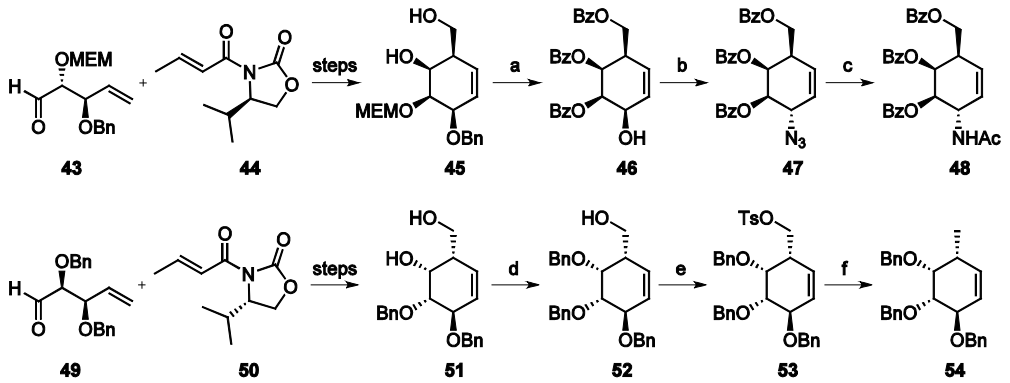

Reagents and conditions: a) *i*) $ZnBr_2$, DCM, *ii*) BzCl, pyridine, *iii*) BCl_3, DCM; b) *i*) Tf_2O, DMAP, pyridine, DCM, *ii*) $TMSN_3$, TBAF, THF; c) *i*) Ph_3P, H_2O, THF, *ii*) Ac_2O, pyridine; d) *i*) Ph_3CCl, Et_3N, DMAP, DMF, *ii*) BnBr, NaH, TBAI, DMF, *iii*) $BF_3.OEt_2$, MeOH/toluene; e) *p*TsCl, pyridine; f) $LiAlH_4$, THF.

derived from D-valine instead of L-valine and aldehyde **49**, which can be obtained from L-xylose instead of D-xylose (Scheme 8.3). Aldol condensation, removal of the Evans template and ring-closing metathesis should lead to compound **51**, after which several protective group manipulations may afford tribenzylated compound **52**. The free hydroxyl group can then be selectively activated by tosylation (**53**) and subsequently substituted with a hydride donor to provide **54**, which serves as a basis for the synthesis of the α-L-fucopyranose-configured inhibitors (**41**, **42**).

The absence of covalent interactions with a substrate in the catalytic mechanism of an enzyme of interest hampers the development of 'classic' ABPs that act via direct alkylation of the catalytically active amino acid residue. A possible solution is the use of suicide substrates, which are cleaved by the enzyme in the same manner as a natural substrate and consequently release a highly reactive species that can react with a nearby nucleophilic amino acid residue. This type of ABPs has for instance been applied to the activity-based profiling of a number of inverting glycosidases.[28-31] Another possibility to label enzymes that do not form a covalent enzyme-substrate intermediate is the use of affinity-based probes (A_fBPs), which also carry a (latent) reactive group but do not require activation by the catalytic machinery of the enzyme. Instead, these probes bind with high affinity to a specific site on the enzyme of interest and achieve labeling by non-specific covalent reaction of an amino acid residue with an electrophile or a photoreactive group in the A_fBP.[32,33] Frequently used photoaffinity labels include aryl azides, benzophenones and diazirines, which are all transformed into a highly reactive species upon activation by light of the appropriate

wavelength and can subsequently crosslink to proximal amino acid residues. A limitation of the use of photoaffinity probes is the propensity of the activated molecules to react with water, so that the success of labeling strongly depends on the speed of crosslinking as well as on the ability of the probes to tightly bind their target enzymes. Since these probes do not bind in a mechanism-based manner, they are strictly no 'true' ABPs. Nonetheless, A_fBPs can be valuable tools to examine the structural integrity of a target enzyme, for example if binding only occurs to an intact active site. Moreover, these probes can be useful to image the cellular localization and/or degradation of proteins and to identify the targets of drugs and inhibitors.[33]

A class of enzymes that does not employ a catalytic nucleophile in the active site is that of the α-ketoglutarate dependent oxygenases, also named 2-oxoglutarate (2-OG) oxygenases.[34-35] These enzymes catalyze the oxidation of C-H bonds in proteins, nucleotides, lipids and small molecules. This process results in hydroxylation of the substrates and can also lead to lysine demethylation. More than 60 different 2-OG oxygenases are known in humans and these are involved in a wide variety of cellular processes, including for example gene control, fatty acid metabolism and the response to hypoxia. The catalytic mechanism of 2-OG oxygenases involves an Fe(II) cofactor that is bound in the active site and in turn coordinates to the cosubstrate 2-OG (Figure 8.8A).[35] Binding of a substrate and O_2 results in oxidative decarboxylation of 2-OG with concomitant formation of CO_2 and oxidation of the substrate. Since the cofactor and cosubstrate binding sites are highly conserved, these sites

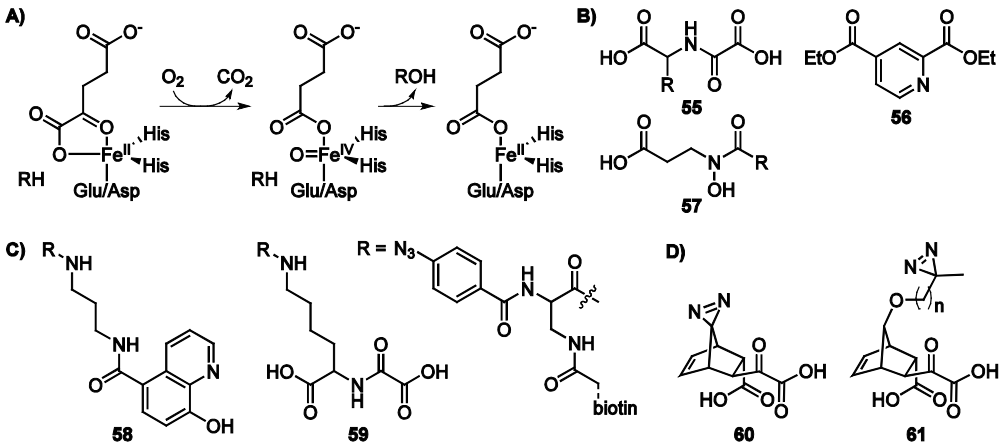

Figure 8.8. A) Catalytic mechanism of 2-OG oxygenases. B, C) Known 2-OG oxygenase inhibitors (**55**-**57**) and probes (**58**-**59**). D) Putative two-step photoaffinity probes for 2-OG oxygenases (**60**, **61**).

form attractive targets for the development of broad-spectrum inhibitors or A$_f$BPs. A number of reversible 2-OG oxygenase inhibitors has been reported in literature, including metal ions, substrate derivatives and analogues of 2-OG such as compounds **55**-**57** (Figure 8.8B), which act via coordination to Fe(II) and competition with binding of 2-OG in the active site.[36-40] The only probe that has been described so far for the labeling of this class of enzymes in complex biological samples is the hydroxyquinoline-based probe **58**, which is derivatized with a biotin tag and an aryl azide as a photoaffinity label (Figure 8.8C).[41] In the same study, the oxalylglycine derivative **59** proved to be only a very weak inhibitor of a small set of 2-OG oxygenases. Hence it appears that in this case the attachment of the relatively large photoreactive group and the biotin tag is not tolerated by the majority of 2-OG oxygenases, indicating that the modifications made to the 2-OG core should be sterically limited. The development of a two-step labeling probe may provide a means to enhance affinity by minimizing the steric bulk that is added to the probe scaffold and may also increase cell permeability. Therefore, two photoreactive 2-OG oxygenase probes were designed that are based on the structure of 2-OG integrated into a norbornene moiety for two-step labeling via tetrazine ligation (**60** and **61**, Figure 8.8D). A diazirine photoaffinity tag is included for crosslinking of the probe to target proteins and is added either directly onto the norbornene core (**60**) or via a short spacer (**61**).

Several strategies have been explored to synthesize A$_f$BPs **60** and **61**. It was reasoned that **60** can be derived from compound **62** (Figure 8.9) by conversion of the ketone into a diazirine moiety via a previously reported procedure[42] followed by deprotection and oxidation of the hydroxyl groups. Compound **61** can be obtained from **63** by functionalization of the hydroxyl group with a diazirine-containing spacer. These key building blocks may in turn be derived from for instance compound **64**, with the hydroxyl groups orthogonally protected to enable separate oxidation steps, or from compound **65** in which an α-keto acid or ester would need to be installed prior to introduction of the diazirine moiety. Initial efforts to synthesize compounds **62** and **63** started with the Et_2AlCl-catalyzed Diels-Alder reaction of silylated diene **67** and dienophile **66** (Scheme 8.4A), which gave a mixture of various diastereomers assumed to be the regio-isomers with the silyl group away

Figure 8.9. Key building blocks for the synthesis of A$_f$BPs **60** and **61**.

from the other substituents (**68a** and **68b** plus the corresponding endo/exo isomers). Next, cyclization of **68b** with bromine was attempted in order to enable silver nitrate-induced desilylation of **69** and intramolecular rearrangement as described in literature (see below).[43] However, the acetonide was not stable towards treatment with bromine. Other conditions for bromocyclization of **68b**, including hydrolysis of the ester with aqueous NaOH followed by reaction with *N*-bromosuccinimide, also failed to give the expected product (**69**).

Scheme 8.4 Synthetic routes towards building blocks **62** and **63**

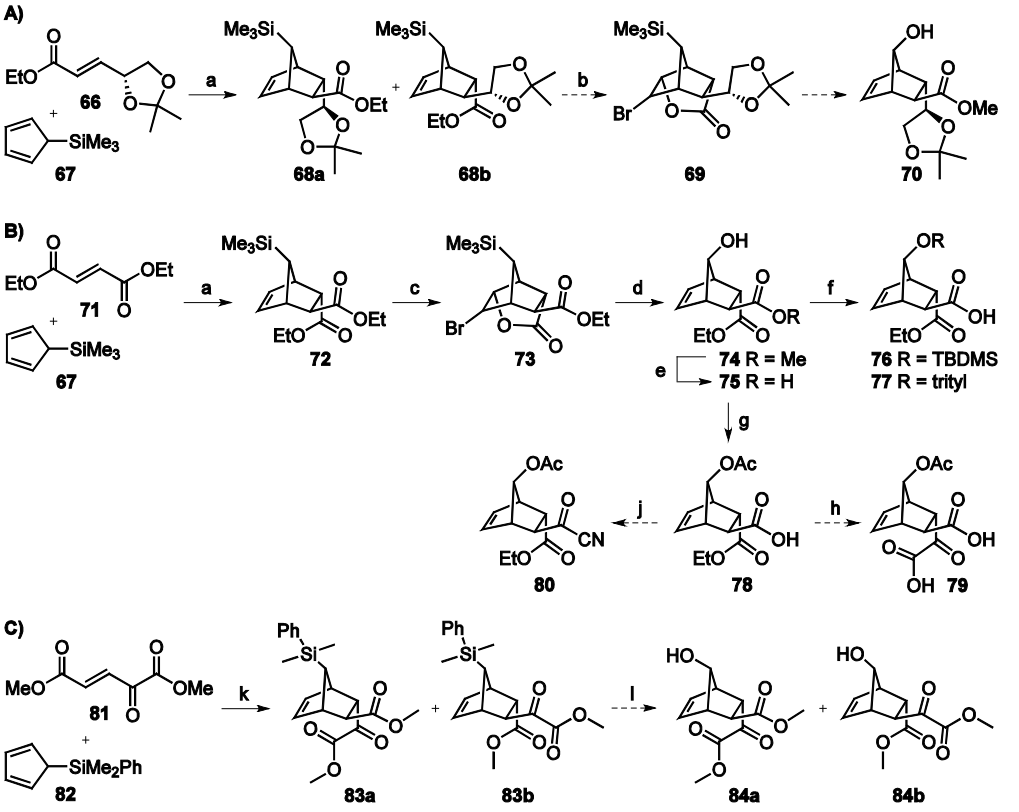

Reagents and conditions: a) Et_2AlCl, toluene, -78 °C → rt, overnight, **68** 86%, **72** quant.; b) Br_2, pyridine, DCM, 0 °C → rt, 6 hrs; c) Br_2, DCM, 0 °C → rt, 4.5 hrs, 83%; d) $AgNO_3$, MeOH, 70 °C, 3.5 hrs, 68%; e) Me_3SnOH, toluene, 100 °C, 5 hrs, 83%; f) TBDMS-Cl, imidazole, DMF, rt, overnight, **76** 28% or TrCl, DMAP, pyridine, 60 °C, 6 hrs, **77** <30%; g) Ac_2O, DMAP, pyridine, 40 °C, 1.5 hrs, 65%; h) *i*) LDA, diethyl oxalate, THF/TMEDA, rt, overnight, *ii*) HCl, 100 °C, 5 hrs; j) *i*) $(COCl)_2$, DMF, DCM, 0 °C → rt, 5 hrs, *ii*) CuCN, ACN, 90 °C, overnight; k) toluene, rt, 1 hr, 80%; l) KBr, NaOAc, AcOOH, AcOH, rt, 1.5 hrs or $Hg(OTFA)_2$, AcOK, AcOH, AcOOH, 0 °C → rt, 4.5 hrs.

Taking into account the difficulties that were associated with the use of **66** as a starting material, resulting in the formation of complicated mixtures of Diels-Alder products including undesired compound **68a**, a second strategy was designed starting from diethyl fumarate (**71**) (Scheme 8.4B). Diels-Alder reaction with silylated diene **67** gave Diels-Alder adduct **72** (plus its enantiomer) in quantitative yield. Treatment with bromine afforded compound **73**, which was then reacted with silver nitrate in methanol to induce desilylation with concomitant opening of the lactone and intramolecular rearrangement,[43] giving compound **74**. Attempts to increase the yield of this reaction by using a longer reaction time resulted in transesterification of the ethyl ester to a methyl ester. Selective hydrolysis of the methyl ester in **74** with Me_3SnOH gave **75**, after which efforts were undertaken to protect the hydroxyl group by silylation or tritylation. Both procedures, however, proceeded slowly and gave low yields of products **76** and **77**, respectively. Moreover, the main product isolated after reaction with TBDMS-Cl appeared to be disilylated (at the hydroxyl group and the carboxylic acid). Acetylation of **75**, on the other hand, successfully afforded compound **78**, which corresponds to one of the potential building blocks shown in Figure 8.9 (**65**). The introduction of an α-keto acid was then attempted by Claisen condensation with diethyl oxalate followed by decarboxylation under acidic conditions (**79**). An alternative procedure involved the formation of an acid chloride and reaction with copper cyanide to give acyl cyanide **80**, which can be hydrolyzed to an α-keto acid. Unfortunately, neither of these procedures proved to yield the desired products.

Therefore, a third route of synthesis was designed in which an α-keto ester is already present in the starting material (**81**) (Scheme 8.4C). Since this procedure does not involve the bromocyclization and rearrangement steps as in routes A and B, a cyclopentadienyl-silane reagent was synthesized in which one of the methyl substituents is replaced with a phenyl substituent (**82**) so that the silyl group can be oxidized to a hydroxyl group. Diels-Alder reaction of **81** and **82** gave a mixture of products (presumably **83a** and **83b** and their enantiomers), which were subjected to several Fleming oxidation procedures. However, compounds **84a** and **84b** could not be isolated. The use of differently substituted silane reagents and/or the use of different oxidation conditions may provide a means to obtain the hydroxylated products **84a** and **84b** (which correspond to building block **63**, Figure 8.9). Alternatively, synthetic route B also holds potential to synthesize the target compounds via selective reduction of the ethyl ester in **78** to an aldehyde, e.g. with DIBAL-H (which will likely also require the use of another hydroxyl protecting group). Stille reaction or Grignard reaction with a hydroxymethylated reagent may then provide an α,β-diol as a precursor of the α-ketoacid.

Another promising option to synthesize putative A_fBPs for 2-OG oxygenases is by making use of 5-methoxymethyl-cyclopenta-1,3-diene (**85**)[44] as a starting material (Scheme 8.5). This compound contains a methoxymethyl substituent that acts as a latent attachment site for the photoreactive group, since it can be mildly converted into a hydroxyl group during a later stage of synthesis. As depicted in Scheme 8.5, the use of cyclopentadiene **85** would lead to probes **88a** and **88b**, the latter of which is structurally similar to compound **61** (Figure 8.8D) except for the placement of the diazirine-containing linker: in probes **88a** and **88b** an extra carbon atom is added between the norbornene core and the alkoxy substituent. The proposed synthetic strategy commences with Diels-Alder reaction of cyclopentadiene **85** with compound **81** to provide adducts **86a** and **86b**, with the hydroxymethyl group away from the (α-keto) ester substituents.[45] In order to prevent isomerization of **85** to 1-methoxymethyl-1,3-cyclopentadiene, Et_2AlCl can be used as a catalyst to accelerate the Diels-Alder reaction and to allow the reaction to proceed at low temperatures (see also Schemes 8.4A and 8.4B). Subsequently, demethylation of the hydroxymethyl group may be achieved by reaction with BBr_3 in DCM and the methyl esters can be hydrolyzed under acidic conditions, procedures that have both been reported to proceed well in the presence of an α-keto moiety.[46-47] The resulting compounds **87a** and **87b** contain the 2-OG motif as well as a primary hydroxyl group for further functionalization with a photoaffinity label.

Scheme 8.5 Proposed strategy to synthesize A_fBPs **88a** and **88b**

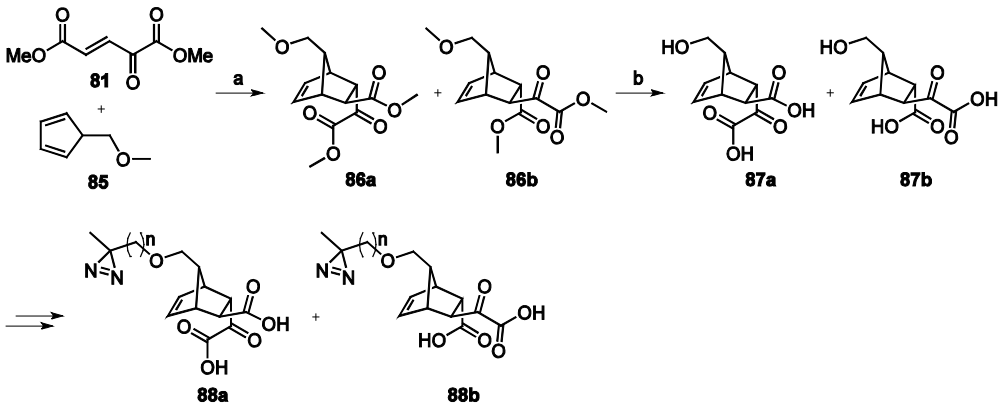

Reagents and conditions: a) Et_2AlCl, toluene, -78 °C → 0 °C; b) *i*) BBr_3, DCM, *ii*) HCl/H_2O.

Conclusion

The work described in this thesis provides novel approaches for the two-step profiling of enzymatic activity and for the simultaneous bioorthogonal labeling of multiple cellular targets, and presents novel probes for the activity-based profiling of two specific classes of enzymes, the retaining α- and β-galactosidases. Two-step labeling strategies are fundamental for enzymes that do not tolerate the attachment of a bulky reporter group onto an inhibitor scaffold. In addition, the application of ABPs for the imaging of enzymatic activity *in vivo* poses additional demands on the cell-permeability of the probes and may therefore necessitate the use of two-step ABPP strategies. At the same time there is an increasing interest in the use of tandem bioorthogonal ligation strategies that allow the monitoring of multiple targets simultaneously. Tandem labeling strategies such as those described in this thesis may provide valuable approaches to study multiple components involved in a particular biological processes or disease state at the same time.

Originally, the development of ABPs was mainly directed towards a few classes of hydrolytic enzymes with well-defined catalytic mechanisms, including serine hydrolases and cysteine/threonine proteases.[48] Nowadays, specific ABPs have also been developed for a variety of other enzyme classes including protein tyrosine phosphatases,[49-51] monooxygenases,[52] monoamine oxidases,[53] and carbohydrate processing enzymes.[54] For those enzymes that do not make use of an active site nucleophile in their catalytic mechanism or that are not susceptible to targeting by ABPs for another reason, the use of A_fBPs can provide a valuable alternative. Such probes have for instance proven successful for the labeling of metalloproteases, phosphatases, histone deacetylases, 2OG oxygenases and kinases.[32] Although A_fBPs do not label their target proteins in an activity-based manner, the careful design of a probe such that binding is dependent on the integrity of the active site may provide a means to monitor the functional state of an enzyme. As the field of ABPP is gradually moving towards the targeting of enzyme classes with different and sometimes poorly understood catalytic mechanisms, tight substrate specificity and/or low expression levels, continuing efforts are being made to generate novel strategies for the activity-based profiling of such difficult to target enzymes. This thesis presents a number of strategies that open up new opportunities for future research directions, both for the activity-based profiling of new enzyme classes as well as for the bioorthogonal labeling of enzymatic activity and other biomolecules.

Experimental procedures

A. Synthesis

General

All reagents were commercial grade and were used as received unless stated otherwise. MeOH was obtained from Biosolve. Toluene, EtOAc and PetEt (Riedel-de Haën) used for column chromatography were of technical grade and distilled before use. DCE, DCM, DMF, and THF (Biosolve) were of analytical grade and when used under anhydrous conditions stored over flame-dried 4 Å molecular sieves. Reactions were monitored by TLC-analysis using DC-alufolien (Merck, Kieselgel60, F254) with detection by UV-absorption (254/366 nm), spraying with a solution of 20% H_2SO_4 in EtOH or a solution of $(NH_4)_6Mo_7O_{24}{\cdot}4H_2O$ (25 g/L) and $(NH_4)_4Ce(SO_4)_4{\cdot}2H_2O$ (10 g/L) in 10% aqueous sulfuric acid followed by charring at ~150 °C or by spraying with an aqueous solution of $KMnO_4$ (7%) and K_2CO_3 (2%). Column chromatography was performed on silica gel (Screening Devices BV, 0.040 - 0.063 mm, 60 Å). LC/MS analysis was performed on an LCQ Adventage Max (Thermo Finnigan) ion-trap spectrometer (ESI+) coupled to a Surveyor HPLC system (Thermo Finnigan) equipped with a C18 column (Gemini, 4.6 mm x 50 mm, 5µm particle size, Phenomenex). The applied buffers were A: H_2O, B: ACN and C: 1 % aqueous TFA. Reported gradients represent the percentage of buffer B in buffer A with 10% buffer C. HRMS analysis was performed on an LTQ Orbitrap (Thermo Finnigan) mass spectrometer equipped with an electronspray ion source in positive mode (source voltage 3.5 kV, sheath gas flow 10 mL min−1, capillary temperature 250 °C) with resolution R = 60000 at m/z 400 (mass range m/z = 150 - 2000) and dioctylphtalate (m/z = 391.28428) as a "lock mass". The high resolution mass spectrometer was calibrated prior to measurements with a calibration mixture (Thermo Finnigan). ^{1}H- and ^{13}C-APT-NMR spectra were recorded on a Brüker AV-400 (400/100MHz) instrument. Chemical shifts are given in ppm (δ) relative to the solvent peak or to tetramethylsilane as internal standard. Coupling constants (*J*) are given in Hz. All presented ^{13}C-APT spectra are proton decoupled. Peak assignments are based on 2D ^{1}H-COSY and ^{13}C-HSQC NMR experiments.

***N*-(Boc-6-aminohexanoyl)-4-(6-(2-pyrimidinyl)-1,2,4,5-tetrazin-3-yl)benzylamine (13)**

Boc-protected tetrazine **12** (0.50 mmol, 0.18 g) was treated with TFA/DCM (1/1, v/v) for 15 min and then concentrated *in vacuo* in the presence of toluene. The residue was dissolved in DCE/DMF under argon atmosphere and DiPEA (1.0 mmol, 0.17 mL, 2.0 eq.) and Boc-6-Ahx-OSu (0.50 mmol, 0.16 g, 1.0 eq.) were added. The reaction mixture was stirred at room temperature overnight before being concentrated *in vacuo*. The crude product was purified by column chromatography (DCM → 2% MeOH in DCM), followed by recrystallization from DCM/n-hexane to yield Boc-Ahx-tetrazine **13** as purple crystals (0.21 g, 0.44 mmol, 88%).^{1}H NMR (400 MHz, $CDCl_3$): δ (ppm) 9.15 (d, *J* = 4.9 Hz, 2H), 8.70 (dd, *J* = 8.3, 1.3 Hz, 2H), 7.61 (t, *J* = 4.9 Hz, 1H), 7.55 (d, *J* = 8.1 Hz, 2H), 6.19 (d, *J* = 7.4 Hz, 1H), 4.61-4.59 (m, 3H), 3.15-3.11 (m, 2H), 2.31 (t, *J* = 7.5 Hz, 2H), 1.79-1.71 (m, 2H), 1.55-1.48 (m, 2H), 1.44 (s, 9H), 1.43-1.35 (m, 2H). ^{13}C NMR: (100 MHz, $CDCl_3$): δ (ppm) 172.95, 164.28, 163.08, 159.57, 158.41, 156.04, 144.43, 130.38, 129.15, 128.57, 122.50, 79.11, 43.23, 40.30, 36.49, 29.80, 28.43, 26.40, 25.25. LC/MS analysis: R_t 6.9 min (linear gradient 10 → 90% B in 15 min), m/z 479.0 $[M+H]^+$, 379.2 $[M-Boc+H]^+$, 957.2 $[2M+H]^+$. HRMS: calcd. for $[C_{24}H_{31}N_8O_3]^+$ 479.25136, found 479.25184; calcd. for $[C_{24}H_{30}N_8O_3Na]^+$ 501.23331, found 501.23367.

***N*-Boc-2-(2-(2-amino-*N*-(1-heptyn-7-oyl)ethoxy)ethoxy)ethylamine (15)**

Boc-protected compound **14**[14] (1.9 mmol, 0.53 g) was dissolved in THF and triphenylphosphine (2.3 mmol, 0.60 g, 1.2 eq.) was added. The reaction mixture was stirred overnight at room temperature, before a few drops of H_2O were added. After stirring for an additional 2 hrs, toluene was added and the mixture was extracted with H_2O. The aqueous layer was washed with toluene and the combined organic layers were again extracted with H_2O until no more product was detected in the organic phase. The combined aqueous layers were concentrated *in vacuo* to give

the monoprotected PEG-diamine. A solution of 6-heptynoic acid (1.9 mmol, 0.24 mL, 1.0 eq.) in toluene was put under argon atmosphere, after which oxalyl chloride (2.9 mmol, 0.25 mL, 1.5 eq.) and one drop of DMF were added. After stirring for 3 hours at room temperature, the mixture was concentrated *in vacuo* and coevaporated with toluene (3x). The acyl chloride was then redissolved in DCE under argon atmosphere, neutralized with DiPEA (2.9 mmol, 0.50 mL, 1.5 eq.) and added to the crude PEG-amine. The mixture was stirred overnight at room temperature, quenched with MeOH and concentrated *in vacuo*. Purification by column chromatography (30% EtOAc in PetEt → EtOAc) yielded alkyne-functionalized PEG spacer **15**, contaminated with some triphenylphosphine oxide (0.37 g, ~1.0 mmol, 54% over two steps). This product was used without further purification for the next step. LC/MS analysis: R_t 6.7 min (linear gradient 10 → 90% B in 15 min), m/z 356.9 $[M+H]^+$, 257.2 $[M\text{-}Boc+H]^+$, 379.1 $[M+Na]^+$. HRMS: calcd. for $[C_{18}H_{33}N_2O_5]^+$ 357.23840, found357.23855; calcd. for $[C_{18}H_{32}N_2O_5Na]^+$ 379.22034, found 379.22042.

***N*-biotin-2-(2-(2-amino-*N*-(1-heptyn-7-oyl)ethoxy)ethoxy)ethylamine (16)**

Boc-protected compound **15** (0.60 mmol, 0.21 g) was treated with TFA/DCM (1/1, v/v) for 20 min and then concentrated *in vacuo* in the presence of toluene. The residue was dissolved in DCE/DMF (1/1, v/v) under argon atmosphere and DiPEA (1.2 mmol, 0.21 mL, 2.0 eq.) and biotin-OSu (0.60 mmol, 0.20 g, 1.0 eq.) were added. The reaction mixture was stirred at room temperature overnight before being concentrated *in vacuo*. The crude product was purified by column chromatography (DCM → 10% MeOH in DCM). To remove final impurities, the product was redissolved in DCM and washed with H_2O (2x), after which the combined aqueous layers were extracted with DCM/MeOH (9/1, v/v) until no more product was detected in the aqueous phase. The combined organic layers were dried over $MgSO_4$, filtered and evaporated *in vacuo* to give alkyne-functionalized and biotin-tagged PEG spacer **16** (0.25 g, 0.52 mmol, 87%). ^{1}H NMR (400 MHz, MeOD): δ (ppm) 4.52 (ddd, *J* = 7.9, 5.0, 1.0 Hz, 1H), 4.33 (dd, *J* = 7.9, 4.5 Hz, 1H), 3.65 (s, 4H), 3.57 (dt, *J* = 5.6, 1.1 Hz, 4H), 3.39 (t, *J* = 5.5 Hz, 4H), 3.23 (ddd, *J* = 8.8, 5.9, 4.5 Hz, 1H), 2.95 (dd, *J* = 12.8, 5.0 Hz, 1H), 2.73 (d, *J* = 12.7 Hz, 1H), 2.27-2.18 (m, 6H), 1.84-1.37 (m, 11H). ^{13}C NMR (100 MHz, MeOD): δ (ppm) 174.75, 174.61, 164.70, 83.28, 69.90, 69.22, 68.40, 61.97, 60.23, 55.60, 39.65, 38.89, 35.34, 35.07, 28.37, 28.10, 27.80, 25.44, 24.70, 17.40. LC/MS analysis: R_t 5.0 min (linear gradient 10 → 90% B in 15 min), m/z 483.3 $[M+H]^+$, 965.1 $[2M+H]^+$. HRMS: calcd. for $[C_{23}H_{39}N_4O_5S]^+$ 483.26357, found 483.26329; calcd. for $[C_{23}H_{38}N_4O_5SNa]^+$ 505.24551, found 505.24477.

Biotinylated levulinoyl linker 17

Azide-modified levulinoyl derivative **18**[13] (0.50 mmol, 0.24 g) and biotin-tagged alkyne **16** (0.50 mmol, 0.24 g, 1.0 eq.) were dissolved in *t*BuOH/toluene/H_2O (2/2/1, v/v/v) (10 mL). Copper(II)sulphate pentahydrate (50 µmol, 1 mL 50 mM in H_2O, 0.1 eq.) and sodium ascorbate (75 µmol, 1 mL 75 mM in H_2O, 0.15 eq.) were added, followed by a few drops of DMF until the mixture became clear. The reaction mixture was heated to 80 °C and stirred overnight, before being concentrated *in vacuo*. The product was purified by column chromatography (DCM/acetone/MeOH, 8/2/0 (v/v/v) → 6.5/2/1.5 (v/v/v)), redissolved in DCM and washed with H_2O, upon which the biotinylated levulinoyl linker **17** precipitated from the organic phase as white crystals (0.29 g, 0.30 mmol, 60%). ^{1}H NMR (400 MHz,$CDCl_3$): δ (ppm) 7.34 (s, 1H), 6.96 (s, 2H), 6.89 (bs, 1H), 6.71 (bs, 1H), 6.63 (bs, 1H), 5.86 (bs, 1H), 4.49 (d, *J* = 7.0 Hz, 1H), 4.33-4.31 (m, 3H), 3.64-3.53 (m, 8H), 3.44-3.42 (m, 4H), 3.14-3.13 (m, 1H), 2.97-2.62 (m, 12H), 2.55-2.50 (m, 4H), 2.24-2.15 (m, 6H), 1.81-1.60 (m, 8H), 1.43 (s, 11H), 1.17 (d, *J* = 6.9 Hz, 12H). ^{13}C NMR (100 MHz,$CDCl_3$): δ (ppm) 207.22, 173.46, 173.28, 172.34, 171.69, 164.18, 143.74, 140.12, 138.76, 123.81, 121.11, 80.31, 70.07, 70.01, 69.94, 69.85, 63.85, 61.80, 60.27, 55.63, 48.98, 40.45, 39.16, 39.11, 38.81, 37.06, 37.00, 36.06, 35.91, 31.00, 29.68, 28.81, 28.20, 28.08, 27.72, 27.43, 25.57, 25.22, 25.12, 24.24. LC/MS analysis: R_t 8.8 min (linear gradient 10 → 90% B in 15 min), m/z 956.5 $[M+H]^+$. HRMS: calcd. for $[C_{49}H_{78}N_7O_{10}S]^+$ 956.55254, found 956.55331; calcd. for $[C_{49}H_{77}N_7O_{10}SNa]^+$ 978.53448, found 978.53480.

Biotin-levulinoyl-tetrazine 11

*t*Bu-protected compound **17** (50 µmol, 48 mg) was treated with TFA/DCM (1/1, v/v) for 30 min and then concentrated *in vacuo* in the presence of toluene. Boc-protected tetrazine **13** (0.10 mmol, 48 mg, 2.0 eq.) was also treated with TFA/DCM (1/1, v/v) for 20 min and then concentrated *in vacuo* in the presence of toluene. The residue was dissolved in DCE/DMF under argon atmosphere, added to the deprotected levulinoyl acid and the mixture was neutralized with DiPEA (0.2 mmol,33 µL, 4.0 eq.). After addition of HCTU (0.15 mmol, 62 mg, 3.0 eq.), the reaction mixture was stirred at room temperature overnight. The mixture was then washed with H_2O, the aqueous layers was extracted with DCM (2x) and the combined organic layers were dried over $MgSO_4$, filtered and concentrated *in vacuo*. Purification by column chromatography (DCM → 10% MeOH in DCM) followed by recrystallization from DCM/PetEt yielded biotin-levulinoyl-tetrazine **11** as a purple powder (44 mg,35 µmol, 70%).^{1}H NMR (400 MHz, $CDCl_3$): δ (ppm) 9.12 (d, *J* = 4.9 Hz, 2H), 8.64 (d, *J* = 8.0 Hz, 2H), 7.60 (t, *J* = 4.9 Hz, 1H), 7.52 (d, *J* = 8.1 Hz, 2H), 7.32 (s, 1H), 7.04-6.92 (m, 4H), 6.89 (t, *J* = 5.6 Hz, 1H), 6.45 (s, 1H), 6.20 (t, *J* = 5.8 Hz, 1H), 5.77 (s, 1H), 4.55 (d, *J* = 5.9 Hz, 2H), 4.46 (dd, *J* = 7.9, 4.8 Hz, 1H), 4.32-4.26 (m, 3H), 3.57-3.52 (m, 8H), 3.41-3.40 (m, 4H), 3.20 (q, *J* = 6.7 Hz, 2H), 3.11 (d, *J* = 4.7 Hz, 1H), 2.98-2.56 (m, 12H), 2.52-2.44 (m, 4H), 2.28 (t, *J* = 7.5 Hz, 2H), 2.21-2.13 (m, 6H), 1.70-1.65 (m, 10H), 1.52-1.28 (m, 6H), 1.14 (d, *J* = 6.9 Hz, 12H). ^{13}C NMR (100 MHz,$CDCl_3$): δ (ppm) 207.35, 173.52, 173.39, 173.35, 172.43, 171.84, 164.29, 164.01, 163.02, 159.47, 158.40, 147.81, 144.82, 143.77, 140.23, 139.06, 130.15, 129.01, 128.49, 123.80, 122.57, 121.23, 70.06, 70.01, 69.91, 69.84, 61.75, 60.20, 55.58, 48.92, 43.09, 40.45, 39.17, 39.15, 39.10, 38.77, 38.47, 36.92, 36.20, 35.98, 35.84, 31.75, 29.68, 29.14, 28.74, 28.14, 28.03, 27.77, 27.42, 26.39, 25.55, 25.11, 25.09, 24.22. LC/MS analysis: R_t 6.9 min (linear gradient 10 → 90% B in 15 min), m/z 1260.8 $[M+H]^+$, 631.1 $[M+H]^{2+}$. HRMS: calcd. for $[C_{64}H_{90}N_{15}O_{10}S]^+$ 1260.67103, found 1260.67164; calcd. for $[C_{64}H_{89}N_{15}O_{10}SNa]^+$ 1282.65298, found 1282.65323.

Ethyl 3-(2,2-dimethyl-1,3-dioxolan-4-yl)-7-(trimethylsilyl)bicyclo[2.2.1]hept-5-ene-2-carboxylate (68)

Compound **66** (5.0 mmol, 0.98 mL) was dissolved in toluene and cooled to -78 °C under argon atmosphere, before Et_2AlCl (5.0 mmol, 2.8 mL 1.8 M in toluene, 1.0 eq.) was added. After stirring for 15 min at -78 °C, cyclopenta-2,4-dien-1-yltrimethylsilane (**67**) (10 mmol, 1.7 mL, 2.0 eq.) was added dropwise and the reaction mixture was stirred overnight while allowing the temperature to slowly rise to room temperature. The reaction was then quenched with saturated aqueous $NaHCO_3$, the aqueous layer was extracted with Et_2O (2x) and the combined organic layers were dried over $MgSO_4$, filtered and concentrated *in vacuo*. Purification by column chromatography (PetEt → 1.5% acetone in PetEt) gave Diels-Alder adduct **68** in two separate fractions with mixtures of 3 and 2 diastereomers, respectively (1st fraction: 1.4 g, 4.1 mmol, 81%; 2nd fraction: 78 mg, 0.23 mmol, 5%). ^{1}H NMR (400 MHz, $CDCl_3$) fraction 1 (3 diastereomers): δ (ppm) 6.25-6.16 (m, 1Ha+1Hb), 6.16-6.08 (m, 2Hc), 5.93 (dd, *J* = 5.6, 2.7 Hz, 1Ha), 5.91-5.87 (m, 1Hb), 4.20-3.87 (m, 4Ha+4Hb+3Hc), 3.79-3.60 (m, 1Ha+1Hb+1Hc), 3.47 (dtd, *J* = 10.6, 5.6, 2.5 Hz, 1Hc), 3.24 (bs, 1Hb), 3.22-3.17 (m, 1Ha), 3.18-3.10 (m, 1Hc), 3.08 (bs, 1Hc), 3.06-2.99 (m, 1Ha), 2.88 (q, *J* = 3.3, 2.5 Hz, 1Hb), 2.56 (d, *J* = 3.0 Hz, 1Hb), 2.45-2.35 (m, 1Ha+1Hc), 2.02 (ddd, *J* = 7.1, 4.5, 2.1 Hz, 1Hb), 1.97-1.88 (m, 1Ha), 1.68 (dd, *J* = 5.0, 2.0 Hz, 1Hc), 1.44 (s, 3Ha+3Hb+3Hc), 1.40 (s, 3Ha+3Hb+3Hc), 1.36 (m, 1Ha+1Hb+1Hc), 1.35-1.19 (m, 3Ha+3Hb+3Hc), -0.02--0.16 (m, 9Ha+9Hb+ 9Hc). ^{1}H NMR (400 MHz, $CDCl_3$) fraction 2 (2 diastereomers): δ (ppm) 6.20 (ddd, *J* = 8.1, 5.5, 3.2 Hz, 1Ha+1Hb), 5.97-5.92 (m, 1Ha), 5.90 (dd, *J* = 5.6, 2.8 Hz, 1Hb), 4.14-4.04 (m, 3Ha+3Hb), 4.04-3.93 (m, 1Ha+1Hb), 3.80-3.68 (m, 1Ha+1Hb), 3.28-3.23 (m, 1Hb), 3.21 (tdq, *J* = 2.7, 1.8, 1.0 Hz, 1Ha), 3.02 (t, *J* = 2.1 Hz, 1Ha), 2.89 (t, *J* = 4.0 Hz, 1Hb), 2.60-2.55 (m, 1Hb), 2.41 (dd, *J* = 4.7, 3.5 Hz, 1Ha), 2.03 (dd, *J* = 7.9, 4.4 Hz, 1Hb), 1.91 (dd, *J* = 8.9, 4.8 Hz, 1Ha), 1.44 (s, 3Ha+3Hb), 1.39 (bs, 3Ha+4Hb), 1.36-1.33 (m, 1Ha), 1.24 (t, *J* = 7.1 Hz, 3Ha+3Hb), -0.04--0.09 (m, 9Ha+9Hb). ^{13}C NMR (100 MHz,$CDCl_3$) fraction 1: δ (ppm) 175.40, 175.06, 173.58, 137.92, 137.64, 136.01, 135.35, 133.44, 133.41, 109.05, 108.94, 108.81, 79.64, 79.44, 79.21, 69.03, 68.70, 68.63, 60.55, 60.35, 60.14, 50.72, 50.46, 49.82, 49.73, 49.20, 48.99, 48.95, 48.72, 48.66, 48.60, 48.45, 48.22, 48.09, 47.53, 47.50,

47.19, 26.96, 26.79, 26.72, 25.94, 25.88, 25.72, 14.27, 14.23, 14.20, -0.18, -0.23. ^{13}C NMR (100 MHz,$CDCl_3$) fraction 2: δ (ppm) 173.96, 173.63, 144.61, 137.94, 133.45, 122.42, 109.09, 108.97, 79.66, 79.46, 69.04, 68.64, 60.39, 60.17, 49.84, 49.23, 49.01, 48.73, 48.67, 48.62, 48.47, 48.12, 47.55, 47.52, 26.80, 26.73, 25.95, 25.73, 14.28, 14.24, -0.18, -0.23. LC/MS analysis: fraction 1: R_t 7.7, 7.8 and 8.3 min (linear gradient 10 → 90% B in 15 min), m/z 338.9 $[M+H]^+$, 299.0 [M-acetonide+H]$^+$; fraction 2: R_t 7.8 and 8.0 min (linear gradient 10 → 90% B in 15 min), m/z 338.8 $[M+H]^+$, 299.0 [M-acetonide+H]$^+$.

(1*R*,2*S*,3*S*,4*S*,7*R*)-diethyl 7-(trimethylsilyl)bicyclo[2.2.1]hept-5-ene-2,3-dicarboxylate and (1*R*,2*R*,3*R*,4*S*,7*R*)-diethyl 7-(trimethylsilyl)bicyclo[2.2.1]hept-5-ene-2,3-dicarboxylate (72)

Diethyl fumarate (**71**) (10 mmol, 1.7 mL) was dissolved in toluene (10 mL) and cooled to -78 °C under argon atmosphere, before Et_2AlCl (10 mmol, 5.6 mL 1.8 M in toluene, 1.0 eq.) was added. After stirring for 15 min at -78 °C, cyclopenta-2,4-dien-1-yltrimethylsilane (**67**) (20 mmol, 3.3 mL, 2.0 eq.) was added dropwise and the reaction mixture was stirred overnight while allowing the temperature to slowly rise to room temperature. The reaction was then quenched with saturated aqueous $NaHCO_3$, the aqueous layer was extracted with Et_2O (3x) and the combined organic layers were dried over $MgSO_4$, filtered and concentrated *in vacuo*. Purification by column chromatography (PetEt → 2% EtOAc in PetEt) gave Diels-Alder adduct **72** (3.1 g, 10 mmol, quant.). ^{1}H NMR (400 MHz, $CDCl_3$): δ (ppm) 6.16 (dd, *J* = 5.7, 3.1 Hz, 1H), 5.94 (dd, *J* = 5.6, 2.8 Hz, 1H), 4.23-4.09 (m, 2H), 4.09-4.03 (m, 2H), 3.34 (t, *J* = 3.9 Hz, 1H), 3.31-3.26 (m, 1H), 3.13 (d, *J* = 3.1 Hz, 1H), 2.71-2.66 (m, 1H), 1.32-1.14 (m, 7H), -0.07--0.17 (m, 9H). ^{13}C NMR (100 MHz,$CDCl_3$): δ (ppm) 174.32, 172.93, 136.95, 134.32, 60.54, 60.26, 50.61, 49.95, 49.17, 48.89, 48.45, 14.10, -0.50.

(1*S*,2*S*,3*S*,7*S*,8*S*,9*S*)-ethyl 2-bromo-5-oxo-8-(trimethylsilyl)-4-oxatricyclo[4.2.1.03,7]nonane-9-carboxylate and (1*R*,2*R*,3*R*,7*R*,8*R*,9*R*)-ethyl 2-bromo-5-oxo-8-(trimethylsilyl)-4-oxatricyclo[4.2.1.03,7]nonane-9-carboxylate (73)

Compound **72** (25 mmol, 7.8 g) was dissolved in DCM under argon atmosphere and cooled to 0 °C. Bromine (50 mmol, 2.6 mL, 2.0 eq.) was added and the reaction mixture was stirred at 0 °C for 40 min and then at room temperature for 4 hrs, before being quenched with saturated aqueous $NaHCO_3$. The aqueous layer was extracted with DCM (3x) and the combined organic layers were dried over $MgSO_4$, filtered and concentrated *in vacuo*. Purification by column chromatography (PetEt → 8% EtOAc in PetEt) gave bromo-functionalized compound **73** (7.5 g, 21 mmol, 83%). ^{1}H NMR (400 MHz, $CDCl_3$): δ (ppm) 4.92 (d, *J* = 4.7 Hz, 1H), 4.26-4.11 (m, 2H), 3.78 (d, *J* = 2.1 Hz, 1H), 3.27 (t, *J* = 4.6 Hz, 1H), 3.11-3.01 (m, 2H), 2.79 (d, *J* = 2.1 Hz, 1H), 1.35-1.30 (m, 1H), 1.26 (t, *J* = 7.2 Hz, 3H), 0.19 (s, 9H). ^{13}C NMR (100 MHz,$CDCl_3$): δ (ppm) 177.34, 170.38, 88.02, 61.86, 53.12, 52.50, 52.32, 49.04, 42.45, 36.98, 14.17, 0.32.

(1*R*,2*S*,3*S*,4*S*,7*R*)-2-ethyl 3-methyl 7-(hydroxy)bicyclo[2.2.1]hept-5-ene-2,3-dicarboxylate and (1*R*,2*R*,3*R*,4*S*,7*S*)-2-methyl 3-ethyl 7-(hydroxy)bicyclo[2.2.1]hept-5-ene-2,3-dicarboxylate (74)

To a solution of bromo-functionalized compound **73** (1.0 mmol, 0.36 g) in MeOH (10 mL) under argon atmosphere was added $AgNO_3$ (5.0 mmol, 0.84 g, 5.0 eq.) and the reaction mixture was stirred at 70 °C for 3.5 hrs. The mixture was then filtered, concentrated *in vacuo* and redissolved in EtOAc. After addition of H_2O, the layers were separated and the aqueous layer was extracted with EtOAc (3x). The combined organic layers were dried over $MgSO_4$, filtered and concentrated *in vacuo*. The crude product was purified by column chromatography (10% EtOAc in PetEt → 50% EtOAc in PetEt) to yield alcohol **74** (0.16 g, 0.68 mmol, 68%). ^{1}H NMR (400 MHz, $CDCl_3$): δ (ppm) 6.23 (dt, *J* = 4.5, 2.3 Hz, 1H), 5.95 (dd, *J* = 6.3, 3.2 Hz, 1H), 4.15 (qd, *J* = 7.1, 2.4 Hz, 2H), 4.03 (bs, 1H), 3.81-3.72 (m, 4H), 3.58 (t, *J* = 4.5 Hz, 1H), 3.13 (td, *J* = 3.4, 1.6 Hz, 1H), 3.11-3.03 (m, 1H), 2.82 (d, *J* = 5.0 Hz, 1H), 1.27 (t, *J* = 7.1 Hz, 3H). ^{13}C NMR (100 MHz,$CDCl_3$): δ (ppm) 175.87, 173.81, 135.63, 132.73, 83.80, 60.82, 52.27, 50.38, 49.79, 45.89, 45.51, 14.08. LC/MS analysis: R_t 5.7 min (linear gradient 10 → 90% B in 15 min), m/z 240.9 $[M+H]^+$.

(1*R*,2*S*,3*S*,4*S*,7*R*)-2-ethyl 7-(hydroxy)bicyclo[2.2.1]hept-5-ene-2-carboxylate-3-carboxylic acid and (1*R*,2*R*,3*R*,4*S*, 7*S*)-3-ethyl 7-(hydroxy)bicyclo[2.2.1]hept-5-ene-3-carboxylate-2-carboxylic acid (75)

Diester **74** (1.2 mmol, 0.29 g) and Me_3SnOH (1.4 mmol, 0.46 g, 1.2 eq.) were dissolved in toluene and stirred at 100 °C for 5 hrs. The mixture was then cooled to room temperature, washed with 1 M HCl and the aqueous layer was extracted with EtOAc (6x). The combined organic layers were dried over $MgSO_4$, filtered and concentrated *in vacuo*. The crude product was purified by column chromatography (PetEt → 50% EtOAc in PetEt) to yield monoester **75** (0.23 g, 1.0 mmol, 83%). ^{1}H NMR (400 MHz, $CDCl_3$): δ (ppm) 7.44 (bs, 1H), 6.21-6.10 (m, 1H), 5.94-5.86 (m, 1H), 4.09 (q, *J* = 7.2 Hz, 2H), 3.74 (t, *J* = 1.9 Hz, 1H), 3.59 (t, *J* = 4.3 Hz, 1H), 3.10 (dd, *J* = 3.7, 1.8 Hz, 1H), 3.03 (td, *J* = 3.6, 1.8 Hz, 1H), 2.78 (d, *J* = 4.7 Hz, 1H), 1.21 (t, *J* = 7.2 Hz, 3H). ^{13}C NMR (100 MHz,$CDCl_3$): δ (ppm) 179.30, 174.00, 135.63, 132.97, 83.61, 60.96, 50.06, 50.00, 45.98, 45.47, 14.20.

(1*R*,2*S*,3*S*,4*S*,7*R*)-2-ethyl 7-((tert-butyl-dimethyl-silyl)hydroxy)bicyclo[2.2.1]hept-5-ene-2-carboxylate-3-carboxylic acid and (1*R*,2*R*,3*R*,4*S*,7*S*)-3-ethyl 7-((tert-butyl-dimethyl-silyl)hydroxy)bicyclo[2.2.1]hept-5-ene-3-carboxylate-2-carboxylic acid (76)

Compound **75** (0.53 mmol, 0.12 g) was dissolved in DMF under argon atmosphere, after which imidazole (0.80 mmol, 54 mg, 1.5 eq.) and TBDMS-Cl (0.66 mmol, 99 mg, 1.3 eq.) were added. The reaction mixture was stirred at room temperature overnight, diluted with H_2O and extracted with EtOAc (3x). The combined organic layers were dried over $MgSO_4$, filtered and concentrated *in vacuo*. Purification by column chromatography (PetEt → 2% EtOAc in PetEt → 50% EtOAc in PetEt) gave monosilylated compound **76** (50 mg, 0.15 mmol, 28%) as well as disilylated byproduct (0.10 g, 0.22 mmol, 42%). ^{1}H NMR (400 MHz, $CDCl_3$) **76**: δ (ppm) 6.18 (ddd, *J* = 6.3, 3.6, 1.1 Hz, 1H), 5.92 (ddd, *J* = 6.3, 3.2, 1.0 Hz, 1H), 4.18-4.03 (m, 2H), 3.73-3.64 (m, 2H), 3.12 (dd, *J* = 3.6, 1.8 Hz, 1H), 2.93 (td, *J* = 3.5, 1.6 Hz, 1H), 2.80 (d, *J* = 4.4 Hz, 1H), 1.24 (t, *J* = 7.1 Hz, 3H), 0.83 (s, 9H), 0.04 (s, 3H), 0.01 (s, 3H). ^{13}C NMR (100 MHz, $CDCl_3$) **76**: δ (ppm) 179.54, 174.04, 135.29, 132.87, 84.30, 60.62, 50.72, 50.55, 46.31, 44.89, 25.50, 14.26, -5.11, -5.30. ^{1}H NMR (400 MHz, $CDCl_3$) disilylated product: δ (ppm) 6.23-6.15 (m, 1H), 5.88-5.83 (m, 1H), 4.09 (dd, *J* = 7.1, 2.7 Hz, 2H), 3.67-3.57 (m, 2H), 3.03 (dd, *J* = 3.7, 1.8 Hz, 1H), 2.88 (dt, *J* = 3.8, 1.8 Hz, 1H), 2.73 (d, *J* = 5.1 Hz, 1H), 1.21 (t, *J* = 7.1 Hz, 3H), 0.89 (s, 9H), 0.84 (s, 9H), 0.24 (s, 3H), 0.23 (s, 3H), 0.03 (s, 3H), 0.01 (s, 3H). ^{13}C NMR (100 MHz, $CDCl_3$) disilylated product: δ (ppm) 174.33, 172.90, 135.85, 132.21, 84.52, 60.42, 50.99, 50.11, 48.10, 44.72, 25.80, 25.44, 18.08, 17.53, 14.26, -4.69, -4.80, -5.00, -5.02. LC/MS analysis: **76**: R_t 10 min (linear gradient 10 → 90% B in 15 min), m/z 340.9 $[M+H]^+$; disilylated product: R_t 14 min (linear gradient 10 → 90% B in 15 min), m/z 455.0 $[M+H]^+$.

(1*R*,2*S*,3*S*,4*S*,7*R*)-2-ethyl 7-((trityl)hydroxy)bicyclo[2.2.1]hept-5-ene-2-carboxylate-3-carboxylic acid and (1*R*,2*R*, 3*R*,4*S*,7*S*)-3-ethyl 7-((trityl)hydroxy)bicyclo[2.2.1]hept-5-ene-3-carboxylate-2-carboxylic acid (77)

Compound **75** (0.44 mmol, 0.10 g) was dissolved in pyridine under argon atmosphere, after which TrCl (0.88 mmol, 0.24 g, 2.0 eq.) and DMAP (88 µmol, 11 mg, 0.2 eq.) were added. The reaction mixture was stirred at 60 °C for 6 hrs, allowed to cool temperature and quenched with MeOH. Next, H_2O was added and the mixture was extracted with EtOAc (5x). The combined organic layers were dried over $MgSO_4$, filtered and concentrated *in vacuo*. After purification by column chromatography (PetEt/EtOAc 1/0 → 6/4) a mixture of product **77** and starting material **75** (ratio 3:7) was obtained that was not further purified. ^{1}H NMR (400 MHz, $CDCl_3$): δ (ppm) 7.45-7.39 (m, 6H **77**), 7.32-7.20 (m, 9H **77**), 6.21 (dd, *J* = 6.2, 3.5 Hz, 1H **75**), 6.05 (dd, *J* = 6.2, 3.6 Hz, 1H **77**), 5.95 (dd, *J* = 6.1, 3.2 Hz, 1H **75**), 5.73 (dt, *J* = 6.2, 3.0 Hz, 1H **77**), 4.18-4.09 (m, 2H **75** + 2H **77**), 3.83-3.72 (m, 1H **75** + 1H **77**), 3.71-3.66 (m, 1H **77**), 3.65-3.61 (m, 1H **75**), 3.57-3.52 (m, 1H **77**), 3.15-3.05 (m, 2H **75**), 2.84 (d, *J* = 4.8 Hz, 1H **75**), 2.77 (d, *J* = 4.9 Hz, 1H **77**), 2.69 (d, J = 3.5 Hz, 1H **77**), 1.30-1.21 (m, 3H **75** + 3H **77**).

(1*R*,2*S*,3*S*,4*S*,7*R*)-2-ethyl 7-((acetyl)hydroxy)bicyclo[2.2.1]hept-5-ene-2-carboxylate-3-carboxylic acid and (1*R*,2*R*, 3*R*,4*S*,7*S*)-3-ethyl 7-((acetyl)hydroxy)bicyclo[2.2.1]hept-5-ene-3-carboxylate-2-carboxylic acid (78)

Compound **75** (0.20 mmol, 45 mg) was dissolved in pyridine under argon atmosphere, after which Ac_2O (0.40 mmol, 40 µL, 2.0 eq.) and DMAP (20 µmol, 2.4 mg, 0.1 eq.) were added. The reaction mixture was stirred at 40 °C for 1.5 hrs and then allowed to cool temperature. Next, H_2O was added and the mixture was extracted with DCM (3x). The combined organic layers were dried over $MgSO_4$, filtered and concentrated *in vacuo*. Purification by column chromatography (PetEt → 25% EtOAc in PetEt) gave acetylated product **78** (35 mg, 0.13 mmol, 65%).^{1}H NMR (400 MHz, $CDCl_3$): δ (ppm) 6.28 (ddd, *J* = 6.2, 3.6, 1.1 Hz, 1H), 6.02 (ddd, *J* = 6.2, 3.3, 0.9 Hz, 1H), 4.54 (t, *J* = 2.0 Hz, 1H), 4.16 (q, *J* = 7.2 Hz, 2H), 3.63 (t, *J* = 4.3 Hz, 1H), 3.40 (dt, *J* = 4.5, 1.5 Hz, 1H), 3.27 (dq, *J* = 4.5, 1.6 Hz, 1H), 2.94 (d, *J* = 4.6 Hz, 1H), 1.96 (s, 3H), 1.27 (t, *J* = 7.1 Hz, 3H). ^{13}C NMR (100 MHz, $CDCl_3$): δ (ppm) 178.53, 172.89, 169.91, 135.21, 132.76, 83.20, 60.99, 47.63, 47.45, 46.01, 45.03, 20.70, 14.19.

Cyclopenta-2,4-dien-1-yl-dimethylphenylsilane (82)

Freshly distilled cyclopentadiene (20 mmol, 1.7 mL) was dissolved in THF under argon atmosphere and cooled to -78 °C, before *n*-BuLi (20 mmol, 13 mL 1.6 M in hexanes, 1.0 eq.) was added. The reaction mixture was stirred at -78 °C for 20 min, then at 0 °C for 40 min and then cooled back to -78 °C. $Me_2PhSiCl$ (20 mmol, 3.5 mL, 1.0 eq.) was added and the reaction mixture was stirred overnight while the temperature was allowed to rise to room temperature. After concentrating the solvents *in vacuo*, H_2O was added and the mixture was extracted with Et_2O (5x). The combined organic layers were dried over $MgSO_4$, filtered and concentrated *in vacuo*. Half of the crude product (**82**) was then purified by column chromatography (pentane) and used directly for the next step (0.2 g, 1.0 mmol, 10%).

Dimethyl 7-(dimethylphenylsilyl)bicyclo[2.2.1]hept-5-ene-3-(2-oxoacetylate)-2-carboxylate and dimethyl 7-(dimethylphenylsilyl)bicyclo[2.2.1]hept-5-ene-2-(2-oxoacetylate)-3-carboxylate (83)

Diester **81**[55] (0.5 mmol, 86 mg) and silane **82** (1.0 mmol, 0.2 g, 2.0 eq.) were dissolved in toluene and stirred at room temperature for 1 hr, before being concentrated *in vacuo*. Purification by column chromatography (pentane → 10% EtOAc in pentane) gave Diels-Alder adduct **83** (0.15 g, 0.40 mmol, 80%) as a mixture of 2 isomers (ratio 3:2). ^{1}H NMR (400 MHz, $CDCl_3$): δ (ppm) 7.60-7.23 (m, 5Ha + 5Hb), 6.32-6.24 (m, 1Hb), 6.18 (t, *J* = 4.2 Hz, 1Ha), 6.11-6.03 (m, 1Hb), 5.93-5.79 (m, 1Ha), 4.05 (t, *J* = 4.2 Hz, 1Ha), 3.96-3.80 (m, 3Ha + 3Hb), 3.73 (s, 3Ha), 3.66 (s, 3Hb), 3.58-3.45 (m, 1Ha + 2Hb), 3.44-3.30 (m, 1Hb), 3.32-3.22 (m, 1Ha + 1Hb), 2.83 (d, *J* = 4.5 Hz, 1Ha), 1.77-1.67 (m, 1Ha), 1.44-1.34 (m, 1Hb), 0.32-0.19 (m, 6Ha + 6Hb). ^{13}C NMR (100 MHz, $CDCl_3$): δ (ppm) 193.48, 192.40, 174.43, 173.07, 161.67, 160.58, 138.85, 138.70, 137.60, 136.85, 135.53, 133.98, 133.63, 133.62, 128.93, 127.77, 55.44, 53.66, 53.12, 53.01, 52.19, 51.89, 51.02, 50.63, 49.55, 49.46, 48.87, 48.25, 47.75, 47.12, -1.36, -1.47.

B. Biochemistry

General

HEK-293T cells were cultured in DMEM supplemented with 10% (v/v) FCS, 10 units/mL penicillin and 10 µg/mL streptomycin in a 5% CO_2 humidified incubator at 37 °C. Cells were harvested, washed with PBS (2x) and lysed in digitonin lysis buffer (50 mM Tris pH 7.5, 250 mM sucrose, 5 mM $MgCl_2$, 1 mM DTT, 2 mM ATP, 0.025% digitonin) for 30 min on ice. After centrifugation of the cells at 16,100 g for 20 min at 4 °C, the supernatants were collected and the protein concentration was determined by Bradford assay. Fibroblasts were obtained with consent from control donors and cultured in DMEM/F-12 medium (Invitrogen) supplied with 10% (v/v) FBS in an incubator at 5% CO_2 and 37 °C. Precipitation of proteins was done using a chloroform/methanol (c/m) precipitation protocol.[56] Western blotting: the proteins were transferred from an SDS-PAGE gel onto a PVDF membrane using a Bio-Rad

Trans-Blot cell system. Membranes were blocked with 1% BSA in TBS-t(+) (0.1% Tween 20) overnight at room temperature, hybridized with Streptavidin-HRP for 1 hr at room temperature (1:10,000 in blocking buffer) (Molecular Probes, Life Technologies), washed with TBS-t(+) and TBS and then visualized using an ECL+ Western blotting detection kit (Amersham Biosciences).

***In vitro* two-step labeling with biotin-cleavable linker-tetrazine 11**

HEK cell lysates (20 µg total protein per experiment) in digitonin lysis buffer (9 µL) were exposed to 1 µM of ABP **19** (1 µL 10 µM in DMSO) for 1 hr at 37 °C in the presence or absence of 100 µM epoxomicin (1 µL 1 mM in DMSO). Next, the indicated concentrations of tetrazine **11**(1.1 µL 10x solution in DMSO) were added and the mixtures were again incubated for 1 hr at 37 °C. After quenching by c/m precipitation, proteins were taken up in 15 µL Laemmli's sample buffer containing 2-mercaptoethanol, boiled for 5 min at 100 °C and resolved on 12.5% SDS-PAGE. Biotinylated proteins were detected by streptavidin Western blotting.

Hydrazine cleavage. After boiling in sample buffer, the samples were treated with 10, 50 or 100 mM hydrazine (5 µL 4x solution in H_2O) and incubated at room temperature overnight. The samples were then again boiled for 5 min at 100 °C and resolved on 12.5% SDS-PAGE. Biotinylated proteins were detected by streptavidin Western blotting.

***In situ* inhibition of α-galactosidase A activity**

Cultured WT fibroblasts were grown to confluency in 12-wells plates and incubated with 0.01 nM - 10 µM aziridine **20** or **21** in medium for 2 hrs at 37 °C. The cells were washed with PBS and lysed by scraping in 25 mM potassium phosphate buffer (pH 6.5, 0.1% (v/v) Triton X-100) with protease inhibitor cocktail (Roche). The protein concentration was determined by BCA assay. The lysates (25 µL) were then mixed with 100 µL substrate mix (1.5 mg/mL 4-methylumbelliferyl-α-D-galactopyranoside in McIlvaine pH 4.6 + 0.1% BSA). After incubation for 1 hr at 37 °C, the reaction was quenched with 2.5 mL 0.3 M glycine, pH 10.6 and fluorescence was measured with a fluorimeter LS55 (Perkin Elmer) using λ_{ex} 366 nm and λ_{em} 445 nm. All samples were corrected for background fluorescence (sample without enzyme) and residual enzyme activity was calculated as compared to control samples from cells incubated without inhibitors. Displayed values represent mean values from duplicate experiments and error bars indicate standard deviation (SD).

References

1. Ovaa, H.; van Swieten, P. F.; Kessler, B. M.; Leeuwenburgh, M. A.; Fiebiger, E.; van den Nieuwendijk, A. M. C. H.; Galardy, P. J.; van der Marel, G. A.; Ploegh, H. L.; Overkleeft, H. S. *Angew. Chem. Int. Ed.* **2003**, *42*, 3626.
2. Devaraj, N. K.; Hilderbrand, S.; Upadhyay, R.; Mazitschek, R.; Weissleder, R. *Angew. Chem. Int. Ed.* **2010**, *49*, 2869
3. Prescher, J. A.; Dube, D. H.; Bertozzi, C. R. *Nature* **2004**, *430*, 873.
4. Rossin, R.; Renart Verkerk, P.; van den Bosch, S. M.; Vulders, R. C. M.; Verel, I.; Lub, J.; Robillard, M. S. *Angew. Chem. Int. Ed.* **2010**, *49*, 3375.
5. Soriano del Amo, D.; Wang, W.; Jiang, H.; Besanceney, C.; Yan, A.; Levy, M.; Liu, Y.; Marlow, F. L.; Wu, P. *J. Am. Chem. Soc.* **2010**, *132*, 16893.
6. Hong, V.; Steinmetz, N. F.; Manchester, M.; Finn, M. G. *Bioconjug. Chem.* **2010**, *21*, 1912.
7. Späte, A.-K.; Busskamp, H.; Niederwieser, A.; Schart, V. F.; Marx, A.; Wittmann, V. *Bioconjugate Chem.* **2014**, *25*, 147.
8. Cole, C. M.; Yang, J.; Šečkutė, J.; Devaraj, N. K. *Chembiochem* **2013**, *14*, 205.
9. Niederwieser, A.; Späte, A.-K.; Nguyen, L. D.; Jüngst, C.; Reutter, W.; Wittmann, V. *Angew. Chem. Int. Ed.* **2013**, *52*, 4265.

10. Vocadlo, D. J.; Hang, H. C.; Kim, E. J.; Hanover, J. A.; Bertozzi, C. R. *Proc. Natl. Acad. Sci. USA* **2003**, *100*, 9116.
11. Homann, A.; Qamar, R. U.; Serim, S.; Dersch, P.; Seibel, J. *Bellstein J. Org. Chem.* **2010**, *6*, doi:10.3762/bjoc.6.24.
12. Kamber, D. N.; Nazarova, L. A.; Liang, Y.; Lopez, S. A.; Patterson, D. M.; Shih, H.-W.; Houk, K. N.; Prescher, J. A. *J. Am. Chem. Soc.* **2013**, *135*, 13680.
13. Geurink, P. P.; Florea, B. I.; Li, N.; Witte, M. D.; Verasdonck, J.; Kuo, C.-L.; van der Marel, G. A.; Overkleeft, H. S. *Angew. Chem. Int. Ed.* **2010**, *49*, 6802.
14. Willems, L. I.; Verdoes, M.; Florea, B. I.; van der Marel, G. A.; Overkleeft, H. S. *ChemBioChem* **2010**, *11*, 1769.
15. Gieselmann, V. *Biochim. Biophys. Acta* **1995**, *1270*, 103.
16. Witte, M. D.; Kallemeijn, W. W.; Aten, J.; Li, K.-Y.; Strijland, A.; Donker-Koopman, W. E.; van den Nieuwendijk, A. M. C. H.; Bleijlevens, B.; Kramer, G.; Florea, B. I.; Hooibrink, B.; Hollak, C. E. M.; Ottenhof R.; Boot, R. G.; van der Marel, G. A.; Overkleeft, H. S.; Aerts, J. M. F. G. *Nat. Chem. Biol.* **2010**, *6*, 907.
17. Stubbs, K. A. *Carbohydr. Res.* **2014**, *390*, 9.
18. Ferraz, M. J.; Kallemeijn, W. W.; Mirzaian, M.; Herrera Moro, D.; Marques, A.; Wisse, P.; Boot, R. G.; Willems, L. I.; Overkleeft, H. S.; Aerts, J. M. *Biochim. Biophys. Acta* **2014**, *1841*, 811.
19. Gold, H.; Mirzaian, M.; Dekker, N.; Ferraz, M. J.; Lugtenburg, J.; Codée, J. D. C.; van der Marel, G. A.; Overkleeft, H. S.; Linthorst, G. E.; Groener, J. E. M.; Aerts, J. M.; Poorthuis, B. J. H. M. *Clin. Chem.* **2013**, *59*, 547.
20. Carlson, J. C. T.; Meimetis, L. G.; Hilderbrand, S. C.; Weissleder, R. *Angew. Chem. Int. Ed.* **2013**, *52*, 6917.
21. Kallemeijn, W. W.; Li, K.-Y.; Witte, M. D.; Marques, A. R. A.; Aten, J.; Scheij, S.; Jiang, J.; Willems, L. I.; Voorn-Brouwer, T. M.; van Roomen, C. P. A. A.; Ottenhoff, R.; Boot, R. G.; van den Elst, H.; Walvoort, M. T. C.; Florea, B. I.; Codée, J. D. C.; van der Marel, G. A.; Aerts, J. M. F. G.; Overkleeft, H. S. *Angew. Chem. Int. Ed.* **2012**, *51*, 12529.
22. Sweeney, J. B. *Chem. Soc. Rev.* **2002**, *31*, 247.
23. Serrano, P.; Llebaria, A.; Delgado, A. *J. Org. Chem.* **2005**, *70*, 7829.
24. Palakurthy, N. B.; Mandal, B. *Tetrahedron Lett.* **2011**, *52*, 7132.
25. Jat, J. L.; Paudyal, M. P.; Gao, H.; Xu, Q.-L.; Yousufuddin, M.; Devarajan, D.; Ess, D. H.; Kürti, L.; Falck, J. R. *Science* **2014**, *343*, 61.
26. Bercier, A.; Plantier-Royon, R.; Portella, C. *Carbohydr. Chem.* **2007**, *342*, 2450.
27. Win-Mason, A. L.; Jongkees, S. A. K.; Withers, S. G.; Tyler, P. C.; Timmer, M. S. M.; Stocker, B. L. *J. Org. Chem.* **2011**, *76*, 9611.
28. Janda, K. D.; Lo, L. C.; Lo, C. H.; Sim, M. M.; Wang, R.; Wong, C. H.; Lerner, R. A. *Science* **1997**, *275*, 945.
29. Kurogochi, M.; Nishimura, S.-I.; Lee, Y. C. *J. Biol. Chem.* **2004**, *279*, 44704.
30. Kwan, D. H.; Chen, H.-M.; Ratananikom, K.; Hancock, S. M.; Watanabe, Y.; Kongsaeree, P. T.; Samuels, A. L.; Withers, S. G. *Angew. Chem. Int. Ed.* **2011**, *50*, 300.
31. Komatsu, T.; Kikuchi, K.; Takakusa, H.; Hanaoka, K.; Ueno, T.; Kamiya, M.; Urano, Y.; Nagano, T. *J. Am. Chem. Soc.* **2006**, *128*, 15946.
32. Geurink, P. P.; Prely, L. M.; van der Marel, G. A.; Bischoff, R.; Overkleeft, H. S. *Top. Curr. Chem.* **2012**, *324*, 85.
33. Sumranjit, J.; Chung, S. J. *Molecules* **2013**, *18*, 10425.
34. Loenarz, C.; Schofield, C. J. *Nat. Chem. Biol.* **2008**, *4*, 152.
35. Hausinger, R. P. *Crit. Rev. Biochem. Mol. Biol.* **2004**, *39*, 21.
36. Rose, N. R.; McDonough, M. A.; King, O. N. F.; Kawamura, A.; Schofield, C. J. *Chem. Soc. Rev.* **2011**, *40*, 4364.
37. Hamada, S.; Kim, T. D.; Suzuki, T.; Itoh, Y.; Tsumoto, H.; Nakagawa, H.; Janknecht, R.; Miyata, N. *Bioorg. Med. Chem. Lett.* **2009**, *19*, 2852.
38. Rose, N. R.; Woon, E. C. Y.; Kingham, G. L.; King, O. N. F.; Mecinovic, J.; Clifton, I. J.; Talib-Hardy, J.; Oppermann, U.; McDonough, M. A.; Schofield, C. J. *J. Med. Chem.* **2010**, *53*, 1810.

39. Hamada, S.; Suzuki, T.; Mino, K.; Koseki, K.; Oehme, F.; Flamme, I.; Ozasa, H.; Itoh, Y.; Ogasawara, D.; Komaarashi, H.; Kato, A.; Tsumoto, H.; Nakagawa, H.; Hasegawa, M.; Sasaki, R.; Mizukami, T.; Miyata, N. *J. Med. Chem.* **2010**, *53*, 5629.
40. Tschank, G.; Brocks, D. G.; Engelbart, K.; Mohr, J.; Baader, E.; Guenzler, V.; Hanauske-Abel, H. M. *Biochem. J.* **1991**, *275*, 469.
41. Rotili, D.; Altun, M.; Kawamura, A.; Wolf, A.; Fischer, R.; Leung, I. K. H.; Mackeen, M. M.; Tian, Y.-m.; Ratcliffe, P. J.; Mai, A.; Kessler, B. M.; Schofield, C. J. *Chem. Biol.* **2011**, *18*, 642.
42. Geurink, P. P.; Klein, T.; Prely, L.; Paal, K.; Leeuwenburgh, M. A.; van der Marel, G. A.; Kauffman, H. F.; Overkleeft, H. S.; Bischoff, R. *Eur. J. Org. Chem.* **2010**, 2100.
43. Breder, A.; Chinigo, G. M.; Waltman, A. W.; Carreira, E. M. *Angew. Chem. Int. Ed.* **2008**, *47*, 8514.
44. Kresze, G.; Schulz, G.; Walz, H. *Liebigs Ann. Chem.* **1963**, *666*, 45.
45. Corey, E. J.; Weinshenker, N. M.; Schaaf, T. K.; Huber, W. *J. Am. Chem. Soc.* **1969**, *91*, 5675.
46. Kende, A. S.; Koch, K.; Smith ,C. A. *J. Am. Chem. Soc.* **1988**, *110*, 2210.
47. Cappon, J. J.; Baart, J.; van der Walle, G. A. M.; Raap, J.; Lugtenburg, J. *Recl. Trav. Chim. Pays-bas* **1991**, *110*, 158.
48. For reviews, see: a) Cravatt, B. F.; Wright, A. T.; Kozarich, J. W. *Annu. Rev. Biochem.* **2008**, *77*, 383; b) Fonovic, M.; Bogyo, M. *Expert Rev. Proteomics* **2008**, *5*, 721; c) Schmidinger, H.; Hermetter, A.; Birner-Gruenberger, R. *Amino Acids* **2006**, *30*, 333.
49. Lo, L. C.; Pang, T. L.; Kuo, C. H.; Chiang, Y. L.; Wang, H. Y.; Lin, J. J. *J. Proteome Res.* **2002**, *1*, 35.
50. Kumar, S.; Zhou, B.; Liang, F.; Wang, W. Q.; Huang, Z.; Zhang, Z. Y. *Proc. Natl. Acad. Sci. USA* **2004**, *101*, 7943.
51. Walls, C.; Zhou, B.; Zhang, Z. Y. *Methods Mol. Biol.* **2009**, *519*, 417.
52. Wright, A. T.; Song, J. D.; Cravatt, B. F. *J. Am. Chem. Soc.* **2009**, *131*, 10692.
53. Krysiak, J. M.; Kreuzer, J.; Macheroux, P.; Hermetter, A.; Sieber, S. A.; Breinbauer, R. *Angew. Chem. Int. Ed.* **2012**, *51*, 7035.
54. For reviews, see: a) S Stubbs, K. A. *Carbohydr. Res.* **2014**, *390*, 9; b) Witte, M. D.; van der Marel, G. A.; Aerts, J. M. F. G.; Overkleeft, H. S. *Org. Biomol. Chem.* **2011**, *9*, 5908.
55. Corey, E. J.; Tramontano, A. *J. Am. Chem. Soc.* **1981**, *103*, 5599.
56. Wessel, D.; Flügge, U. I. *Anal. Biochem.* **1984**, *138*, 141.

Samenvatting

Chemisch biologisch onderzoek richt zich op het toepassen van chemische benaderingen voor het bestuderen en controleren van biologische processen. Principes en kennis uit de organische chemie worden gebruikt om bepaalde biomoleculen te manipuleren in een biologisch systeem. Op die manier kan inzicht worden verkregen in de processen waarbij de betreffende moleculen betrokken zijn. Dit proefschrift beschrijft de ontwikkeling van nieuwe chemische verbindingen en methodes voor ´activity-based protein profiling´ (ABPP), een vakgebied binnen de chemische biologie met als doel de activiteit van enzymen zichtbaar te maken en te kwantificeren in de context van een complex biologisch systeem. Om dit doel te bereiken wordt er gebruik gemaakt van verbindingen die covalent en irreversibel binden aan het actieve centrum van een specifiek enzym of een klasse van enzymen, op een dusdanige manier dat alleen de actieve enzympopulatie wordt gelabeld. Deze zogenoemde ´activity-based probes´ (ABPs) worden onderverdeeld in twee typen afhankelijk van de identiteit van de detecteerbare groep waarmee ze zijn uitgerust. Directe ABPs bevatten een label, zoals een fluorescent label of biotine, waarmee de target enzymen direct gevisualiseerd, geïsoleerd, gekwantificeerd en/of geïdentificeerd kunnen worden. Tweestaps ABPs zijn uitgerust met een kleine reactieve groep die kan worden gebruikt om het label in een later stadium te introduceren, nadat de ABP aan zijn target enzym is gebonden. Om de labeling te realiseren wordt er gebruik gemaakt van bioorthogonale ligatiereacties. Bioorthogonale chemie kenmerkt zich door een hoge mate van selectiviteit, een hoge efficiëntie en vooral ook door de afwezigheid van enige interacties met het biologische systeem waarin de reactie wordt uitgevoerd. **Hoofdstuk 1** beschrijft de principes van ABPP en het ontwerp van ABPs.

In **Hoofdstuk 2** wordt een overzicht gegeven van de verscheidene bioorthogonale ligatiereacties die tot nu toe in de literatuur zijn beschreven, met de nadruk op het gebruik van deze methodes voor de tweestaps labeling van enzymactiviteit. Voorafgaand aan het werk beschreven in dit proefschrift berustten alle gerapporteerde tweestaps ABPP methodes op het gebruik van een azide of een alkyn als reactieve groep in een ABP. Labeling

van enzymactiviteit werd gerealiseerd via Staudinger-Bertozzi ligatie, de reactie tussen een azide en een phosphine, of via azide-alkyn cycloadditie ('click' reactie), die ofwel gekatalyseerd wordt door koper(I) of wordt gedreven door de ring-spanning in een cyclooctyn.

In **Hoofdstuk 3** wordt een nieuwe tweestaps ABPP methode beschreven die is gebaseerd op de Diels-Alder cycloadditie. De Diels-Alder strategie maakt gebruik van ABPs die zijn uitgerust met een geconjugeerd dieen en een maleimide reagens als de dienofiel waaraan een fluorescent Bodipy label is gekoppeld. Deze strategie werd succesvol toegepast voor de labeling van de endogene activiteit van het 20S proteasoom en van cathepsines, een klasse van cysteine proteases, in celextracten. Daarnaast werd aangetoond dat de ontwikkelde ligatiemethode gecombineerd kan worden met de Staudinger-Bertozzi ligatie voor de labeling van twee verschillende enzymactiviteiten in hetzelfde experiment. De Diels-Alder ABPP strategie vormt een bruikbaar alternatief voor bestaande methodes die gebaseerd zijn op Staudinger-Bertozzi ligatie en click chemie. Desondanks wordt de bredere toepasbaarheid ervan gelimiteerd door de noodzaak om cysteine residuen te beschermen vóór toevoeging van de dienofiel, waardoor *in situ* en *in vivo* toepassingen niet mogelijk zijn. Een ander nadeel van deze methode is de aanzienlijke hoeveelheid achtergrond labeling, waardoor de detectie van eiwitten met lage endogene activiteit wordt bemoeilijkt.

Hoofdstuk 4 beschrijft de ontwikkeling van een alternatieve ABPP strategie die is gebaseerd op de 'inverse-electron-demand' Diels-Alder reactie. Het gebruik van tetrazine als een dieen en norborneen als een dienofiel, welke beide niet met cysteine residuen reageren, resulteert in een ligatiereactie met sterk verbeterde selectiviteit en verhoogde snelheid. Een norborneen-gemodificeerde proteasoom ABP werd gebruikt om endogene proteasoom activiteit efficiënt en selectief te labelen in celextracten en in levende cellen via reactie met Bodipy- en biotine-gelabelde tetrazines. Bovendien werd er een drievoudige bioorthogonale ligatiestrategie ontwikkeld waarbij de tetrazine ligatie werd gecombineerd met de Staudinger-Bertozzi ligatie en de koper(I)-gekatalyseerde click reactie voor de simultane labeling van drie verschillende enzymactiviteiten met verschillende labels in een enkel experiment. Ondanks het feit dat tetrazines niet stabiel zijn onder de condities voor koper(I)-gekatalyseerde click chemie, maakt een simpele wasstap tussen de twee ligatiereacties het mogelijk beide ligaties opeenvolgend uit te voeren in hetzelfde experiment. Dit onderzoek creëert de mogelijkheid drie verschillende biomoleculen tegelijkertijd te bestuderen via bioorthogonale labeling in een complex biologisch systeem.

Het tweede deel van dit proefschrift beschrijft de synthese en biologische evaluatie van nieuwe glycosidase ABPs. Glycosidases zijn enzymen die verantwoordelijk zijn voor de hydrolyse van glycosidische bindingen in (oligo)sacchariden en glycoconjugaten en zijn cruciaal voor de afbraak van glyco(sphingo)lipiden in lysosomen. Een deficiëntie in één van de lysosomale glycosidases kan ophoping van de corresponderende substraten in lysosomen veroorzaken, wat op zijn beurt kan leiden tot een lysosomale stapelingsziekte. Ondanks de vergelijkbare defecten die ten grondslag liggen aan de verschillende lysosomale stapelingsziekten, zijn deze opvallend heterogeen wat betreft loop van de ziekte, phenotypes en klinische manifestatie. ABPP kan een nuttige techniek zijn om de verschillende glycosidases en hun rol in de verscheidene ziektes te bestuderen. Tot op heden is er slechts een beperkt aantal glycosidase ABPs ontwikkeld, waarschijnlijk vanwege de nauwe substraatspecificiteit en de afwezigheid van covalente interacties met het substraat in het katalytische mechanisme van vele van deze enzymen. Niettemin vormen de meeste glycosidases met een 'retaining' mechanisme wel een covalent enzym-substraat intermediair en zijn daarom geschikte kandidaten voor ABPP studies, waarbij ABPs ontworpen kunnen worden die covalent reageren met het katalytisch actieve nucleofiel van één (of meerdere) van deze enzymen.

Hoofdstuk 5 beschrijft het ontwerp en de synthese van irreversibele remmers en ABPs voor twee klassen van glycosidases, de retaining α- en β-galactosidases. De galactopyranose-geconfigureerde probes bevatten een electrofiele epoxide of aziridine groep die op een dusdanige manier is gepositioneerd (in een α- of β-configuratie) dat deze aangevallen kan worden door de katalytisch actieve nucleofiel van respectievelijk α- en β-galactosidases. Voor beide enzymen werden vier epoxide probes gesynthetiseerd, waaronder één niet-gelabelde remmer en drie ABPs waarin de hydroxyl group op C6 (koolhydraat nummering) is gesubstitueerd met een Bodipy label, biotine of een azide voor tweestaps labeling. Daarnaast werden er twee α-galactosidase aziridine probes gesynthetiseerd waarin een azide of Bodipy label werd geïntroduceerd via acylering van de aziridine amine. Pogingen om ook β-galactosidase aziridine probes te isoleren waren tot dusver niet succesvol, aangezien zelfs het gebruik van volledig zuurvrije procedures voor zuivering en vriesdrogen van deze verbindingen resulteerde in opening van de geacyleerde aziridine.

In **Hoofdstuk 6** wordt de remming en labeling van humane retaining α-galactosidases door de α-galactopyranose-geconfigureerde probes beschreven. De aziridine ABPs bleken zeer potente remmers te zijn van α-galactosidase A (αGal A), het humane lysosomale enzym dat deficiënt is in patiënten met de ziekte van Fabry, een lysosomale stapelingsziekte. Verder werd aangetoond dat deze probes geen reactiviteit vertonen tegen een retaining β-

galactosidase, galactocerebrosidase, en een retaining β-glucosidase, glucocerebrosidase. De niet-gelabelde epoxide remmer was een factor 10.000 minder potent op αGal A dan de aziridine probes. Daarentegen vertoonde geen van de C6-gelabelde epoxide ABPs enige remming van dit enzym, wat aantoont dat de primaire hydroxyl groep op C6 essentieel is voor binding van de probes. De fluorescent gelabelde aziridine kan gebruikt worden om de endogene activiteit van αGal A te labelen in celextracten van wild-type fibroblasten. Naast αGal A labelt de ABP ook de activiteit van *N*-acetyl-galactosaminidase (αGal B), het tweede humane enzym in de familie van retaining α-galactosidases. In fibroblast celextracten die afkomstig zijn van klassieke Fabry patiënten is overeenkomstig het gebrek aan αGal A activiteit uitsluitend labeling van αGal B zichtbaar. Een mogelijk zeer waardevolle toepassing van de Bodipy-gelabelde probe is het labelen en vergelijken van de retaining α-galactosidase activiteit in celextracten van Fabry patiënten met verschillende mutaties in αGal A en/of phenotypische varianten van de ziekte.

In **Hoofdstuk 7** worden de β-galactopyranose-geconfigureerde epoxide probes geëvalueerd met betrekking tot remming en labeling van het humane enzym galactocerebrosidase. Deficiëntie van deze lysosomale β-galactosidase leidt eveneens tot een lysosomale stapelingsziekte, de ziekte van Krabbe. De meest potente remmer van galactocerebrosidase was de niet-gelabelde epoxide, terwijl substitutie van de hydroxyl groep op C6 met een azide resulteerde in een factor 2.000 lagere potentie. Daarentegen bleek de introductie van een Bodipy label, en in mindere mate biotine, op dezelfde positie de potentie weer gedeeltelijk te herstellen. Zowel de Bodipy- als de biotine-gelabelde probes werden toegepast om katalytisch actief galactocerebrosidase te visualiseren op gel. Verder werd aangetoond dat de probes selectief zijn voor dit enzym ten opzichte van retaining α-galactosidases en β-glucosidases. Eerdere publicaties hebben laten zien dat deze laatste klasse van enzymen selectief kan worden gelabeld met ABPs die slechts verschillen van de β-galactosidase probes in de configuratie van een enkele hydroxyl substituent. Het onderzoek beschreven in hoofdstukken 6 en 7 laat zien dat het mogelijk moet zijn verschillende klassen van retaining glycosidases te labelen door ABPs te ontwikkelen die dusdanig gemodificeerd zijn dat de configuratie overeenkomt met het natuurlijke substraat van de target enzymen. Bovendien vormen de beschreven α- en β-galactosidase remmers en ABPs nuttige middelen voor het bestuderen van de betreffende enzymen en hun betrokkenheid bij de corresponderende lysosomale stapelingsziekten.

In **Hoofdstuk 8** wordt een overzicht gegeven van het onderzoek dat in dit proefschrift is beschreven. Daarnaast worden verdere toepassingen van de ontwikkelde probes en methodes besproken en worden voorstellen gedaan voor nieuwe glycosidase ABPs die andere eigenschappen hebben (stabiliteit, reactiviteit) en/of gericht zijn tegen andere enzymklassen. Ook worden twee lopende projecten geïntroduceerd, waarvan de eerste betrekking heeft op tweestaps labeling van enzymactiviteit met behulp van de tetrazine ligatie. Een biotine-gelabeld tetrazine reagens waarin een splitsbare linker is opgenomen kan gebruikt worden om gelabelde eiwitten te isoleren met behulp van geïmmobiliseerd streptavidine en vervolgens selectief af te splitsen onder milde condities om zo een zuiver preparaat te verkrijgen. Het tweede project beschrijft het ontwerp en de (gedeeltelijke) synthese van probes voor 2-oxoglutaraat-afhankelijke oxygenases. Omdat deze klasse van enzymen geen covalent enzym-substraat intermediair vormt, is er gekozen voor het gebruik van 'affiniteit-gebaseerde probes' in plaats van ABPs. De probes zijn gebaseerd op de structuur van 2-oxoglutaraat en bevatten een norborneen groep voor labeling via tetrazine ligatie en een 'fotoreactieve' groep, waarmee door middel van fotochemie irreversibele binding aan target enzymen gerealiseerd kan worden.

De focus binnen het vakgebied van ABPP verschuift in steeds hogere mate richting het labelen van enzymklassen met andere en soms slechts deels opgehelderde katalytische mechanismes, nauwe substraatspecificiteit en/of lage expressie niveaus. Daarom worden voortdurend inspanningen gewijd aan het ontwikkelen van nieuwe benaderingen die het mogelijk maken de activiteit van deze enzymen zichtbaar te maken en/of te kwantificeren. Het onderzoek beschreven in dit proefschrift biedt een aantal nieuwe strategieën die aanzet geven tot verdere onderzoekslijnen, zowel voor het labelen van de activiteit van nieuwe enzymklassen als ook voor de bioorthogonale labeling van enzymactiviteit en andere biomoleculen.

List of publications

Azido-BODIPY acid reveals quantitative Staudinger-Bertozzi ligation in two-step activity based proteasome profiling

Verdoes, M.; Florea, B. I.; Hillaert, U.; Willems, L. I.; van der Linden, W. A.; Sae-Heng, M.; Filippov, D. V.; Kisselev, A. F.; van der Marel, G. A.; Overkleeft, H. S. *ChemBioChem* **2008**, *9*, 1735-1738.

A panel of subunit-selective activity-based proteasome probes

Verdoes, M.; Willems, L. I.; van der Linden, W. A.; Duivenvoorden, B. A.; van der Marel, G. A.; Florea, B. I.; Kisselev, A. F.; Overkleeft, H. S. *Org. Biomol. Chem.* **2010**, *8*, 2719-2727.

Small molecule antagonists for chemokine CCR3 receptors

Willems, L. I.; IJzerman, A. P. *Med. Res. Rev.* **2010**, *30*, 778-817.

Two-step labeling of endogenous enzymatic activities by Diels-Alder ligation

Willems, L. I.; Verdoes, M.; Florea, B. I.; van der Marel, G. A.; Overkleeft, H. S. *ChemBioChem* **2010**, *11*, 1769-1781.

Proteasome activity imaging and profiling characterizes bacterial effector syringolin A

Kolodziejek, I.; Misas-Villamil, J. C.; Kaschani, F.; Clerc, J.; Gu, C.; Krahn, D.; Niessen, S.; Verdoes, M.; Willems, L. I.; Overkleeft, H. S.; Kaiser, M.; van der Hoorn, R. A. L. *Plant Physiol*. **2011**, *155*, 477-489.

Bioorthogonal chemistry: applications in activity-based protein profiling

Willems, L. I.; van der Linden, W. A.; Li, N.; Li, K.-Y.; Liu, N.; Hoogendoorn, S.; van der Marel, G. A.; Florea, B. I.; Overkleeft, H. S. *Acc. Chem. Res.* **2011**, *44*, 718-729.

Synthesis of pH-activatable red fluorescent BODIPY dyes with distinct functionalities
Hoogendoorn, S.; Blom, A. E. M.; Willems, L. I.; van der Marel, G. A.; Overkleeft, H. S. *Org. Lett.* **2011**, *13*, 5656-5659.

Activity-based chemical proteomics accelerates inhibitor development for deubiquitylating enzymes
Altun, M.; Kramer, H. B.; Willems, L. I.; McDermott, J. L.; Leach, C. A.; Goldenberg, S. J.; Kumar, K. G. S.; Konietzny, R.; Fischer, R.; Kogan, E.; Mackeen, M. M.; McGouran, J.; Khoronenkova, S. V.; Parsons, J. L.; Dianov, G. L.; Nicholson, B.; Kessler B. M. *Chem. Biol.* **2011**, *18*, 1401-1412.

Discovery of a potent and highly β1 specific proteasome inhibitor from a focused library of urea-containing peptide vinyl sulfones and peptide epoxyketones
van der Linden, W. A.; Willems, L. I.; Shabaneh, T. B.; Li, N.; Ruben, M.; Florea, B. I.; van der Marel, G. A.; Kaiser, M.; Kisselev, A. F.; Overkleeft, H. S. *Org. Biomol. Chem.* **2012**, *10*, 181-194.

Triple bioorthogonal ligation strategy for simultaneous labeling of multiple enzymatic activities
Willems L. I.; Li, N.; Florea, B. I.; Ruben, M.; van der Marel, G. A.; Overkleeft, H. S. *Angew. Chem. Int. Ed.* **2012**, *51*, 4431-4434.

Tuning the leaving group in 2-deoxy-2-fluoroglucoside results in improved activity-based retaining β-glucosidase probes
Walvoort, M. T. C.; Kallemeijn, W. W.; Willems, L. I.; Witte, M. D.; Aerts, J. M. F. G.; van der Marel, G. A.; Codée, J. D. C.; Overkleeft, H. S. *Chem. Commun.* **2012**, *48*, 10386-10388.

Novel activity-based probes for broad-spectrum profiling of retaining β-exoglucosidases in situ and in vivo
Kallemeijn, W. W.; Li, K.-Y.; Witte, M. D.; Marques, A. R. A.; Aten, J.; Scheij, S.; Jiang, J.; Willems, L. I.; Voorn-Brouwer, T. M.; van Roomen, C. P. A. A.; Ottenhoff, R.; Boot, R. G.; van den Elst, H.; Walvoort, M. T. C.; Florea, B. I.; Codée, J. D. C.; van der Marel, G. A.; Aerts, J. M. F. G.; Overkleeft, H. S. *Angew. Chem. Int. Ed.* **2012**, *51*, 12529-12533.

Relative quantification of proteasome activity by activity-based protein profiling and LC-MS/MS

Li, N.; Kuo, C.-L.; Paniagua, G.; van den Elst, H.; Verdoes, M.; Willems, L. I.; van der Linden, W. A.; Ruben, M.; van Genderen, E.; Gubbens, J.; van Wezel, G. P.; Overkleeft, H. S.; Florea, B. I. *Nat. Protoc.* **2013**, *8*, 1155-1168.

Gaucher disease and Fabry disease: New markers and insights in pathophysiology for two distinct glycosphingolipidoses

Ferraz, M. J.; Kallemeijn, W. W.; Mirzaian, M.; Herrera Moro, D.; Marques, A.; Wisse, P.; Boot, R. G.; Willems, L. I.; Overkleeft, H. S.; Aerts, J. M. *Biochim. Biophys. Acta* **2014**, *1841*, 811-825.

Acylazetine as a dienophile in bioorthogonal inverse electron-demand Diels-Alder ligation

Engelsma, S. B.; Willems, L. I.; van Paaschen, C. E.; van Kasteren, S. I.; van der Marel, G. A.; Overkleeft, H. S.; Filippov, D. V. *Org. Lett.* **2014**, doi: http://dx.doi.org/10.1021/ol501049c.

Potent and selective activity-based probes for human retaining α-galactosidases

Willems, L. I.; Beenakker, T. J. M.; Murray, B.; Scheij, S.; Kallemeijn, W. W.; Boot, R. G.; Verhoek, M.; Donker-Koopman, W. E.; Ferraz, M. J.; van Rijssel, E. R.; Florea, B. I.; Codée, J. D. C.; van der Marel, G. A.; Aerts, J. M. F. G.; Overkleeft, H. S. *Submitted for publication.*

Current developments in activity-based protein profiling

Willems, L. I.; Overkleeft, H. S.; Van Kasteren, S. I. *Submitted for publication*.

Synthesis of α- and β-galactopyranose-configured isomers of cyclophellitol and cyclophellitol aziridine

Willems, L. I.; Beenakker, T. J. M.; Murray, B.; Gagestein, B.; van den Elst, H.; van Rijssel, E. R.; Codée, J. D. C.; Kallemeijn, W. W.; Aerts, J. M. F. G.; van der Marel, G. A.; Overkleeft, H. S. *Submitted for publication*.

Curriculum Vitae

Nederlands

Lianne Willems werd op 18 januari 1986 geboren te Leiden. Zij behaalde in 2004 *cum laude* het Gymnasium diploma (profielen Natuur&Gezondheid en Natuur&Techniek) aan het Adelbert College te Wassenaar. Datzelfde jaar begon zij aan de bacheloropleiding Bio-Farmaceutische Wetenschappen aan de Universiteit Leiden, die zij in 2006 *cum laude* afrondde. Aansluitend begon ze aan de masteropleiding Bio-Pharmaceutical Sciences aan dezelfde universiteit.

In het kader van de bacheloropleiding en de masteropleiding deed zij twee onderzoeksstages bij de vakgroep Bio-organic Synthesis onder leiding van dr. M. Verdoes, prof. dr. H.S. Overkleeft en prof. dr. G.A. van der Marel. Dit onderzoek was gericht op het ontwikkelen van een nieuwe methode voor de tweestapslabeling van enzymactiviteit via Diels-Alder cycloadditie. Daarnaast werd een onderzoeksstage uitgevoerd aan Oxford University (UK) in de Ubiquitin Proteolysis Group onder leiding van dr. H.B. Kramer en dr. B.M. Kessler. Het doel van dit onderzoek was het evalueren van nieuwe reversible remmers voor deubiquitinerende enzymen met behulp van gelabelde ubiquitine derivaten. In augustus 2009 behaalde zij *cum laude* het Master of Science diploma.

In september 2009 begon zij als assistent in opleiding met het onderzoek beschreven in dit proefschrift bij de vakgroep Bio-organic Synthesis onder leiding van prof. dr. H.S. Overkleeft en prof. dr. G.A. van der Marel. Een deel van het beschreven onderzoek werd uitgevoerd op het AMC te Amsterdam in de vakgroep Medische Biochemie onder leiding van prof. dr. J.M.F.G. Aerts en dr. R.G. Boot. Posters over delen van het promotieonderzoek werden gepresenteerd op verscheidene nationale en internationale conferenties (2010-2013). Mondelinge presentaties werden gegeven op de West European Activity-Based Proteomics Meeting in Essen (Duitsland, 2011), de Netherlands Proteomics Centre Progress Meeting in Utrecht (2012), de COST Chemical Proteomics Meeting in Jeruzalem (Israël, 2012) en de NWO-CW 'Design and Synthesis' conferentie in Lunteren (2012).

In februari 2015 zal zij beginnen met postdoctoraal onderzoek in de vakgroep van prof. dr. D. J. Vocadlo aan Simon Fraser University in Vancouver (Canada).

Curriculum Vitae

English

Lianne Willems was born on January 18th 1986 in Leiden. In 2004 she completed her high school (Gymnasium) diploma with distinction at the Adelbert College in Wassenaar (majors in Life Science&Health and Life Science&Technology). Subsequently, she started with the bachelor's programme Bio-Pharmaceutical Sciences at Leiden University, followed by the master's programme Bio-Pharmaceutical Sciences at the same university. She obtained both degrees with distinction in 2006 and 2009, respectively.

As part of the bachelor's and master's programmes, she performed two research internships in the Bio-organic Synthesis group at Leiden University under the supervision of dr. M. Verdoes, prof. dr. H.S. Overkleeft and prof. dr. G.A. van der Marel. This research was aimed at the development of a new method for the two-step labeling of enzymatic activity via Diels-Alder cycloaddition. In addition, she performed a research internship at Oxford University (UK) in the Ubiquitin Proteolysis Group under the supervision of dr. H.B. Kramer and dr. B.M. Kessler. The aim of this research was to evaluate new reversible deubiquitinating enzyme inhibitors by using labeled ubiquitin derivatives.

In September 2009 she started with her doctoral studies in the Bio-organic Synthesis group at Leiden University under the supervision of prof. dr. H.S. Overkleeft and prof. dr. G.A. van der Marel. Part of the research described in this thesis was conducted at the Amsterdam Medical Center in the Medical Biochemistry group under the supervision of prof. dr. J.M.F.G. Aerts and dr. R.G. Boot. Posters on parts of the Ph.D. research were presented at various national and international conferences (2010-2013). Oral presentations were given at the West European Activity-Based Proteomics Meeting in Essen (Germany, 2011), the Netherlands Proteomics Centre Progress Meeting in Utrecht (The Netherlands, 2012), the COST Chemical Proteomics Meeting in Jeruzalem (Israël, 2012) and the NWO-CW 'Design and Synthesis' conference in Lunteren (The Netherlands, 2012).

In February 2015 she will start with postdoctoral research in the group of prof. dr. D. J. Vocadlo at Simon Fraser University in Vancouver (Canada).